



OpenAIR@RGU

The Open Access Institutional Repository at Robert Gordon University

<http://openair.rgu.ac.uk>

Citation Details

Citation for the version of the work held in 'OpenAIR@RGU':

SKENE, K. E., 2010. Studies on the role of the endocannabinoid anandamide, as a possible modulator of events during neointimal formation. Available from *OpenAIR@RGU*. [online]. Available from: <http://openair.rgu.ac.uk>

Copyright

Items in 'OpenAIR@RGU', Robert Gordon University Open Access Institutional Repository, are protected by copyright and intellectual property law. If you believe that any material held in 'OpenAIR@RGU' infringes copyright, please contact openair-help@rgu.ac.uk with details. The item will be removed from the repository while the claim is investigated.

**STUDIES ON THE ROLE OF THE
ENDOCANNABINOID
ANANDAMIDE, AS A POSSIBLE
MODULATOR OF EVENTS DURING
NEOINTIMAL FORMATION.**

Karen E Skene

PhD

2010

**STUDIES ON THE ROLE OF THE
ENDOCANNABINOID ANANDAMIDE, AS A
POSSIBLE MODULATOR OF EVENTS DURING
NEOINTIMAL FORMATION.**

KAREN E. SKENE

A thesis submitted in partial fulfilment of the requirements of

The Robert Gordon University

for the degree of Doctor of Philosophy

April 2010

Declaration

This thesis in candidature for the degree of Doctor of Philosophy has been composed entirely by myself. The work which is documented was carried out by myself unless otherwise stated. All sources of information contained within the text which have not arisen from the results generated have been specifically acknowledged.

Karen E Skene

For my Granda
Who was always so proud

Contents	Page
Acknowledgements	I
Publications	II
Abstract	III
Abbreviations	IV
Chapter 1: General Introduction.	1
1.1.1. Blood vessel morphology	2
1.1.2. Smooth muscle cells	2
1.1.3. PDGF	3
1.1.4. Smooth muscle cell proliferation	3
1.1.5. The ERK signalling cascade	4
1.1.6. Smooth muscle cell migration	6
1.1.7. Apoptosis	7
1.2. Atherosclerosis	8
1.2.1. Inflammation and atherosclerosis	8
1.2.2. Smooth muscle cells and atherosclerosis	9
1.2.3. Plaque structure and rupture	9
1.3. Restenosis	10
1.3.1. The initiating phase	11
1.3.2. The intermediate phase	11
1.3.3. The chronic phase	12
1.3.4. Smooth muscle cell origin	12
1.3.5. Restenosis and the inflammatory response	14
1.3.6. Cytokines	14
1.3.7. Protective role of cytokines	17
1.3.8. The endothelium and neointimal formation	17
1.3.9. Nitric oxide	17
1.3.10 Drug eluting stents	18
1.4 Cannabinoids	19
1.4.1. The CB ₁ receptor	19
1.4.2. The CB ₂ receptor	20
1.4.3. Cannabinoid agonists	20
1.5 Endocannabinoids	20
1.5.1. Anandamide biosynthesis	22

1.5.2. 2-AG biosynthesis	23
1.5.3. Endocannabinoid metabolism	23
1.5.3.1. FAAH	23
1.5.3.2. Cyclooxygenase	25
1.5.3.3. Lipoxygenase metabolism	26
1.5.3.4. CYP450	26
1.5.4. 2-AG metabolism	28
1.5.5. Anandamide accumulation and transport	28
1.5.5.1. Facilitated diffusion	28
1.5.5.2. Transport mediated uptake	29
1.5.5.3. Cellular sequestration	30
1.5.5.4. Endocytotic uptake	30
1.6. Cannabinoid action at vanilloid, non cannabinoid, and novel receptors	31
1.6.1. Vanilloid receptors	31
1.6.2. PPARS	32
1.6.3. Novel receptors	33
1.6.4. GPR455	34
1.7. Cannabinoid receptor signalling	34
1.7.1. Adenylate cyclase	35
1.7.2. Cannabinoid modulation of ion channels and Ca ²⁺ concentration	35
1.7.3. MAPK	36
1.8 Cellular effects of cannabinoids	36
1.8.1. Cannabinoids and apoptosis	36
1.8.2. Cannabinoids and cell proliferation	37
1.8.3. Cannabinoids and migration	37
1.9. Cannabinoids and inflammation	38
1.10. Cardiovascular effects of cannabinoids	39
1.10.1. Cannabinoids and atherosclerosis	42
1.11. Hypothesis	43
1.11.1 Objectives	43

Chapter 2: General Methods.	44
2.1. Animals	45
2.2. Small vessel myography	45
2.3. Histological staining	47
2.3.1. Fixing and tissue embedding	47
2.3.2. Haematoxylin and Eosin staining	48
2.3.3. Massons Trichrome staining protocol	49
2.4. Immunohistochemical staining	50
2.4.1. The avidin-biotin complex/alkaline phosphatase (ABC/AP) procedure	50
2.4.2. Basic staining protocol	52
2.4.3. Primary vascular smooth muscle cell extraction from murine aortic rings	53
2.4.4. Passage of vascular smooth muscle cells	53
2.4.5. Sub culture of VSMC in chamber slides	54
2.4.6. Immunocytochemical staining	55
2.5. Cell proliferation studies	55
2.5.1. Bradford Assay	55
2.5.2. Measurement of ERK1/2 phosphorylation in SMC by ELISA	56
2.5.3. Cell extraction and lysis	57
2.5.4. Sample preparation	57
2.5.5. Phospho ERK ELISA protocol	57
2.5.5.1. Plate preparation	57
2.5.5.2. Assay procedure	58
2.5.6. Total ERK ELISA	58
2.5.6.1. Plate preparation	58
2.5.6.2. Assay protocol	59
2.5.7. Determination of DNA synthesis using the BrdU assay	59
2.5.7.1. Cell preparation	59
2.5.7.2. Cell stimulation and assay protocol	60
2.6. Measurement of cell viability by MTT assay	60
2.7. Cell migration studies	61
2.7.1. Preparation of cells for the chemotaxis chamber	61
2.7.2. Preparation of the chamber	64
2.7.3. Removal of unmigrated cells and cell fixation	64
2.7.4. Staining of filter	65
2.8. LCMS/MS detection of AEA and 2-AG in aortic samples	65
2.8.1. Tissue extraction procedure	65

2.8.2. LC conditions	66
2.9. Materials	66
2.9.1. Histology solutions	66
2.9.2. ELISA solutions	68
2.9.3. Reagent preparation for phospho ERK ELISA	68
2.9.4. Reagent preparation for total ERK ELISA	70
2.9.5. BrdU solutions	70
2.9.6. Solution required for MTT assay	71
2.9.7. Solutions required for migration studies	71

Chapter 3: Development and characterisation of an *in vitro* model of neointimal formation. 72

3.1. Introduction	73
3.1.1. Neointimal formation	73
3.1.2. Experimental models of neointimal formation	73
3.1.2.1. <i>In vivo</i> models of neointimal formation	73
3.1.2.2. The use of cell cultures	74
3.1.2.3. Models of organ culture	74
3.1.3. The cannabinoid system	75
3.1.3.1. Endocannabinoids and disease	75
3.2. Aim	76
3.3. Method	81
3.3.1. Tissue preparation and standard culture method	77
3.3.2. Methodological developments to produce vessel injury	77
3.3.2.1. Ligature method	77
3.3.2.2. Vessel injury induced by culturing alone	78
3.3.2.3. Vessel injury induced by intraluminal injury by a wire	78
3.3.2.4. Wire-induced injury	79
3.3.3. Expression and quantification of vessel injury	79
3.3.3.1. Calculation of neointimal area	79
3.3.3.2. Calculation of medial area	79
3.3.3.3. Calculation of adventitial area	80
3.3.3.4. Medial thickness	80
3.3.3.5. Adventitial thickness	80
3.3.4. Injury characterisation	81

3.3.4.1. CB ₁ and CB ₂ antibody staining	82
3.3.5. LCMS-MS analysis of endocannabinoid concentration in normal and injured artery segments.	82
3.3.5.1. Production of endocannabinoid standard curve	83
3.3.5.2. Normalisation of endocannabinoid concentration	83
3.4. Data analysis	83
3.5. Antibodies	83
3.6. Results	85
3.6.1. Morphological assessment of in vitro models of neointimal formation in the murine aorta	85
3.6.1.1. Morphology of control uncultured vessels	85
3.6.1.2. Morphological changes following injury induced by vessel Ligation	85
3.6.1.3. Morphological changes induced by culture	88
3.6.1.4. Morphological changes induced by intraluminal wire injury	90
3.6.2. Quantitative comparison of injury produced by culture with and without wire injury.	90
3.6.2.1. Medial area and thickness	90
3.6.2.2. Adventitial area and thickness	90
3.6.2.3. Neointimal area	91
3.6.3. Vessel characterisation	96
3.6.3.1. Cellular composition of injury response	96
3.6.4. Cannabinoid receptor antibody optimisation	99
3.6.5. Cannabinoid receptor staining of aortic tissue	99
3.6.6. LCMS-MS analysis of AEA concentration	104
3.6.7. LCMS analysis of 2-AG concentration	104
3.7. Discussion	109
Chapter 4: Functional response of murine blood vessels to AEA	115
4.1. Introduction	116
4.1.1. In vitro effects of endocannabinoids	116
4.1.2. Anandamide metabolism	116
4.1.3. Receptors involved in mediating cannabinoid responses in the vasculature	117
4.2. Aim	117

4.3. Myography method	117
4.3.1. Normalisation procedure	118
4.4 Experimental protocols	120
4.4.1. Determination of optimum contractile agent	120
4.4.2. Production of relaxant responses	120
4.4.3. SNP relaxations	121
4.4.4. Vessel responses to anandamide	121
4.4.5. Vessel responses to the CB ₁ receptor agonist ACEA	121
4.4.6. Vessel responses to the endogenous cannabinoid virodhamine	122
4.5. Drugs	122
4.6. Data analysis and statistics	123
4.7. Results	125
4.7.1. Determination of optimum KCL sensitisation concentration	125
4.7.2. Determination of optimum contractile agent	125
4.7.3. Determination of relaxant ability of blood vessel sections and endothelial integrity.	125
4.7.4. Assessment of the relaxant response to anandamide and effect of FAAH inhibition in both the mouse aorta and carotid artery.	133
4.7.5. The effects of COX1 and COX2 inhibition on the relaxant response to anandamide	133
4.7.6. The effects of the CB ₁ antagonist AM251 on the vasorelaxant response produced by AEA.	138
4.7.7. The effect of the CB ₂ antagonist AM630 on the vasorelaxant response produced by AEA	138
4.7.8. The effect of the CB ₁ agonist ACEA on the murine carotid artery	138
4.7.9. The effect of the endogenous cannabinoid virodhamine on the murine carotid artery.	138
4.8 Discussion	142
Chapter 5: The effects of cannabinoids on murine vascular smooth muscle cell proliferation.	148
5.1. Introduction	149
5.1.1. Smooth muscle cells and neointimal formation	149
5.1.2. Cannabinoids and cell proliferation	149
5.1.2.1. Cannabinoid receptors and intracellular growth signalling pathways	149

5.1.2.2. Anti-tumour effects of cannabinoids	150
5.1.2.3. Cannabinoids and smooth muscle cells	150
5.2. Aim	151
5.3. Method	151
5.3.1. Optimisation of PDGF concentration and incubation time for ERK1/2 ELISA	151
5.3.2. Effects of cannabinoid treatment on PDGF induced ERK 1/2 phosphorylation	152
5.3.3. Data Expression of ERK 1/2 phosphorylation	154
5.3.4. Optimisation of PDGF concentration, BrdU incorporation time and cell seeding density for BrdU assay	154
5.3.5. Rationale for choice of cannabinoid ligands to study BrdU incorporation	154
5.3.6. Cannabinoid treatment of cells	155
5.3.7. Data Expression	156
5.3.8. Drug treatments for MTT assay	156
5.3.9. Data Expression	157
5.4. Data Analysis	157
5.5 Drugs	158
5.6. Results	158
5.6.1. Determination of optimum conditions	158
5.6.1.1. Determination of optimum conditions for measuring ERK 1/2 phosphorylation	158
5.6.1.2. Determination of optimum conditions for the BrdU assay	159
5.6.2. The effect of CB receptor ligands on ERK1/2 phosphorylation	164
5.6.2.1. CB ₁ agonist ACEA	164
5.6.2.2. CB ₂ agonist JWH015	164
5.6.2.3. GPR55 agonist O-1602	164
5.6.2.4. Raising endogenous AEA concentration	164
5.6.3. The effect of CB receptor ligands on BrdU incorporation	169
5.6.3.1. The effect of CB ₂ agonists and antagonist on BrdU incorporation	169
5.6.3.2. The effect of the CB ₁ agonist ACEA	169
5.6.3.3. The effect of AEA on BrdU incorporation	173
5.6.3.4. The effect of 2-AG on BrdU incorporation	173
5.6.3.5. The effect of AEA and 2-AG on BrdU incorporation	173
5.6.4. The effect of the CB ₂ agonists/antagonist and their corresponding vehicles on % cell viability	178
5.6.4.1. The effects of CB ₂ agonists on % cell viability	178

5.6.4.2. The effects of a CB ₂ antagonist on cell viability	178
5.6.5. The effects of the endocannabinoids AEA and 2-AG on cell viability	178
5.7. Discussion	184
Chapter 6: The effect of cannabinoids on vascular smooth muscle cell migration	191
6.1. Introduction	192
6.1.1. Smooth muscle cells and neointimal formation	192
6.1.2. Cannabinoids and cell migration	192
6.1.3. Cannabinoids and smooth muscle cells	193
6.2. Aim	193
6.3. Method	194
6.3.1. Method optimisation	194
6.3.2. Determination of optimum incubation time and cell number	194
6.3.3. Determination of optimum staining technique	195
6.3.3.1. Coomassie brilliant blue stain	195
6.3.3.2. Giemsa stain	196
6.3.3.3. Haematoxylin	196
6.3.3.4. Haematoxylin and Eosin	196
6.3.4. Determination of the optimum PDGF concentration	197
6.3.5. Cannabinoid treatment of cells prior to migration assay	198
6.4. Data Expression and Analysis	199
6.5. Drugs	201
6.6. Results	202
6.6.1. Determination of optimum experimental conditions	202
6.6.1.1. Determination of optimum incubation time for measuring cell migration	202
6.6.1.2. Determination of optimum staining technique	202
6.6.1.3. Determination of optimum PDGF concentration	203
6.6.2. The effect of cannabinoid agonists on cell migration	212
6.6.2.1. The effect of a CB ₁ agonist on both un-stimulated and stimulated cell migration	212
6.6.2.2. The effect of a CB ₂ agonist on both un-stimulated and stimulated cell migration.	212
6.6.2.3. The effect of a CB ₂ antagonist on both un-stimulated and stimulated cell migration	215

6.6.2.4. The effect of the endogenous cannabinoid AEA on both un-stimulated and stimulated cell migration.	215
6.6.2.5. The effect of the endogenous cannabinoid 2-AG on both un-stimulated and stimulated cell migration.	215
6.7. Discussion	219
Chapter 7: General Discussion.	224
7.1. Main findings	225
7.2. Clinical relevance	229
7.3. Future Work	230
7.4. Conclusion	231
Appendix : Drug incubation study	233
8.1. Aim	234
8.2. Method	234
8.2.1. Tissue preparation and drug incubation method	234
8.3. Results	236
References	245

List of figures

Chapter 1: General Introduction

Figure 1.1 The PDGF signalling cascade	5
Figure 1.2 A schematic diagram highlighting the processes involved in neointimal formation.	13
Figure 1.3 Illustrating the self propagating nature of cytokines.	16
Figure 1.4. The structures of Δ^9 THC, 2-AG, AEA and arachidonic acid	21
Figure 1.5. The biosynthetic pathways of AEA and 2-AG	24
Figure 1.6. The metabolic pathways of both AEA and 2-AG	27

Chapter 2: General Methods

Figure 2.1. A schematic diagram illustrating the location of the murine carotid artery and thoracic aorta.	46
Figure 2.2. A schematic diagram of a mounted vessel segment for the Myograph 510	47
Figure 2.3. A schematic diagram demonstrating the streptavidin-biotin enzyme complex reacting with a biotinylated secondary antibody	51
Figure 2.4. The components of the 48 well chemotaxis chamber	62
Figure 2.5. An example of the assembled chemotaxis chamber	63

Chapter 3: Development and characterisation of an in vitro model of neointimal formation

Figure 3.1 An Illustration of the aorta with a ligature attached, and the serial sectioning.	78
Figure 3.2 An illustration of a transverse aortic section highlighting the different areas of the vessel	81
Figure 3.3 Original LCMS-MS chromatograms of standards used to produce the standard curve.	84
Figure 3.4 A transverse section of a control non cultured murine aorta	86
Figure 3.5 Sections of murine aorta injured by placement of a ligature	87
Figure 3.6 A transverse section of a cultured murine aorta	89
Figure 3.7 A transverse section of aorta following wire injury	92
Figure 3.8. Medial area of control, cultured and injured aortic tissue	93
Figure 3.9 A comparison of medial thickness of control, cultured and injured aortic tissue	93

Figure 3.10. A comparison of adventitial area of control, cultured and injured aortic tissue	94
Figure 3.11. A comparison of adventitial thickness of control, cultured and injured aortic tissue.	94
Figure 3.12. A comparison of neointimal area of cultured and injured aortic tissue	95
Figure 3.13. Transverse sections of wire injured aorta	97
Figure 3.14. Transverse sections of mouse aorta that had been cultured	98
Figure 3.15. Immunocytochemical staining of CB ₂ transfected CHO cells with a CB ₁ receptor antibody.	100
Figure 3.16. Immunocytochemical staining of CB ₂ transfected cells with a CB ₂ antibody	101
Figure 3.17. Immunohistochemical staining of uncultured aortic tissue for cannabinoid receptors	102
Figure 3.18. Immunocytochemical staining of murine aortic smooth muscle cells for both the CB ₁ and CB ₂ receptors.	103
Figure 3.19. An original LCMS-MS chromatogram showing the AEA peak	105
Figure 3.20. AEA concentration in aortic tissue sections	106
Figure 3.21. An original LCMS-MS chromatogram showing the 2-AG peak	107
Figure 3.22. 2-AG concentration in aortic tissue	108

Chapter 4. Functional response of murine blood vessels to AEA

Figure 4.1. An example of a normalisation trace in the mouse carotid artery	118
Figure 4.2. Shows an example of a normalisation curve showing how the optimum internal diameter is determined.	119
Figure 4.3. An example trace of a time control experiment	124
Figure 4.4. Concentration response curve to increasing concentrations of KCl	126
Figure 4.5. KCl sensitisation of vessels	127
Figure 4.6. Concentration response curve to 5-HT in murine aorta	128
Figure 4.7. Concentration response curve to U46619 in murine aorta	128
Figure 4.8. A comparison of the E max values for 5-HT and U46619	129
Figure 4.9. Concentration response curve to carbachol	130
Figure 4.10. Concentration response curve to calcimycin	130
Figure 4.11. Concentration response curve to SNP	131
Figure 4.12. Example traces of SNP induced relaxations	132

Figure 4.13. Concentration response curve to AEA alone and in the presence of URB597 in the murine aorta	134
Figure 4.14. Concentration response curve to AEA alone or in the presence of URB597 in the mouse carotid artery	134
Figure 4.15. Comparison of AEA concentration response curves in the carotid artery and thoracic aorta in the presence of URB597	135
Figure 4.16. Responses produced in response to AEA in the aorta and carotid artery in response to AEA	136
Figure 4.17. Concentration response curve to AEA alone and in the presence of a COX inhibitor	137
Figure 4.18. Concentration response curve to AEA alone and in the presence of the COX2 inhibitor DUP697	137
Figure 4.19. Concentration response for AEA alone and in combination with the CB ₁ antagonist AM251	139
Figure 4.20. Concentration response curve to AEA alone and in combination with the CB ₂ antagonist AM630.	140
Figure 4.21. Concentration response curve for ACEA alone and in combination with the CB ₁ antagonist AM251	140
Figure 4.22. Concentration response for virodhamine alone and in the presence of AM251	141

Chapter 5 The effects of cannabinoids on murine vascular smooth muscle cell proliferation

Figure 5.1. An example of the plate layout used in the ELISA, and the typical arrangement of samples	153
Figure 5.2. An example of a standard curve produced from phospho ERK standards	153
Figure 5.3. ERK1/2 phosphorylation in response to increasing PDGF concentrations in MVSMC	160
Figure 5.4. ERK1/2 phosphorylation in response to increasing PDGF incubation time in MVSMC	161
Figure 5.5. Increasing concentrations of PDGF on BrdU incorporation at both 12 and 24 hour time points at cell seeding density of 2000 cells/well	162
Figure 5.6. Increasing concentrations of PDGF on BrdU incorporation at both 12 and 24 hour time points at a cell seeding density of 5000 cells/well	163
Figure 5.7. The effect of ACEA on PDGF stimulated ERK1/2 phosphorylation	165

Figure 5.8. The effect of JWH015 on PDGF stimulated ERK1/2 phosphorylation	166
Figure 5.9. The effect of O-1602 on PDGF stimulated ERK1/2 phosphorylation	167
Figure 5.10. The effect of URB597 on PDGF induced ERK1/2 phosphorylation	168
Figure 5.11. The effect of the CB ₂ agonists JWH015 and JWH133 and CB ₂ antagonist AM630 on PDGF stimulated BrdU.	170
Figure 5.12. The effect of JWH133 on PDGF stimulated BrdU incorporation	171
Figure 5.13. The effect of ACEA on PDGF stimulated BrdU incorporation	172
Figure 5.14. The effect of AEA on PDGF stimulated BrdU incorporation	174
Figure 5.15. The effect of AEA (1x10 ⁻⁵ M) on PDGF stimulated BrdU incorporation	175
Figure 5.16. The effect of treating cells with 2-AG on PDGF stimulated BrdU incorporation	176
Figure 5.17. The effect of 2-AG (1x10 ⁻⁵ M) on PDGF	177
Figure 5.18. The effect of AEA and 2-AG combined on PDGF stimulated BrdU incorporation.	177
Figure 5.19. The effect on cell viability following treatment with vehicle, JWH015 and JWH133 (1x10 ⁻⁵ M), measured by MTT assay	179
Figure 5.20. The effect on cell viability following 24 and 48 hour incubation with the CB ₂ antagonist AM630 measured by MTT assay.	180
Figure 5.21. A comparison between the effect on cell viability following 24 hour or 48 hour incubation with the CB ₂ antagonist AM630 in combination with CB ₂ agonists, measured by the MTT assay.	181
Figure 5.22. The effect of AEA (1x10 ⁻⁵ M) at both 24 and 48hrs on cell viability, measured by MTT assay.	183
Figure 5.23. The effect of 2-AG (1x10 ⁻⁵ M) on cell viability, measured by MTT assay	183

Chapter 6 The effect of cannabinoids on vascular smooth muscle cell migration

Figure 6.1. An example of the layout of the chamber	198
Figure 6.2. An illustration of the layout of the chemotaxis chamber for the cannabinoid drug study.	200
Figure 6.3. Illustration of the five non overlapping fields of vision used to count the migrated cells.	201
Figure 6.4. The effect of increasing concentrations of PDGF on smooth muscle cell migration	204
Figure 6.5. Smooth muscle cells stained with Coomassie brilliant blue	205

Figure 6.6. The effect of increasing concentrations of PDGF on smooth muscle cell migration	206
Figure 6.7. The effect of increasing concentrations of PDGF on smooth muscle cell migration	207
Figure 6.8. Smooth muscle cells stained using a variety of techniques	208
Figure 6.9. Smooth muscle cells stained using a variety of techniques	209
Figure 6.10. The effect of increasing concentrations of PDGF on fold change in cell number	210
Figure 6.11. The effect of increasing concentrations of PDGF on smooth muscle cell migration	211
Figure 6.12. The effect of ACEA on un-stimulated cell migration	213
Figure 6.13. The effect of ACEA on PDGF stimulated cell migration	213
Figure 6.14. The effect of JWH133 on un-stimulated cell migration	214
Figure 6.15. The effect of JWH133 on PDGF stimulated cell migration	215
Figure 6.16. The effect of AM630 on un-stimulated cell migration	216
Figure 6.17. The effect of AM630 on PDGF stimulated cell migration	216
Figure 6.18. The effect of AEA on un-stimulated cell migration	217
Figure 6.19. The effect of AEA on PDGF stimulated cell migration	217
Figure 6.20. The effect of 2-AG on un-stimulated cell migration	218
Figure 6.21. The effect of 2-AG on PDGF stimulated cell migration	218

Appendix 1

Figure 8.1. Illustrates the method by which tissue samples either injured or non injured were incubated with cannabinoid drugs	235
Figure 8.2. The individual areas of samples that had been cultured in the presence of cannabinoid agents	238
Figure 8.3. The individual areas of samples that had been injured prior to culture in the presence of cannabinoid agents	238
Figure 8.4. The individual adventitial areas of samples that were cultured in the presence of cannabinoid agents	240
Figure 8.5. The individual adventitial areas of samples that were injured prior to culture in the presence of cannabinoid agents	240
Figure 8.6. The mean medial thickness value for each sample that had been cultured along with cannabinoid agents	242
Figure 8.7. The mean medial thickness value for each sample that had been injured prior to culture along with cannabinoid agents	242

Figure 8.8. The mean adventitial thickness values for each sample that had been cultured along with cannabinoid agents	244
Figure 8.9. The mean adventitial thickness values for each sample that had been injured prior to culture along with cannabinoid agents.	244

List of Tables

Chapter 1 General Introduction

Table 1.1 Summarises a selection of studies that have investigated the effects of AEA on isolated vessels in different species, highlighting the variability between species and vessels.	41
---	----

Chapter 2 General Methods

Table 2.1. The volume of accutase solution required for complete removal of a cell monolayer in various containers	54
Table 2.2. The volume of medium required for each container	54
Table 2.3. The dilutions of BSA standards required for use in the Bradford assay	56
Table 2.4. Composition of controls performed in the BrdU assay	60
Table 2.5. The composition of the diluents and lysis buffer required for the ERK ELISAs	69
Table 2.6. Indicates the dilutions required for the Phospho ERK standards	69
Table 2.7. Shows the dilutions required for the Total ERK 1/2 standards	70

Chapter 3 Development and characterisation of an in vitro model of neointimal formation

Table 3.1. The morphological changes observed following ligature induced injury	88
Table 3.2. The morphological changes observed following vessel culture	89
Table 3.3. The morphological changes observed following vessel injury	92

Chapter 4 Functional response of murine blood vessels to AEA

Table 4.1. An example of measurements of the vessels used in this study	120
Table 4.2. The % relaxation values produced by the time controls	124

Chapter 5 The effects of cannabinoids on murine vascular smooth muscle cell proliferation

Table 5.1. Treatment protocols for drug interventions required for a single experiment	152
Table 5.2. Controls included for all drug treatment groups in the BrdU assay	155
Table 5.3. Details the concentrations of drugs investigated in the MTT assay	157
Table 5.4. The individual values of ERK1/2 phosphorylation in response to increasing PDGF incubation time.	161
Table 5.5. Individual results of increasing PDGF concentration on BrdU incorporation at both 12 and 24 hour time points at a cell seeding density of 2000 cells/well	162
Table 5.6. Individual experimental values of increasing concentrations of PDGF on BrdU incorporation at both 12 and 24 hour time points at a cell seeding density of 5000 cells/well.	163
Table 5.7. Individual experimental values of the control cells treated with $1 \times 10^{-7} \text{M}$ ACEA	165
Table 5.8. Individual experimental values of the control cells	168

Chapter 6 The effects of cannabinoids on vascular smooth muscle cell migration

Table 6.1 Drugs used in this study and the well concentration at which they were used	200
---	-----

Appendix

Table 8.1. Drugs and their medium concentrations used in the drug incubation study	234
Table 8.2. The individual medial areas of samples that had been cultured in combination with cannabinoid agents	237
Table 8.3. The individual areas of tissue samples that had been injured then cultured in the presence of cannabinoid agents	237
Table 8.4. The individual adventitial areas of samples that were cultured in the presence of cannabinoid agents	239
Table 8.5. The individual adventitial areas of tissue samples that had been injured then cultured in the presence of cannabinoid agents.	239
Table 8.6. The mean medial thickness value for each sample that had been cultured along with cannabinoid agents	241

Table 8.7. The mean medial thickness values for each sample that had been injured prior to culture along with cannabinoid agents	241
Table 8.8. The mean adventitial thickness values for each sample that had been cultured along with cannabinoid agents.	243
Table 8.9. The mean adventitial thickness values for each sample that had been injured prior to culture, along with cannabinoid agents.	243

Acknowledgements

I would like to extend my sincere thanks to the following people, without whom I could not have got this far:

Firstly, my director of studies Prof Cherry Wainwright for all her expert advice, supervision and guidance, and for always being so positive!! To my other supervisors Dr Stuart Cruickshank for his help and patience during my myography work, Prof Roger Pertwee for his expert cannabinoid knowledge, and Dr Rachel Knott for all her advice and encouragement, and allowing me time off from my current job to finish my write up.

To the technical staff for all their assistance, especially Dorothy Moir.

To the British Heart Foundation for funding my PhD

To Dr Marie Goua and Dr Giovanna Bermano for their help and advice with the ELISA assays, and to Dr Lesley Macintosh for her help with the migration assays.

To my fellow PhD students past and present, firstly Cip for being an invaluable source of information during my early days in the lab, to Claire and Lisa for the countless cups of tea and keeping me entertained throughout my write up, also to Ray, Barbara, Pramod and Scott for their good company.

To Emma and Sarah who have helped me so much over the years and have become such good friends.

To my friends for always managing to get my mind off my PhD with some good conversation, nights out, and games of squash.

Last but by no means least I would like to thank my family, my brother Logan for his handy excel tips and lending me his computer, and my mum and dad for their love and encouragement, and for always being there for me.

Publications

Markos F, Ruane-O'Hora T, Snow HM, Kelly R, Wainwright CL, Skene K, Drake-Holland AJ, Noble MI, (2008). [Dilatation in the femoral vascular bed does not cause retrograde relaxation of the iliac artery in the anaesthetized pig](#). Acta Physiol. **194**, 207-13.

Skene K, Cruickshank S, Knott R, Pertwee R, Wainwright CL, (2009). Studies on Endocannabinoids and Neointimal Proliferation in an in Vitro Murine Model. (Abstract, Arteriosclerosis, Thrombosis, and Vascular Biology Annual Conference 2009 29;e9-e130).

Skene K, Hector E, Cruickshank S, Pertwee R, Wainwright CL, (2008). Characterisation of the response produced by AEA in the murine carotid artery and effects of cannabinoids on ERK1/2 phosphorylation. (Abstract, 18th annual symposium of the International Cannabinoid research society pg 87).

Skene K, Stewart C, Middleton D, Pertwee R, Wainwright CL, (2006). Studies on the receptors mediating relaxant responses to the endocannabinoid anandamide in the porcine coronary artery. (Abstract, 16th annual symposium of the International cannabinoid research society pg 173).

Abstract

Neointimal formation is a complex process that occurs due to the over compensatory healing response produced by the vessel following injury. Three key events, SMC proliferation, SMC migration and the inflammatory response, occur in unison to drive the formation of a neointima. Cannabinoids/endocannabinoids have been shown to elicit antiproliferative, anti-migratory and anti-inflammatory effects, highlighting modulation of the endocannabinoid system as possible therapeutic strategy.

The aims of this study were to; (i) develop an organ culture model of neointimal formation, and investigate the presence of the endocannabinoid system, (ii) investigate the functional response of anandamide (AEA) in the murine carotid artery, (iii) investigate the effects of cannabinoids on SMC proliferation, and (iv) to establish the effects of cannabinoids on SMC migration.

The organ culture model developed in this study demonstrated the presence of both CB receptors on SMCs, LCMS/MS analysis of tissue samples showed that endocannabinoid concentration was significantly (2-arachidonoylglycerol / 2-AG) increased in injured artery sections. Isolated vessel studies demonstrated that AEA produces a small (~20%) relaxation of the murine carotid artery which was not dependant on the production of active metabolites, but involved activation of the CB₁ receptor. Studies investigating the effects of cannabinoids on cell proliferation revealed that paradoxically both a CB₂ agonist and a CB₂ antagonist reduced markers of cell proliferation without any effect on cell viability; high concentrations of AEA (10µM) reduced SMC proliferation, however this was associated with an apparent cytotoxic/cytostatic effect. The preliminary data from cell migration studies suggests that a CB₂ agonist may function to reduce stimulated cell migration and that 2-AG can increase migration of unstimulated SMCs.

In conclusion, although further research is required, the data within this thesis provides evidence that the endocannabinoid system (in particular the CB₂ receptor) may have the potential to be manipulated for therapeutic gains in terms of restenosis.

Abbreviations

A	Adventitia
ABC/AP	Avidin-biotin complex/ alkaline phosphatase
Abhd4	alpha beta hydrolase 4
ACEA	Arachidonyl-2'-chloroethylamide
ACh	Acetylcholine
AEA	Anandamide
D4-AEA	Anandamide with 4 hydrogens replaced with deuterium
2-AG	2-arachidonoylglycerol
Akt	Protein kinase B
ANOVA	Analysis of variance
ApoE	Apolipoprotein
AT	Adventitial thickness
bFGF	Basic fibroblast growth factor
BMK	Big mitogen activated kinase
BK _{Ca}	Large conductance calcium activated potassium channel
BrdU	5-bromo-2'-deoxy-uridine
BSA	Bovine serum albumin
CAMP	Cyclic adenosine monophosphate
CB	Cannabinoid
CB ₁	Cannabinoid receptor 1
CB ₂	Cannabinoid receptor 2
CCR2	Receptor for monocyte chemoattractant protein
CDK	Cyclin dependent kinase
CDKI	Cyclin dependent kinase inhibitor
CHO	Chinese Hamster Ovary
COX	Cyclooxygenase
CO ₂	Carbon dioxide
CYP450	Cytochrome P450
DAG	Diacylglycerol
DES	Drug eluting stent
DMSO	Dimethylsulphoxide
DMT	Danish Myograph Technology
DNA	Deoxyribonucleic acid
EC ₅₀	The concentration that produces 50% of the maximum response

ECM	Extracellular matrix
EEL	External elastic lamina
EGF	Epidermal growth factor
ELISA	Enzyme linked immunosorbent assay
E_{max}	The maximum response produced by an agonist
eNOS	Endothelial nitric oxide synthase
ERK 1/2	Extracellular signal regulated kinase $\frac{1}{2}$
FAAH	Fatty acid amide hydrolase
FAK	Focal adhesion kinase
FBS	Foetal bovine serum
FGF	Fibroblast growth factor
Gp-AEA	Glycerophospho-arachidonyl ethanolamide
GPCR	G protein coupled receptor
HCL	Hydrochloric acid
HRP	Horse radish peroxidase
HSL	Hormone sensitive lipase
H_2SO_4	Sulphuric acid
5-HT	5-hydroxytryptamine (serotonin)
IC	Internal circumference
ICAM	Intercellular adhesion molecule
ICC	Immunocytochemistry
IEL	Internal elastic lamina
IHC	Immunohistochemistry
iNOS	Inducible nitric oxide synthase
IL	Interleukin
IP_3	Inositol triphosphate
IGF	Insulin like growth factor
JNK	Jun amino-terminal kinase
KCl	Potassium chloride
K_i	The inhibition constant, denotes the affinity of a ligand for a receptor
KO	Knock out
L	Lumen
LCMS/MS	Liquid chromatography mass spectroscopy/ mass spectroscopy
LDL	Low density lipoprotein
LOX	Lipoxygenase
LPI	Lysophosphatidylinositol

LPS	Lipo-polysaccharide
M	Media
MAPK	Mitogen activated protein kinase
MMP	Matrix metalloproteinase
MAGL	Monoacylglycerol lipase
MCP-1	Monocyte chemoattractant protein 1
M-csf	Macrophage colony stimulating factor
Meth-AEA	Methanandamide
MLCK	Myosin light chain kinase
mRNA	Messenger Ribonucleic acid
MT	Medial thickness
mTOR	Mammalian target of rapamycin
m/z	Mass/charge ratio
n	Number of replicates
NFκB	Nuclear factor kappa B
NAE	N-acylethanolamines
NAPE	N-arachidonoyl phosphatidylethanolamine
NAPE-PLD	NAPE- Phospholipase D
NGF	Nerve growth factor
NI	Neointima
NMDA	N-methyl D aspartic acid
NO	Nitric oxide
NTE	Neuropathy target esterase
PBS	Phosphate buffered saline
PCTE	Polycarbonate track-etch
PEA	Palmitoylethanolamide
PDGF	Platelet derived growth factor
PG	Prostaglandin
PGE ₂	Prostaglandin E ₂
PI3K	Phosphoinositide-3 kinase
PKB	Protein kinase B
PKC	Protein kinase C
PKG	Protein kinase G
PLA	Phospholipase A
PLC	Phospholipase C
PLD	Phospholipase D
PMN	Polymorphonuclear neutrophils

PMSF	Phenyl methyl sulphonyl fluoride
PPAR	Peroxisome proliferator activated receptors
PTX	Pertussis Toxin
RANTES	Regulated on activation normally T expressed and presumably secreted
ROS	Reactive oxygen species
RTK	Receptor tyrosine kinase
RTX	Resiniferatoxin
SEM	Standard error of the mean
α SMA	Alpha Smooth muscle actin
SMC	Smooth muscle cell
SNP	Sodium nitroprusside
SRM	Selected Reaction Monitoring
STWS	Scotts tap water solution
TGF β	Tumour growth factor beta
Δ^9 -THC	Delta nine tetrahydrocannabinol
TNF α	Tumour necrosis factor alpha
TRPV1	Transient receptor potential channels
TXA	Thromboxane A
VCAM-1	Vascular adhesion molecule-1
VEGF	Vascular endothelial growth factor
VSMC	Vascular smooth muscle cell
WASP	Wiskott-Aldrich syndrome protein
WAVE	Verprolin-homologous protein

Chapter 1

General Introduction

1.1 Introduction

1.1.1 Blood vessel morphology

Blood vessels are composed of three well defined layers that encompass the vessel lumen, referred to as the intima, the media and the adventitia. These three layers are demarcated by layers of elastin; between the intima and media is the internal elastic lamina, and separating the media and adventitia, the external elastic lamina. The outermost layer is the adventitia, this functions as a protective layer and is composed of collagen, fibroblasts, smooth muscle cells and a loose matrix of elastin.

The media consists primarily of smooth muscle cells, these take on a layering formation with the quantity of layers depending on arterial size. Smooth muscle cells are held together by extracellular matrix (ECM), composed of elastic fibres, collagen and a small portion of proteoglycans (Stocker *et al.*, 2004). The intima, the innermost layer, is primarily composed of endothelial cells with the occasional smooth muscle cell.

The endothelium is the single cell layer that lines the internal surface of all blood vessels; its primary function is to act as a protective barrier between the vascular wall and blood, and to maintain vascular homeostasis. The endothelium has the ability to secrete a variety of vasoactive compounds that not only affect vascular tone but regulate underlying cell growth.

1.1.2 Smooth muscle cells

The smooth muscle cell is a highly specialised cell whose primary function is to maintain vascular tone. Under normal physiological conditions smooth muscle cells proliferate at a low rate, and are comprised of the contractile proteins actin and myosin; three isoforms of actin exist α , β , and γ , in adults the α form predominates. In addition to contractile proteins smooth muscle cells also contain intermediate filaments vimentin and desmin (Reviewed in Shwartz *et al.*, 1986). Smooth muscle cells have the unique feature of not being permanently differentiated. In normal conditions smooth muscle cells display a contractile phenotype however following injury they are able to switch to a synthetic phenotype. The synthetic phenotype is characterised by reduced contractile protein expression, and an increase in organelles associated with proliferation, for example ribosomes and rough endoplasmic reticulum (Reviewed in Schwartz *et al.*, 1986). Smooth muscle cells are activated by interaction with a variety of growth factors and cytokines, many of which can be released from the cells themselves or from circulatory cells. Some of the key growth factors include, platelet derived growth factor (PDGF), fibroblast

growth factor (FGF), TGF β , IGF-1, endothelin and thrombin (reviewed in Schwartz *et al.*, 1995).

1.1.3 PDGF

PDGF (the stimulatory agent used throughout this study) was originally isolated from platelets, however it is now accepted that the majority of cells in the blood vessel can secrete this mitogen (Reviewed in Raines 2004). PDGF exists as five different subtypes; PDGF-AA, PDGF-AB and PDGF-BB and the more recently discovered PDGF-CC and PDGF-DD (Li *et al.*, 2000; Bergsten *et al.*, 2001). These isoforms differ in the receptors they activate (Pekny *et al.*, 1994). PDGF receptors exist as inactive monomers (PDGF α or PDGF β ; Hart *et al.*, 1988) until activated by ligand binding. To become activated the receptors must first form dimers and undergo autophosphorylation (Hughes *et al.*, 1996; reviewed in Henrik Heldin *et al.*, 1999), which culminates in the formation of PDGF $\alpha\alpha$, PDGF $\beta\beta$ or PDGF $\alpha\beta$ receptor subtypes, which are members of the receptor tyrosine kinase family. The affinity of the isoforms of PDGF for the receptor units differs; PDGF-AA only binds to PDGF $\alpha\alpha$, while PDGF-AB prefers to bind to PDGF $\alpha\beta$ or PDGF $\alpha\alpha$ (although it can bind to PDGF $\beta\beta$ with lower affinity). PDGF-BB, on the other hand, binds to all variations of receptor dimers (Drozdoff *et al.*, 1991). Upon activation the PDGF receptor activates a vast quantity of signalling molecules, all of which contribute to either cell proliferation or cell migration (summarised in Figure 1.1).

In normal healthy vessels expression of PDGF is minimal, however in atherosclerotic and injured arteries the expression is increased, for example a 10-12 fold increase in PDGF-A mRNA was observed in the rat carotid artery following balloon denudation (Majesky *et al.*, 1990; reviewed in Raines 2004).

1.1.4 Smooth muscle cell proliferation

Like all other cells, smooth muscle cells proliferate by completion of the cell cycle. The cell cycle is a regulated series of events that enables the cell to replicate. Smooth muscle cells normally exist in the G₀ phase, however their activation promotes them to enter the G₁ phase, where cells prepare for DNA synthesis, and then enter the S phase where DNA synthesis occurs. Once synthesis is complete the cells progress to the G₂ phase in preparation for mitosis, which subsequently occurs during the M phase. Regulation of this cycle is performed at two restriction points, firstly between the G₁ and S, and secondly between G₂ to M (Sriram *et al.*, 2001). The cell cycle restriction points are regulated by cyclins and their corresponding cyclin dependant

kinase (CDK), which encourage movement through the cycle. Cyclin dependant kinase inhibitors (CDKI) have a negative effect on movement through the cycle. Transcription factors are able to modulate the cell cycle by influencing cyclin CDK/CDKI expression, for example antiproliferative signals activate P53 which results in the transcription of P21 which subsequently inhibits the cyclin CDK union that promotes entry through G₁ (Reviewed in Sriram *et al.*, 2001).

1.1.5 The ERK signalling pathway

Cells interact with the extracellular environment through means of signalling cascades, perhaps one of the most important signalling pathways is the Map Kinase (MAPK) pathway. Four distinct MAPK pathways have been identified; ERK, JNK, P38 and BMK, although the pathway of most importance in regards to this study is the ERK pathway. The extracellular signal regulated kinase (ERK) pathway is fundamental in cellular function. Its complex regulation controls cellular processes such as proliferation, differentiation, cell survival, migration and even apoptosis. The pathway can be activated by either receptor tyrosine kinase (RTK) activation, or by G protein coupled receptors (Reviewed in Force *et al.*, 1998). Upon activation of a RTK by a growth factor (for example PDGF) the activated receptor recruits the GTP binding protein Ras, which is then converted to its active state and activates Raf, which in turn activates the dual specific kinase MEK. MEK then phosphorylates ERK of which there are two isoforms, ERK1 and ERK2, which then translocate to the nucleus to activate transcription factors including c-myc, ELK1, P53 and c-Jun. In this example where stimulation came from PDGF, the transcription factors produced then encourage cells to pass through the cell cycle, inducing proliferation.

As mentioned above, the ERK cascade controls a wide variety of cellular functions, including cell proliferation and apoptosis. The mechanism by which activation of the same signalling pathway can result in such diverse cellular endpoints, has received much attention. Five mechanisms have been proposed to explain how the ERK pathway can distinguish and respond specifically to a stimulus.

(i) One of the most convincing mechanisms is through the strength and duration of the signal (Marshall *et al.*, 1995), an example of which occurs in PC12 cells. When these cells are stimulated with EGF a strong but transient activation of ERK occurs, resulting in cell proliferation. When the same cells are stimulated with NGF, a strong but sustained activation of ERK occurs, resulting in cell differentiation. From these findings it is speculated that the

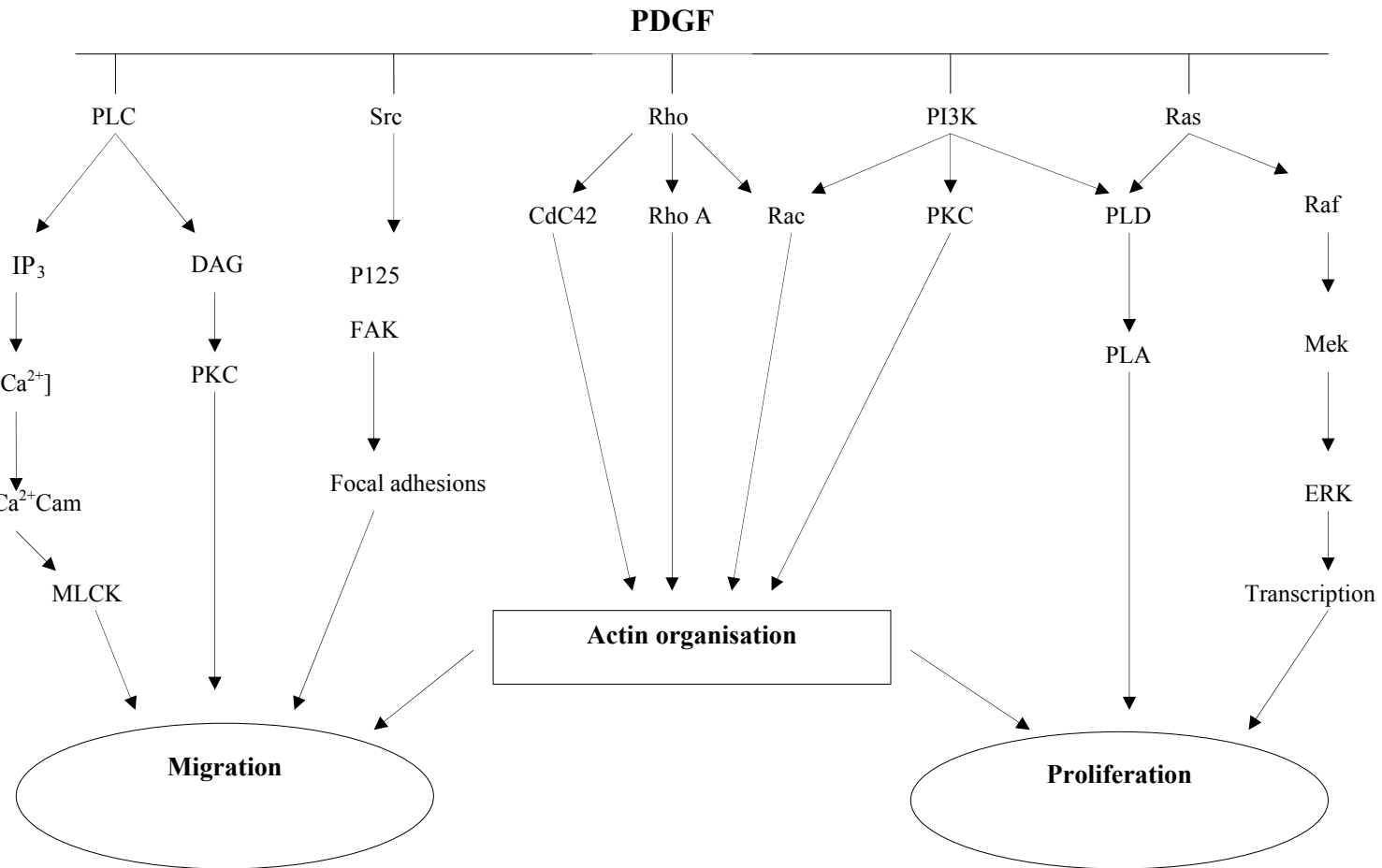


Figure 1.1The PDGF signalling pathways. Adapted from Hughes et al., 1996

duration of ERK activation mediates the ability to activate certain transcription factors (Nguyen *et al.*, 1992; Traverse *et al.*, 1994).

(ii) The interaction of ERK with scaffolding proteins is also thought to regulate the specific actions of ERK. It is thought that scaffolding proteins can organise components of a signalling pathway bringing the desired molecules together (Kolch *et al.*, 2007).

(iii) The third mechanism suggested is that the outcome of ERK activation may vary depending on the cellular location. For example, if components of the ERK cascade are localised to differing target organelles, then the end points of the ERK cascade may vary (Matallanas *et al.*, 2006).

(iv) Interference from other signalling pathways may also contribute to the specificity of the ERK cascade (Shaul *et al.*, 2007).

(v) Different isoforms may regulate the differing functions of ERK. As mentioned previously there are two isoforms of ERK, ERK1 and ERK2. Although these are normally regarded to function together, it may be that the isoforms function differently. Interestingly, the difference between the roles of ERK 1 and ERK2 can be observed in knockout mice, ERK1 knockout mice grow to a normal size (Pages *et al.*, 1999). However it was discovered that ERK2 is essential during development as the mice did not survive (Hatano *et al.*, 2003; Yao *et al.*, 2003). These interesting and complex regulatory mechanisms of ERK are reviewed in detail in Shaul *et al.*, 2007, and Ebisuya *et al.*, 2005.

1.1.6 Smooth muscle cell migration

Smooth muscle cell migration is a complex process which to occur requires prior activation of either a RTK or a G protein coupled receptor (GPCR). Smooth muscle cells normally exist in a non migratory state, with migration only occurring during either vascular development, as a result of vascular injury, or during atherogenesis. There are many activators of cell migration; these include PDGF and other growth factors, cytokines, extracellular matrix components, changes in blood flow, and shear stress (Gerthoffer, 2007; Li *et al.*, 2003; Ward *et al.*, 2001). In order for smooth muscle cells to migrate they must (i) extend lamellipodia in the direction of the stimulus by actin polymerisation, (ii) detach the trailing end of the cell through degradation of focal contacts then (iii) generate enough force to propel the cell in the desired direction.

(i) Actin is the backbone of the lamellipodia, its polymerisation and depolymerisation allows the cell to move in the desired direction. The polymerisation process is regulated by a large variety

of cellular mediators including the formins (mDia1 and mDia2), the formins are molecules that enhance the extension of new filaments and are activated by RhoA and Cdc42 respectively. Similarly the proteins WAVE (verprolin-homologous protein) and WASP (Wiskott-Aldrich syndrome protein) are essential in the nucleation and branching of new actin filaments and are regulated by Rac and Cdc42. Actin depolymerisation occurs in unison with polymerisation to maintain a ready supply of actin, and to stabilise the filament. These processes generate force to aid the protrusion of the leading edge of the cell (Gerthoffer 2007; Prass *et al.*, 2006).

(ii) The formation and degradation of focal contacts maintains the delicate balance of cell attachment and detachment required to enable the cell to move. Focal contacts form at the leading edge of the cell to provide an anchor and aid movement of the cell in the desired direction. One of the key components in focal contacts is focal adhesion kinase (FAK) (Hauck *et al.*, 2000), whose importance has been confirmed by the finding that its expression is up regulated during intimal hyperplasia (Owens *et al.*, 2001). While new contacts are being formed, the redundant focal contacts at the trailing edge of the cell are degraded by metalloproteinases and calpains (Gerthoffer 2007; Paulhe *et al.*, 2001; Bendeck *et al.*, 1994).

(iii) The force that drives the cell in the desired direction comes from the activation of myosin light chain kinase (MLCK) in response to increased Ca^{2+} or activation from Rho A.

Also essential to the process of cell migration is the remodelling of microtubules. These actively assemble and disassemble during cell movement, providing instability in the structure of the cell, a prerequisite for cell migration. The importance of microtubule remodelling is evident from results of treating cells with paclitaxel, which inhibits PDGF induced cell migration through stabilisation of microtubules (Sollott *et al.*, 1995).

1.1.7 Apoptosis

Apoptosis is a carefully controlled method of cell death, regulating the removal of un-required or injured cells (Best *et al.*, 1999). The process of apoptosis begins following activation of death receptors; this can be induced by free radicals, cytokines, growth factor withdrawal and many more noxious stimuli (Mallat *et al.*, 2000). The next step in the apoptotic cascade is the activation of caspase enzymes, which initiate mitochondrial dysfunction and therefore induce cell death (Muto *et al.*, 2007). The Bcl-2 family of proteins are also important regulators of cell death. The family is composed of two groups of proteins; those that are anti apoptotic (such as Bcl-2 and A1) and those that are pro-apoptotic (including Bad and Bid), the balance between these proteins determines cell life or cell death (Muto *et al.*, 2008). Certain cellular pathways

can elicit a protective effect on cells. For example the Akt pathway inhibits apoptosis through the phosphorylation of Bad, thus preventing any association with pro-apoptotic molecules and consequently tipping the balance away from apoptosis (Sen *et al.*, 2003).

1.2 Atherosclerosis

Atherosclerosis is a chronic inflammatory disease of the blood vessels, characterised by plaque formation. Its progression can lead to myocardial infarction and strokes, making atherosclerosis one of the major causes of death in the western world. Atherosclerosis progression is highly complex involving the cumulative effects of circulatory cells, inflammatory cells, and cells of the vessel wall.

1.2.1 Inflammation and atherosclerosis

Atherosclerosis is believed to originate from the accumulation of low density lipoprotein (LDL) in the vessel wall. This tends to occur at locations in the vasculature which are susceptible to high levels of sheer stress, such as bifurcations or curvatures of the arteries (Zand *et al.*, 1999). Accumulated LDL can become oxidised by circulating free radicals, this induces endothelial cell activation and triggers an immune reaction. Activation of endothelial cells initiates the expression of the adhesion molecules ICAM and VCAM-1, which are responsible for the adhesion of circulating monocytes to the endothelium (Khan *et al.*, 1995; Huo *et al.*, 2000; reviewed in Mestas *et al.*, 2008). Under the guidance of macrophage colony- stimulating factor (M-CSF), monocytes enter the arterial wall and differentiate into activated macrophages, which subsequently engulf the oxidised LDL and become foam cells.

Adhesion molecules also facilitate the entry of T lymphocytes into the vascular wall where they become activated and differentiate into T helper cells (either Th1 or Th2). Th1 cells secrete inflammatory mediators and chemokines which function to enhance atherosclerotic progression. However, in established plaques these cells can also contribute to plaque vulnerability through unfavourable interactions with the extracellular matrix (Bui *et al.*, 2009; Hansson and Libby 2006). Mast cells are another inflammatory cell involved in the progression of atherosclerosis. Through the release of histamine they increase the permeability of the endothelium, expediting further inflammatory cell infiltration, they also add to plaque instability in fully established lesions (Sun *et al.*, 2007).

1.2.2 Smooth muscle cells and atherosclerosis

SMCs are primarily found in the media of blood vessels, however a small but significant number exist in the intima. In certain locations, such as those that experience high levels of shear stress, the intima can become thickened due to the presence of additional SMCs (Stary *et al.*, 1992). It has been found that locations of intimal thickening correlate to the locations where atherosclerosis is observed in later life (Stary *et al.*, 1992; Stary 2000). It has been suggested that even in non diseased/injured conditions, SMCs that locate in the intima differ in phenotype from those in the media. SMCs in the intima possess lower quantities of proteins required for contractile function and more that are required for the synthesis of extracellular matrix and release of cytokines (Owens *et al.*, 2004). In diseased conditions the release of inflammatory cytokines and growth factors stimulate the migration of smooth muscle cells from the media to the intima, where they proliferate and contribute to the progression of the plaque.

The lipid content of an atherosclerotic plaque or lesion is not solely due to macrophage derived foam cells; SMCs also possess the ability to accumulate lipid (Stary *et al.*, 1994) as they express the LDL uptake receptor, via which the uptake of LDL is enhanced following cell exposure to IL-1 β (Ruan *et al.*, 2006). SMCs also facilitate monocyte accumulation. In a similar fashion to endothelial cells, SMC express the adhesion molecules ICAM and VCAM-1, which permit monocyte and lymphocyte interactions (Braun *et al.*, 1999). It has been suggested that interactions with SMC protect monocytes from apoptosis through increased activity of the Akt and MAPK pathways (Cai *et al.*, 2004). SMCs are also involved in the secretion of cytokines, which enhance disease progression through potentiating the inflammatory response, stimulating further SMC proliferation, migration, and inducing extracellular matrix production (reviewed in detail in Raines *et al.*, 2005).

Smooth muscle cells constitutively synthesise ECM, which in healthy vessels, is primarily composed of type I and type III fibrillar collagen. In diseased arteries however, the ratios are altered with the ECM consisting of mostly proteoglycans, type I collagen, and fibronectin (Ross 1999). ECM not only contributes to the structure of the lesion it also functions to add to its mass, ECM traps LDL which adds further fuel to the atherosclerotic fire.

1.2.3 Plaque structure and rupture

Early stage atherosclerotic plaques are characterised by a small necrotic core which is protected from the blood supply by a strong fibrous cap, composed of smooth muscle cells and

extracellular matrix; these plaques are referred to as stable. Over time, these stable plaques continue to grow until they become weakened due to the release of metalloproteinases (MMPs), from the ever-accumulating macrophages. MMPs have many functions including the degradation of collagen, thus resulting in thinning of the fibrous cap and rendering the plaque unstable. Unstable or vulnerable plaques have the morphology of a large necrotic core, containing dead cells, lipid, foam cells and cell debris, surrounded by a thin fibrous cap comprised of only a small amount of smooth muscle cells. A unique feature of unstable plaques is that they possess their own blood supply. Neovascularisation of plaques also contributes to disease progression, as these newly formed vessels have the capability to leak, leading to red blood cells and platelets infiltrating the plaque and the deposition of iron (Kolodgie *et al.*, 2003; Kaartinen *et al.*, 1996).

The rupture of a vulnerable plaque is due to a culmination of factors including the size of the necrotic core, fibrous cap thickness and the extent of positive vessel remodelling (Ohayon *et al.*, 2009). Plaques that are most likely to rupture have a dense population of inflammatory cells either within or in close proximity to the fibrous cap (Bui *et al.*, 2009). Once the plaque ruptures the necrotic core comes into contact with the circulation initiating platelet aggregation and the formation of a thrombus, which can result in either myocardial infarction or a stroke.

There is no cure for atherosclerosis but many things can slow or prevent its progression. Lifestyle changes such as improved diet and exercise, and cessation of smoking can reduce the risk of disease. Lipid lowering drugs such as statins and anti-hypertensives can also slow and reduce disease progression. Despite these preventative measures many cases become critical and require surgical intervention (Lewis 2008).

1.3 Restenosis

Percutaneous transluminal angioplasty is now the most common clinical approach to the treatment of patients with atherosclerotic lesions that are of sufficient size to cause angina. Angioplasty involves plaque compression and arterial stretching by the use of either a balloon or the placement of a stent. The implantation of stents has now replaced balloons as they are distinctly advantageous, for example they prevent the initial vessel recoil and improve the long term viability of the blood vessel (Winslow *et al.*, 2005). Despite revascularisation being effective in the immediate restoration of blood flow, the long term benefits of surgical intervention are plagued by restenosis. Restenosis is characterised as the reduction in luminal area due to the formation of a neointima and occurs following 20-80% of insertions of bare metal stents (Topol *et al.*, 1998). In a similar fashion to atherosclerosis, restenosis is a complex

disease that occurs due to the combined coordinated effects of cells within the vessel wall, circulatory cells, and inflammatory cells. Neointimal formation is suggested to occur in three key stages, the initiating phase, the intermediate phase and the chronic phase (Lee *et al.*, 1993).

1.3.1 The initiating phase

This early stage of disease progression is characterised by the interaction of platelets with the vessel wall and the subsequent activation (i.e. change in phenotype) of smooth muscle cells. In a rat model of restenosis, platelets were found to aggregate and adhere to the injury site within seconds of injury and remain there for up to 7 days (Fingerle *et al.*, 1989). While present at the site of injury platelets release mitogenic substances including PDGF (Ross 1981). The placement of a stent results in large scale apoptosis of the SMCs in close proximity to the stent, and indeed it has been reported that up to 70% of the medial smooth muscle cells undergo apoptosis following injury (Perlman *et al.*, 1997). It is thought that apoptosis occurs in response to stimulation of MAPK, as MAPK expression is increased following mechanical injury of vessels (Pollman *et al.*, 1999). Dying smooth muscle cells release bFGF that initiates SMC activation and proliferation and functions to stimulate endothelial cell proliferation, to encourage healing of the injury site (Lindner *et al.*, 1991; Lindner *et al.*, 1990). In addition to this SMCs can become activated purely as a result of mechanical stress. Stretching of SMCs can induce the activation of receptor tyrosine kinases, enhance receptor expression and induce apoptosis (Reviewed in detail Haga *et al.*, 2007).

Between 48-72 hours post injury the majority of SMC, having fulfilled their purpose, return to their quiescent state. Despite this, an important sub-population of cells are resistant to growth inhibition and migrate towards the lumen following directional cues from chemoattractants released from smooth muscle cells; these migrated cells are the progenitor cells of the restenotic lesion (Clowes *et al.*, 1990; Casscells *et al.*, 1992; Majesky *et al.*, 1994).

1.3.2 The intermediate phase

This phase is characterised by intimal hyperplasia, the active proliferation and further migration of SMCs. Migration of smooth muscle cells from the media to the intima is normally inhibited by the extracellular matrix, following injury however, the ECM becomes modified to allow the passage of cells, which is supported by findings that MMPs (enzymes that digest collagen and elastin) are up regulated following injury (Bendeck *et al.*, 1994).

Once SMCs arrive at the intima they can proliferate for months, most likely due to the continued stimulation from growth factors including PDGF, TGF β and IGF (Reviewed in Schwartz *et al.*, 1995). There is some debate over the role of PDGF to enhance SMC proliferation following injury, as it has been reported that antibodies inhibiting the actions of PDGF do not inhibit SMC proliferation during this phase of disease progression (Majesky *et al.*, 1990; Ferns *et al.*, 1991). Instead it is speculated that in this stage of the disease PDGF is more heavily involved in the regulation of SMC migration (Jawien *et al.*, 1992).

1.3.3 The chronic phase

The chronic phase of restenosis is characterised by the large scale production of extracellular matrix. Approximately 2 weeks post injury SMC proliferation becomes reduced, however neointimal thickness continues to increase due to the production of ECM. At a time point of 3 months after injury it was found that 80% of intimal mass was attributed to ECM (Clowes *et al.*, 1983). ECM not only contributes to the size and structure of the neointima, it propagates further SMC proliferation. For example fibronectin has been shown to induce SMC phenotype modulation from contractile to synthetic, although this is not the case for all types of ECM as laminin and collagen have been shown to have no such effects (Hedin *et al.*, 1988). The mechanisms involved in neointimal formation are summarised in Figure 1.2.

1.3.4 Smooth muscle cell origin

It has been suggested that the smooth muscle cells that contribute to neointimal lesions are derived from circulating hematopoietic stem cells that differentiate into smooth muscle cells. This notion was founded from findings that neointimal SMCs have an altered phenotype compared to medial SMCs, and that their gene expression was altered. Indeed, a study by Sata *et al.*, 2002 found that vascular progenitor cells contribute substantially to vascular lesions. This is highly controversial as many other studies contradict these findings, confirming the origin of SMCs in vascular lesions to be the local vessel wall (Bentzon *et al.*, 2006; Rodriguez-Menocal *et al.*, 2009). Aside from the controversy over the importance of progenitor cells, the importance of the adventitia during neointimal formation has also come into question. Various studies have suggested that adventitial fibroblasts become activated following vessel injury and subsequently migrate to the intima to contribute to the restenotic lesion. These findings are also controversial, as in a recent study it was shown that less than 2% of the mass of restenotic lesions was

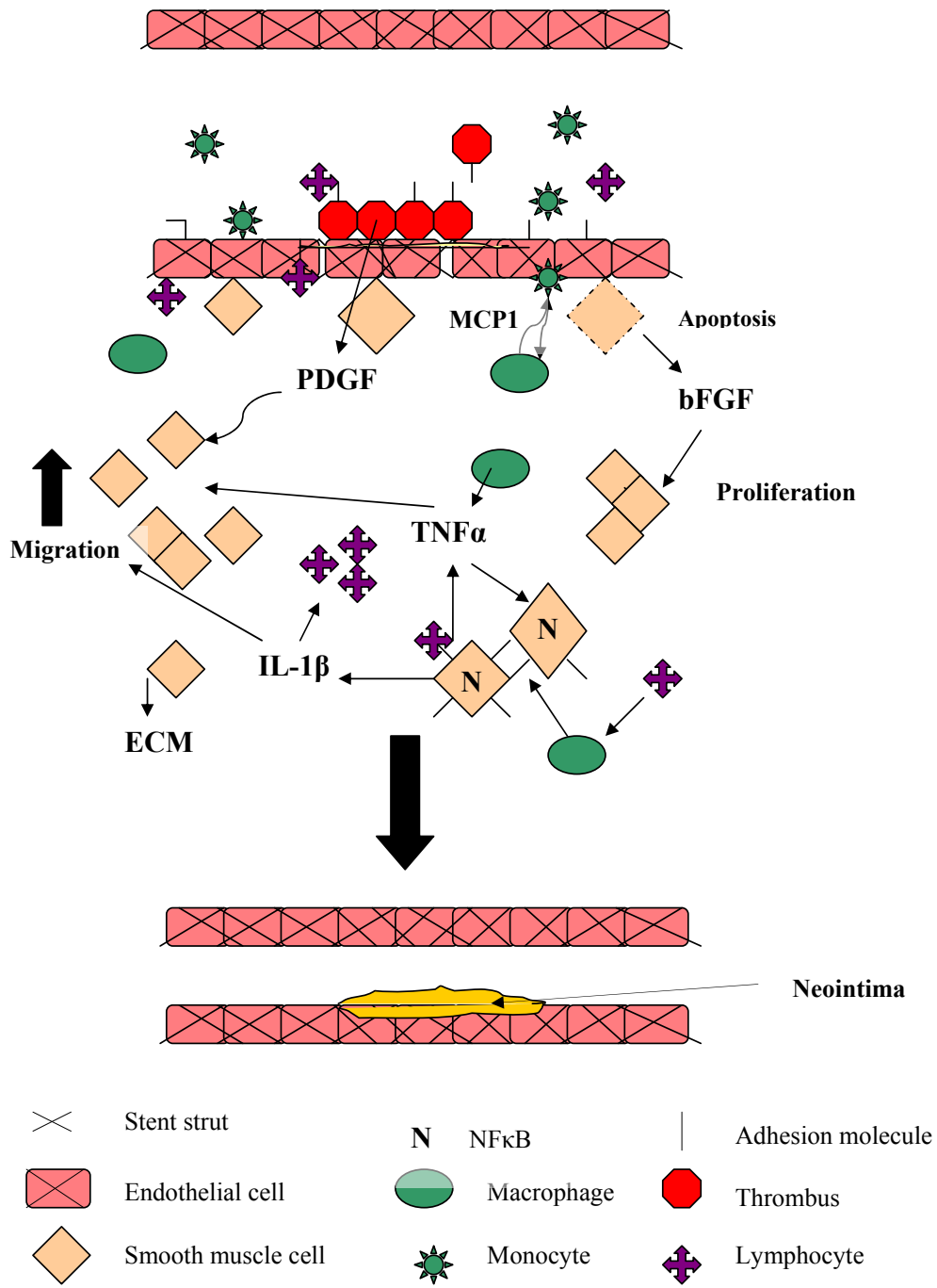


Figure 1.2. A schematic diagram highlighting the processes involved in neointimal formation

composed of adventitial fibroblasts (Fleenor *et al.*, 2009), similarly an earlier study demonstrated SMCs were the principal cell of the lesion (Christen *et al.*, 2001).

1.3.5 Restenosis and the inflammatory response

Inflammation plays a pivotal role in the progression and initiation of restenosis. Immediately following injury platelets adhere to the injury site and become activated. They release a plethora of inflammatory mediators and express adhesion molecules, all of which result in the initiation of an inflammatory response. As mentioned earlier, SMCs alter their phenotype following injury, resulting in morphological changes, and increased proliferation. In addition to this, neointimal SMCs also express a pro-inflammatory phenotype, characterised by increased expression of adhesion molecules and cytokines. This inflammatory phenotype is attributed to the upregulation of NF- κ B (Zeiffer *et al.*, 2004). NF- κ B is a family of transcription factors that can induce the expression of a variety of adhesion molecules, cytokines, COX-2 and iNOS (Reviewed in de Martin *et al.*, 2000).

Mac-1 is a β_2 integrin which is expressed on activated leukocytes and binds to receptors on platelets, and fibrinogen. Mac-1 expression has been found to be increased following coronary stenting (Inoue *et al.*, 2003), and it is speculated that this integrin receptor plays a central role in the recruitment of leukocytes by adhering them to sites on the injured vessel wall (Inoue *et al.*, 2003). This is supported by findings that antibody blockade of Mac-1 reduced neointimal thickening in an experimental model (Rogers *et al.*, 1998). Following balloon induced injury polymorphonuclear leukocytes (PMN) are thought to be the first cell recruited to the lesion site and it is thought that these cells drive the restenotic response. Interestingly in stent induced injury monocytes/macrophage infiltration over days and weeks are thought to be the driving force of disease progression (Horvath *et al.*, 2002). Studies have also demonstrated that neointimal smooth muscle cells exhibit a higher expression of the adhesion molecule P-selectin, aiding monocyte infiltration (Zeiffer *et al.*, 2004). Similarly expression of E selectin and VCAM-1 were also found to be increased in a rabbit model of injury (Kennedy *et al.*, 2000). Leukocytes add to the progression of restenosis through the release of free radicals, proteolytic enzymes, growth factors, chemokines and cytokines.

1.3.6 Cytokines

Cytokines play an essential role in the progression of neointimal formation since they have the ability to influence all the contributing factors that drive the progression of restenosis. The vast

majority of cytokines have the ability to induce immune cell proliferation. In contribution to this cytokines can also facilitate the adhesion of immune cells to the endothelium, and increase endothelial permeability (Sprague *et al.*, 2009). For example TNF α has been found to stimulate the expression of adhesion molecules, and if TNF α is inhibited a reduction in leukocyte infiltration is observed (Ahn *et al.*, 2004; Neumann *et al.*, 1996). Cytokines also have the ability to activate the inflammatory NF κ B pathway (Sprague *et al.*, 2009).

Chemokines are involved in the recruitment of inflammatory cells, most commonly monocytes and T cells. During vascular remodelling MCP-1 and Regulated on Activation, Normally T – Expressed, and presumably Secreted (RANTES) are up regulated, their function being to attract leukocytes to the area of injury (Raines *et al.*, 2005). In neointimal lesions RANTES, is located in smooth muscle cells and also on the surface of endothelial cells, (Schober *et al.*, 2008). The importance of RANTES in neointimal formation has been confirmed in experimental models, as blockade of the RANTES receptors resulted in an inhibition of neointimal formation and macrophage infiltration (Krohn *et al.*, 2007). Another chemokine essential in neointimal formation is monocyte chemoattractant protein (MCP-1) and its receptor CCR2 (Schober *et al.*, 2008). MCP-1 production is increased within hours of vascular injury, this increase however is only short lived supporting a role of MCP-1 in the early phases of neointimal formation (Furukawa *et al.*, 1999; Schober *et al.*, 2004). MCP-1 induces the transendothelial migration of monocytes thus contributing to macrophage infiltration of the neointimal lesion (Schober *et al.*, 2008).

A variety of cytokines have demonstrated an ability to modulate SMC migration and proliferation, this is thought to be mediated through activation of MAPK (Goetze *et al.*, 1999). SMCs have also been shown to release cytokines which can have a cytoprotective effect on neutrophils (Stanford *et al.*, 2001). As mentioned earlier ECM plays a pivotal role in facilitating SMC motility, TNF α increases the fibronectin integrin receptor thus promoting cell migration (Barillari *et al.*, 2003).

Cytokines have also been linked with an increase in reactive oxygen species (ROS), which can induce signalling events such as cell growth and cell death, depending on their concentration. It is speculated that TNF α can induce an increase in the production of ROS, which then in turn results in further cytokine release (Griendling *et al.*, 2000). The self propagating nature of cytokines is illustrated in Figure 1.3.

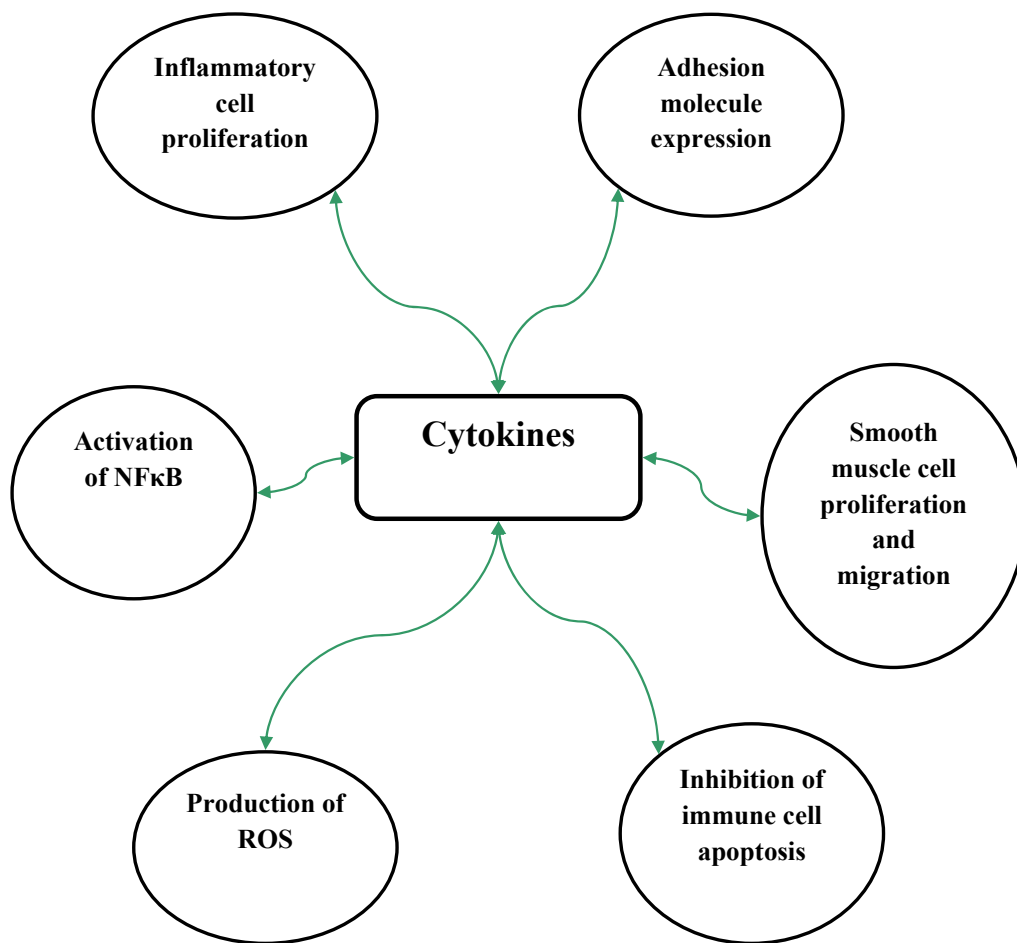


Figure 1.3. Illustrating the self propagating nature of cytokines. The majority of the cellular functions of cytokines result in further production of cytokines.

1.3.7 Protective role of cytokines

Aside from their many pro-inflammatory disease progressing properties, certain cytokines can exhibit anti-inflammatory effects. IL-10 and TGF β have been shown to have inhibitory actions on the activation of NF κ B (Mazighi *et al.*, 2004), this is supported from findings that in a rabbit model of balloon injury SMC proliferation was reduced by 81% following an infusion of IL-10 (Feldman *et al.*, 2000). A beneficial role of cytokines has also been demonstrated in the endothelium, and it is speculated that certain IL-11 can prevent endothelial cell apoptosis and thereby prevent further inflammatory response through the regulation of survivin (an inhibitor of apoptosis; Kirkiles-Smith *et al.*, 2004). The effects of cytokines in vascular injury are reviewed in detail in Sprague *et al.*, 2009; Raines *et al.*, 2005; Tedgui *et al.*, 2006).

1.3.8 The endothelium and neointimal formation

As mentioned earlier endothelial disruption is the initiating event in neointimal formation. Endothelial cell proliferation is an essential part of the healing process, it is initiated in unison with smooth muscle cells through stimulation from bFGF less than 24 hours following injury (Lindner *et al.*, 1990). Endothelium regeneration is a timely yet extremely favourable process taking up to several weeks before the injured surface is completely restored; once the endothelium is restored neointimal growth is attenuated (Asahara *et al.*, 1995).

1.3.9 Nitric oxide

Aside from being a protective barrier the endothelium is also the source of nitric oxide (NO) generation. The release of NO from the endothelium is a sought after process in terms of limiting the progression of neointimal formation, as it has many desirable disease limiting qualities. NO is produced in the endothelium by the enzyme nitric oxide synthase (NOS) from L-arginine. There are two forms of NOS in the vasculature, constitutively expressed eNOS, and an inducible form (iNOS) (Ahanchi *et al.*, 2007). iNOS is expressed in conditions of cellular stress and can synthesis 100-1000 times more NO than eNOS (Morris *et al.*, 1994; Nathan *et al.*, 1994).

NO appears to have an inhibitory effect on the initial inflammatory response through its limiting effects on platelet aggregation and leukocyte chemotaxis. An experimental model of injury demonstrated iNOS knockout mice to show increased leukocyte rolling and adhesion compared to the corresponding wild type control (Ahanchi *et al.*, 2007; Hickey *et al.*, 1997). NO also

exhibits highly desirable effects on SMCs through inhibition of both cell proliferation and migration. Experimental evidence has shown that NO can induce cell cycle arrest at the G₀/G₁ checkpoint and also at the G₁/S checkpoint, the latter due to the inhibition of phosphorylation of the retinoblastoma protein (Sarkar *et al.*, 1997; Ishida *et al.*, 1997). Similarly NO donors have been found to inhibit stimulated SMC migration *in vitro* (Dubey *et al.*, 1995). As previously discussed SMC migration depends on changes in the ECM through the activation of MMPs, NO has also been shown to have inhibitory effects on MMPs therefore reducing cell migration (Reviewed in Ahanchi *et al.*, 2007; Kibbe *et al.*, 1999).

In contrast to the inhibitory effects of NO on SMC, NO evokes a stimulatory effect on endothelial cells through increased endothelial cell proliferation and inhibition of endothelial cell apoptosis (Ahanchi *et al.*, 2007; Ziche *et al.*, 1994). Increasing endothelial cell survival would propagate further release of NO thus inducing more beneficial effects.

1.3.10 Drug eluting stents

Drug eluting stents have been developed to combat the development and progression of restenosis, two agents that have proven effectiveness in limiting neointimal formation are Rapamycin (Siromilus) and Paclitaxel.

Rapamycin is an immunosuppressive agent that produces its antiproliferative effect through inhibition of the cell cycle regulatory protein mTOR (mammalian target of rapamycin), thus preventing cell cycle progression from the G₁ to the S phase (Marx *et al.*, 1995; Sabers *et al.*, 1995; Costa *et al.*, 2005). In addition to its antiproliferative effects rapamycin also prohibits SMC migration (Poon *et al.*, 1996). As a result of its many beneficial anti restenotic properties, stents coated with rapamycin showed reduced neointimal formation compared to bare metal stents in clinical trials (Moses *et al.*, 2003).

Paclitaxel was originally used in the treatment of cancer however its cellular actions made it an ideal anti restenotic drug. Paclitaxel binds to the β tubulin subunit of microtubules and inhibits their disassembly; thus prevents cells from completing mitosis (Costa *et al.*, 2005). Drug eluting stents coated with Paclitaxel have shown in clinical trials to inhibit neointimal formation compared with bare metal stents (Stone *et al.*, 2009).

Despite the benefits of these two drugs, DES also have their drawbacks. While the antiproliferative properties of these agents are beneficial for SMCs, an antiproliferative effect on endothelial cells is a negative effect, as it delays the reendothelialisation process (Joner *et al.*, 2006). Other adverse effects to the current DES are endothelial dysfunction in vessel areas

surrounding the stent (Hofma *et al.*, 2006), and also the potential link to thrombus formation (Takahashi *et al.*, 2007; Joner *et al.*, 2006), DES are also thought to be less effective in patients with diabetes (Lemos *et al.*, 2003).

Aside from these two main agents other drugs including free radical scavengers, estradiol, and the corticosteroid dexamethasone have been investigated as novel drug eluting compounds, however results have been disappointing (Reviewed in Costa *et al.*, 2005), supporting the continued need for identification of novel therapeutic strategies.

1.4 Cannabinoids

For over 5000 years extracts from the *Canabis sativa* plant have been used as medicines, for religious ceremonies, and recreationally. The cannabis plant is a unique source of at least 66 compounds collectively known as cannabinoids, amongst these compounds is tetrahydrocannabinol (Δ^9 -THC), the cannabinoid primarily responsible for the psychotropic effects produced following exposure to cannabis (reviewed in Pertwee 2006). The observation that the activity of psychotropic cannabinoids was reliant on structure, and that cannabinoids with chiral centres demonstrated stereoselectivity, suggested that cannabinoids may act through specific receptors (Howlett *et al.*, 2002; Pertwee 2006), a notion that had previously been thought unlikely. In the 1980s two important findings confirmed the presence of cannabinoid receptors. Firstly that psychotropic cannabinoids inhibited adenylate cyclase through activation of $G_{i/o}$ receptors, and secondly that the radiolabelled synthetic cannabinoid CP55940 showed high affinity binding sites in rat brain membranes (Howlett *et al.*, 1984; Howlett *et al.*, 1985a; Howlett *et al.*, 1985b). Following this discovery two CB receptors were cloned and identified, firstly the CB₁, then in 1993 the CB₂ receptor (Matsuda *et al.*, 1990; Munro *et al.*, 1993).

1.4.1 The CB₁ receptor

The CB₁ receptor has been cloned in mouse, rat, and human tissue, and demonstrates 97-99% homology in amino acid sequence between species. It is located on the q14-q15 region of chromosome 6 (reviewed in Pertwee 1997) and has the classic structure of 7 transmembrane domains, a requisite of a G protein coupled receptor (reviewed in Howlett *et al.*, 2002; Pertwee, 1997). CB₁ receptors were originally found primarily in the brain but recent evidence has confirmed their presence in the periphery including the heart and vasculature, lungs, bladder and adrenal gland (Rajesh *et al.*, 2008; Sugiura *et al.*, 1998; Reviewed in Pertwee 1997).

1.4.2 The CB₂ receptor

The CB₂ receptor exhibits 48% homology with the CB₁ receptor and is found primarily in the periphery, especially in the immune system. CB₂ receptors have also been identified in the adrenal gland, heart, lungs, pancreas, uterus and prostate (Munro *et al* 1993) as well as on microglial cells and in some brain neurones (Van Sickle *et al.*, 2005). Aside from these two receptors there is mounting evidence for the existence of novel cannabinoid receptors, which will be discussed later.

1.4.3 Cannabinoid agonists

Cannabinoid receptor agonists can be classified into one of four categories (reviewed in Pertwee, 1997 and Howlett *et al.*, 2002). The classical cannabinoids, are dibenzopyran derivatives and included in this group is Δ^9 -THC. The second group is the non- classical cannabinoids, which are synthetic analogues of Δ^9 -THC and include CP55940, the compound that helped confirm the presence of cannabinoid receptors. The third group is made up of aminoalkylindoles, which are structurally different from the compounds in the other groups; the prototypic member of this group is the compound WIN55-212-2. The final and most important group of cannabinoid agonists (for the scope of this study) is the eicosanoid group; compounds in this group are arachidonic acid derivatives and include the endogenous cannabinoids (reviewed in Pertwee, 1997 and Howlett *et al.*, 2002).

1.5 Endocannabinoids

Following the identification of the two cannabinoid receptors, the hunt began for endogenous ligands. In 1992 the first endocannabinoid was discovered from extracts of porcine brain and named anandamide (AEA) (Devane *et al.*, 1992). AEA is a partial cannabinoid receptor agonist with slightly greater affinity for the CB₁ receptor than the CB₂, but shows much less efficacy at CB₂ compared to CB₁ (Pertwee, 1999). Soon after the discovery of AEA another endocannabinoid 2-arachidonoyl glycerol (2-AG) was discovered. This was first isolated in the canine gut but has subsequently been detected in the brain (Structures can be seen in Figure 1.4,

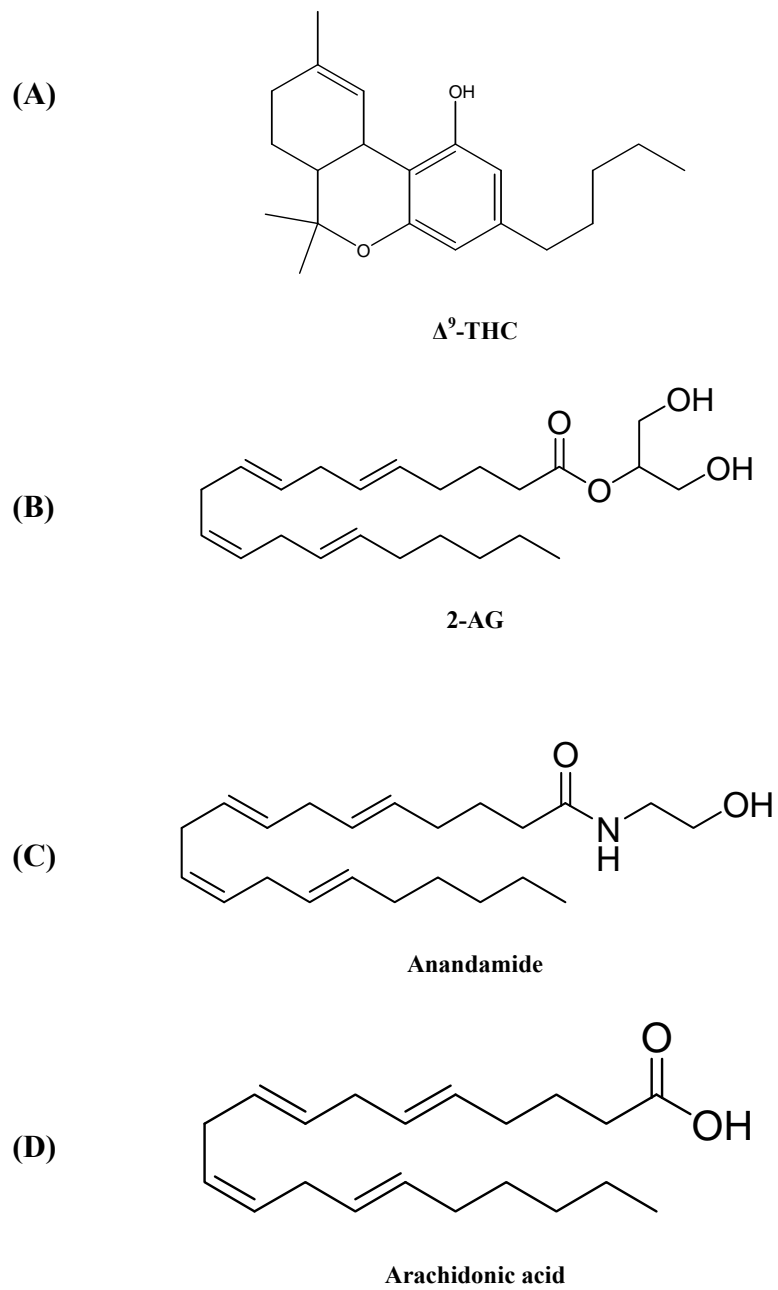


Figure 1.4 The structure of (A) Δ^9 -THC (B) 2-AG, (C) Anandamide and (D) Arachidonic acid.

Mechoulam *et al.*, 1995; Sugiura *et al.*, 1995). The affinity of 2-AG for CB receptors is similar to AEA, however 2-AG demonstrates higher efficacy at CB₂ and possibly also CB₁ compared to AEA (Hanus *et al.*, 2001; Gonsiorek *et al.*, 2000; Pertwee 2002). Other endocannabinoids have since been discovered but have not been subjected to the same amount of scrutiny; these include virodhamine (a CB₁ receptor antagonist/inverse agonist, Porter *et al.*, 2002) and noladin ether (Hanus *et al.*, 2001). All together these compounds and their receptors define the endocannabinoid system.

1.5.1 Anandamide biosynthesis

Anandamide is synthesised from the phospholipid precursor N-arachidonoyl phosphatidylethanolamine (NAPE). It was originally thought to be produced by the simple phosphodiesterase mediated cleavage of NAPE (Di Marzo *et al.*, 1994) as a specific NAPE-Phospholipase D (PLD) was identified which hydrolysed NAPE to yield AEA in a Ca²⁺ dependant manner. This was confirmed when cells over expressing NAPE- PLD showed reduced levels of NAPE and increased AEA (Okamoto *et al.*, 2004; Okamoto *et al.*, 2005). While this method of AEA synthesis is not disputed, recent evidence has highlighted that the biosynthesis of AEA is in fact more complicated than first thought. In NAPE-PLD knockout mice it was found that there was no reduction in AEA concentration, and that the knockout mice retained the ability to synthesise AEA from NAPE in a Ca²⁺ independent manner (Leung *et al.*, 2006). Similarly NAPE-PLD has been proved redundant in the synthesis of AEA in LPS stimulated macrophages. Instead, phospholipase C (PLC) produced the lipid phosphoanandamide (pAEA) from NAPE, which was then converted to AEA by phosphatases, including PTPN22 (Liu *et al.*, 2006). This is supported by previous findings demonstrating the presence of phosphoanandamide in brain tissue and macrophages, and that its concentration is increased following phosphatase inhibition (Liu *et al.*, 2006). AEA is a member of the N-acylethanolamines (NAEs) that include palmitoylethanolamide (PEA). During AEA biosynthesis, PEA is produced in tandem, its function is to act as a protective molecule, inhibiting the degradation of AEA, and therefore increasing AEA concentration. The mechanism by which PEA inhibits AEA degradation is unknown, as it does not directly inhibit FAAH (Smart *et al.*, 2002). PEA also increases the affinity and the potency of AEA at TRPV1 receptors (De Petrocellis *et al.*, 2001), and can target PPARs (O'Sullivan 2007).

A recently discovered phospholipase A₂ has been found to convert NAPE to 2-lyso NAPE which is then metabolised to AEA by a Ca²⁺ independent process (Sun *et al.*, 2004). In slight contradiction to this it was found that tissue distribution of PLA₂ was limited, suggesting therefore, that other enzymes may be involved in this pathway. It has been proposed that the

newly discovered $\alpha\beta$ -hydrolase 4 (Abhd4) functions to convert either NAPE directly, or 2-lysoNAPE, to glycerophospho-arachidonyl ethanolamide (GpAEA), which is then converted to AEA by a phosphodiesterase (Simon and Cravatt, 2006). In a recent study the three pathways described above were investigated, it was found that macrophages could only synthesise AEA on demand through the PLC pathway, and that in brain tissue the immediate production of AEA (in the first minute) is reliant on the PLC pathway. The Abhd4 pathway was found to play a dominant role in the longer term production of AEA (Liu *et al.*, 2008). The pathways discussed above are illustrated in Figure 1.5.

1.5.2 2-AG biosynthesis

2-AG is synthesised from membrane phospholipids containing arachidonic acid, for example the inositol phospholipids. Two central pathways for the synthesis of 2-AG have been identified; (i) the conversion of inositol phospholipids to diacylglycerol (DAG) by PLC β , then subsequent hydrolysis of DAG by diacylglycerol lipase (DAG lipases) to 2-AG. This pathway that was first discovered to explain arachidonic acid breakdown in platelets but has since been found to result in the production of 2-AG (Prescott *et al.*, 1983; Stella *et al.*, 1997 nature). (ii) The conversion of phospholipids to lyso- phospholipids by Phospholipase A₁, this is then converted to 2-AG by lyso-PLC (Reviewed in Sugiura *et al.*, 2002). 2-AG synthesis is illustrated in Figure 1.5.

1.5.3 Endocannabinoid metabolism

1.5.3.1 FAAH

Anandamide is primarily hydrolysed into arachidonic acid and ethanolamine by the enzyme fatty acid amide hydrolase (FAAH). This was confirmed following findings from FAAH knockout mice which demonstrated brain anandamide concentrations 15 times greater than that of the normal wild type mouse (Cravatt *et al.*, 2001). FAAH is a membrane bound protein which in humans has been located in a variety of tissues, including the pancreas, brain, kidney and skeletal muscle (Giang *et al.*, 1997). Due to the similarity in chemical composition of AEA to arachidonic acid, it was speculated that there may be more than one route of metabolism for

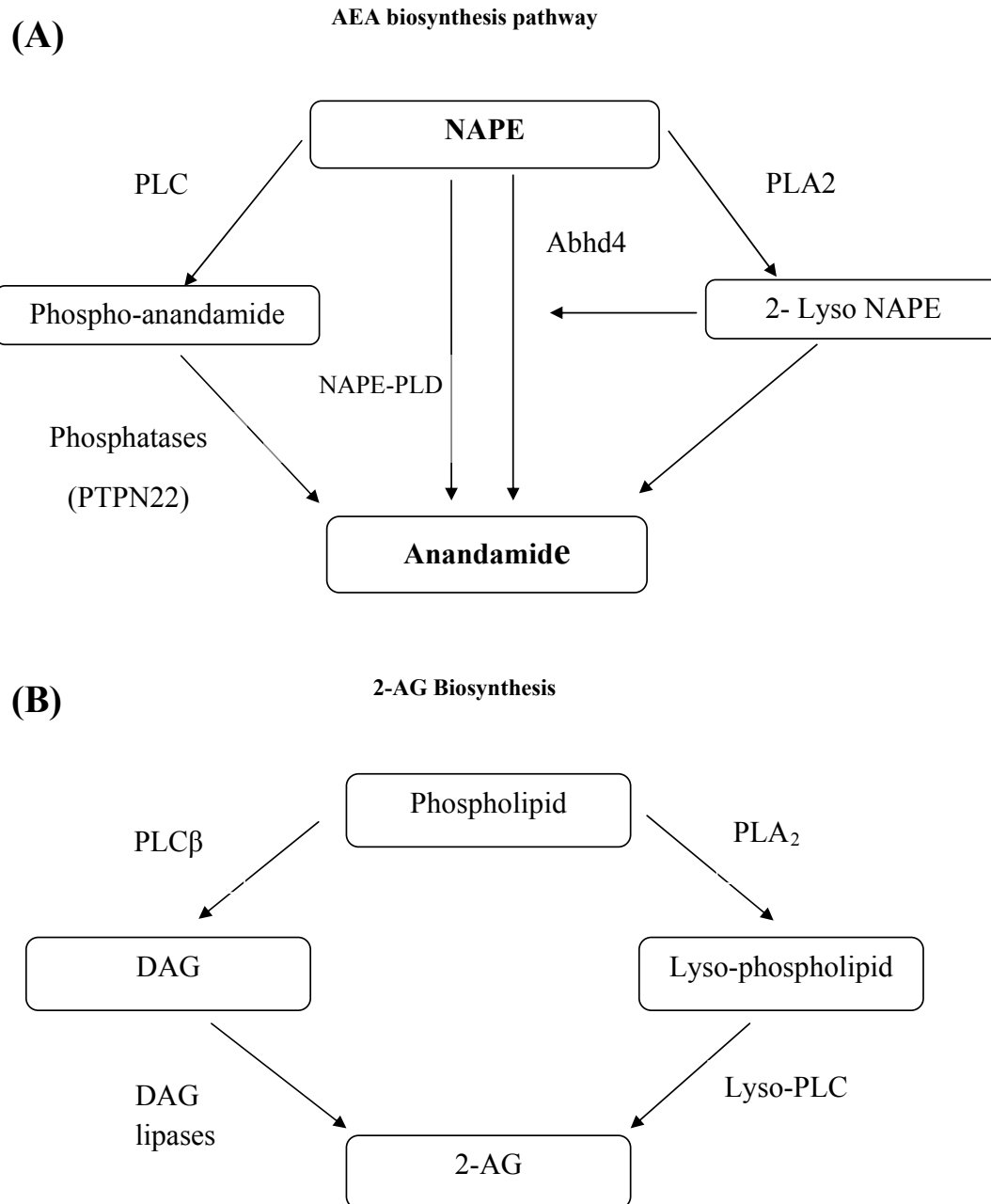


Figure 1.5. An illustration of the pathways involved in the biosynthesis of AEA (A) and 2-AG (B). Pathways described in section 1.5.1 & 1.5.2.

AEA. It has been found that certain cyclooxygenase (COX) and lipoxygenase (LOX) enzymes are capable of metabolising AEA.

1.5.3.2 Cyclooxygenase

COX-1 is a constitutively expressed enzyme that performs general “housekeeping tasks” (Kozak *et al.*, 2002), COX-2 on the other hand is an inducible enzyme that produces prostaglandins (PGs) in inflammatory cells (Dubois *et al.*, 1998). It has been shown that COX-2 has the ability to metabolise AEA in a similar way to arachidonic acid. Cells cultured with AEA produced prostaglandin (PG) D_2 -, PGE $_2$ -, and PGF $_{2\alpha}$ -ethanolamide, a family of compounds known collectively as prostamides (Yu *et al.*, 1997; Yang *et al.*, 2005). COX-1 is unable to metabolise AEA, thought to be due to the differing chemical structure of the enzyme active site (Kozak *et al.*, 2003; Yu *et al.*, 1997).

The discovery of prostamide products from the metabolism of AEA has led to much research to try and understand the pharmacology of these compounds. Prostamides have been shown to be much less active at their corresponding PG receptor compared to PGs (Ross *et al.*, 2002). For example, prostamide E $_2$ is 100-1000 fold less active than PGE $_2$ in binding experiments utilising human prostanoid EP receptors (Ross *et al.*, 2002). It has been found that prostamides can weakly activate the CB receptors (Berglund *et al.*, 1999) and that only prostamide F $_{2\alpha}$ could elicit very weak activation of the TRPV1 receptor (see section 1.6.1 Matias *et al.*, 2004). Prostamides produce a potent contractile effect on the cat iris sphincter and it has been suggested that this effect is mediated by novel prostamide receptors. A notion that has been supported by findings that the compound AGN-204396 antagonises the effects of the prostamides on the cat iris sphincter but not the effects of prostaglandins (Matias *et al.*, 2004; Woodward *et al.*, 2007). It has also been suggested that prostamides may be produced to enhance the concentration of AEA by competing at the active site of FAAH; however this is unlikely as prostamides are not substrates of FAAH (Matias *et al.*, 2004).

Despite the extensive research in to the metabolism and pharmacology of the AEA metabolites produced by COX-2, the physiological relevance of COX-2 metabolism comes into question. The concentration of AEA in physiological conditions is habitually in the nanomolar region (Di Marzo *et al.*, 1999; Bisogno *et al.*, 1999), while the K_m of COX-2 is in the micromolar range, suggesting that COX metabolism of AEA is unlikely to occur. However, it is well established that AEA concentration increases in pathological conditions (Reviewed in Di Marzo, 2008).

This along with the fact that COX-2 only functions in pathological conditions, raises the possibility that if, under certain conditions FAAH mediated metabolism was inhibited, then AEA might be metabolised by COX-2 *in vivo*. This theory is supported by the discovery of an endogenous FAAH inhibitor 2-octyl-g-bromoacetoacetate, this compound was originally found in the cerebrospinal fluid but has since been identified in other tissues (Patricelli *et al.*, 1998). The metabolism of AEA is summarised in Figure 1.6.

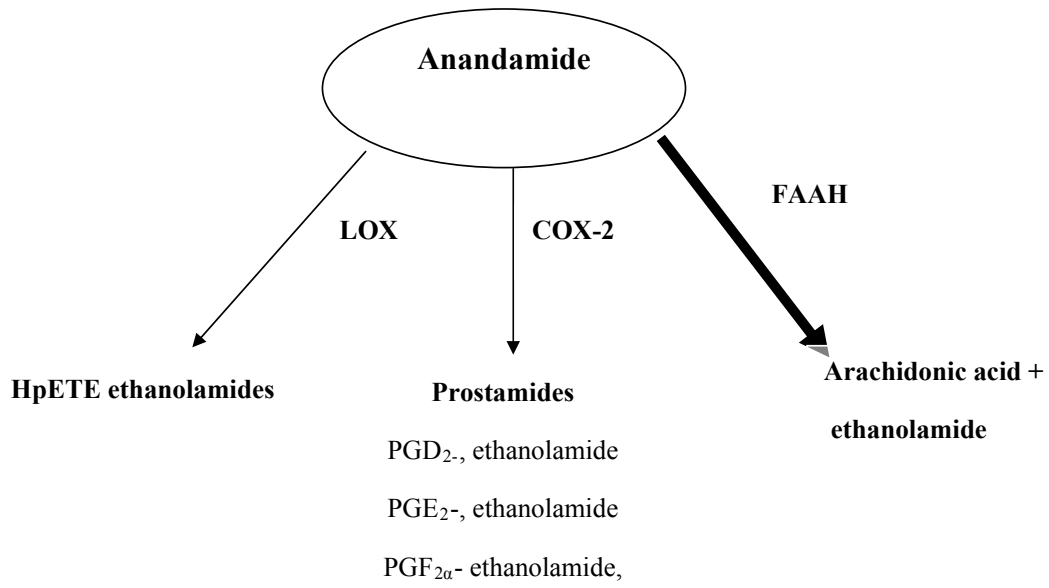
1.5.3.3 Lipoxygenase metabolism

Lipoxygenases (LOX) are a group of enzymes that catalyse the addition of an oxygen molecule to fatty acids and other compounds. The products of LOX mediated metabolism of arachidonate are hydroperoxyeicosatetraenoic acids (HpETEs) (Kozak *et al.*, 2002). Due to the known ability of LOX to metabolise fatty acids and phospholipids, it was speculated that it may also metabolise AEA. Confirmation of this came from findings that AEA incubated with LOX, resulted in the production of HpETE-EA (Ueda *et al.*, 1995). Indeed, it has been suggested that lipoxygenation is the primary route of AEA metabolism in platelets, as these cells have only COX-1 and very little amounts of FAAH (Kozak *et al.*, 2002). It is established that AEA produces contractions of the guinea pig bronchus through activation of vanilloid receptors (Craib *et al.*, 2001); interestingly this effect is inhibited by a combined COX and LOX inhibitor, and attenuated by a specific LOX inhibitor. It is suggested that AEA is metabolised to hydroperoxyeicosatetraenoyl ethanoloamides and lipoxin A₄, both of which function as vanilloid receptor agonists (Craib *et al.*, 2001). Interestingly, it has been discovered that the lipoxygenase mediated metabolites of arachidonic acid, 12 HPETE, 5-HETE and leukotriene B₄, are agonists of the TRPV1 receptor (Hwang *et al.*, 2000). It is speculated that AEA could either function as an arachidonic acid donor through its metabolism by FAAH, or through direct metabolism by LOX to produce metabolites that subsequently activate TRPV1 receptors. It may also compete with arachidonic acid for metabolism by LOX, and therefore would reduce the arachidonic acid derived LOX metabolites.

1.5.3.4 CYP450

Aside from the two oxygenation pathways previously described there is also evidence that AEA can be metabolised by the cytochrome P450 (CYP450) superfamily of enzymes. In the mouse, AEA was metabolised into at least 20 different polar lipids by CYP450 (Bornheim *et al.*, 1995).

Anandamide metabolism



2-AG metabolism

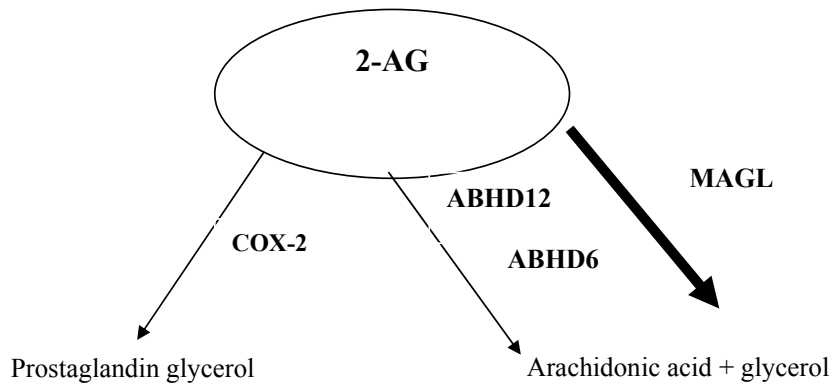


Figure 1.6 The metabolic pathways for both AEA and 2-AG. Thick arrows represents dominant pathway.

1.5.4 2-AG metabolism

2-AG metabolism has not been studied as extensively as AEA metabolism; however the key enzyme involved is thought to be the cytosolic enzyme monoacylglycerol lipase (MAGL), after findings that over expression of MAGL in rat neurones reduced accumulation of 2-AG (Dinh *et al.*, 2002). Other enzymes including FAAH, neuropathy target esterase (NTE) and hormone sensitive lipase (HSL) are also thought to metabolise 2-AG. A recent study was directed at investigating the importance of these enzymes and identifying the dominant metabolic pathway. It was found that 85% of the hydrolysis of 2-AG was mediated by MAGL, the majority of the remaining 15% of activity was discovered not be due to either NTE or HSL but to two previously uncharacterised enzymes ABHD12 and ABHD6. The same study also demonstrated that in the brain these three enzymes exhibited different distribution suggesting that these enzymes have access to their own supply of 2-AG (Blankman *et al.*, 2007). It is also suggested that ABHD12 and ABHD6 may be responsible for the metabolism of 2-AG in cells lacking MAGL such as microglial cells (reviewed in Blankman *et al.*, 2007).

Like AEA, 2-AG can also be metabolised by COX-2, however 2-AG is metabolised much more efficiently. The major metabolite produced following 2-AG metabolism by COX-2 is PGH₂ glycerol ester (PGH₂G) as yet the biological significance of this molecule is elusive (Kozak *et al.*, 2000, 2001). The metabolism of 2-AG is summarised in Figure 1.6.

1.5.5 Anandamide accumulation and transport

In order for endocannabinoids to be metabolised they must first enter the cells, the mechanism/s by which AEA accumulates in cells is highly controversial. One finding that researchers in the field do agree on is that the process of AEA uptake is saturable (Reviewed in Hillard *et al.*, 2000); however the cellular component that is being saturated is still open to debate. The four proposed mechanisms of AEA accumulation are; (i) facilitated diffusion, (ii) uptake by means of a transporter/carrier protein, (iii) cellular sequestration and (iv) AEA uptake via lipid rafts.

1.5.5.1 Facilitated diffusion

Experimental evidence has shown that in FAAH expressing neuroblastoma cells AEA uptake is reduced by 50% in the presence of a FAAH inhibitor (MAFP) (Deutsch *et al.*, 2001). This is consistent with findings from HeLa cells, which, when transfected with FAAH demonstrated a 2 fold increase in AEA uptake (Day *et al.*, 2001). The demonstrable importance of FAAH in AEA

accumulation leads to the speculation that FAAH functions to provide an inward concentration gradient, to facilitate diffusion across the membrane (Reviewed in McFarland *et al.*, 2004; Hillard *et al.*, 2003). It has been shown in neuroblastoma cell lines that AEA uptake is entirely dependent on FAAH, and that no other process is involved; this conclusion was based on the fact that many of the AEA transport inhibitors also inhibit FAAH (Glaser *et al.*, 2003). In this proposed mechanism of AEA uptake FAAH is the saturable component.

As an argument against this proposed mechanism, it has been pointed out that the FAAH inhibitor used in the studies mentioned above (MAFP) is structurally similar to AEA and may in fact be inhibiting AEA accumulation. This is supported by findings that a second FAAH inhibitor PMSF, which is not structurally similar to AEA, failed to inhibit AEA uptake (Day *et al.*, 2001). Further evidence against this mechanism of uptake has come from FAAH knockout mice; these retained saturable accumulation of AEA although it was reduced compared to wild type mice (Ligresti *et al.*, 2004). It has also been shown that FAAH knockout mice and their wild type counterparts exhibit temperature sensitive, rapid, saturable uptake of AEA that can be inhibited by AM404 and AM1172, a compound that does not inhibit FAAH (Fegley *et al.*, 2004). Therefore, it can be seen that although FAAH plays a role in the uptake of AEA in some experimental preparations, it is unlikely that this is the sole mode of AEA uptake into cells. While AEA would have the capabilities of simply diffusing across the membrane it is thought that this process would be too slow to account for the rapid accumulation of AEA (McFarland *et al.*, 2004).

1.5.5.2 Transporter mediated uptake

Structure activity studies have led to the hypothesis that AEA is transported across the membrane by a carrier which is stereoselective (Melck *et al.*, 1999; Piomelli *et al.*, 1999). In support of this it has been found that cerebellar granule neurones exhibit trans flux coupling for AEA. Trans flux coupling is indicative of bidirectional carriers, it occurs when carrier proteins (which have only one binding site) have their binding sites on the *trans* side of the membrane, despite accumulation of substrate on the *cis* side of the membrane, effectively transporting compounds against their concentration gradient (Hillard *et al.*, 2000; Hillard *et al.*, 2003). AM404 has been identified as an AEA transport inhibitor although it is also a FAAH inhibitor (Beltramo *et al.*, 1997; Jarrahian *et al.*, 2000). AM404 has been found to inhibit AEA efflux (Beltramo *et al.*, 1997), thus if AM404 was functioning through inhibition of FAAH then it would be expected that the rate of AEA efflux would increase as opposed to decrease, supporting an independent role of AM404, possibly at the proposed carrier protein (Beltramo *et al.*, 1997; Hillard *et al.*, 2003; McFarland *et al.*, 2004). In support of this it has also been found

that AM404 demonstrates competitive inhibition of AEA uptake (Rakhshan *et al.*, 2000). Despite this mounting evidence in support of an AEA transporter research has focused on neurones and endothelial cells, whether this proposed transporter exists in the majority of cell types remains to be investigated.

1.5.5.3 Cellular sequestration

In further disagreement with facilitated diffusion as a mechanisms of AEA transport, it has been suggested that AEA concentration in cells is much greater than in the extracellular media (Hillard *et al.*, 2000; from Hillard 2003). It was found that cerebellar granule neurones possessed a concentration of AEA that was a thousand times greater than that of the extracellular media (Hillard *et al.*, 2000). Similar findings were also observed in RBL-2H3 cells and N8 neuroblastoma cells (Rakhshan *et al.*, 2000; Deutsch *et al.*, 2001). As there is no evidence for an active process transporting AEA against its concentration gradient, it is suggested that only some of the intracellular AEA is free and in equilibrium with extracellular AEA, and that the remainder of the AEA is being “sequestered or bound” (Hillard *et al.*, 2003). Two possible explanations have been put forward to explain this, the first being that AEA is contained within membranous compartments which would have the potential to become saturated (McFarland *et al.*, 2003). The second that AEA is bound to an intracellular protein that functions to move AEA between cellular compartments (Stremmel *et al.*, 2001). The binding of AEA to binding proteins would keep in line with the saturable nature that has been established for AEA uptake.

1.5.5.4 Endocytotic uptake

The final proposed mechanism of AEA uptake is by means of endocytosis. It has been suggested that one of the ways by which cells sequester AEA is by maintaining it in membranous compartments. To expand on this, it has been put forward that AEA may be taken up into cells by caveolae-related endocytosis (McFarland *et al.*, 2004). Lipid rafts are areas in the plasma membrane that are enriched with cholesterol, sphingolipids, and arachidonic acid (Brown *et al.*, 2000; Pike *et al.*, 2002), caveolae are similar in composition to lipid rafts and found as invaginations in the plasma membrane (Pike *et al.*, 2002). It has been suggested that caveolae or lipid rafts may function to transport AEA into cells (McFarland *et al.*, 2004; 2005). RBL-2113 cells (mast cells) have been shown to accumulate AEA; treatment of these cells with inhibitors of caveolae mediated endocytosis, resulted in a 50% reduction in AEA uptake

(McFarland *et al.*, 2004). To add support to this, it was found that fluorescently labelled AEA co-localised with caveolin-1 and flotillin-1 (markers for caveolae and lipid rafts Muthian *et al.*, 2000). It is suggested that within the lipid rafts/caveolae there are binding proteins or carriers for AEA, this would satisfy the required saturable component that has been established for AEA uptake (McFarland *et al.*, 2005). This proposed mechanism of uptake would allow the transport of AEA to FAAH where it would be metabolised and thereby make the binding proteins available. This supports the theory that AEA uptake is mediated by, but not reliant upon FAAH (McFarland *et al.*, 2005).

Therefore, it can be seen that despite extensive research into this area, no definitive mechanism of uptake of AEA has yet been established. Valid evidence supports each mechanism described above, so it may be that they are all involved in the uptake of AEA or perhaps some mechanisms are cell specific (for example uptake mediated by a transporter). Further research is also required to explain some pieces of evidence that cannot be explained by mechanisms put forward so far, for example the finding that NO increases AEA accumulation in endothelial cells and human mast cells (Maccarrone *et al.*, 2000a and b).

1.6 Cannabinoid action at vanilloid, non cannabinoid, and novel receptors

1.6.1 Vanilloid receptors

Vanilloid receptors (TRPV1) are members of the transient receptor potential (TRP) channels; they are non selective cation channels primarily located on primary afferent fibres (Benham *et al.*, 2002; reviewed recently in Starowicz *et al.*, 2007). Vanilloid receptors are activated by capsaicin, resiniferatoxin (RTX) and noxious stimuli such as heat and acid. Similarities in chemical structure between AEA and capsaicin, and the finding that AEA could activate vanilloid receptors led to the proposition that AEA was in fact an endovanilloid (Zygmunt *et al.*, 1999; 452; Di Marzo *et al.*, 2001).

AEA activates TRPV1 in a manner that can be inhibited by TRPV1 receptor specific, but not CB receptor, antagonists. Pre-treatment with capsaicin (to render vanilloid receptors inactive) also abolishes any effect of AEA (Ross, 2003). AEA has a similar affinity for TRPV1 to capsaicin however it has a much lower potency, and whether AEA is a full or partial agonist at vanilloid receptors varies between tissues (reviewed in Ross 2003). Interestingly AEA has been found to exhibit low intrinsic activity at the TRPV1 receptor, which means that AEA will attenuate the effects of a full agonist. This has been observed in neurones where the combined addition of AEA and capsaicin resulted in a reduction of the effects of capsaicin (Roberts *et al.*,

2002; Ross. 2003). As vanilloid receptors are involved in inflammatory pain, it raises the possibility that AEA may function to inhibit this process via these receptors.

The low intrinsic activity of AEA at vanilloid receptors has called the physiological relevance of AEA acting at vanilloid receptors into question. However research has shown that many environmental conditions can increase the efficacy of AEA at vanilloid receptors. For example increased receptor expression in conditions of disease (Szallasi *et al.*, 2002; Di Marzo *et al.*, 2002), the production of LOX metabolites that function as TRPV1 agonists (Hwang *et al.*, 2001; Craib *et al.*, 2001; Ross. 2003), receptor sensitisation by phosphorylation (Di Marzo *et al.*, 2002) and the presence of an AEA biosynthesis by-product (PEA) that enhances the affinity and potency of AEA at vanilloid receptors (De Petrocellis *et al.*, 2001; Smart *et al.*, 2002; reviewed by Ross 2003).

1.6.2 PPARs

Peroxisome proliferator-activated receptors (PPARs) are a family of nuclear receptors that exist in three isoforms α , γ and δ . These receptors dimerise with the retinoid X receptor to bind to DNA sequences called PPAR response elements, these then initiate the transcription of target genes following activation. PPARs are involved in the regulation of metabolism, energy homeostasis and inflammation (Reviewed Moraes *et al.*, 2006; Rizzo *et al.*, 2006; Bensinger *et al.*, 2008). PPAR α is found in the heart and liver and is involved in fatty acid catabolism and inflammation (Stienstra *et al.*, 2007). PPAR γ is involved in insulin sensitivity and inflammation (Stienstra *et al.*, 2007; Fievet *et al.*, 2006) and PPAR δ whose function was unknown until quite recently, is now thought to function by regulating metabolism (Barish *et al.*, 2006). PPARs are also found in the CNS (Moreno *et al.*, 2004). Due to the large binding site present on PPARs they have the capability of binding many substances, including fatty acids and eicosanoids (O' Sullivan. 2007).

Endocannabinoid involvement with PPARs first became evident when it was found that a LOX produced metabolite of 2-AG could activate PPAR α (Kozak *et al.*, 2002). PEA (as described previously) is synthesised alongside AEA, PEA has been found to activate PPAR α and subsequently produce anti inflammatory and analgesic actions (Lo Verme *et al.*, 2005; Lo Verme *et al.*, 2006). Anandamide, virodhamine and noladin ether have also been shown to activate PPAR α (Sun *et al.*, 2006). Similarly, AEA can also bind to and activate PPAR γ , it is through this receptor that AEA inhibits production of IL-2 (Bouboula *et al.*, 2005; Rockwell *et al.*, 2004). 2-AG has also been shown to activate PPAR γ (Bouboula *et al.*, 2005). The effects of endocannabinoids on PPAR δ have not been investigated to the same extent; however, one study

has shown that if PPAR δ receptors are silenced an increase in CB₁ receptor expression is observed; the reverse of this is seen if CB₁ receptors are silenced, when an increase in PPAR δ expression is observed (Yan *et al.*, 2007).

1.6.3 Novel Receptors

As discussed above, endocannabinoids/cannabinoids have been shown to be active at the CB₁ and CB₂ receptors, vanilloid receptors, and PPARs, however these receptors do not account for all cannabinoid mediated effects. There is substantial evidence supporting the existence of at least two other receptors (i) the endothelial CB_x receptor/AEA receptor/abnormal cannabidiol receptor and (ii) the orphan receptor GPR55.

The first indication that a novel cannabinoid receptor may exist came from studies in the rat mesenteric arterial bed. It was found that both AEA and its metabolically stable analogue produced a long lasting vasodilatory effect that was not mimicked by other synthetic cannabinoids (Wagner *et al.*, 1999). Further research demonstrated that the CB₁ receptor antagonist SR141716A could inhibit this vasodilatation but only at much higher concentrations than would be required to antagonise CB₁ (Jarai *et al.*, 1999; Wagner *et al.*, 2001; White *et al.*, 2001). The antagonistic effect of SR141716A was found to be endothelium dependent, as the effect was abolished following endothelial denudation. This led to the hypothesis that a novel endothelial cannabinoid receptor exists (Jarai *et al.*, 2002; Wagner *et al.*, 2001). This putative receptor is also thought to be present in the rat coronary circulation (Ford *et al.*, 2002). Abnormal cannabidiol is a structural analogue of cannabidiol (a non psychotropic phytocannabinoid), and has been found to be a specific agonist at this CB_x receptor. It demonstrates an endothelium dependant, CB₁ and CB₂ independent relaxation, which is antagonised by high concentrations of SR141716A and unaffected by the vanilloid receptor antagonist capsazepine (Jarai *et al.*, 1999; Offertaler *et al.*, 2003). The previous finding that AEA relaxation in the mesenteric artery is mediated by vanilloid receptors suggests a possible interplay between the CB_x receptors and vanilloid receptors in the response to AEA (Jarai *et al.*, 1999; Begg *et al.*, 2005). This is supported from findings in the rabbit aorta, where AEA produced a vasodilatation that was primarily endothelium dependent (antagonised by SR141716A) but also demonstrated a residual relaxation that was endothelium independent which was antagonised by vanilloid receptor antagonists (Mukhopadhyay *et al.*, 2002).

1.6.4 GPR55

GPR55 is an orphan G protein coupled receptor that has been put forward as a novel cannabinoid receptor (Reviewed in Baker *et al.*, 2006; and Brown, 2007; Ross 2009). Despite this receptor receiving much attention, its role as a cannabinoid receptor remains controversial. GPR55 shares only 13.5% and 14.4% homology with CB₁ and CB₂ receptors respectively, and its reported receptor expression is much lower than that of the established CB receptors (Ryberg *et al.*, 2007). GPR55 receptor mRNA has been located both in the brain and the periphery and has been suggested to be present in certain vascular beds (Baker *et al.*, 2006). It was initially questioned whether the CB_x receptor (described previously) and GPR55 were one and the same; however research has shown this not to be the case (Johns *et al.*, 2007).

The ability of endogenous cannabinoids to activate GPR55 is contentious, depending on the marker of activation and the cell type (reviewed in Ross 2009). Both AEA and 2-AG show no effect on ERK phosphorylation (a chosen marker of GPR55 activation) in GPR55 expressing cells (Oka *et al.*, 2007). In some cases AEA has been shown to activate GPR55 at concentrations greater than 5µM and 10µM. These are far greater than would be observed either physiologically or pathologically and are much higher than would be required to activate CB receptors (Lauckner *et al.*, 2008; Ryberg *et al.*, 2007; Ross. 2009). Despite the controversy over the ability of endocannabinoids to activate GPR55 a likely candidate for an endogenous ligand of this receptor has been identified. Lysophosphatidylinositol (LPI) has been shown convincingly to activate GPR55 (Oka *et al.*, 2007; Henstridge *et al.*, 2009), while it is not thought to bind to cannabinoid receptors. The synthetic analogue of cannabidiol, 0-1602, has also been shown to activate GPR55, however in GPR55^{-/-} knockout mice this ligand still elicited a functional vasodilatory effect (Johns *et al.*, 2007).

1.7 Cannabinoid receptor signalling

Cannabinoid signalling, like all other aspects of cannabinoid pharmacology is extremely complex. There are four main mechanisms of signalling which cannabinoid receptors are believed to regulate, these are: (i) adenylate cyclase (ii) MAP kinase (iii) ion channels and intracellular Ca²⁺ concentration.

1.7.1 Adenylate cyclase

Early studies into the signalling pathways of the CB₁ receptor established that in neuroblastoma cells, CB₁ signals through the G_{i/o} family of PTX sensitive G proteins resulting in the inhibition of adenylate cyclase and in the reduction of cAMP production (Howlett *et al.*, 1984; Howlett *et al.*, 1986). This signalling mechanism was also confirmed in CHO cells (Matsuda *et al.*, 1990). CB₁ mediated inhibition of adenylate cyclase has also widely been demonstrated in brain slices (Bidaut-Russell *et al.*, 1990). In contrast to this, some experimental results have demonstrated that CB₁ receptor activation can result in an increase in adenylate cyclase activation, and thus an increase in cAMP (Glass *et al.*, 1997; Busch *et al.*, 2004). CB₂ receptor activation, on the other hand is thought to result purely in an inhibition of adenylate cyclase, and therefore in a reduction in cAMP (Glass and Felder *et al.*, 1997; Demuth *et al.*, 2006).

1.7.2 Cannabinoid modulation of ion channels and Ca²⁺ concentration

Cannabinoids can also signal through the modulation of a variety of ion channels, including the inward rectifying K⁺ channel, and L, N, P and Q voltage gated Ca²⁺ channels. It is thought that it is through modulation of these ion channels that cannabinoid inhibition of neurotransmitter release occurs at presynaptic terminals (Reviewed in Howlett *et al.*, 2002; Demuth *et al.*, 2006). Due to their activity at Ca²⁺ channels, cannabinoids are thought to be important regulators of intracellular Ca²⁺ concentration. In human arterial endothelial cells AEA produces an increase in Ca²⁺ by opening intracellular stores. It has been hypothesised that one of the ways in which AEA produces vasodilatation is by increasing intracellular Ca²⁺ concentration, resulting in an increase in NO release and subsequent vasodilatation (Fimiani *et al.*, 1999; Demuth *et al.*, 2006).

Research has also been undertaken to understand the signalling mechanisms of the endothelial AEA/abnormal cannabidiol/CB_x receptor. In a similar fashion to the established cannabinoid receptors, the CB_x receptor is thought to couple to G_{i/o} receptors and activate P42/44 MAP kinase and PKB/Akt (Offertaler *et al.*, 2003). The CB_x receptor is also thought to elicit its vasodilatory effect through PKG activation of BK_{Ca} (Begg *et al.*, 2003).

The orphan receptor GPR55 signals through different signalling pathways compared to the cannabinoid receptors. GPR55 is coupled to Gα₁₃ which upon activation stimulates RhoA, cdc42, and rac (Ryberg *et al.*, 2007). Other downstream targets of GPR55 receptor activation remain controversial and are reviewed in (Ross 2009).

1.7.3 MAPK

The MAP kinase pathway is possibly one of the most important cellular signalling pathways, regulating many cellular activities such as proliferation, migration and cell death (discussed in detail in section 1.1.5). CB₁ receptors have been shown to activate MAPK (p38) in CHO and HUVEC cells (Rueda *et al.*, 2000; Liu *et al.*, 2000). Similarly, in astrocytes and CHO cells CB₁ receptor activation activates p42/p44 MAP kinase (Bouaboula *et al.*, 1995; Galve-Roperh *et al.*, 2002). CB₂ receptors appear to signal through MAPK in a fashion comparable to CB₁, showing activation of p42/p44 MAP kinase in both CHO and HL-60 cells expressing CB₂ (Bouaboula *et al.*, 1996; Kobayashi *et al.*, 2001). It is not clear how cannabinoid receptors activate MAP kinase however two mechanisms have been suggested. The first is that cannabinoid receptor activation results in the activation of PI3K which through tyrosine phosphorylation activates Raf; it is also suggested that PI3K activates PKB/Akt which in turn activates MAPK (Gomez del Pulgar *et al.*, 2000; Galve-Roperh *et al.*, 2002). The second proposed pathway by which cannabinoid receptors can activate MAPK is through the actions of the second messenger ceramide. Ceramide is a sphingolipid second messenger important in the regulation of cell fate. Changes in ceramide concentration can make the decision between cell survival and cell death. It is also suggested that inhibition of PKA induced by CB receptors may lead to MAP kinase inhibition. (Sanchez *et al.*, 1998 54;834; Galve-Roperh *et al.*, 2000 ; Demuth *et al.*, 2006).

1.8 Cellular effects of cannabinoids

Cannabinoids can activate a variety of regulators of cellular function including ERK, c-jun and p38 MAPK, AKT/PKB, PKA and ceramide (Wartmann *et al.*, 1995; Liu *et al.*, 2000; Rueda *et al.*, 2000; Gomez del Pulgar *et al.*, 2000; GalveRoperh *et al.*, 2000). This evidence strongly suggests that cannabinoids can influence cellular behaviour. Indeed evidence already supports cannabinoid involvement in cell proliferation, apoptosis and cytoprotection. To date the vast majority of information regarding the influence of cannabinoids on cellular function has come from studies with neuronal cells or with cancer cell lines.

1.8.1 Cannabinoids and apoptosis

Cannabinoids have been shown to induce apoptosis in a wide variety of cancer cell lines (Reviewed in Guzman *et al.*, 2002). Moreover, in one *in vivo* study, rats with malignant gliomas that were treated with Δ^9 -THC survived longer than control rats; in addition 20-35% of the animals demonstrated complete eradication of the tumours (Galve-Roperh *et al.*, 2000; Sanchez

et al., 2001). Investigations into the cellular mechanisms by which cannabinoids induce apoptosis have confirmed a role for sustained ceramide production and subsequent sustained activation of ERK; production of superoxide which resulted in activation of caspases 3; and raised intracellular Ca^{2+} , inducing mitochondrial disruption, cytochrome C release, and activation of caspases (Galve-Roperh *et al.* 2000, Mimeault *et al.*, 2003; reviewed in Guzman *et al.*, 2002). For example in colorectal cancer cells Δ^9 -THC induced apoptosis through CB_1 receptor mediated inhibition of the Ras-MAPK pathway and PI3K-Akt pathways (Greenhough *et al.*, 2007).

1.8.2 Cannabinoids and cell proliferation

The effects of cannabinoids on cell proliferation are extremely complex and contradictory, with both antiproliferative and pro-proliferative effects being reported. In a human breast cancer cell line, AEA demonstrated an antiproliferative effect which was attributed to CB_1 receptor mediated blockade of the G1-S transition phase, thought to be the result of decreased availability of PKA and sustained activation of the ERK signalling cascade (De Petrocellis *et al.*, 1998; Melck *et al.*, 1999). Similarly, anti proliferative effects of cannabinoids have been reported in other cell lines including prostate cancer cell lines (Mimeault *et al.*, 2003, Reviewed in Bifulco *et al.*, 2006; Guzman *et al.*, 2002; Parolaro *et al.*, 2002). In contrast to this, cannabinoids have also been shown to exhibit stimulatory effects on cell proliferation. For example Hart *et al.*, 2004, demonstrated a stimulatory effect of AEA, HU-210 and WIN55,212-2 on MAP kinase activity and Akt, they also showed a direct stimulatory effect of Δ^9 -THC (nM) on DNA synthesis. This is a complete contradiction to previous findings where Δ^9 -THC was shown to induce cell death, however in those studies Δ^9 -THC was used at micromolar concentrations. Therefore this clearly indicates that cannabinoid concentration influences the cellular decision between proliferation and growth arrest.

1.8.3 Cannabinoids and Migration

The effects of cannabinoids on cell migration have been studied primarily in immune cells. An anti-inflammatory role for cannabinoids has been suggested since 1974, when it was discovered that Δ^9 -THC elicited an inhibitory effect on the migration of leukocytes (Schwartzfarb *et al.*, 1974). Low concentrations of Δ^9 -THC have also been shown to inhibit the migration of macrophages in response to monocyte chemoattractant protein-1 (Steffens *et al.*, 2005). In contrast, studies investigating the endogenous cannabinoid 2-AG have shown it to induce the

migration of human monocytic cells (Kishimoto *et al.*, 2003) and microglia, an effect that was abolished by an inhibitor of ERK phosphorylation and an antagonist of the putative abnormal cannabidiol receptor (Walter *et al.*, 2003). 2-AG has also been shown to induce directional migration of B lymphocytes in a CB₂ dependant manner (Jorda *et al.*, 2002) and to regulate CB₂ mediated migration of myeloid leukaemia cells (Jorda *et al.*, 2002). Intriguingly AEA does not share the pro-migratory profile of 2-AG. AEA only weakly stimulates migration of microglial cells and elicits only 20% of the migratory response produced by 2-AG in a leukaemia cell line (Walter *et al.*, 2003; Jorda *et al.*, 2002). The poor ability of AEA to stimulate immune cell migration has been attributed to the finding that AEA only weakly activates the CB₂ receptor (Hillard *et al.*, 1999). Interestingly 2-AG was found to have no effect on human neutrophil migration whereas both AEA and virodhamine (another endogenous cannabinoid) have both been shown to inhibit migration of these cells (McHugh *et al.*, 2007).

1.9 Cannabinoids and inflammation

The anti-inflammatory effects of Δ^9 -THC have been recognised since the 1970s (reviewed in Berdyshev, 2000), since then the effects of cannabinoids on various individual immune cells have been studied intensively. Cannabinoid receptors have been located on a wide variety of immune cells, despite the presence of both CB receptors, the CB₂ receptor is more highly expressed (reviewed in Croxford *et al.*, 2005)

Macrophages are pivotal in the inflammatory response, they are the first line of defence and are responsible for the release of inflammatory mediators such as NO, TNF α , IL-1 and IL-6. It has been shown both *in vivo* and *in vitro* that administration of cannabinoids can inhibit macrophage activation following inflammatory stimuli (reviewed in Berdyshev *et al.*, 2000). An essential function of macrophages is to produce NO. It has been demonstrated that one mechanism by which cannabinoids can inhibit macrophages is through the inhibition of NO production. In a macrophage cell line cannabinoids inhibited LPS stimulated NO production a process which involved the CB₂ receptor (Ross *et al.*, 2000). The endogenous cannabinoid AEA was also shown to inhibit NO in a macrophage cell line, although interestingly it was found that 2-AG enhanced NO production, a finding attributed to 2-AG functioning as an arachidonic acid donor (Chang *et al.*, 2001). Evidence also supports the idea that cannabinoids have an inhibitory effect on TNF α , IL-6 release and can inhibit phagocytosis (Reviewed in Croxford *et al.*, 2005).

Cannabinoids have also been shown to affect lymphocytes, AEA can inhibit both T and B cell proliferation and induce apoptosis (reviewed in Klein *et al.*, 1998), however experiments have also shown that the effect of cannabinoids on lymphocytes is complex and may depend on the

concentration of the cannabinoid agent. For example, in human B cells, nM concentrations of CP55940, WIN55212-2, and Δ^9 -THC increased DNA synthesis (Derocq *et al.*, 1995). T cells produce two groups of inflammatory cytokines the Th1 group (IFN γ , TNF α), and the Th2 group (IL-4, IL-5). Evidence conflicts as to the effects of cannabinoids on these cytokines, with studies showing both stimulatory and inhibitory effects (reviewed in Croxford *et al.*, 2005; Klein *et al.*, 2000).

Similar contradictory effects are observed following cannabinoid treatment of polymorphonuclear neutrophils (PMNs). Kraft *et al.*, 2004 reported that CP55940 (μ M range) elicited a suppressive effect on stimulated PMNs resulting in reduced production of oxygen radicals as well as the recruitment of activated PMNs. This report implicated a mechanism of action independent of the CB receptors, the same study found a negligible role of AEA and meth-AEA on PMN's. In contrast, a more recent study from the same group documented a stimulatory effect of meth-AEA and CP55940 when the concentration of these agents was in the nM region (Kraft *et al.*, 2005).

1.10 Cardiovascular effects of cannabinoids

It is well established that cannabinoids can elicit functional effects on the cardiovascular system. Indeed, people who smoke marijuana most commonly develop peripheral vasodilatation and tachycardia, effects which culminate in an increase in peripheral blood flow, an increase in cardiac output, and changes in blood pressure (Hillard *et al.*, 2000). In anaesthetised animals, administration of Δ^9 -THC produces a short pressor response followed by a long lasting hypotensive effect (reviewed in Hillard 2000). When AEA is applied to anaesthetised animals a triphasic response is observed: phase I, bradycardia with a short lasting hypotension, phase II, a vasopressor response, and phase III, a sustained hypotensive effect (Varga *et al.*, 1995,1996). It was originally hypothesised that cannabinoids/endocannabinoids produced their effects on the cardiovascular system by acting centrally; however current evidence suggests that whereas some effects may be mediated centrally the majority result from actions on the peripheral nervous system and directly from the vasculature (Reviewed in Pacher *et al.*, 2005; Hillard *et al.*, 2000; Randall *et al.*, 2002). Regarding the three phases of the AEA response, it is thought that the initial bradycardia and associated hypotension is vagally mediated, while the sustained hypotensive effect (phase III) has been attributed to peripheral CB₁ receptor activation which is thought to induce presynaptic inhibition of sympathetic outflow (Varga *et al.*, 1995,1996; Lake *et al.*, 1997 Randall 2002). In contrast the pressor response (phase II) is not fully understood, although it has been shown to be independent of central, peripheral, and CB₁ receptors (Varga *et al.*, 1996; Lake *et al.*, 1997) but may involve β_2 adrenoreceptors and NMDA receptors

(Kwolek *et al.*, 2005). Whether or not AEA produces a triphasic response has been questioned, in contrast to studies performed in urethane-anaesthetised rats, rats under pentobarbitone anaesthesia lacked the phase II pressor response (Kwolek *et al.*, 2005). To add further confusion to the *in vivo* effects of AEA, when AEA is administered to conscious animals quite different responses are observed and include a bradycardic response followed by a sustained pressor response that is unaffected by AM251 (Gardiner *et al.*, 2002; Stein *et al.*, 1996). In contrast, AEA administered to conscious mice produced an initial depressor response followed by a sustained hypotension, effects that were absent in CB₁ knockout mice (Ledent *et al.*, 1999).

Despite the confusion and controversy over the effects of AEA *in vivo*, substantial evidence unarguably demonstrates that AEA can act directly on the vasculature. Although there is consensus on the direct vascular effect of AEA, the underlying mechanism varies between species and even between vessels of the same species (Reviewed in Randall *et al.*, 2004, 2002). The effects of AEA on the vasculature have been most extensively studied in the rat; using this one species as an example will highlight the variability in AEA responses. The rat mesenteric artery, coronary artery, aorta and hepatic artery (O'Sullivan *et al.*, 2004; Zygmunt *et al.*, 1999) all dilate in response to AEA; however the rat carotid artery does not respond (Holland *et al.*, 1999). The vasodilatory response also varies in magnitude between vessels, the rat coronary artery relaxes around 50% in response to AEA (Pratt *et al.*, 1998; White *et al.*, 2001) whereas the aorta undergoes a maximum relaxation of 20% (O'Sullivan *et al.*, 2004). Further variability arises in the receptors involved in the AEA response, in the rat mesenteric artery vanilloid receptors are implicated, where as in the rat coronary artery and smaller mesenteric arteries a novel endothelial cannabinoid receptor is thought to be involved. Other factors which add to the complex pharmacology of the AEA response include endothelial dependence/independence, the production of active metabolites, and the involvement of ion channels (summarised in Table 1.1).

Aside from AEA other endocannabinoids have been shown to be vasoactive; 2-AG has been shown to relax mesenteric arterial segments through an endothelium independent mechanism (Kagota *et al.*, 2001). Similarly, virodhamine has been shown to relax the small mesenteric artery of the rat, it is believed to activate the putative endothelial CB_x/anandamide receptor (Ho *et al.*, 2004).

These extensive research findings characterising the effects of AEA on the vasculature raise the question as to the physio/pathological purpose of endocannabinoids in the vasculature. One area that has received substantial attention is that endocannabinoids may be produced to combat shock. In a rat model of haemorrhagic shock it was found that activated macrophages produced

Artery	Is AEA a vasodilator	Endothelium dependant	CB ₁ receptor mediated	Vanilloid receptor mediated	Due to production of metabolites	Involves other mechanism	Reference
Rat aorta	Yes	No	No	No	No	-	O'Sullivan <i>et al.</i> , 2005
Rat Superior mesenteric	Yes	No	Yes	Yes	No	-	O'Sullivan <i>et al.</i> , 2004
Rat mesenteric resistance artery	Yes	Yes	Yes	Yes	No	Yes	O'Sullivan <i>et al.</i> , 2004 Zygmunt <i>et al.</i> , 1999
Rat carotid artery	No	No	No	No	No	-	Holland <i>et al.</i> , 1999
Rat coronary artery	Yes	No	No	No	No	Yes	White <i>et al.</i> , 2001
Rat hepatic artery	Yes	No	No	Yes	No	-	Zygmunt <i>et al.</i> , 1999
Sheep coronary artery	Yes	Partial	No	No	Yes	Yes	Grainger <i>et al.</i> , 2001
Rabbit aorta	Yes	Partial	Possible	Partial	-	Yes	Mukhopadhyay <i>et al.</i> , 2002
Bovine coronary	Yes	Yes	No	No	Yes	-	Pratt <i>et al.</i> , 1998

Table 1.1 Summarises a selection of studies that have investigated the effects of AEA on isolated vessels in different species, highlighting the variability between species and vessel.

AEA. A similar finding was also observed following endotoxic shock where the synthesis of 2-AG in platelets was increased (Wagner *et al.*, 1997; Varga *et al.*, 1998). These findings have been confirmed in human plasma samples, where it was found that plasma concentrations of both AEA and 2-AG were increased (Wang *et al.*, 2001). Whereas it is speculated that endocannabinoids may have a protective role in conditions of shock, in liver cirrhosis endocannabinoids are thought to have a negative effect. It has been shown that the vasodilatation observed in liver cirrhosis can be inhibited by a CB₁ antagonist, CB₁ receptor expression on endothelial cells was also found to be increased (Batkai *et al.*, 2001).

Endogenous cannabinoid concentration is increased during myocardial infarction (Wagner *et al.*, 2001). It has been found that CB₁ antagonism promoted left ventricular remodelling in rats that had suffered experimentally induced myocardial infarction (Wagner *et al.*, 2003). CB₁ antagonism also resulted in worsening of endothelial function (Wagner *et al.*, 2001) suggesting that endocannabinoids may play a protective role following myocardial infarction.

1.10.1 Cannabinoids and atherosclerosis

Cannabinoids have been shown to influence the progression of atherosclerosis. In 2005 Steffens *et al* demonstrated that oral administration of Δ^9 -THC significantly reduced atherosclerotic plaque progression in ApoE^{-/-} mice. Investigations revealed that this effect was due to CB₂ receptor mediated immunomodulatory effects on lymphoid and myeloid cells. This same study also showed the CB₂ receptor to be present in human and mouse atheroma, interestingly CB₂ receptors were not present in healthy arteries and the CB₁ receptor was not present in either diseased or healthy arteries. A CB₁ receptor antagonist has also been shown effective in limiting atherosclerosis. In LDLR^{-/-} mice rimonabant (SR141716A) exhibited a dose dependant inhibitory effect on atherosclerosis, an effect that was ascribed to cholesterol lowering and anti-inflammatory properties of rimonabant (Dol-Gleizes *et al.*, 2008). Another study confirmed a role of endocannabinoids in coronary artery disease, endocannabinoid concentrations were found to be increased in blood samples of patients with coronary artery disease, CB₁ receptor expression was increased in coronary atheroma and similarly anti-inflammatory effects of CB₁ blockade were observed (Sugamura *et al.*, 2008). The STRADIVARIUS clinical trial aimed to investigate the effectiveness of rimonabant on progression of coronary disease in patients with abdominal obesity and metabolic syndrome. The findings obtained in this trial revealed some favourable properties of rimonabant but the overall outcome was a non significant effect on percent atheroma volume (Nissen *et al.*, 2008). Therefore it can be seen that manipulation of the endocannabinoid system may be beneficial in the treatment of atherosclerosis, however further

development of agents that are devoid of adverse psychiatric effects would be required before these could be used again therapeutically.

1.11 Hypothesis

The development of restenosis following balloon angioplasty or insertion of a stent is a result of the combined effects of three key processes, increased smooth muscle cell proliferation, increased cell migration and the induction of an inflammatory response. It can be clearly seen from the literature that cannabinoid agents have the potential to influence all three of these fundamental processes. Cannabinoids have already been shown to limit atherosclerosis through their immunomodulatory effects (Steffens *et al.*, 2005), and also to inhibit stimulated smooth muscle cell proliferation *in vitro* (Rajesh *et al.*, 2008). What remains to be elucidated is the functional role of the endocannabinoid system in this disease. It has been well documented that endocannabinoid concentration increases in pathological conditions (Di Marzo 2008), however this has not been investigated in restenosis. If an increase in concentration were to occur, then understanding the functional effects of the endogenous cannabinoids (i.e. establishing if they exhibit negative or positive effects on disease progression) would be imperative to unmasking the potential of modulating the cannabinoid system for therapeutic gains, in terms of restenosis.

1.11.1 Objectives

The aim of this project was to investigate the role of the endogenous cannabinoids, AEA and 2-AG in the processes involved in a murine *in vitro* model of neointimal formation. The specific objectives were to

- develop a murine organ culture model of neointimal formation that would permit the investigation of endogenous cannabinoid concentration and allow the effects of cannabinoid agents on neointimal formation to be determined;
- establish a primary cell line of murine aortic smooth muscle cells;
- investigate the effect of AEA on murine vasculature and identify its mechanism of action;
- investigate the effects of cannabinoid agents on two indicators of cell proliferation, ERK1/2 phosphorylation and BrdU incorporation;
- establish the effect cannabinoid agents have on smooth muscle cell migration.

Chapter 2

General Methods

2.1 Animals

All mice were obtained as required from the Medical Research Facility (MRF) at Aberdeen University. Mice were either humanely euthanized within the MRF by CO₂ asphyxiation or cervical dislocation, or transported to Robert Gordon University (RGU) and kept in the holding facility until euthanasia by a schedule 1 method.

2.2 Small vessel myography

C57/B16J mice of either sex were euthanized by CO₂ asphyxiation and the aorta and carotid arteries dissected out (illustrated in Figure 2.1). The vessels were cleared of adherent tissue and placed in a Krebs solution of the following composition (mM): NaCl 118.4, NaHCO₃ 25, Glucose 11, KCL 4.7, KH₂PO₄ 1.2, MgSO₄ 1.2, and CaCL₂ 2.5. The arteries were then cut into rings of less than 2mm in length and mounted on to an Auto Dual Wire Myograph System model 510A (Danish Myograph Technology; Figure 2.2).

The mounting procedure involved insertion of two intra-luminal wires (40µm) which were then secured to the jaw heads by tightening the wire underneath the screws. The jaws in turn were connected to a force transducer which had been calibrated (prior to vessel mounting) as detailed in the manual.

The myograph baths (5ml) were filled with Krebs solution, aerated (20% O₂/5% CO₂) and maintained at 37°C. Once successfully mounted the vessels then underwent the classic normalisation procedure using the DMT Normalisation module (detailed in Chapter 3.3.1) to determine optimum resting tension (Danish Myo Technology 2003). Upon completion of this process the vessels were then left to equilibrate for 1hour, after which time they were sensitised by repeat (routinely 3-4) additions of 80mM KCl until consistent responses were obtained, the baths being washed out with fresh Krebs solution between each addition. The vessels were then left for between 30 and 45 minutes before experimentation began and subsequently between each experiment to allow time for the vessels to recover.

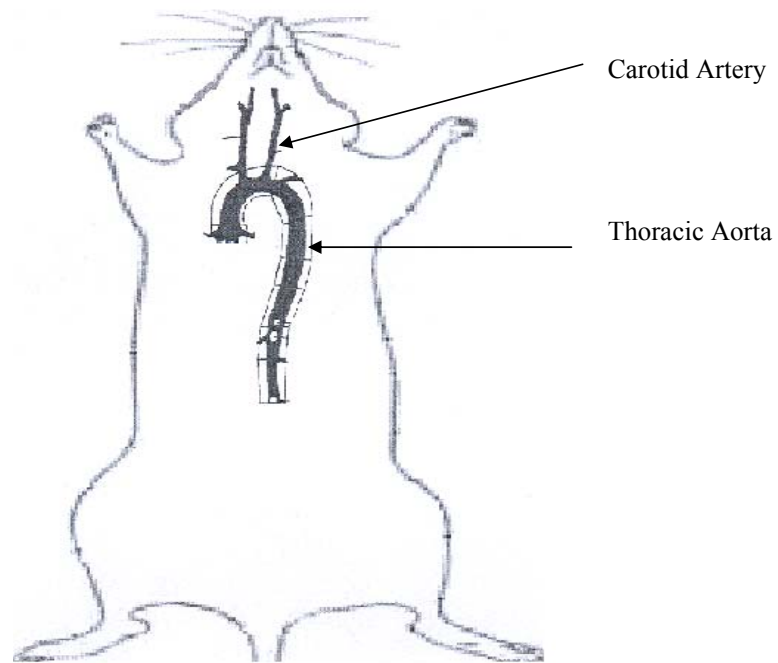


Figure 2.1 A schematic diagram illustrating the location of the murine carotid artery and thoracic aorta.

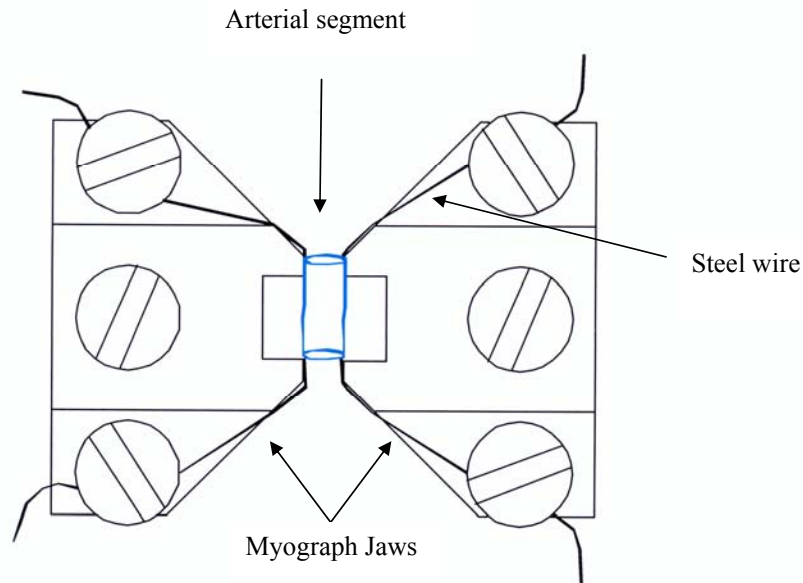


Figure 2.2 A schematic diagram of a mounted vessel segment for the Myograph 510A. The example shows an arterial segment mounted between two jaws secured with 40 μ m steel wire. Image adapted from M.J.Mulvany 2004.

2.3 Histological Staining

2.3.1 Fixing and tissue embedding

Mouse aortas were dissected and cut into rings as described above. The rings were submerged in 10% neutral buffered formalin for 2 days then transferred to phosphate buffered saline (PBS) until required. To begin the fixation process the aortic samples were placed in cassettes (Shandon microsette biopsy cassettes) then processed using an auto processor (Citadel 1000, Thermo Shandon, Cheshire, UK) through alcohol solutions, histosolve and paraffin wax as follows:

1. Alcohol (100%)	2 hours
2. Alcohol (100%)	2 hours
3. Alcohol/histosolve (50:50)	1 hour
4. Histosolve (100%)	1 hour
5. Histosolve (100%)	1 hour

6.Paraffin wax	2 hours
7.Paraffin wax	2 hours

Following this procedure the tissue was embedded in paraffin wax with the aid of a tissue embedding system (Histocentre 2, Thermo Shandon, Cheshire, UK). The resulting wax blocks were then cut into 5µm sections using a microtome (Finesse 325, Thermo Shandon). The wax sections were then floated out in a water bath (Thermo Shandon, Cheshire, UK) at 50°C and mounted on either basic glass slides (for standard histological staining) or polysine slides (for immunohistochemical staining). The slides were then placed in a section dryer (Thermo Shandon) for 2 hours at 70°C after which they were either stored for future use or allowed to cool to room temperature for immediate staining.

2.3.2.Haematoxylin and Eosin staining

Haematoxylin and Eosin are stains used to highlight the morphology of tissue sections; haematoxylin stains the nuclei of the cells blue where as the eosin stains the cytoplasm and other cellular areas red. To ensure consistency of staining, slides were stained using an autostainer (Varistain Thermo Shandon, Cheshire, UK) programmed with the following protocol.

1. HistoClear	5 mins
2. HistoClear	2 mins
3. HistoClear	2 mins
4. Absolute Alcohol	5 mins
5. Absolute Alcohol	4 mins
6. 70% Alcohol	3 mins
7. Distilled Water	1 min
8. Haematoxylin	1 min
9. Distilled Water	2 min
10.0.5% Acid Alcohol	1 min
11.Distilled Water	2 min
12.STWS	2 min
13.Distilled Water	2 min
14.Eosin	30 secs
15.Distilled Water	2 mins
16.Absolute Alcohol	2 mins

17.Absolute Alcohol	2 mins
18 Absolute Alcohol	2 mins
19.Histoclear	3 mins
20.Histoclear	3 mins
21.Histoclear	3 mins
22.Histoclear	3 mins

Upon completion of the staining process cover slips were applied using a Xylene substitute mountant (Thermo Shandon, Cheshire, UK) and left to air dry. Tissue analysis was performed using a Leica DMLB light microscope (Leica Microsystems, Bucks, UK). For analysis of tissue area, micrographs of the sections were taken using the Leica DC150 camera (Leica Microsystems, Bucks, UK) utilising the Leica QWin software. The micrographs were then analysed using ImageJ software which allowed calculation of specific areas of the cross section of blood vessel.

2.3.3 Massons Trichrome staining protocol

Massons trichrome is a stain that enables the differentiation between the cellular matter and connective tissue present in a section. Successful use of this stain results in cell nuclei appearing a blue/black colour, the cytoplasm staining red, and collagen staining blue.

1. Histoclear	5 min
2. Histoclear	2 min
3. Histoclear	2 min
4. Absolute Alcohol	5 min
5. Absolute Alcohol	4 min
6. 70% Alcohol	3 min
7. Distilled Water	1 min
8. Biebrich scarlet acid fuchsin solution	2 min
9. Distilled water	1 min
9. Distilled Water	1 min
10. phosphomolybdic-phosphotungstic acid solution	5 min
11. Aniline Blue Solution	1 min
12. Distilled water	1 min
13. Acetic acid	2 min
14. Distilled water	1 min
16.Absolute Alcohol	2 min
17.Absolute Alcohol	2 min

18 Absolute Alcohol	2 min
19.Histoclear	3 min
20.Histoclear	3 min
21.Histoclear	3 min
22.Histoclear	3 min

2.4 Immunohistochemical Staining

2.4.1 The Avidin-Biotin complex/ alkaline phosphatase (ABC/AP) procedure

The ABC/AP method is a procedure that allows the detection of specific antigens through light microscopy. The method is based on the high affinity that streptavidin has for a biotinylated secondary antibody which is directed against the primary antibody. The streptavidin has alkaline phosphatase attached to it which functions as an enzymatic label; this acts on a chromagenic substrate (the fast red solution) to produce a red colour which allows clear visualisation of the antigen of interest. This process is summarised in Figure 2.3.

Key:

▲ Biotin

X Streptavidin

● Alkaline Phosphatase

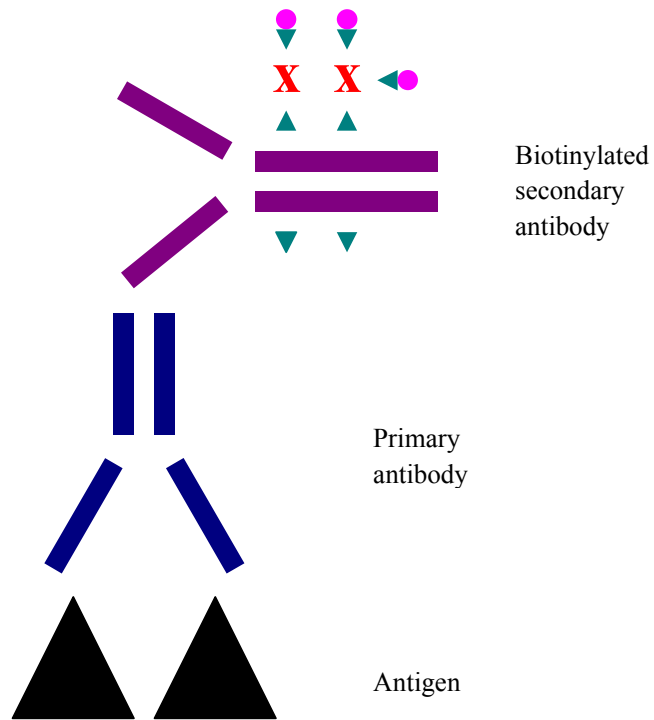


Figure 2.3. Schematic diagram demonstrating the streptavidin- biotin enzyme complex reacting with a biotinylated secondary antibody (adapted from *Immunochemical Staining Methods Handbook*, 3rd edition Dako Corporation)

2.4.2 Basic staining protocol

Sections were processed and cut as previously described in section 2.3.1, they were then deparaffinized and re-hydrated through histosolve and alcohol solutions.

1. HistoClear	5 mins
2. HistoClear	2 mins
3. HistoClear	2 mins
4. Absolute Alcohol	5 mins
5. Absolute Alcohol	4 mins
6. 70% Alcohol	3 mins
7. Distilled Water	1 min

1 Litre of PBS was heated in the microwave until boiling (12 minutes) in a pressure cooker without the lid. The slides were then placed in the pressure cooker and heated on full power for 6 minutes to enable antigen unmasking. The pressure cooker was left to cool before being opened, and the slides subsequently cooled with tap water and placed in PBS for 5 minutes. Non specific binding of the antibody was prevented by blocking the sections with 5% goat serum (Biosource), this was left for 20 minutes blotted then washed in PBS for 5 minutes. The primary antibody was then added to the sections at the appropriate dilution (see relevant chapter) and incubated in a humidifying chamber at 4°C overnight. The following day the slides were then washed in PBS twice each time for 5 minutes. The secondary antibody, biotinylated goat anti-rabbit (Dako) was diluted to 1:200 in PBS; this was then added to the sections and incubated in the humidifying chamber at room temperature for 30 minutes. The secondary antibody was then blotted and washed in PBS for 3 x 10 minutes. The streptavidin alkaline phosphatase solution (Zymed) was then prepared at a 1:300 dilution using PBS and applied to the sections for 30 minutes; the slides were then washed in PBS for 3 x 10 minutes. The fast red solution was prepared in veronyl acetate buffer and added to the slides for between 2-3 minutes (until a red colour could be observed), the slides were then rinsed in PBS left to dry then cover-slips were applied using immunomount (Thermo Shandon UK).

2.4.3 Primary vascular smooth muscle cell extraction from murine aortic rings

C57/B16J mice of either sex were euthanized by cervical dislocation, sprayed with ethanol and the aorta's were dissected and cleared of adherent tissue using sterile technique. The vessels were placed in a 6 well plate containing 3ml of sterile medium composed of 42% Waymouths, 42% Hams F-12, 1% penicillin streptomycin, 15% foetal bovine serum (FBS), 0.05% fungizone and transferred to the laminar flow hood (Bioair Instruments). The vessels were then cut into sections and cleaned gently using a syringe containing media to remove remaining blood from the lumen. The segments were then transferred to a sterile 6 well plate containing 3ml of medium and placed in a 5% CO₂ Galaxy S incubator (Wolf Laboratories). The vessel segments were maintained in culture for 14 days with the medium being aspirated and replaced every alternate day. The aortic sections were removed from culture and fixed in 10% neutral buffered formalin for subsequent histological analysis as previously described in section 2.3.1. During the 14 day period vascular smooth muscle cells (VSMC) migrate from the vessel and adhere to the plate surface; once the tissue ex-plant was removed the cells were left to grow until they reached 90% confluence, again with medium changes every alternate day.

2.4.4 Passage of vascular smooth muscle cells

Once cells had reached confluence the monolayer was rinsed in warm sterile PBS to remove all traces of medium. The cells were then removed from their container by addition of undiluted accutase solution (for volume see Table 2.1) which was left to incubate for 10 minutes; gentle shaking ensured complete removal of cells. The cell solution was then poured into a sterile universal tube and added to 3ml of medium to neutralise enzymatic action. The universal tube was then centrifuged for 6 minutes at 13000 rpm to produce a pellet; this was then re-suspended in 1ml of medium. Once the pellet was completely resuspended the 1ml cell suspension was routinely divided into two 500µl aliquots into flasks to which the appropriate volume of medium was added (Table 2.2).

Container	Volume of Accutase
6 well plate	1ml
25cm ² flask	3ml
75cm ² flask	5ml

Table 2.1 indicates the volume of accutase solution required for complete removal of a cell monolayer in various containers.

Container	Volume of media
6 well plate	3ml
25cm ² flask	6ml
75cm ² flask	15ml

Table 2.2 indicates the volume of medium required for each container.

2.4.5 Sub culture of VSMC in chamber slides

Cells were passaged as described above; once the pellet was re-suspended a cell count was performed to estimate the number of cells present per ml of medium. 20 µl of the cell suspension was added to 20 µl of Trypan blue solution (Gibco), after 2 minutes (sufficient time to enable the dye to penetrate any non-viable cells) a small volume was pipetted onto the edge of the coverslip on the haemocytometer. Capillary action enabled the solution to completely cover the area of the grid. Using a microscope to visualise the grid, the number of viable cells were counted in the 25 squares contained within the large central square. The number of cells was calculated by the following equation.

$$\text{Number of cells/ml} = \text{Number of cells in large square} \times \text{Dilution Factor} \times 10000$$

The cell suspension was then diluted accordingly so that approximately 10000 cells were seeded onto each well of the 8 well chamber slide (Lab Tek II Nunc) to which 300µl of media was added.

To optimise antibody dilutions for the CB₁ and CB₂ receptors, CB₂ transfected Chinese hamster ovary (CHO) cells, provided as a gift from Aberdeen University, were used. Sub culture of CHO cells into chamber slides employed the same method as described previously only differing in medium composition, 500ml Hams F12 (Gibco) 50ml FBS 3ml of Penicillin streptomycin and 4ml of Geneticin (G418).

2.4.6 Immunocytochemical Staining

Once the cells had reached 80~90% confluence the chamber slides were removed from the incubator and the medium removed by blotting. The plastic wells were then removed from the slides following the manufacturer's instructions and the key provided. The slides were left to air dry for 1-2 hours then fixed in 4% paraformaldehyde for 30 minutes in a fume hood; they were then left to air dry on the bench for another 10 minutes. Once the slides were dry the wells were delineated using a wax pen then washed in PBS for 5 minutes. The following stages apply the same principles as described in section 2.3.1. Unspecific binding was inhibited by blocking with 5% goat serum for 20 minutes, this was then blotted and the slides washed in PBS for 5 minutes. The primary antibody (for specific antibody see relevant chapter) was then added at the appropriate dilution and incubated in a humidifying chamber at 4°C overnight. The following day the slides were then washed in PBS twice each time for 5 minutes. The secondary antibody biotinylated goat anti- rabbit was diluted to 1:200 in PBS; this was then added to the sections and incubated in the humidifying chamber at room temperature for 30 minutes. The secondary antibody was then blotted and washed in PBS 3 x 10 minutes. The strepavidin alkaline phosphatase solution was then prepared at a 1:300 dilution using PBS and applied to the sections for 30 minutes; the slides were then washed in PBS for 3 x 10 minutes. The fast red solution was prepared in veronyl acetate buffer and added to the slides for between 2-3 minutes (until a red colour could be observed); the slides were then rinsed in PBS. The slides were then allowed to air dry before being mounted using Immu-mount (Thermo Shandon) and applying a cover slip.

2.5 Cell proliferation studies

2.5.1 Bradford Assay

The protein concentration of samples was quantified using the Bradford Assay, the principle of which compares solutions of known concentration of protein (bovine serum albumin BSA) to unknown samples (Table 2.3). A 1mg/ml solution of BSA was prepared by dissolving 100 mg of albumin bovine in approximately 70ml distilled water; this was then made up to 100ml with

distilled water when fully dissolved. The protein solution was then aliquoted and stored at -20°C for future use.

Standard Concentration (mg/ml)	Volume of BSA 1mg/ml (µl)	Volume of distilled water (µl)
0	0	30
0.2	6	24
0.4	12	18
0.6	18	12
0.8	24	6
1	30	0

Table 2.3 Shows the Dilutions of BSA standards required for use in the Bradford assay.

The Bradford reagent was made by dissolving 100mg Coomassie brilliant blue G-250 in 50ml 95% ethanol, with 100ml 85% (weight/ volume) phosphoric acid. This was diluted to 1 litre with distilled water when the dye had completely dissolved. The solution was then filtered using Whatman No.1 filter paper and stored at room temperature in a dark coloured bottle.

Comment [c1]: Karen – be consistent with the spacing after each paragraph – some times it is single space, others it is double.

10µl of each sample was added to a 96 well microtitre plate in duplicate (leaving the first row blank); 200µl of Bradford reagent was then added to the blank first row and to each sample and standard on the plate producing a colour change from brown to blue. Samples were then read on a colorimetric plate reader (Bio-tec) at 595nm.

2.5.2 Measurement of ERK1/2 phosphorylation in smooth muscle cells by ELISA.

ELISA kits (DuoSet IC phospho ERK and Total ERK) were purchased from R and D systems. The protocols used were adapted from the accompanying protocol leaflet. The protocols described here are the final protocols employed for all assays based on results from preliminary studies, where cells were incubated for various times and at different stimulant concentrations to determine the optimum experimental conditions, outlined in Chapter 5.

The principle of the ERK1/2 ELISA utilises a capture antibody that targets both phosphorylated and non phosphorylated MAP kinase, a biotinylated detection antibody then recognises only phosphorylated ERK1/2 for the Phospho- ERK1/2 ELISA or all ERK1/2 present for the total

ERK1/2 ELISA. The concentration of ERK1/2 was quantified by comparison to standards of known ERK1/2 concentration. An example of a standard curve used in this assay and details on how data was expressed is detailed in Chapter 5.

2.5.3 Cell extraction and lysis

Cells were grown in 75cm² flasks till they were 80-90% confluent, the cells were then quiesced for 24hrs in medium containing 1% penicillin streptomycin || 0.3% serum. Drug or vehicle was added to the quiesced cells and incubated for 20 minutes; the cells were then stimulated with 30ng/ml PDGF-AB and incubated for a further 15 minutes. The medium was poured off and the monolayer rinsed three times in ice cold PBS. To extract the cells from the flask the monolayer was scraped into 1ml of PBS, the suspension was centrifuged for 8 minutes at 10,000rpm and the supernatant discarded. Cell pellets were then lysed directly by adding 100µl of lysis buffer #6 (detailed in materials section 2.9.2) gently vortexed then left on ice for 15 minutes, the lysate was then either used directly in the assay or stored at -80°C for future use.

Comment [c2]: You use various ways of expressing this – at time in full and at time abbreviated. I would recommend using the full terminology throughout.

2.5.4 Sample Preparation

Samples were allowed to defrost thoroughly at room temperature and then centrifuged at 2000rpm for 5 minutes and the supernatant transferred to a clean tube. To ensure comparable results the amount of protein in each sample was quantified using the Bradford assay (described in section 2.5.1); the samples were then diluted 6 fold in IC diluent #8 in preparation for the assay.

2.5.5 Phosph ERK ELISA protocol

2.5.5.1 Plate preparation

The capture antibody was diluted to a working concentration of 4 µg/ml in PBS and 100 µl immediately added to each well of a 96 well microplate (Nunc). The plate was then sealed and incubated overnight at room temperature. The following day each well was thoroughly aspirated 3 times with wash buffer using a 20ml syringe. It was essential to ensure complete removal of liquid at each step to optimise the experiment; this was done by inverting the plate and blotting it against a clean paper towel. Non specific binding of antibody was prevented by addition of 300µl of block buffer to each well; the plate was then sealed and incubated at room temperature for 1-2 hours.

The plate was then washed 3 times as described above.

2.5.5.2 Assay Procedure

100 μ l of sample or standards in IC Diluent#3 (for preparation see materials section 2.9.2) were added to the wells; the first row of the plate contained only IC#3 to serve as a blank control (an example of plate layout is shown in chapter 5). The plate was then sealed and left to incubate for 1 hour at room temperature. The plate was then thoroughly aspirated as detailed above.

The detection antibody was diluted to a working concentration of 0.5 μ g/ml in IC#1 (supplemented with 2% heat inactivated goat serum and prepared 1-2 hours prior to use), 100 μ l of this antibody was then added to each well. The plate was then sealed and incubated at room temperature for 2 hours then washed as detailed above. Prior to use, the streptavidin-HRP was diluted to the concentration indicated on the vial using IC Diluent #1. 100 μ l of this solution was then added to each well; the plate was sealed and incubated for 20 minutes at room temperature then washed as described above. 100 μ l of substrate solution was then added to each well and incubated for 20 minutes at room temperature avoiding direct sun light, 50 μ l of stop solution was added to each well the plate; gently tapping ensured thorough mixing. The optical density of each well was determined immediately using a microplate reader set to 450nm with wavelength correction set to 540nm, an example of a standard curve produced and details on data expression can be found in chapter 4.

2.5.6 Total ERK ELISA

Samples were prepared in the same way as detailed in section 2.6.2. The principle of the assay was the same as for the phosphorylated ERK ELISA described above the only difference being the biotinylated detection antibody detects both phosphorylated and non phosphorylated ERK. Diluents and lysis buffers were the same as used in the phospho ERK ELISA as detailed in materials section 2.9.

Comment [c3]: If the plate preparation and assay protocol is identical to that for phospho-ERK then these two sections could be combined and you simply need to identify the differences in the detection kits. If there are marked differences leave as it is, but I couldn't find any.

2.5.6.1 Plate Preparation

The capture antibody was diluted to a working concentration of 1 μ g/ml in PBS this was then used to coat the plate by adding 100 μ l to each well, the plate was then sealed and left to incubate overnight at room temperature. The remainder of the plate preparation process is as described in section 2.5.5.1.

2.5.6.2 Assay Protocol

100µl of either sample or standard was added to the desired well, the first row contained only 100 µl of IC#3. The plate was then sealed and left to incubate at room temperature for 2 hours. The plate was washed as described above. The detection antibody was diluted to a working concentration of 0.5µg/ml in IC#1, 100 µl of this solution was then added to each well, the plate was then sealed and incubated at room temperature for 2 hours. The plate was then washed as described above. Streptavidin –HRP was diluted to the working concentration specified on the label using IC#1, 100 µl of this solution was then added to each well and incubated for 20 minutes avoiding direct light. The plate was then washed as previously described. 100µl of substrate solution was added to each well this was then left to incubate for 20 minutes at room temperature again avoiding direct light. 50 µl of stop solution was added to each well, the plate was gently tapped to ensure complete mixing. The optical density of each well was determined immediately by using a microplate reader set to 450nm with wavelength correction set to 540nm.

2.5.7 Determination of DNA synthesis using the BrdU assay

The BrdU assay is an effective non radioactive method to measure cellular proliferation by monitoring DNA synthesis. 5-bromo-2-deoxyuridine (BrdU) is a pyrimidine analogue that replaces thymidine and becomes incorporated into DNA at the synthesis stage; the incorporated BrdU is then measured by immunoassay. BrdU kits which included BrdU labelling solution, FixDenat, Anti-BrdU-POD, antibody dilution solution, washing buffer and substrate solution were purchased from Roche. The following protocol was developed from that provided in the instruction manual that accompanied the kit. Details of the solutions used in this assay can be found in the materials section 2.9.5. The protocol described is the final protocol determined from preliminary experiments to determine the optimum concentration and incubation time of the BrdU (detailed in Chapter 5).

2.5.7.1 Cell preparation

Cells were grown to 80-90% confluence in 75cm³ flasks then seeded at the appropriate cell number (as detailed in Chapter 5) in 100µl of normal medium into a tissue culture grade flat bottomed 96 well plate (for method see Section 2.4.3). The cells were returned to the incubator for 6 hours to allow them time to adhere and grow. Following this the cells were then quiesced, the medium was removed from the plate by tapping and was replaced with 100µl of medium containing 0.3% serum 1%, penicillin streptomycin the plate was then returned to the incubator

overnight. A blank control was included in each experiment; a background control was performed only once. For details of the requirements for each control see Table 2.4

2.5.7.2 Cell stimulation and assay protocol

The quiesced cells were incubated for 15 minutes with drug then stimulated for 24 hours with the appropriate concentration of PDGF. After 24hr the medium was supplemented with 10µl BrdU labelling solution (for dilution see materials section 2.9.5) and left for a further 24hrs. At the end of this period the medium was then tapped off. Once the plate was dry, 200µl of Fixdenat solution was added to each well for 30min to allow the denaturing of the DNA which facilitated access of the antibody to the incorporated BrdU. The Fixdenat solution was removed by tapping and blotting to ensure complete removal of liquid and 100µl of the anti BrdU –POD solution (materials section 2.9.5) was added to each well for 90minutes. Following this incubation, each well was washed 3 times with the wash buffer provided in the kit (for dilution see materials section) then 100µl of chromagenic substrate solution was added to each well and incubated for 20 minutes avoiding direct sun light. Once the colour had developed the reaction was then stopped by adding 25µl of 1M H₂SO₄ . The absorbances were immediately read (within 5 minutes) on a plate reader at 450nm with reference wavelength 690nm.

Comment [c4]: Which was?

Comment [c5]: You need to identify which section number this is at the end of the chapter

Well Contents	Blank	Background control
Culture Medium	100µl	-
Cells	-	100µl
BrdU	10µl	-
Anti-BrdU-POD	100µl	100µl

Table 2.4 Composition of controls performed in the BrdU assay.

2.6 Measurement of cell viability by MTT assay

To ensure that the drugs employed in the cell proliferation studies were having a genuine effect on proliferation and not inducing cytotoxicity, cell viability was measured by the MTT assay. To ensure comparable results with the BrdU assay cells were seeded and quiesced in the exact same way as detailed in section 2.5.7.1. Cells were then treated with the appropriate concentration of drug (detailed in chapter 5) and left to incubate at 37°C 5% CO₂ for either 24 or 48 hours. To enable % cell viability to be calculated a negative control of cells treated with

triton X and a positive control of healthy cells containing medium were required. Details on data calculation can be found in Chapter 5.

Following incubation with drug, 50µl of MTT solution was then added to each well (taking care not to expose the solution to light), the plates were then wrapped in tinfoil to avoid light exposure and incubated for 4 hours at 37°C 5 % CO₂. The solution was then removed from the wells using a multi channel pipette ensuring complete removal of liquid; at this stage purple crystals were visible on the bottom of the wells. 200µl of DMSO was then added to each well to dissolve the crystals and produce a purple coloured solution in wells that contained viable cells; the wells that contained triton x remained clear. 25µl of glycine buffer was then added to each well and the plate was then read at 570nm.

2.7 Cell migration studies

A 48 well chemotaxis chamber (AP48 Neuroprobe) was used to investigate the effects of cannabinoids on cell migration. The chemotaxis chamber is composed of 3 sections, the lower wells which contain the chemoattractant, the silicon gasket, and the upper wells (Figure 2.4) which contain the cells. The chamber is assembled as illustrated in Figure 2.5 with the upper and lower wells being separated by a Polycarbonate track-etch (PCTE) membranes with a pore size of 8µm (Neuroprobe). The principal behind the assay is that the cells in the upper wells migrate towards the chemoattractant solution in the lower wells across the filter. Cells that migrate across the filter and adhere are stained and counted.

2.7.1 Preparation of cells for the chemotaxis chamber

Cells were grown to 90% confluence in 75cm² flasks as previously described; they were quiesced overnight in medium containing 0.3% serum 1% penicillin streptomycin then removed from the flask using accutase solution as detailed in section 2.4.4. The cells were counted as previously described and re-suspended in a 1.5ml tube at the appropriate density (as determined from optimising experiments detailed in chapter 6) in medium containing 0.3% serum 1% penicillin streptomycin.

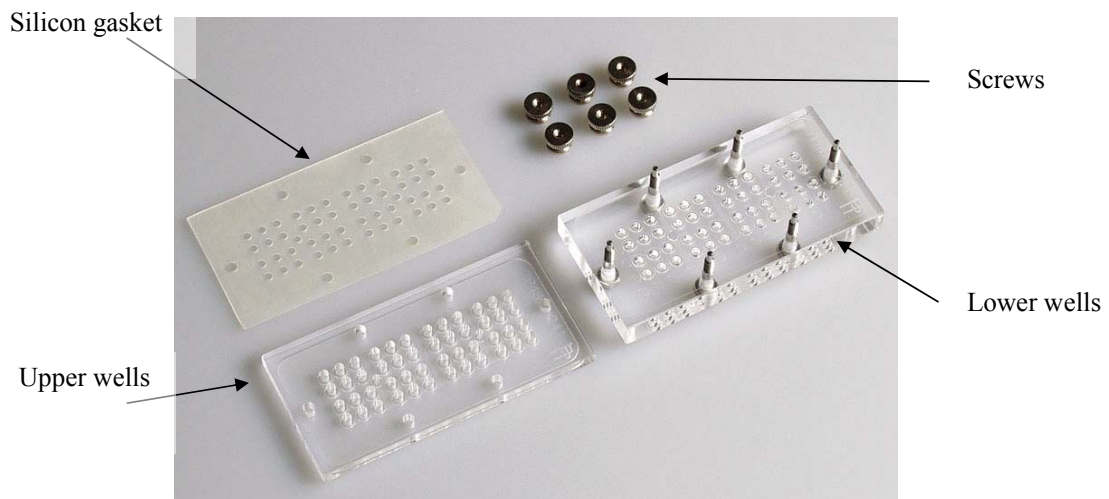


Figure 2.4. The components of the 48 well chemotaxis chamber.



Figure 2.5. An example of the assembled chemotaxis chamber.

2.7.2 Preparation of the chamber

The polycarbonate filter was carefully removed from its box; with the shiny side facing downwards, a small notch was cut in the top left hand corner. The filter was

then placed in a Petri dish containing a 0.2% gelatine solution and left for 30minutes at room temperature; the filter was then turned over and left for a further 30minutes. Once the filter was coated it was held in warmed PBS until time for use.

A chemoattractant solution of 30ng/ml of PDGF-BB was made up in serum free medium and warmed to 37°C. The solution was gently vortexed before 26.5µl was added to each of the lower wells, except for those wells that were to be used as un-stimulated controls, which contained only warmed serum free medium. With the lower wells filled, the filter was removed from the PBS (with the excess PBS being allowed to drip off) and, with the shiny side facing downwards (with the notched corner at the top left of the chamber), the filter was placed on top of the lower wells. The silicon gasket was then placed on top of the filter (again with the notched corner on the top left), the upper wells placed on top of the gasket, and the chamber secured using the screws. 50µl of the **cell suspensions** (described above 2.7.1) were then added to the upper wells, the chamber placed inside a humidifying chamber (to prevent evaporation) and then incubated for 3 hours at 37°C and 5% CO₂.

Comment [c6]: Do you mean those containing the stimulant PDGF-BB?– if so, indicate this explicitly

2.7.3 Removal of un-migrated cells and cell fixation

To remove the filter from the chamber the screws were loosened and then the chamber turned upside down. When the bottom wells were removed the filter was stuck to the gasket with the migrated cells facing upwards (with the notched corner now on the top right hand corner). Using curved forceps the right end of the filter was carefully attached to a large filter clamp (Neuroprobe accessory kit), the filter was then lifted by the clamp and a smaller filter clamp was attached to the bottom edge. With the migrated cell side still facing upwards the underside (non-migrated cell side) of the filter was dipped in a dish containing PBS (ensuring that PBS did not wash over the cell side of the filter). Holding the filter by the large clamp, with the small clamp attached to the other end freely hanging, the non-migrated cell side of the filter was wiped by running the filter over a wiper blade (Neuroprobe accessory kit) which was attached to a clamp stand. This was repeated 4 times with the un-migrated side of the filter being dipped in PBS between each wipe. The wiper blade was also cleaned between each wipe with a PBS soaked swab. This process was performed quickly to prevent the drying of un-migrated cells as this would prevent complete removal. Once the un migrated cells were removed the filter was then completely immersed in 100% methanol for 7 minutes then left to air dry.

2.7.4 Staining of filter

Once the filter was completely dry the filter was stained using a modified H and E protocol (detailed below) to enable visualisation of cells to permit quantification.

1. Distilled Water	1 min
2. Haematoxylin	5 min
3. Distilled Water	2 min
4. 0.5% Acid Alcohol	1 min
5. Distilled Water	2 min
6. STWS	2 min
7. Distilled Water	2 min
8. Eosin	15 secs
9. Distilled Water	2 min
10. Haematoxylin	5 min
11. Distilled water	1 min

The filter was then cut in half (as the filter was too large to fit whole on a slide) and mounted onto a slide using Shandon xylene substitute mountant (Thermo Scientific) and a coverslip was added (22x50mm). Cells were counted as detailed and illustrated in chapter 6.

2.8 LC-MS/MS Detection of Anandamide and 2-arachidonylglycerol in aorta samples

Sections of aorta were prepared as described in Chapter 3 section 3.3.5. then immediately flash frozen in liquid nitrogen. The samples were then transported on ice to Aberdeen University mass spectroscopy department where the analysis was performed by Mr G Cameron (Department of Medicine and Therapeutics, Aberdeen University).

2.8.1 Tissue extraction procedure

Tissue sections were homogenised in 0.6ml 50/50 methanol/acetonitrile, containing 60pmol of d4-anandamide as internal standard. 1.4ml of water was added and the solution vortexed. The samples were then centrifuged at 13000rpm for 5 minutes.

The supernatant was applied to a preconditioned Strata-X SPE cartridge; this was washed with 2ml 70/30 water/methanol followed by 2ml 30/70 water/methanol. This was eluted with 1ml of

methanol then evaporated to dryness under nitrogen then reconstituted in 50µl 85/15 methanol/water.

2.8.2 LC Conditions

Injection volume: 20µl

Tray temperature: 4°C

Column: ACE 5µ C8 (150 x 2.2mm)

Column temperature: 30°C

Mobile phase: 85% methanol :15% water (both containing 0.5% formic acid)

Flow rate: 200µl/min

MS/MS Conditions

Interface: +ve ion ESI

Spray voltage: 3500V

Sheath gas: 40 arbitrary units

Aux gas: 10 arbitrary units

Capillary temp: 375°C

Collision pressure: 1.5mTorr

Collision energy : 13V

Skimmer offset : -10V

Selected Reaction Monitoring (SRM) transitions :

(m/z = mass charge/ratio)

Anandamide: m/z 348.20 – m/z 62.20

2-arachidonylglycerol: m/z 379.00 – m/z 287.00

D4-anandamide: m/z 352.20 – m/z 66.20

2.9 Materials

All drugs and chemicals were purchased from Sigma Aldrich UK unless otherwise stated; paraffin wax and PBS tablets were from Fisher Scientific.

2.9.1 Histology Solutions

PBS: 1 PBS tablet was dissolved in 100mls of distilled water resulting in a final concentration of 137mM NaCl, 10mM Phosphate, 2.7mM KCl.

0.5% Acid Alcohol for 1 L

- 5% HCL (50ml)
- 2.5ml of HCL (conc) +47.5ml distilled water
- 0.5% Acid in Alcohol (1L)
- 50ml of 5%HCL +950ml Ethanol

STWS = Scotts Tap Water Substitute for 1L distilled water

- $\text{MgSO}_4 \cdot 7\text{H}_2\text{O}$ 20g,
- NaHCO_3 3.5g

Biebrich Scarlet-Acid Fuchsin solution:

- Biebrich Scarlet 1% aqueous -90ml
- Acid Fuchsin 1% aqueous 10ml
- Acetic Acid 1% - 1ml

Phosphomolybdic-Phosphotungstic Acid Solution:

- 5% Phosphomolybdic acid in 25ml
- 5% Phosphotungstic acid in 25ml

Aniline Blue Solution:

- Aniline Blue 2.5g
- Acetic Acid 1% 2ml
- Distilled water 99ml

Veronyl Acetate Buffer

- 0.97g of sodium Acetate
- 1.47g of sodium diethyl barbituate in 200ml
- Adjust pH to 9.2 with 0.1M HCL
- Make up to 250ml with distilled water

- 25mg Naphthol AS-MX phosphate
- 12mg Levamisal
- 25mg Fast Red TR salt

2.9.2 ELISA SOLUTIONS

Sample Diluent Concentrate 1, Reagent Diluent Concentrate, Substrate solution and Stop solution were purchased from R and D systems. Capture antibodies, detections antibodies, standards and Streptavidin-HRP were provided with the kits.

Wash Buffer : 0.05% Tween 20 in PBS

Block Buffer: 1% BSA, 0.05% NaN₃ in PBS

ERK 1/2 ELISA.

Proteases and Phosphate inhibitors required for Lysis Buffer #6: 10µg/ml leupeptin, 10 µg/ml pepstatin, 100 µM PMSF, 3 µg/ml aprotinin

Substrate Solution: 1:1 mixture of colour reagent A (H₂O₂) and colour reagent B (Tetramethylbenzidine)

Stop Solution: 2N H₂SO₄

2.9.3 Reagent Preparation for Phospho ERK ELISA

Phospho-ERK capture antibody: This was reconstituted in 200µl of PBS producing a concentration of 720µg/ml this was aliquoted and stored at -20°C.

Phospho- ERK detection antibody: This was reconstituted in 1ml of IC diluent #1 giving a concentration of 18µg/ml this was then aliquoted and stored at -20°C.

Diluents and Lysis Buffer:

Diluent Name	Volume of Sample Diluent concentrate¹	Urea Required	0.5M NaF required	Protease and Phosphate inhibitors required	Adjust with Distilled H₂O
IC Diluent #3	10ml	3.003g	0.5ml	no	50ml
IC Diluent #7	10ml	18.02g	0.5ml	no	50ml
IC Diluent #8	10ml	n/a	0.5ml	no	50ml
Lysis Buffer #6	2ml	3.604g	0.1ml	yes	10ml

Table 2.5 Indicates the composition of the diluents and lysis buffer required for

Phospho ERK standard: 115ng/ml when reconstituted with 500µl of IC Diluent #7. An initial 6 fold dilution was made in IC#8 (2.5ml giving a total volume of 3ml), further 2 fold serial dilutions were made using IC#3 immediately before use. A seven point curve using 2 fold serial dilutions and a high standard of 12ng/ml was used.

Concentration of Standard	Volume of Standard	Volume of IC#3
12ng/ml	3ml	1.7ml
6ng/ml	500µl of 12ng/ml	500µl
3ng/ml	500µl of 6ng/ml	500 µl
1500pg/ml	500µl of 3ng/ml	500 µl
750pg/ml	500 µl of 1500pg/ml	500 µl
375pg/ml	500 µl of 750pg/ml	500 µl
0	0	500 µl

Table 2.6. Indicates the dilutions required for the Phospho ERK 1/2 standards

2.9.4 Reagent Preparation for Total ERK ELISA

Total ERK capture antibody: 180µg/ml was reconstituted in 200µl of PBS this was stored in aliquots at -20°C.

Total ERK2 detection antibody: 18µg/ml of biotinylated rabbit anti-human ERK2 antibody was reconstituted in 1ml of IC#1. This was then stored at -20°C.

Total ERK standard: 600ng/ml of recombinant human ERK2 was reconstituted in 500µl of IC diluent#7 An initial 6 fold dilution was made by adding 2.5ml of IC#8 giving a total volume of 3ml at a concentration of 100ng/ml. 12ml of IC#3 was then added to give a concentration of 20ng/ml. 2 fold serial dilutions of the maximum concentration allowed a seven point standard curve to be made.

Concentration of Standard	Volume of Standard	Volume of IC#3
10ng/ml	500µl of 20ng/ml	500 µl
5ng/ml	500 µl of 10ng/ml	500 µl
2.5ng/ml	500 µl of 5ng/ml	500 µl
1250pg/ml	500 µl of 2.5ng/ml	500 µl
625pg/ml	500 µl of 1250pg/ml	500 µl
0	0	500 µl

Table 2.7 Shows the dilutions required for the Total ERK 1/2 standards.

2.9.5 BrdU solutions

BrdU labelling solution: BrdU labelling solution was diluted 1:100 in sterile culture medium giving a final concentration of 100µM BrdU.

Anti-BrdU-POD stock solution: This was dissolved in 1.1ml of double distilled water for 10 minutes and mixed thoroughly.

Anti-BrdU –POD working solution: The stock solution was diluted 1:100 with the antibody dilution solution.

Wash Buffer: This was diluted 1:10 with double distilled water.

2.9.6 Solutions required for MTT assay

MTT solution: 0.05g of MTT powder was dissolved in 10ml of PBS preventing exposure to light.

Glycine Buffer: 3.75g of glycine and 2.93g of NaCl was dissolved in 500ml of distilled water, the pH was then adjusted using NaOH to 10.5.

2.9.7 Solutions required for migration studies

0.2% gelatine solution: 0.04g gelatine was dissolved in 20ml PBS and heated until completely in solution.

30ng/ml PDGF solution: 3 μ l of 10 μ l/ml stock solution was added to 997 μ l of serum free medium to make a 30ng/ml solution.

Coomassie brilliant blue:

- 7% Acetic acid
- 35% Methanol
- 0.5% Coomassie blue R250 (w/v)

De Stain:

- 7% Acetic acid
- 35% Methanol

Giemsa

- 1% Giemsa (w/v) dissolved in methanol

Chapter 3

Development and characterisation of an *in vitro* model of neointimal formation

3.1 Introduction

3.1.1 Neointimal formation

Percutaneous coronary angioplasty or more recently, the placement of stents, are the most common methods of revascularization following coronary artery disease. Recent advances in these techniques, such as the development of drug eluting stents, has reduced the occurrence of restenosis to less than 10% of surgical interventions (Epstein *et al.*, 2008), however, research still continues to identify new treatments that may be more suitable. Restenosis is a condition that occurs following vessel injury, and is characterised by a reduction in luminal area due to the formation of a neointima. Neointimal formation is a complex process that occurs due to the over compensatory healing response produced by the vessel following injury (discussed in detail in chapter 1). The response involves a large variety of cells and cell mediators, with the key pathological events being smooth muscle cell proliferation and migration, adventitial remodelling and matrix production (Ferns *et al.*, 2000).

3.1.2 Experimental models of neointimal formation

3.1.2.1 *In vivo* models of neointimal formation

The most common method used to study the restenosis process is through the use of *in vivo* models. The most established and characterised model is the rat carotid balloon injury model, (Guyton *et al.*, 1980; Kantor *et al.*, 1999), this has been a fundamental tool in the understanding of PDGF and its function as a smooth muscle cell mitogen (Fingerle *et al.*, 1989). An alternative approach to studying restenosis is in rabbits fed a high cholesterol diet, which can induce atherosclerotic like lesions. Vessel injury is then induced by passing inflated balloons across either the carotid, subclavian (Hadoke *et al.*, 1995) or femoral arteries. The neointima that results is highly comprised of lipid, making this model less useful for investigations into antiproliferative agents (Faxon *et al.*, 1982). An alternative method of inducing neointimal formation in high fat/cholesterol fed rabbits is to crush the central ear arteries, after 21 days substantial neointima and smooth muscle cell proliferation occur (Banai *et al.*, 1991). The dog has also been investigated as a potential model of restenosis, however dogs have different fibrinolytic activity compared to humans and the neointimal response produced following injury is minimal. For these reasons the dog is considered a poor model (Schwartz *et al.*, 1994).

The cardiovascular system of pigs is similar to that of humans in aspects of morphology and physiology. Porcine vessels react to vessel injury by producing a large neointima that is almost identical to that produced in humans, in terms of cell density and histological appearance (Schwartz *et al.*, 1990, Arturo *et al.*, 2006). For these reasons the porcine model has become an invaluable tool in the further understanding and the identification of novel therapeutic strategies including research into drug eluting stents (Scheller *et al.*, 2008; Hamada *et al.*, 2009). *In vivo* models have also been developed in the mouse. Carotid artery ligation produces a reproducible injury response, however the neointima produced is not in response to endothelial denudation and may therefore differ in its mechanism of development. Endothelial denudation is another method used *in vivo* to produce neointimal formation, this method also has its drawbacks as the technique is challenging (Reviewed in Hui *et al.*, 2008). Despite the difficulties of performing surgical techniques in mice, a very recent study has documented the development of a murine model of in stent restenosis, this technique involves the placement of a stent in the mouse aorta (Rodriguez-Menocal *et al.*, 2009).

3.1.2.2 The use of cell cultures

As mentioned above intimal smooth muscle cell proliferation is pivotal in the formation of a neointimal. The use of cultured isolated cells from both humans and animals has been crucial in helping us to understand this process and investigate novel therapeutic strategies. For example, this approach has provided insight into the effects of many growth factors on smooth muscle cells, including bFGF, and IL-1 (Lindner *et al.*, 1991; Libby *et al.*, 1988). However, it has been reported that smooth muscle cells originating from vascular lesions may behave differently to cells obtained from healthy vessels. For example, human smooth muscle cells isolated from atheromatous plaques demonstrated a higher sensitivity to the agent photofrin II (an agent used in photodynamic therapy of tumours) compared to smooth muscle cells derived from healthy vessels (Dartsch *et al.*, 1990). Notwithstanding the fact that smooth muscle cell cultures are an essential *in vitro* screening tool for the study of smooth muscle cell proliferation, they do not replace the need for whole vessel studies. Only in the whole vessel can the anatomical orientation of cells, the presence of a vessel wall, and production of extracellular matrix, all of which which may impact on cell to cell interactions and proliferation be studied together (Holt *et al.*, 1992).

3.1.2.3 Models of organ culture

Organ culture models of neointimal formation have been developed in a variety of human vessels including the mammary, coronary, and renal arteries (Holt *et al.*, 1992, Holt *et al.*, 1994; Voisard *et al.*, 1999). These models have led to the discovery and identification of factors released by the vessel following injury such as PDGF (Holt *et al.*, 1992, Holt *et al.*, 1994). The

Comment [c7]: What about mouse models? Considering you have employed mouse tissues for your experiments it is worth outlining what there is available in the form of *in vivo* mouse models – particularly if they are problematic!

use of organ culture is the only *in vitro* method available to investigate the response to injury produced in humans; however the effectiveness of this method is reliant on the availability of human tissue. To overcome this problem organ culture models have been developed using blood vessels from other animals, the most commonly used being the porcine model. One important limitation to these organ culture models is that they employ healthy vessels. Development of a murine organ culture model would enable the use of tissues from transgenic mice developed to mimic human disease (such as the ApoE K/O mouse) which would provide a more pathological environment for experimentation. While *in vivo* models of murine neointimal formation are already established, an organ culture method would remove the need for complicated surgery and allow the simultaneous screening of a range of compounds for selection prior to *in vivo* testing.

3.1.3 The cannabinoid system

As detailed in Chapter 1, the endocannabinoid system is composed of the endogenous cannabinoids (of interest in this study are AEA and 2-AG), the receptors to which they bind, and the enzymes involved in their biosynthesis and degradation. It is accepted that endocannabinoids are synthesised on demand, then immediately released from cells as there is no evidence of vesicle storage (Di Marzo, 2008; Mechoulam *et al.*, 1998).

3.1.3.1 Endocannabinoids and disease

The endocannabinoid system has been linked to many diseases due to observed alterations in endocannabinoid concentration. Indeed, alterations in AEA and 2-AG concentration have been observed in pain, cancer, gastrointestinal and hepatic conditions, obesity, eye disorders (Matias *et al.*, 2006; Jhaveri *et al.*, 2007; Storr *et al.*, 2007; Matias *et al.*, 2007; Alpini *et al.*, 2009) and, most importantly for the scope of this study, in cardiovascular disease. The involvement of the endocannabinoid system in disease states is complex, with both protective and detrimental effects occurring following cannabinoid receptor activation. It has also been observed that each endocannabinoid may have opposing effects, as AEA and 2-AG levels can differ within the same tissue (Di Marzo, 2008). An example of the complex nature of the endocannabinoid system can be observed in investigations into pain and inflammation. It has been shown that irritant and inflammatory stimuli induce an increase in the concentrations of endocannabinoids in the skin and peripheral nerves of rodents (Oka *et al.*, 2006) and it has been postulated that these changes aim to reduce pain and inflammation, a theory supported by the fact that inhibition of endocannabinoid metabolism counteracts pain (Jhaveri *et al.*, 2006). In contradiction to this, some models of pain show that CB₁ receptor antagonists can induce analgesic effects (Costa *et al.*, 2005), highlighting the complexities of the involvement of the endocannabinoid system.

Comment [c8]: Which ones?

Comment [c9]: Inhibition of EC's would increase pain if the postulation were correct – need to read through this again to remove inconsistencies

In the cardiovascular system, studies into the effects of endocannabinoids on disease have primarily been focused on their role in hypertension and different types of shock, (cardiogenic, septic and haemorrhagic) all of which have demonstrated an increase in AEA and 2-AG concentration in platelets, monocytes, macrophages or blood (Reviewed in Malinowska *et al.*, 2008). AEA is thought to be released to combat pathological hypertension, a theory supported by the finding that AEA produced from endothelial cells, macrophages and platelets induced a long lasting hypotensive effect in spontaneously hypertensive rats, compared to normotensive rats (Lake *et al.*, 1997; Batkai *et al.*, 2004). Endocannabinoids have also been shown to have a cardioprotective effect by reducing infarct size, a process thought to involve the CB₂ receptor (Lepicier *et al.*, 2003), and a novel cannabinoid receptor (Underdown *et al.*, 2005). There is mounting evidence for a protective role of cannabinoids in the progression of atherosclerosis. Δ⁹-THC reduced atherosclerotic plaque progression (Steffens *et al.*, 2005) and AEA has been shown to attenuate TNF-α induced expressions of ICAM-1 and VCAM-1 and also to reduce the adhesion of monocytes to endothelial cells (Batkai *et al.*, 2007). In support of this, 2-AG concentration was found to be increased in a mouse model of atherosclerosis (Montecucco *et al.*, 2009), and similarly human patients suffering coronary artery disease were found to have increased blood endocannabinoid concentrations (Sugamura *et al.*, 2009). However, in contradiction, endocannabinoids may also be pro atherosclerotic as it has been shown that 2-AG can activate platelets (Maccarrone *et al.*, 2001).

3.2 Aim

The development of an *in vitro* murine model of neointimal formation would be an exceedingly useful experimental model as it would permit the use of transgenic mice to explore the roles of either disease or of specific receptors in the development of neointima. The primary aim of this study was to develop a murine organ culture model of neointimal formation that could be utilised to (i) characterise the injury response produced in the mouse and investigate the presence and location of cannabinoid receptors within the vascular wall (ii) determine whether the endocannabinoid system becomes activated in this model of vessel injury and (iii) investigate the effects of cannabinoid agents on the formation of neointima.

3.3 Method

3.3.1 Tissue preparation and standard culture method

C57/B16J mice of either sex were euthanized by cervical dislocation, sprayed with ethanol and the aorta dissected out and cleared of adherent tissue using sterile technique. The vessels were placed in a 6-well plate containing 3ml of sterile medium (composed of 42% Waymouths, 42% Hams F-12, 1% penicillin streptomycin, 15% foetal bovine serum (FBS), 0.05% fungizone) and transferred to the laminar flow hood. The vessels were then cut into segments of approximately 3mm and cleaned gently using a syringe containing media to remove remaining blood from the lumen. The segments were then transferred to a sterile 6-well plate containing 3ml medium and placed in a 5% CO₂ Galaxy S incubator (Wolf Laboratories). The vessel segments were maintained in culture for 14 days with the medium being aspirated and replaced every alternate day. The aortic sections were removed from culture and fixed in 10% neutral buffered formalin for subsequent histological analysis as previously described in section 2.3.1.

3.3.2 Methodological development to produce vessel injury

3.3.2.1. Ligature method

To induce an injury response in the aorta similar to that observed following angioplasty or placement of a stent, a method for injuring the vessels had to be identified. The first method employed to induce injury was through the placement of a ligature. Once the aorta was dissected and cleaned of adherent tissue, a ligature was placed round the middle of the aortic segment (illustrated in Figure 3.1). The vessel was then placed in culture under the conditions described above. Following the 14 day culture period the aortas were removed, fixed and embedded in wax (as detailed in method section 2.3.1), and serial sectioned at 25µm intervals from the edge of the segment towards the ligature. The wax sections were then stained with H&E as detailed in Section 2.3.2.

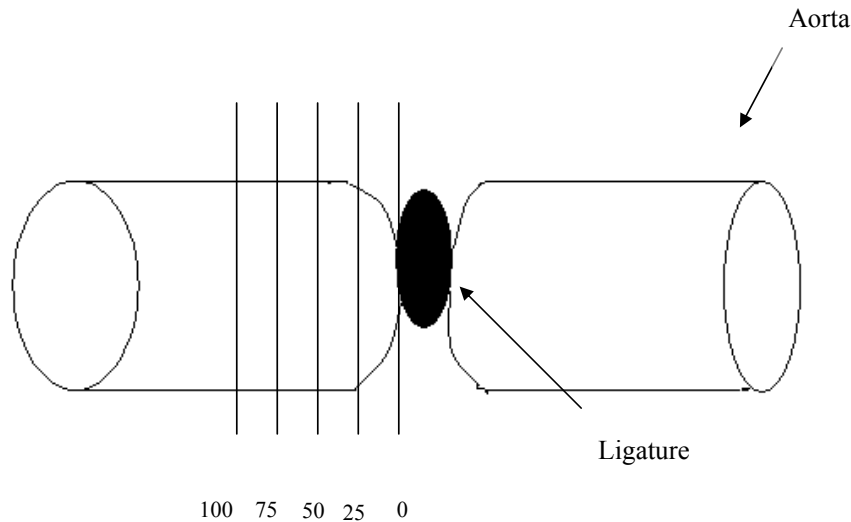


Figure 3.1 An illustration of the aorta with a ligature attached, and the serial sectioning. Distance was measured in μm .

3.3.2.2 Vessel injury induced by culturing alone

Once the aortas were dissected and cleaned of adherent tissue they were cut into segments, rinsed free of blood then placed in culture for 14 days as described in method section 2.4.3. Following the 14 day culture period the aortas were removed, the tissues were then processed, embedded in wax, sectioned ($4\mu\text{m}$ thick) and subsequently stained with H&E as detailed in method section 2.4.3.

3.3.2.3 Vessel injury induced by intraluminal injury by a wire

The aorta was dissected and cleaned of adherent tissue, it was then cut into segments and rinsed free of blood. In an attempt to induce vessel injury the endothelium was disrupted by rubbing the luminal surface with a piece of stainless steel wire ($40\mu\text{m}$ in diameter), the tissue sections were then placed in culture for 14 days as described in method section 2.4.3. Following the culture period the tissues were then processed, embedded in wax, sectioned and subsequently stained with H&E as detailed in method section 2.3.2. Vessel injury with the wire proved the most suitable method and was used in this study.

Comment [c10]: This section should come before the previous one

3.3.2.4 Wire-induced injury

The aorta was dissected and cleaned of adherent tissue, cut into three ~3mm segments and then rinsed free of blood. The vessel segments were then subjected to the following conditions: (i) one was immediately fixed in formalin (control) (ii) the second was placed in culture and (iii) the third was injured with the wire (by rubbing the internal surface) then placed in culture. The vessel segments were processed, embedded in wax, sectioned and subsequently stained with H&E as detailed in section 2.3.2.

Comment [c11]: Explain how the wire injury was induced

3.3.3 Expression and quantification of vessel injury

The injury response produced by both culturing vessels and injuring them prior to culture was analysed in three ways;

(1) Visual analysis- identifying four key morphological changes archetypal of vessel injury: (i) medial thickening (ii) rupture of the internal elastic lamina (IEL) (iii) neointimal growth and (iv) adventitial thickening.

(2) Measuring the area of (i) any neointima produced (ii) the media (iii) and the adventitia.

(3) Measurement of medial and adventitial thickness.

Area measurement was performed using the image J (National institute of health, Bethesda) software as illustrated in Figure 3.2

3.3.3.1 Calculation of neointimal area

Neointimal area = Area within the boundary of the IEL – Luminal area

Comment [c12]: Do you mean luminal area?

(Area of shaded circle – area of white circle as shown in Figure 3.2)

3.3.3.2 Calculation of medial area

Medial Area = Area within the boundary of the external elastic lamina (EEL) – Area within the boundary of the IEL

(Area of green circle – area of shaded circle as shown in Figure 3.2)

3.3.3.3 Calculation of adventitial area

Adventitial Area = Area of outer edge of blood vessel – Area within the boundary of the EEL

(Area of beige circle – area of green circle as shown in Figure 3.2)

3.3.3.4 Medial thickness

The distance between the EEL and the IEL was measured at 4 locations of a vessel section then averaged (illustrated on Figure 3.2). This was repeated for each vessel section, the values were expressed as mean \pm SEM.

Comment [c13]: Were they averaged for a single vessel to give one value and then the means calculated for the whole group? This needs to be made clearer.

3.3.3.5 Adventitial thickness

The distance between the outer boundary of the vessel and the EEL (as illustrated on Figure 3.2) was measured at 4 locations of the vessel 90° apart. This was repeated for all vessel sections, then expressed as mean \pm SEM.

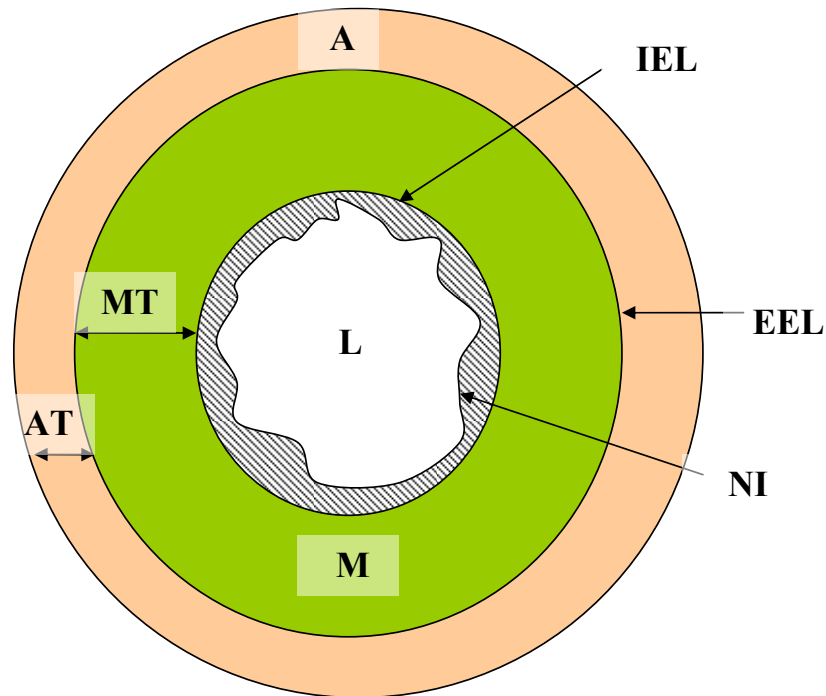


Figure 3.2 An illustration of a transverse aortic section highlighting the different areas of the vessel. The white circle represents the area of the lumen (L), the shaded area represents any neointima that may be present, the green circle represents the area of the media (M) and the beige circle represents the area of the adventitia (A). MT= medial thickness, AT= adventitial thickness, IEL = internal elastic lamina, EEL= external elastic lamina, NI = neointima.

3.3.4 Injury characterisation

To characterise the injury response produced in the murine aorta, both histological and immunohistological staining was performed. Once vessel sections were embedded in wax and cut into 4 μ m sections they were then stained with H&E (described in section 2.3.2) or Massons Trichrome (detailed in section 2.3.3). Immunohistochemical staining using an antibody directed at α smooth muscle actin (α -SMA) was used to identify and locate smooth muscle cells (IHC method detailed in section 2.4).

3.3.4.1 CB₁ and CB₂ antibody staining

To identify the optimum dilutions at which both cannabinoid receptor antibodies should be utilised, CB₂ transfected CHO cells were used as both a positive (CB₂ receptors) and a negative (CB₁) control. CHO cells were grown and subcultured onto 8 well chamber slides (as detailed in method section 2.4.5) ICC was then performed using the method described in section 2.4.6. Once the optimum dilutions of CB receptor antibodies had been identified, 4µm wax sections were then stained for both CB₁ and CB₂ receptors using IHC. To confirm the presence of CB receptors on smooth muscle cells, murine smooth muscle cells (MVSMCs) were grown on chamber slides (as detailed in section 2.4.5) and stained for both the CB receptors using ICC (described in section 2.4.6).

3.3.5 LCMS-MS analysis of endocannabinoid concentration in normal and injured artery segments

Murine aorta was dissected, cleaned of adherent tissue and rinsed free of blood and the vessel cut into 3 segments. Segment 1 functioned as the fresh tissue control and was placed immediately in liquid nitrogen and stored at -80°C until subsequent analysis. Segment 2 was placed in culture for 14 days (as described in section 2.4.3), the tissue was then rinsed free of media with PBS, flash frozen in liquid nitrogen then stored at -80°C. Segment 3 was injured intraluminally (as described in section 3.3.2.3) prior to placing in culture for 14 days. The tissue was then rinsed free of media using PBS, flash frozen in liquid nitrogen, then transferred to -80°C. Frozen samples were then transported to the department of Medicine and Therapeutics at Aberdeen University where the LCMS-MS analysis of AEA and 2-AG levels was performed by Mr Gary Cameron. All samples were homogenised as detailed in section 2.8.1. Tissue homogenates and standards were all supplemented with 60pM d4-Anandamide which functioned as the internal standard. d-4-anandamide is anandamide which has had four of the hydrogen atoms on the ethanolamine portion of the molecule replaced with deuterium atoms (deuterium is a stable isotope of hydrogen with an extra neutron in the nucleus for example H mass =1, D mass =2), d4-AEA was synthesised at Aberdeen University. Samples were then analysed using the LCMS-MS conditions detailed in method section 2.8.2.

3.3.5.1 Production of the endocannabinoid standard curve

A standard of known concentration was analysed by measuring the area of the peak produced by the standard (shown in Figure 3.3A), and the area of the peak produced by the internal standard (shown in Figure 3.3 B). The area ratio was then calculated as shown below.

$$\text{Area ratio of standard} = \frac{\text{Area of AEA standard peak (Figure 3.3A)}}{\text{Area of internal standard peak (Figure 3.3B)}}$$

This was then plotted against the concentration of the known standards producing a standard curve as shown in Figure 3.3C. The standard curve allowed the concentrations of unknown samples to be calculated from their area ratios.

3.3.5.2 Normalisation of endocannabinoid concentration

To allow accurate comparison of samples, results were normalised in accordance to their individual protein concentration (as established by Bradford Assay) to a uniform 1mg/ml as shown below.

$$[\text{Endocannabinoid}] \text{ at } 1\text{mg/ml} = \frac{1}{[\text{Protein of sample}]} \times [\text{endocannabinoid}]$$

3.4 Data Analysis

Outliers were determined by using the Grubs test. Statistical analysis was carried out using a one-way analysis of variance (ANOVA) with a Dunnetts post test (GraphPad Prism 4) unless otherwise stated, significance was accepted when $P < 0.05$

3.5 Antibodies

- α -SMA (Abcam): Stored in aliquots at -20°C , diluted before use to 1:100 in PBS.
- CB_1 (Abcam): Stored in aliquots at -20°C , diluted to 1:500 in PBS (section 3.5.4.)
- CB_2 (Abcam): Stored in aliquots at -20°C , diluted to 1:1000 in PBS (section 3.5.5)

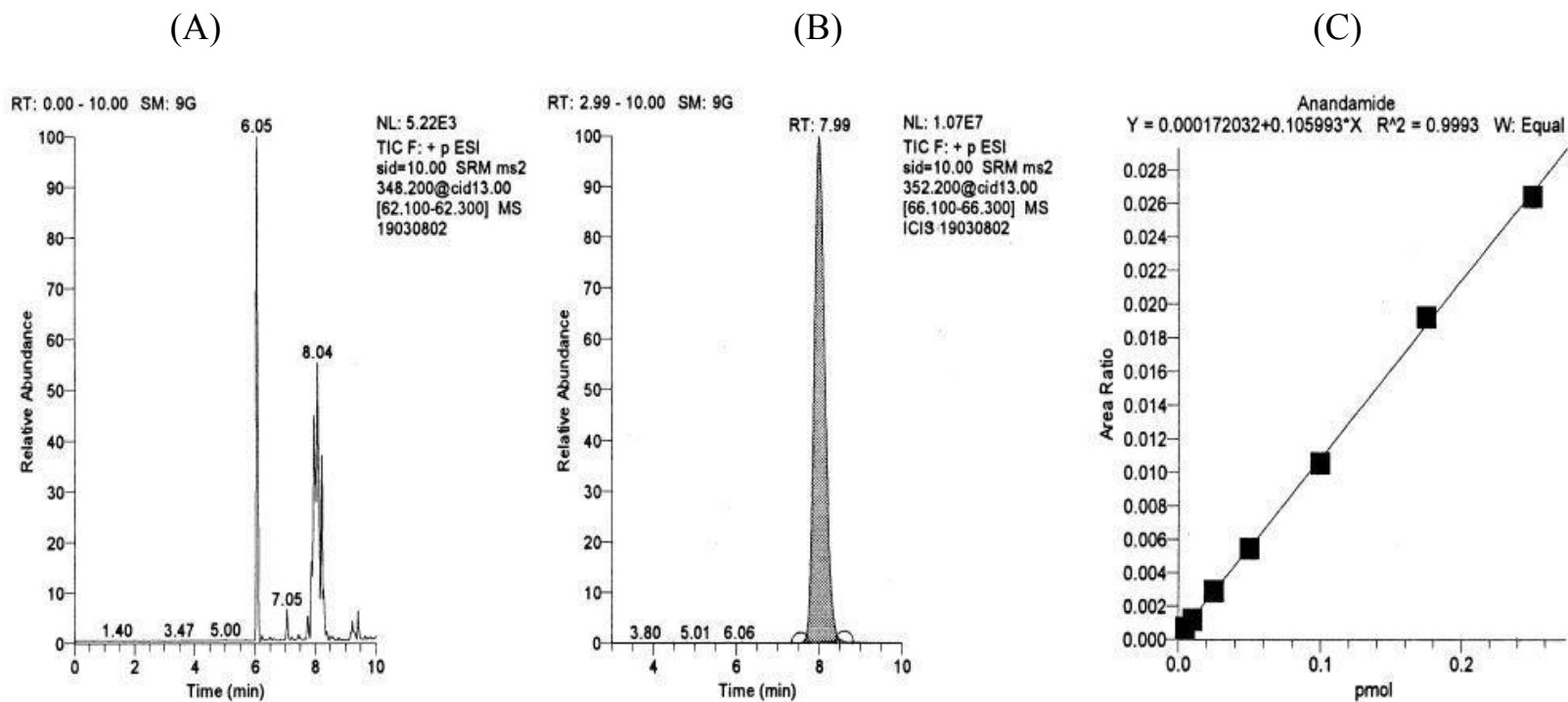


Figure 3.3 Original LCMS-MS chromatograms of standards used to produce the standard curve. Example chromatograms showing (A) the peak produced by a standard sample, (B) the peak produced by the internal d4-Anandamide standard, and (C) the standard curve produced when all the standards were calculated as area ratios and plotted against concentration.

3.6. Results

3.6.1 Morphological assessment of *in vitro* models of neointimal formation in the murine aorta

3.6.1.1 Morphology of control uncultured vessels

Histological staining with H&E highlights the morphology of an uncultured control transverse vessel section (Figure 3.4). It can be seen that the IEL is intact and that the media is organised by highly convoluted layers of elastin. The EEL can also be visualised surrounded by a very thin layer of adventitia.

3.6.1.2 Morphological changes following injury induced by vessel ligation

The first method implemented to induce vessel injury was the placement of a ligature prior to vessel culture. At 100 μ m (Figure 3.5A) from the ligature there was no apparent signs of injury, however at 75 μ m from the ligature visible signs of injury could be observed. It can be seen (Figure 3.5B) that at localised areas of the vessel there is substantial medial thickening and disruption of the organised convoluted layers of elastin. Adventitial thickening can also be observed at the same location. At 50 μ m from the ligature (Figure 3.5 C), signs of vessel disruption become more apparent, it can be seen that at localised areas the media is thicker and that adventitial width has increased. Cell outgrowth from the adventitia can also be observed. At 25 μ m from the ligature it can be seen that the vessel lumen is nearly occluded. Again medial thickening can be observed but most obvious is the substantial adventitial thickening occurring at localised areas round the vessel. Upon inspection of the adventitial areas it can be seen that the cellular matter is contained within a very definite cellular boundary. At 25 μ m from the ligature, similar to all other distances measured, there was no cell growth towards the lumen and the IEL remained intact. Analysis of the morphological changes produced by the ligature induced injury model in vessels originating from 3 different mice (Table 3.1) show that if any changes in vessel morphology occurred with this model, they were confined to medial and adventitial thickening; neointimal formation was not observed in any of the samples.

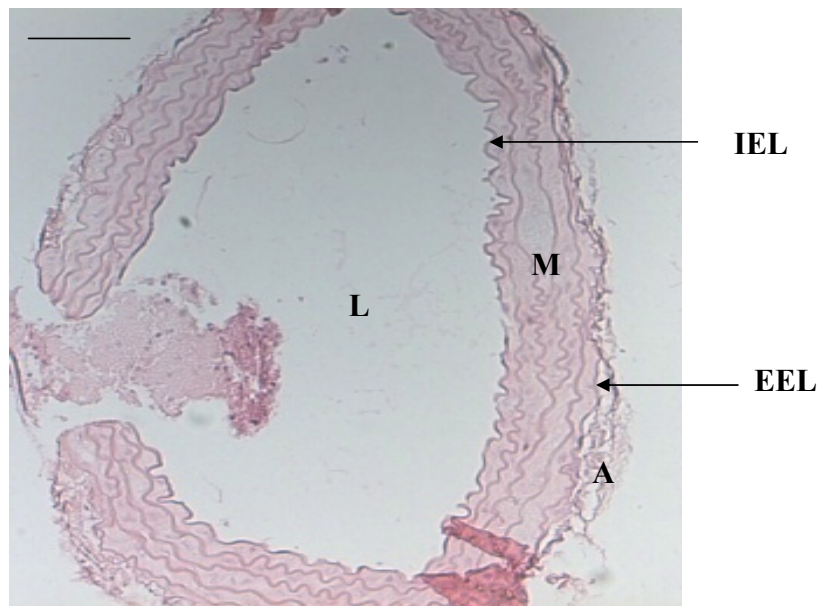


Figure 3.4 A transverse section of a control non cultured murine aorta. Light micrograph (x200) of a transverse section of fresh, uncultured control tissue. The section is stained with H & E demonstrating physiological morphology. IEL=internal elastic lamina, M=media, EEL=external elastic lamina, A=adventitia, L=lumen. Black line represents 50 μ m.

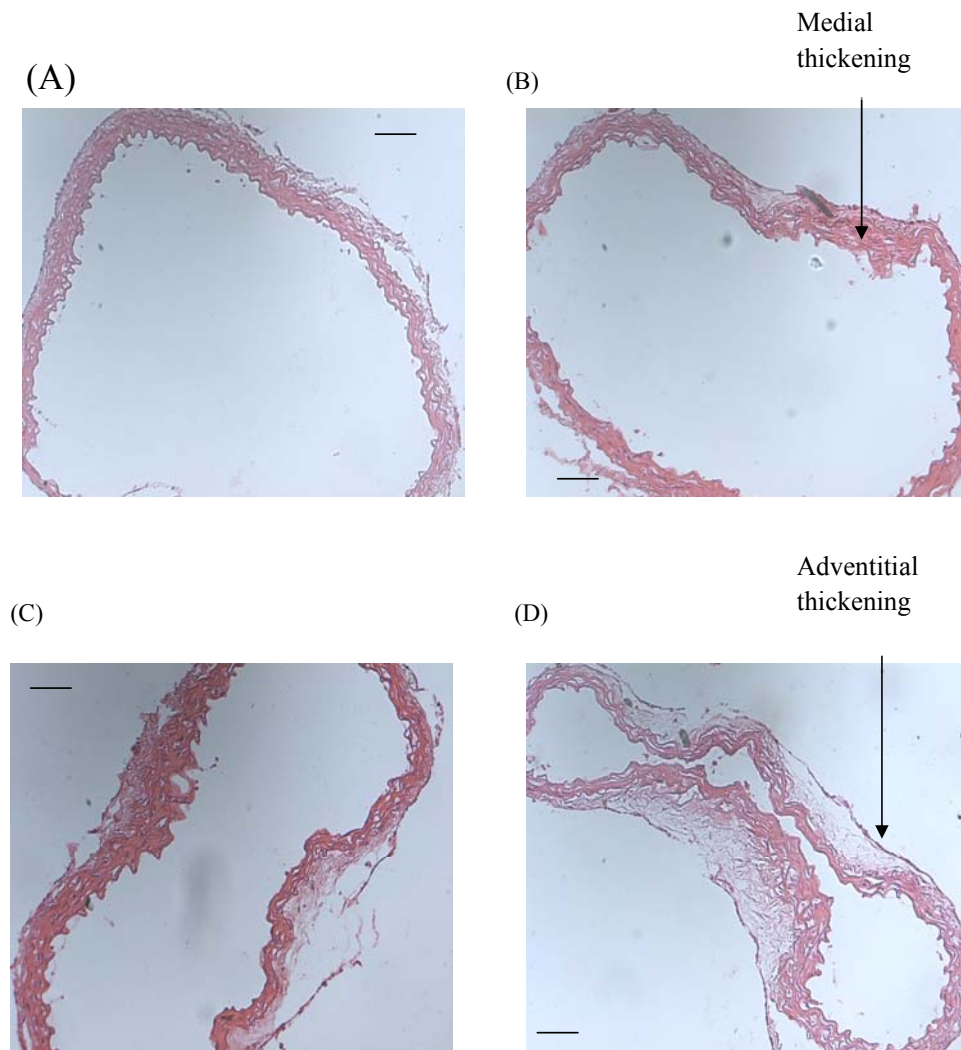


Figure 3.5 Sections of murine aorta injured by placement of a ligature. Light micrographs (x100) showing transverse sections of murine aorta which had been injured by placement of a ligature prior to vessel culture. Micrographs are shown at decreasing distances from the ligature (A) 100µm from ligature (B) 75µm from ligature (C) 50µm from ligature and (D) 25µm from ligature. Sections are stained with H & E. Black lines represent 50µm.

Comment [c14]: You could put in some arrows indicating the key changes you have identified in the text rather than leaving the reader to work it out for themselves.

	Medial Thickening	Rupture of IEL	Neointimal Growth	Adventitial thickening
Sample 1	N	N	N	N
Sample 2	Y	N	N	Y
Sample 3	Y	Y	N	Y

Table 3.1 The morphological changes observed following ligature induced vessel injury

Aortas originating from three different mice had a ligature placed round them and were cultured for 14 days. The vessels were serial sectioned, then at a distance of 25µm from the ligature four markers of vessel injury were examined, (i) media thickening, (ii) rupture of the IEL, (iii) neointimal growth and finally (iv) adventitial thickening. n=3. Due to the small sample size and the lack of neointimal response these were not quantified.

Comment [c15]: You need to put a statement in here somewhere about why this was not quantified – insufficient numbers?

3.6.1.3 Morphological changes induced by culture

The second method implemented to induce neointimal formation was by placing the aortic sections in culture for 14 days, as this has previously been shown to induce neointimal growth in porcine arteries (Work PhD thesis, University of Strathclyde 1999). Histological staining with H&E highlighted the morphology of the vessel to be highly disrupted, possessing many characteristics of vessel remodelling. An example of these changes is illustrated in Figure 3.6. Marked cell infiltration into the luminal space was observed and, in vessels where the IEL was ruptured, the layers of elastin in the media appeared disorganised and damaged. Medial thickening and adventitial thickening was also frequently observed, with the adventitial thickening contained within the confinement of a well defined cellular boundary. The morphological changes observed in six different mice are shown in Table 3.2. It can be seen that vessels from 4 of the 6 mice displayed medial thickening and rupture of the IEL; however neointimal growth was only observed in 3 of the 6 vessels. Adventitial thickening was observed in 5 of the 6 vessels investigated.

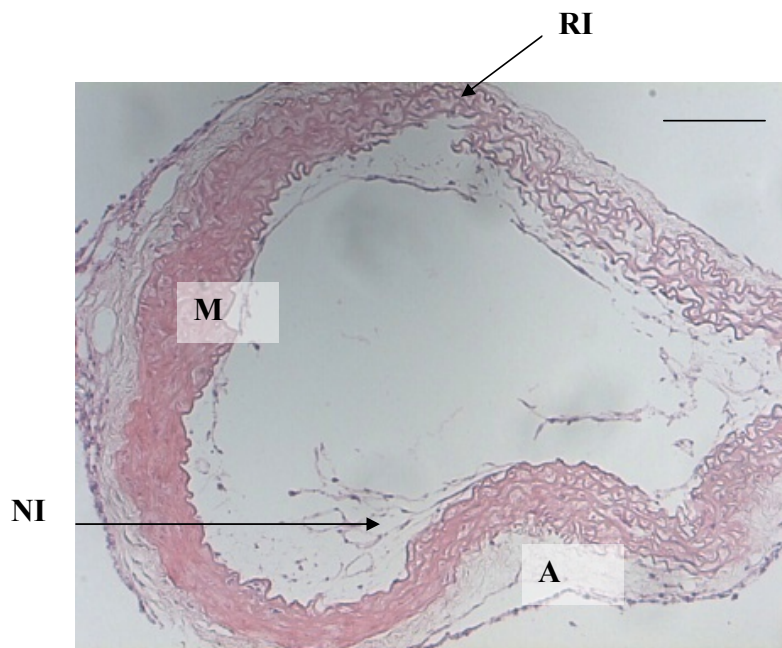


Figure 3.6 A transverse section of a cultured murine aorta. Light micrograph (x200) of a transverse section of aorta that had been cultured for 14 days and stained with H&E. M = media, NI=Neointima, A=Adventitia, RI=Ruptured internal elastic lamina. Black line represents 50µm.

	Medial Thickening	Rupture of IEL	Neointimal Growth	Adventitial Thickening
Sample 1	Y	Y	Y	Y
Sample 2	Y	Y	N	Y
Sample 3	Y	N	N	N
Sample 4	Y	N	Y	Y
Sample 5	N	Y	N	Y
Sample 6	N	Y	Y	Y

Table 3.2 The morphological changes observed following vessel culture. Vessels originating from six different mice were cultured for 14 days then analysed for four markers of vessel injury, media thickening, rupture of the IEL, neointimal growth and finally adventitial thickening.

3.6.1.4 Morphological changes induced by intraluminal wire injury

The third method of injuring vessels to induce an injured response was to rub the luminal surface of the vessel with stainless steel wire then place them in culture for 14 days. Histological staining with H&E highlighted the morphology of the wire injured vessel to be highly disrupted, possessing many characteristics of vessel injury (an example is illustrated in Figure 3.7) including cell infiltration into the lumen. However, the appearance of the cells within the lumen was unlike that reported for neointima observed in established models, in that the cells occupied most of the lumen in a network like fashion. The vessels also demonstrated substantial medial thickening. In the example shown in Figure 3.7, one area of the vessel had folded inwards, in this area the elastin layers were less convoluted and there is significant adventitial cell growth. Assessment of the response to wire injury in vessels from four different mice demonstrated that medial thickening, rupture of the IEL and neointimal growth occurred in all vessels and adventitial thickening was present in all but one vessel (Table 3.3).

3.6.2 Quantitative comparison of injury produced by culture with and without wire injury

3.6.2.1 Medial area and thickness

Both cultured and injured/cultured vessels demonstrated increases in both medial thickness and area compared to non-cultured control arteries (Figure 3.8). Vessel sections that had been injured prior to culture exhibited the largest increase in area from $0.067 \pm 0.004 \text{mm}^2$ (uncultured control $n=4$) to $0.124 \pm 0.024 \text{mm}^2$ (wire injured). Despite both culture alone and prior injury resulting in increased medial areas the differences did not reach significance (One way ANOVA with Dunnett's post test $P=0.0858$ $n=3$ and 4 respectively). Medial thickness was also increased from $0.04 \pm 0.001 \text{mm}$ (uncultured control $n=4$) to $0.11 \pm 0.043 \text{mm}$ in cultured tissue ($n=3$) and $0.076 \pm 0.005 \text{mm}$ in injured/cultured arteries, $n=4$ (Figure 3.9). Once again these changes failed to reach statistical significance (One-way ANOVA with Dunnett's post test).

3.6.2.2 Adventitial area and thickness

Adventitial area was increased in both tissue that had been cultured ($0.04 \pm 0.005 \text{mm}^2$ $n=3$) and injured prior to culture ($0.09 \pm 0.04 \text{mm}^2$ $n=4$) compared to the uncultured control ($0.03 \pm 0.007 \text{mm}^2$ $n=4$; Figure 3.10) although these changes did not reach statistical significance (One-way ANOVA with Dunnett's post test $P=0.1961$). Adventitial thickness was also increased in tissue that had been cultured ($0.063 \pm 0.02 \text{mm}$, $n=3$) and injured prior to culture ($0.09 \pm 0.03 \text{mm}$ $n=4$) compared to the uncultured controls ($0.02 \pm 0.002 \text{mm}$, $n=4$; Figure 3.11). Despite this apparent increase in adventitial thickness this did not reach statistical significance (One-way ANOVA with Dunnett's post test $P=0.1455$).

Comment [c16]: Karen – I suggest you move some of the figures so that they are closer to the text describing them – all micrograph figures and associated tables should come before you move on to the quantification section.

3.6.2.3 Neointimal area

As expected, no neointima was present in uncultured control vessels. However, tissues that were either cultured or subjected to injury prior to culture both produced a measurable neointima (Figure 3.12). Wire injured tissue produced a neointima that was marginally larger than that produced by cultured tissue (0.052 ± 0.023 and 0.03 ± 0.016 respectively; $P>0.05$ One-way ANOVA with Dunnett's post test $n=4$ and 3 respectively).

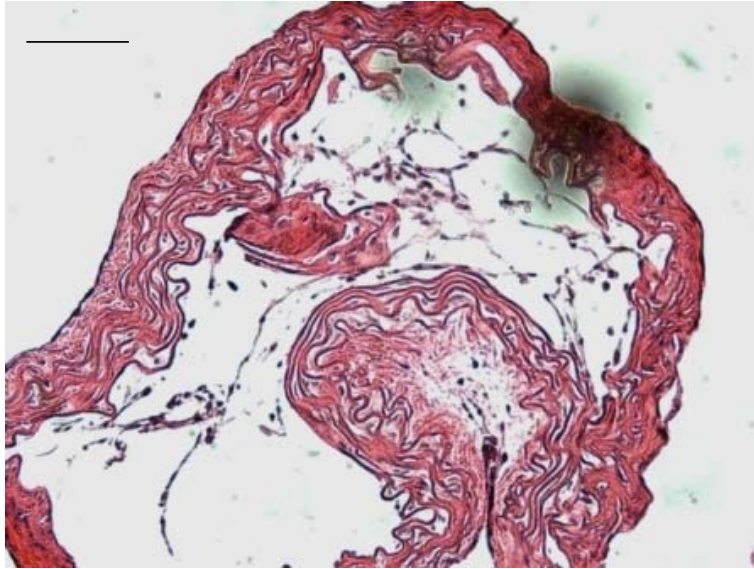


Figure 3.7 A transverse section of aorta following wire injury. Light micrograph showing a section of aorta that had been injured intraluminally by a wire prior to culture; the section has been stained with H&E. Magnification x200. Thin black line represents 50µm.

	Medial Thickening	Rupture of IEL	Neointimal Growth	Adventitial Thickening
Sample 1	Y	Y	Y	N
Sample 2	Y	Y	Y	Y
Sample 3	Y	Y	Y	Y
Sample 4	Y	Y	Y	Y

Table 3.3 The morphological changes observed following vessel injury. Vessels originating from six different mice were injured intraluminally with wire then cultured for 14 days. The sections were stained with H&E and analysed for four markers of vessel injury; media thickening, rupture of the IEL, neointimal growth and adventitial thickening.

Comment [c17]: Changes all legends to match

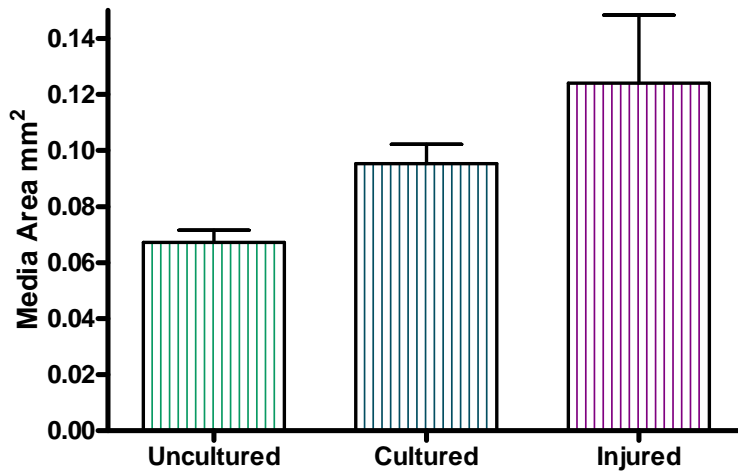


Figure 3.8 Medial area of control, cultured and injured aortic tissue. Tissue sections were either fixed immediately following dissection (uncultured control), cultured for 14 days or injured then cultured for 14 days. Values are mean + SEM; n=4 for uncultured and injured, n=3 for cultured.

Comment [c18]: Make similar changes in punctuation etc in other legends.

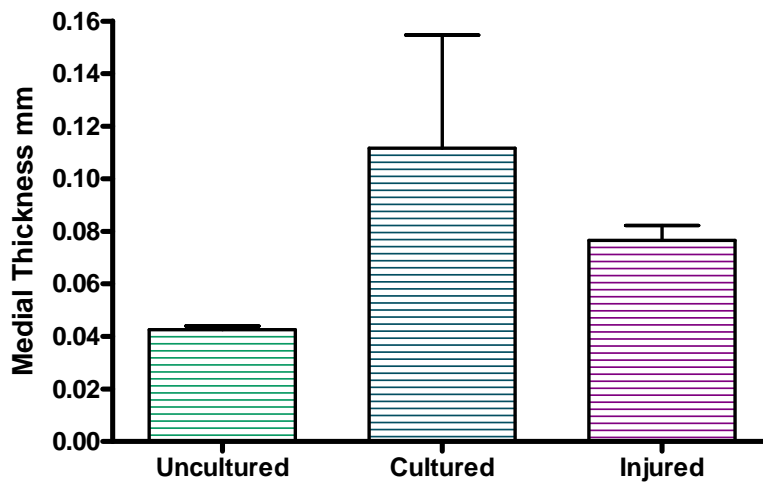


Figure 3.9 A comparison of medial thickness of control, cultured and injured aortic tissue. Tissue sections were either fixed immediately following dissection (uncultured control), cultured for 14 days or injured then cultured for 14 days. Values are mean + SEM; n=4 for uncultured and injured, n=3 for cultured.

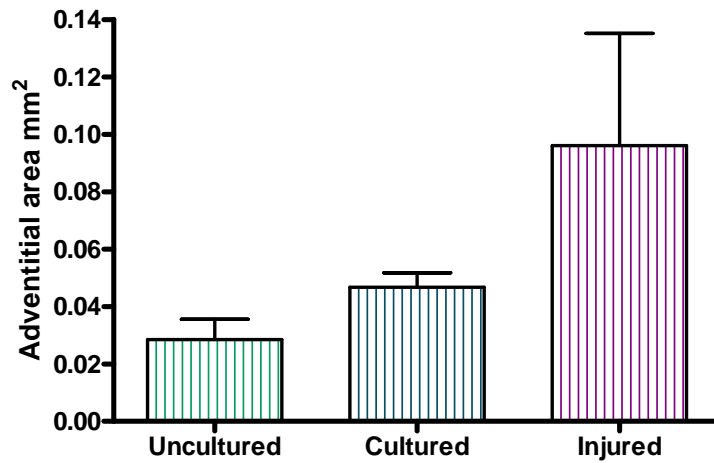


Figure 3.10 A comparison of adventitial area of control, cultured and injured aortic tissue.

Tissue sections were either fixed immediately following dissection (uncultured control), cultured for 14 days or injured then cultured for 14 days. Values are mean + SEM; n=4 for uncultured and injured, n=3 for cultured.

Comment [c19]: Make similar changes in punctuation etc in other legends.

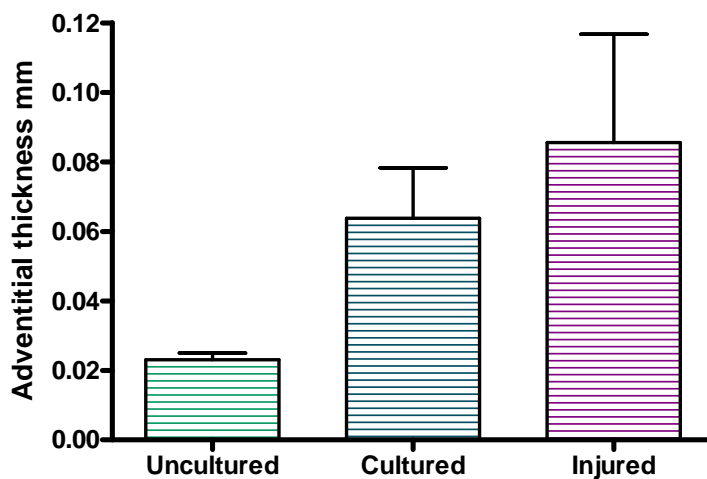


Figure 3.11 A comparison of adventitial thickness of control, cultured and injured aortic tissue.

Tissue sections were either fixed immediately following dissection (uncultured control), cultured for 14 days or injured then cultured for 14 days. Values are mean + SEM; n=4 for uncultured and injured, n=3 for cultured.

Comment [c20]: Make similar changes in punctuation etc in other legends.

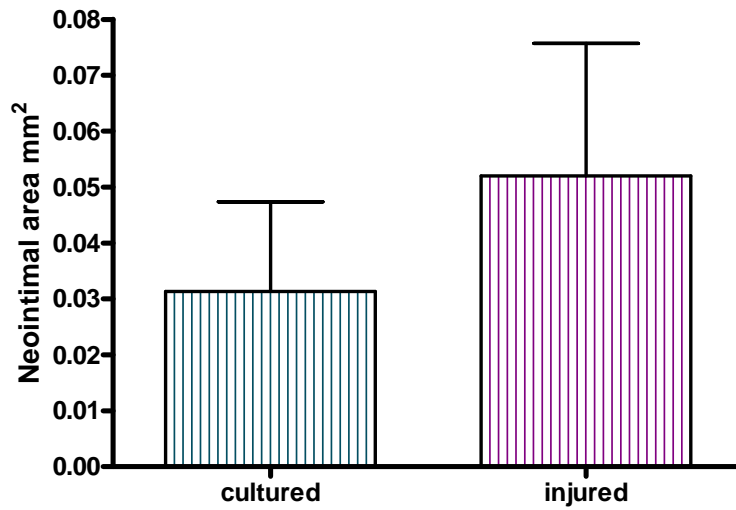


Figure 3.12 A comparison of neointimal area of cultured and injured aortic tissue. Tissue sections were either cultured for 14 days or injured then cultured for 14 days. Values are mean + SEM; n=4 for injured, n=3 for cultured.

Comment [c21]: Make similar changes in punctuation etc in other legends.

3.6.3 Vessel characterisation

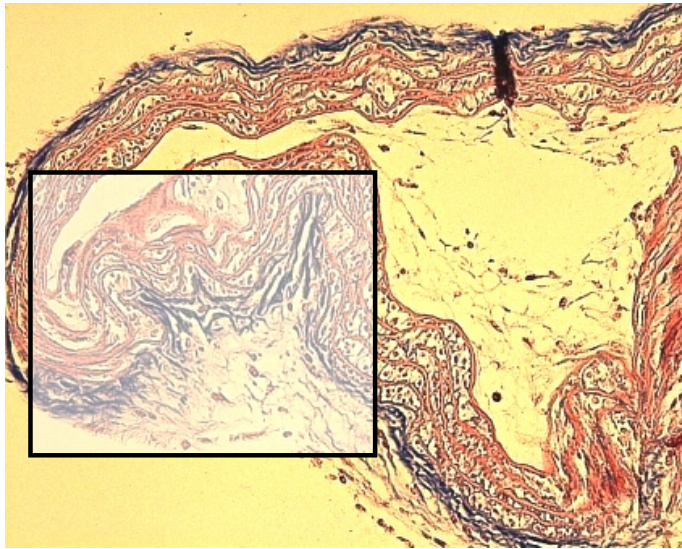
3.6.3.1 Cellular composition of injury response

To identify the cells involved in the injury response produced in the murine aorta, sections were stained with Masson Trichrome, which stains extracellular matrix blue, cellular material red, and nuclei black. Figure 3.13 (A) shows a transverse section of wire injured tissue, the thickened media is stained bright red and the adventitia can be clearly visualised by the blue colour. The cells that have infiltrated the lumen are stained a mixture of blue/black and red, giving no clear indications of their identity. The cell growth in the adventitia is stained a mixture of blue and red showing cellular accumulation and the presence of collagen.

In an attempt to precisely identify the location of smooth muscle cells in the injury response produced following wire injury, sections were stained by IHC for α -SMA (a marker of smooth muscle cells). Figure 3.13 (B) clearly shows (by presence of pink/red colour) that smooth muscle cells are most abundant in the media, as evident by the dense red colour. In the area of adventitial thickening a small amount of red staining can be observed indicating that smooth muscle cells are present but not the most abundant cell type, as the majority of the adventitial mass showed no positive staining. The cells present in the lumen exhibit faint red staining in some areas but not in others, indicating that smooth muscle cells may contribute to a small proportion of the neointimal mass but not the majority. This is confirmed in Figure 3.14 (A) and (B) which show that the cellular accumulation which occurs in the lumen and adventitial following culture is a mixture of smooth muscle cells and other unidentified cells.

Comment [c22]: Re-organise figures so that the relevant figures appear before this section of text.

(A)



(B)

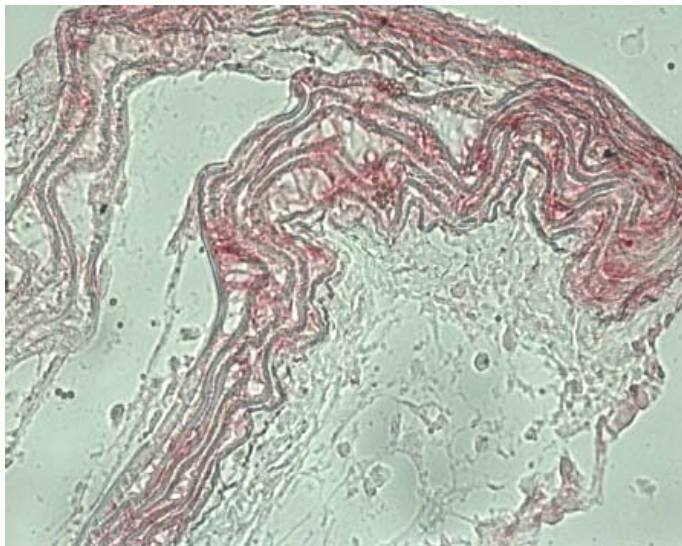
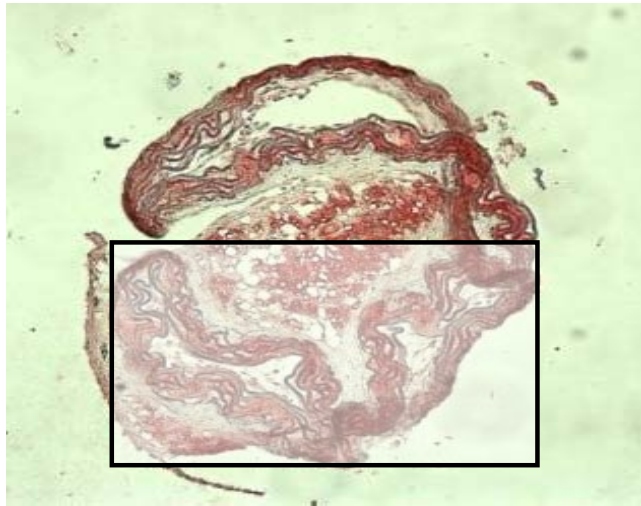


Figure 3.13 Transverse sections of wire injured aorta. Light micrographs showing wire injured aorta sections stained with (A) Masson Trichrome (x200), (red colour indicates muscle, blue indicates collagen and black staining shows cell nuclei), the area shown in black box is that shown in picture B (B) Immunohistochemical staining with α -SMA antibody, positive staining shown by pink/red colour (x400).

(A)



(B)

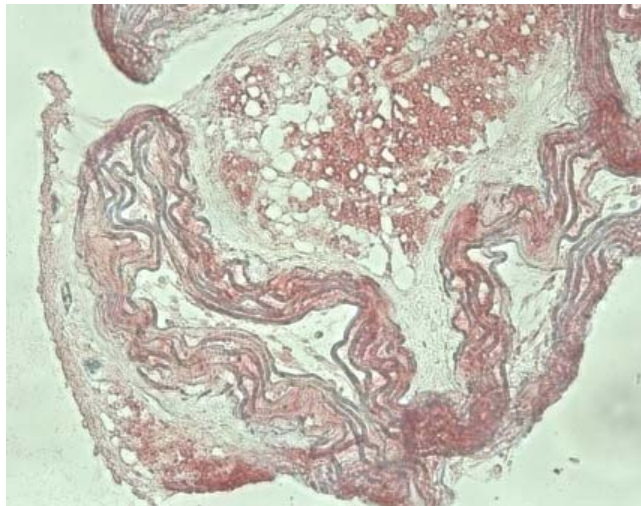


Figure 3.14 A transverse section of a mouse aorta that had been cultured. Light micrographs showing an example of a cultured vessel that had collapsed (A) immunohistological staining with an antibody directed at α -SMA, shows locations of smooth muscle cells, positive staining shown by pink-red colour (x100). Area in black box shown in picture B. (B) Immunohistological staining with α -SMA antibody shows location of smooth muscle cells, positive staining shown by pink-red colour (x200)

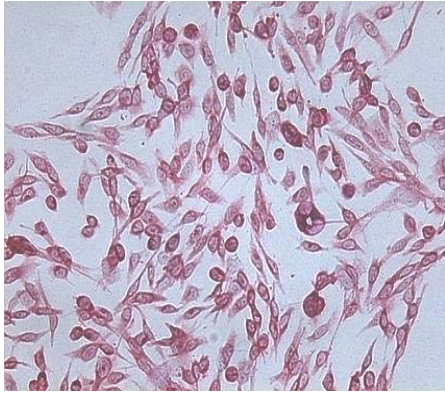
3.6.4 Cannabinoid receptor antibody optimisation

CB₂ transfected CHO cells displayed positive staining (pink/red colour) for CB₁ receptors at antibody dilutions as low as 1:500 (Figure 3.15) for this reason the CB₁ antibody was only used at dilutions of 1:500 or lower. CB₂ transfected CHO cells displayed positive staining (pink/red colour) for CB₂ receptors at antibody dilutions as low as 1:1000 (Figure 3.16), to avoid unspecific binding 1:1000 was identified as the optimum dilution.

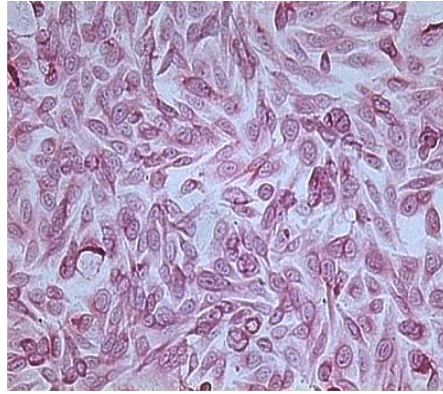
3.6.5 Cannabinoid receptor staining of aortic tissue

Aortic tissue stained by IHC with antibodies directed against the CB₁ and CB₂ receptors, showed positive staining for both receptors (Figure 3.17). It appears from the micrographs that the staining is concentrated in the media although there also appears to be positive staining in the adventitia. This is confirmed in Figure 3.18 which shows murine vascular smooth muscle cells displaying positive staining for both CB₁ and CB₂ receptors.

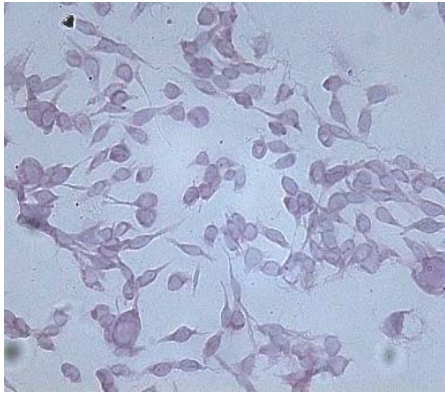
(A)



(B)



(C)



(D)

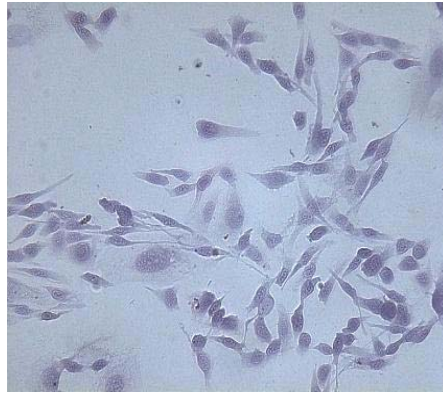
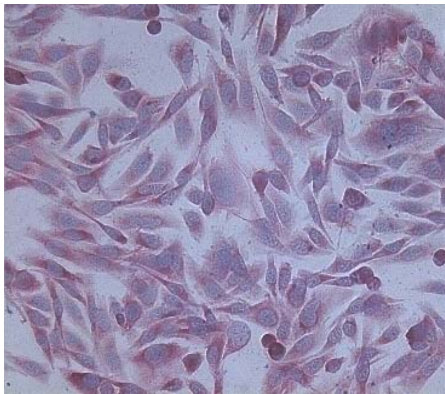
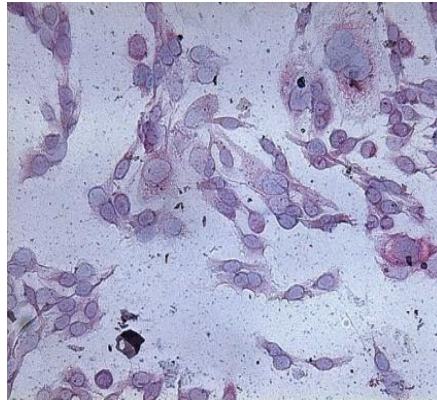


Figure 3.15 Immunocytochemical staining of CB₂ transfected CHO cells with a CB₁ receptor antibody. Light micrographs (x200) of CB₂ transfected CHO cells stained with CB₁ antibody at (A) 1:50 dilution, (B) 1:100 dilution (C) 1:500 dilution (D) IgG 1:50

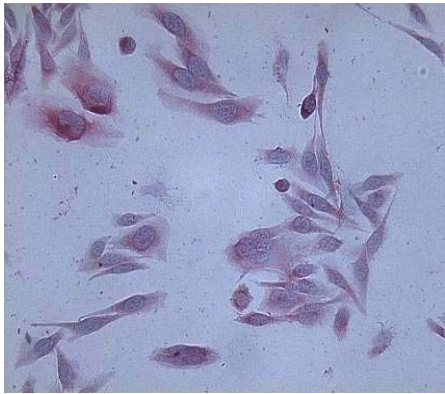
(A)



(B)



(C)



(D)

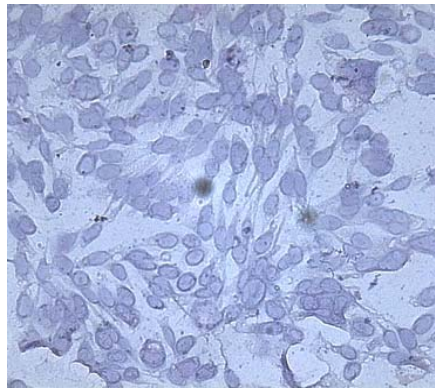
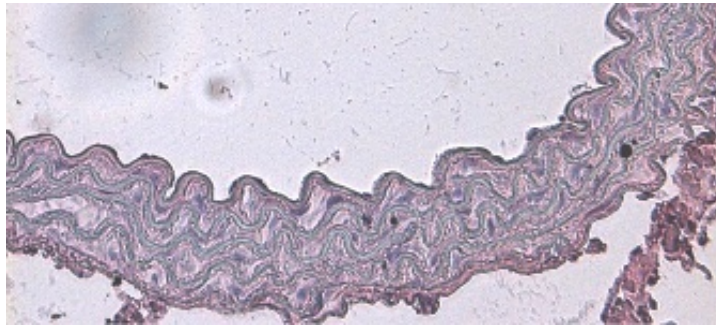


Figure 3.16 Immunocytochemical staining of CB₂ transfected cells with a CB₂ antibody. Light micrographs (x200) of CB₂ transfected CHO cells stained with a CB₂ antibody at (A) 1:500 dilution (B) 1:700 dilution (C) 1:1000 dilution (D) 1:5000 dilution positive staining shown by pink/red colour.

(A)



(B)



(C)

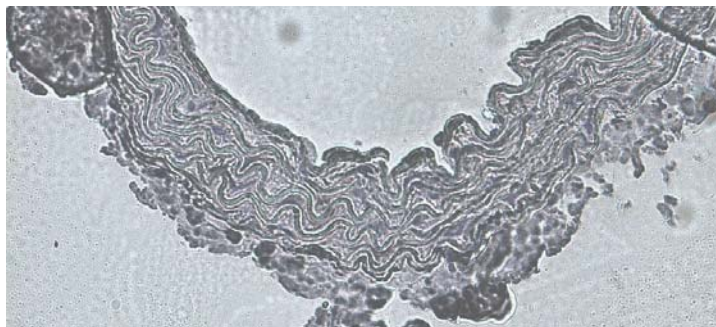
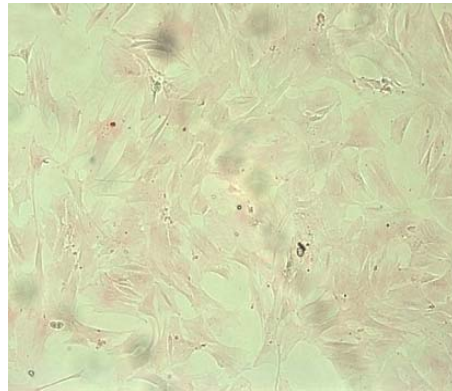
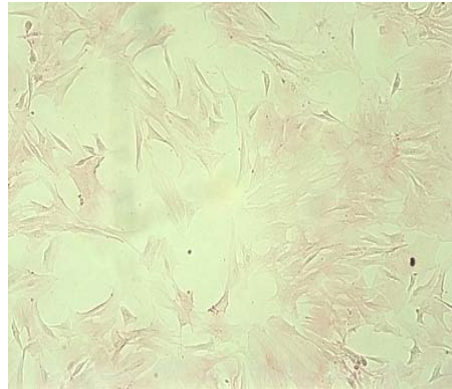


Figure 3.17 Immunohistochemical staining of uncultured aortic tissue for cannabinoid receptors. Light micrographs (x200) of murine aortic uncultured tissue stained with (A) CB₁ receptor antibody at 1:500 dilution. (B) CB₂ antibody at 1:1000 dilution. Pink/red colour indicates positive staining. (C) Negative IgG control 1:500

(A)



(B)



(C)



Figure 3.18 Immunocytochemical staining of murine aortic smooth muscle cells for both the CB₁ and CB₂ receptors. Light micrographs (x100) of murine vascular smooth muscle cells stained with either (A) CB₁ antibody (1:700) or (B) CB₂ antibody (1:1000) positive staining shown by pink/red colour (C) negative IgG control.

3.6.6 LCMS-MS analysis of AEA concentration.

Anandamide concentration was increased in tissue that had been cultured compared to the uncultured control tissue ($0.22\pm 0.03\text{pM/mg}$ of protein and $0.03\pm 0.004\text{pM/mg}$ of protein, respectively $n=6$). The concentration of AEA was increased further in tissue that had been wire injured prior to culture ($1.08\pm 0.72\text{pM/mg}$ of protein $n=4$). Due to the presence of a sample that was close to being excluded as an outlier, the increase in AEA concentration between samples did not reach significance (One-way ANOVA with Dunnett's post test $P>0.05$).

3.6.7 LCMS-MS analysis of 2-AG concentration

2-AG concentration was significantly increased in tissue that had been cultured compared to control tissue ($358.8\pm 52.5\text{pM/mg}$ of protein and $0.2\pm 0.04\text{pM/mg}$ of protein respectively $n=6$, Figure 3.22); there was a further significant increase in 2-AG concentration between samples that had been cultured and those that had been injured prior to culture ($358.8\pm 52.5\text{pM/mg}$ of protein and $697.4\pm 213.5\text{pM/mg}$ of protein, respectively; $P<0.05$; One way ANOVA with Dunnett's post test $n=4$ for injured tissue).

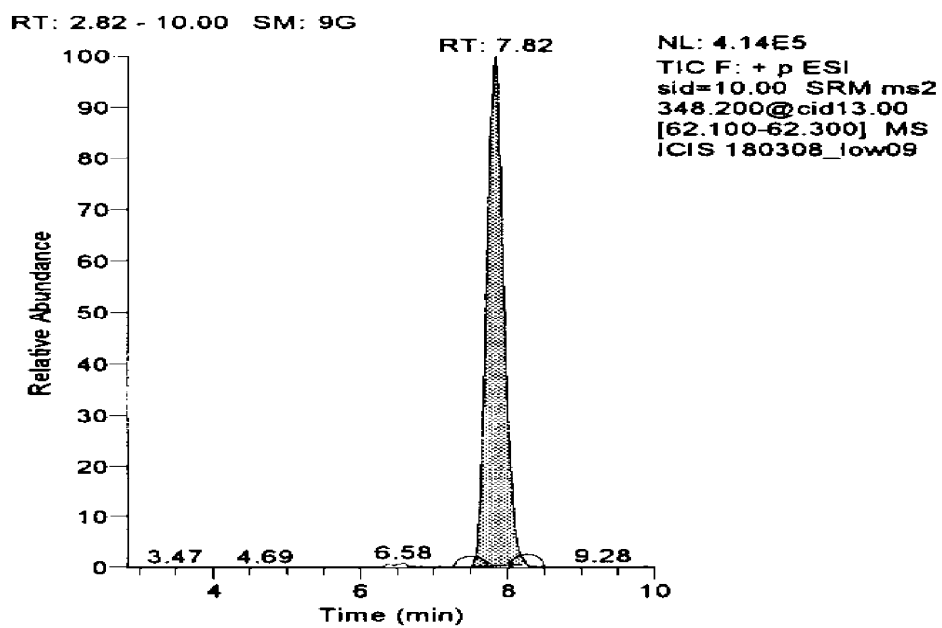


Figure 3.19 An original LCMS-MS chromatogram showing the AEA peak. The trace illustrates the peak produced by AEA following LCMS-MS analysis of a tissue sample. The shaded area was measured to calculate the concentration of AEA in the sample.

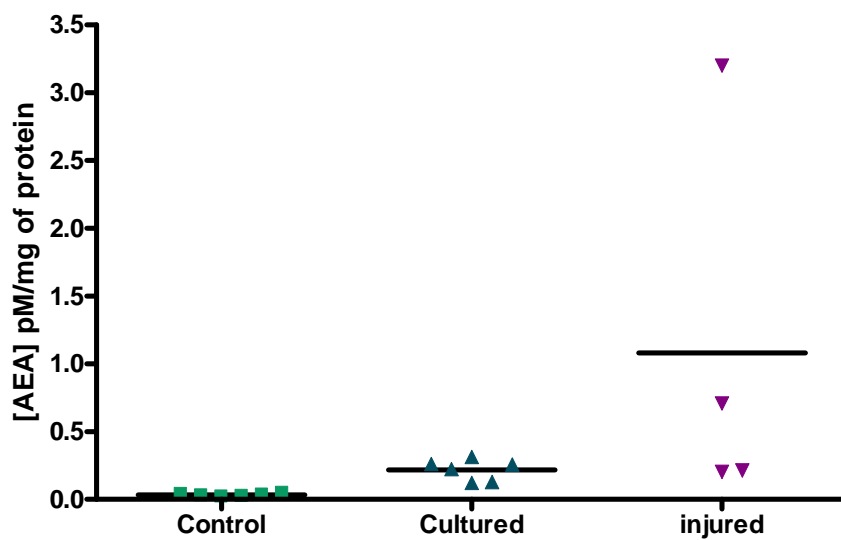


Figure 3.20 AEA concentration in aortic tissue sections. Tissue sections were either frozen immediately following dissection (uncultured control), cultured for 14 days or injured then cultured for 14 days. Anandamide concentration was then measured using LCMS-MS. n=6 for control and cultured, n=4 for injured tissue.

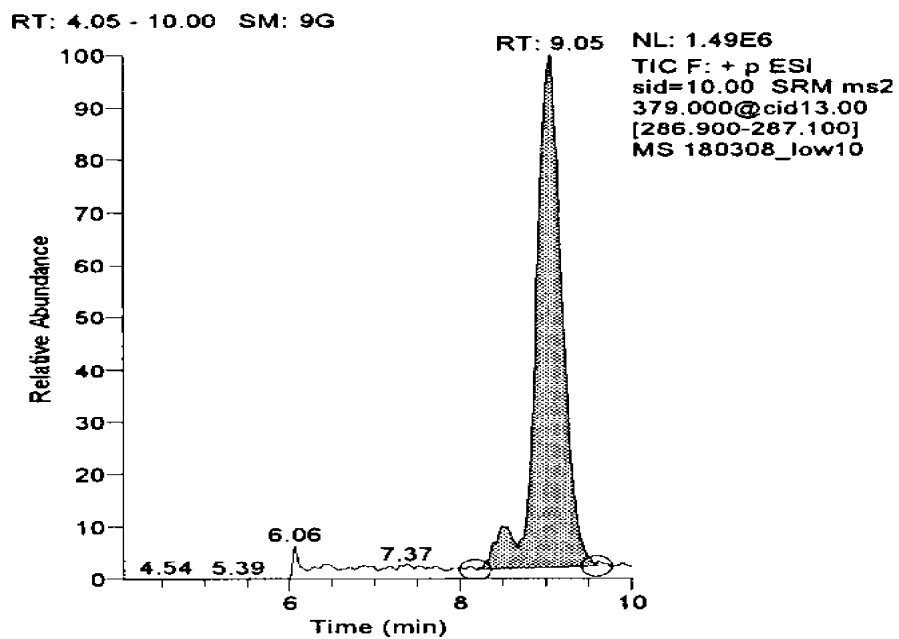


Figure 3.21 An original LCMS-MS chromatogram showing the 2-AG peak. The trace illustrates the peak produced by 2-AG following LCMS-MS analysis of a tissue sample. The shaded area was measured to calculate the concentration of 2-AG in the sample.

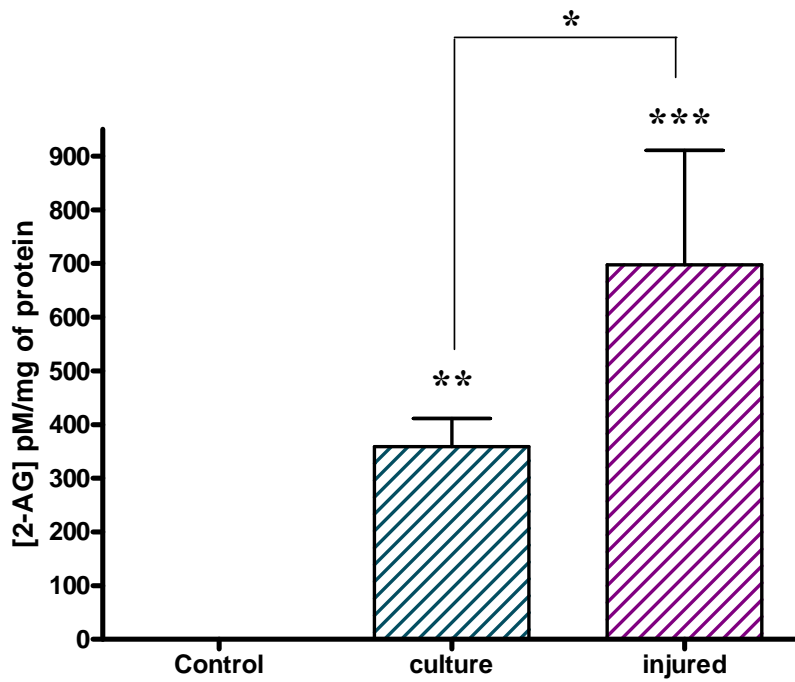


Figure 3.22 2-AG concentration in aortic tissue sections. Tissue sections were either frozen immediately following dissection (uncultured control), cultured for 14 days or injured then cultured for 14 days. 2-AG concentration was measured using LCMS-MS. n=6 for control and cultured, n=4 for injured tissue. Data shown as mean \pm SEM * Indicates $P < 0.05$, * indicates $P < 0.01$, *** indicates $P < 0.001$ compared to control (one way ANOVA with a Dunnetts post test).

3.7 Discussion

The aim of this study was to (i) develop a murine organ culture model of neointimal formation that could allow the investigation of the effects of cannabinoid agents (ii) characterise the injury response produced and investigate the presence and location of cannabinoid receptors, and to (iii) investigate whether the endocannabinoid system becomes activated in this model of vessel injury. It can be seen from the results of this study, that a successful reproducible model of vessel injury can be established in the murine aorta, by culturing vessel sections following luminal injury with stainless steel wire. The injury response produced by the murine aorta manifests as cellular growth in the intima, media thickening and adventitial thickening. This study has also confirmed the presence of both CB₁ and CB₂ receptors on the murine aorta and on smooth muscle cells. This study has also demonstrated that endocannabinoid concentration is significantly increased (2-AG) in injured tissue.

Murine aortic organ culture

Placement of a ligature round the carotid arteries of mice is a common method of inducing reproducible neointimal formation *in vivo* (Moura *et al.*, 2007; Wang *et al.*, 2007). For this reason it was the first method to be investigated for the organ culture model. Tying a ligature round the mouse aorta then placing it in culture for 14 days, did not prove to be a suitable injury model; the injury response produced was primarily adventitial thickening, with some localised medial thickening, and proved to be nonreproducible. *In vivo* this model is successful due to the reduction in vessel diameter and blood flow, and the resulting changes in shear stress (Hui *et al.*, 2008), these factors are obviously not present in an organ culture model and may therefore explain the failure of this method.

Culturing vessels produced a measurable injury response, which included the presence of cells in the lumen, medial thickening, and adventitial thickening. This response was more reproducible than the ligature model. Endothelial denudation by mechanical injury is also a common method of inducing neointimal formation *in vivo*. To emulate this method, vessels were injured with wire prior to culture. This method provided a reproducible injury response that included medial thickening, neointimal growth, and adventitial thickening. Comparison of the two methods showed that injuring the vessels prior to culture produced the largest increases in medial area, adventitial area and thickness, and neointimal area, for that reason it was considered the optimum method. Despite the results being reproducible and exhibiting small standard errors the differences in areas and thickness did not reach significance, most likely due to the small group size.

When the neointima produced in this model is compared to neointima produced in *in vivo* models, it can be seen that there is a notable difference in appearance. In established *in vivo* models, neointimal cells invade the lumen as a compact cellular mass (Moura *et al.*, 2007; Wang *et al.*, 2007), whereas the neointima produced in the murine organ culture preparation spreads out with a diffuse lattice-like appearance, in some cases completely filling the lumen. Interestingly, when the neointima produced in the murine culture model is compared to that produced in the porcine organ culture model, similarities in the appearance can be observed, in that the neointima appears more sparse in cell density (Yau *et al.*, 2008). It is assumed that the cells infiltrating the lumen are smooth muscle cells, although this is not completely confirmed in this study. Masson Trichrome staining highlighted cellular material along with extracellular matrix in the lumen, faint staining for α -SMA could also be observed. Together these findings suggest that smooth muscle cells migrate to the lumen then secrete extracellular matrix to form the lattice-like network observed in the lumen.

The most pronounced marker of injury that occurred in all three models investigated in this study was adventitial thickening. The adventitia was originally thought to function as purely a structural component, having little importance in the vascular response to injury; however recent evidence has challenged this. It has been shown that functional changes in the adventitia can contribute to coronary artery bypass vein graft failure and neointimal formation following angioplasty, through the activation, differentiation, and migration of adventitial fibroblasts (Siow *et al.*, 2007; Zalewski *et al.*, 1997; Li *et al.*, 2000; Shi *et al.*, 1996). Factors which are thought to activate the adventitial response include increased growth factor release, increased extracellular matrix production, and the accumulation of progenitor cells (Shi *et al.*, 1996; Shi *et al.*, 1997; Torsney *et al.*, 2005). Despite this, the importance of adventitial derived fibroblasts in neointimal formation is controversial, with different laboratories and varying experimental techniques producing conflicting evidence. For example, it has been shown that adventitial fibroblasts migrate to the lumen and contribute to the neointimal mass in both rodents and pigs. In the latter adventitial fibroblasts have been shown to contribute 86% and 43% of total neointimal cells (Fleenor *et al.*, 2009; Shi *et al.*, 1996; Scott *et al.*, 1996). However in pigs this finding has been contradicted, as a recent study found that adventitial fibroblasts contributed less than 2% to the neointimal cell mass (Fleenor *et al.*, 2009). In the same study it was found that adventitial thickness increased 3 days post angioplasty, suggesting that following injury adventitial fibroblasts proliferate and produce matrix, as opposed to migrating towards the lumen. The adventitial response produced in the present murine organ culture model is not in complete compliance with that described for in *in vivo* models. In this study, it was observed that smooth muscle cells are present in some areas of adventitial thickening, suggesting, that

instead of migrating towards the lumen, the smooth muscle cells are in fact migrating into the adventitia. This suggests that an essential homing signal is lacking in the *in vitro* environment, for example inflammatory mediators or circulatory cells. This is in agreement with findings, that following mechanical injury, leukocytes are essential for intimal growth (Simon *et al.*, 2000; Tanaka *et al.*, 1993; Miller *et al.*, 2001). Circulatory cells such as monocytes are recruited following release of cytokines from platelets, and have been shown to be important in the process of neointimal formation. Experiments inhibiting macrophage infiltration resulted in the abolition of neointimal formation, a reduction in intimal hyperplasia was also observed when cytokine release from platelets was inhibited. These findings highlight the importance of circulatory cells in the process of neointimal formation (Reviewed in Hui *et al.*, 2008).

Cannabinoids and organ culture

This study has demonstrated that both the CB₁ and CB₂ receptors are present on murine vascular smooth muscle cells, as shown by staining of both aortic tissue sections, and sub cultured smooth muscle cells. This is similar to findings in human tissue, where CB₁ and CB₂ receptors have been located on smooth muscle cells (Rajesh *et al.*, 2008; Sugiura *et al.*, 1998). An important finding from this study was the lack of selectivity exhibited by the CB₁ receptor antibody at high concentrations. In this study the use of CHO cells transfected with only the CB₂ receptor were used as a negative control for the CB₁ receptor antibody. ICC staining showed that these cells showed positive staining for the CB₁ receptor at dilutions above 1:500. For this reason this antibody was always used in more dilute concentrations than 1:500. As a similar negative control was not available for the CB₂ receptor, a range of dilutions were investigated and the lowest dilution to show positive staining was decided as optimum. The lack of selectivity of currently commercially available antibodies for cannabinoid receptors has been commented on before, since Rajesh *et al.*, 2008a reported that they could not find any CB₂ receptor antibodies that did not produce positive staining in CB₂ receptor knockout mice. It should be noted however, that the antibody used in that study was different to that used in this present study, they also used their antibody at a concentration of 1:100 which is relatively high and there is no mention of whether or not they investigated a range of dilutions.

Aortic segments that were either cultured, or injured prior to culture, both demonstrated a trend of increasing AEA concentration, respectively. However, due to the presence of a sample that was very close to being removed as an outlier, there was no significant difference between samples (it is noteworthy that if the sample in question was removed, then the difference between the samples is statistically significant; one way ANOVA). When the same sample groups were analysed for 2-AG, a significant increase was observed between both interventions

and the control. There was also a further significant increase between tissues that had been cultured and those that had been injured, which is an important observation as it confirms that the endocannabinoid response produced by the vessel is in fact a response to injury and not a response to culture. These results are similar to findings that 2-AG levels were elevated in a mouse model of atherosclerosis and also that endocannabinoid concentration was increased in patients with coronary artery disease (Sugamura *et al.*, 2009; Montecucco *et al.*, 2009). The findings of this study are thus very important, as they show that the endocannabinoid system in the mouse becomes activated following vessel injury in a similar way to that of human tissue (in terms of increased endocannabinoid concentration), supporting the further use of the mouse as an experimental tool.

It is well established that endocannabinoid concentration increases in tissues in pathological conditions (reviewed recently in Di Marzo, 2008). Endocannabinoids are generally thought to have a protective role in disease states, for example cancer, pain and gastrointestinal disorders. However in reality, experimental evidence surrounding the pathological importance of endocannabinoids is highly conflicting and complex (reviewed recently in Di Marzo 2008; Alpini *et al.*, 2009). Nevertheless, the observation that endocannabinoid concentrations are increased following vessel injury suggests that they must play a role in the injury response, whether it be a positive healing effect or a negative pro-injury effect. Three possible ways in which the endocannabinoid system could influence vascular injury are hypothesised below.

- (1) It is widely accepted that in many vessels AEA elicits a relaxant effect on precontracted arteries *in vitro*, and produces a hypotensive effect *in vivo* although its mechanism of action seems to vary depending on the vessel and species (Reviewed in Hillard, 2000; Randall *et al.*, 2004; Hogestatt *et al.*, 2002). One possibility is that following injury blood vessels synthesise and secrete endocannabinoids to induce vasodilatation.
- (2) As discussed in Chapter 1, it has been established that endocannabinoids can affect cellular proliferation, having both anti and pro- proliferative effects (De Petrocellis *et al.*, 1998; Alpini *et al.*, 2009; Hart *et al.*, 2004). This, along with the recent finding that both a CB₂ agonist and a CB₁ antagonist can inhibit stimulated smooth muscle cell proliferation (Rajesh *et al.*, 2008 a & b), and similar results from this study (Chapter 5), raises the postulation that endocannabinoids are released to combat the proliferative response produced following vessel injury.
- (3) Endocannabinoids have been shown to have an effect on cell migration, although the majority of research has focused on their effect on immune cells where it has been

Comment [c23]: This is the perfect opportunity for you to refer to your own data within the thesis – please do so.

shown that the two endocannabinoids AEA, and 2-AG, can have dissimilar effects. 2-AG has been shown to induce migration in a variety of immune cells (Kishimoto *et al.*, 2003; Walter *et al.*, 2003; Jorda *et al.*, 2002). On the other hand, AEA does not share the pro-migratory profile of 2-AG and only weakly stimulates immune cell migration (Walter *et al.*, 2003; Jorda *et al.*, 2002). Endocannabinoids can also effect migration of cells out with the immune system (Song and Zhong 2000; Blazquez *et al.*, 2003), for example embryonic kidney cells (Song and Zhong 2000) and vascular endothelial cells (Mo *et al.*, 2004) This evidence, along with the recent finding that both a CB₂ agonist and a CB₁ antagonist can inhibit smooth muscle cell migration (Rajesh *et al.*, 2008 A&B), leads to the notion that since cell migration is a pivotal step in neointimal formation, endocannabinoids are released following blood vessel injury to either inhibit or induce cell migration.

Despite the results of this study showing increased production of endocannabinoids following injury, there is no insight as to the location of the source of production. As the vessel is intact in culture there would be endothelial cells present on the intima (although these would be minimal in injured vessels), smooth muscle cells in the media and adventitial fibroblasts and sensory neurones present in the adventitia. It has been shown that endothelial progenitor cells can release both AEA and 2-AG in a basal manner, which is increased following stimulation with TNF- α (Opitz *et al.*, 2007). This is in agreement with an earlier study which shows that human vascular endothelial cells can synthesise and release 2-AG in response to stimulation by thrombin (Sugiura *et al.*, 1998), 2-AG has also been found to be released from the endothelium of bovine coronary arteries (Gauthier *et al.*, 2005). Evidence also suggests that endocannabinoids can be released from sensory neurones, as this has been shown to be the case in the CNS (Di Marzo *et al.*, 1994). Evidence of non-endothelium derived endocannabinoids in the vasculature has come from a study by Rademacher *et al.*, (2005), who showed that endocannabinoid concentration increased in the rat cerebral artery preparations without an endothelium. Therefore, although there is no direct evidence confirming that smooth muscle cells can produce endocannabinoids, the prospect seems likely.

Limitations and further work

A possible limitation to this study may be the strain of mice used. It has been reported that the C57BL/6 strain of mice (the strain used in this study) can be resistant to neointimal hyperplasia following endothelial denudation *in vivo* (Hui *et al.*, 2008). As the organ culture model used in this study was dependant on endothelial denudation induced injury it may explain the unusual neointimal response observed.

Had time allowed it would have been interesting to determine whether cannabinoid receptor expression increased following injury, which could have been assessed by polymerase chain reaction (PCR). It may also have been beneficial to confirm the ability of smooth muscle cells to produce AEA and 2-AG, which could have been done by measuring the concentration of endocannabinoids in conditioned smooth muscle cell medium.

In conclusion it can be seen that the murine organ culture model produces a neointimal response that is both reproducible and quantifiable. Despite the neointima being atypical in appearance, other markers of injury such as increased medial and adventitial thickness could be measured. It can also be concluded that an endocannabinoid system is present, as shown by the presence of both types of cannabinoid receptor, and functional, evidenced by the rise in endogenous cannabinoid concentrations following vessel culture and injury, in the murine vasculature. Together these original findings lead to the hypothesis that endocannabinoids may play a role in the vascular response to injury.

Chapter 4

Functional response of murine blood vessels to AEA

4.1 Introduction

4.1.1 *In vitro* effects of endocannabinoids

The first finding from *in vitro* studies demonstrating that AEA was a direct vasorelaxant came in 1995 from experiments in the rabbit cerebral artery (Ellis *et al.*, 1995). Since then many studies have confirmed that endogenous cannabinoids are vasodilators, however to date there is no real consensus regarding the molecular target or the mechanism of action for these compounds. The confusion over the receptor(s) important in mediating the direct vascular effect of AEA still remains, due to the variation in the responses produced by AEA, both between species and also between vessels of the same species. For example, AEA produces relaxation in the rat hepatic artery but not in the rat carotid artery or aorta (Zygmunt *et al.*, 1999; Holland *et al.*, 1999). Some of the key mechanisms of action that have been investigated are the role of the endothelium, AEA metabolism to active products, the CB₁ receptor, vanilloid receptors and novel receptors.

4.1.2 Anandamide Metabolism

The main route of metabolism for AEA is by the enzyme fatty acid amine hydrolase (FAAH) which hydrolyses AEA to arachidonic acid and ethanolamine (Cravatt *et al.*, 1996). FAAH knock out mice demonstrate a 15 fold increase in endogenous AEA concentration, and FAAH has been detected in many tissues, including endothelial cells (Cravatt *et al.*, 2001; Deutsch *et al.*, 2001).

There is also evidence that AEA can be metabolised by cyclooxygenase (COX)-2 but not COX-1, with the major metabolic products being prostaglandin (PG)E₂, D₂ and F_{2 α} ethanolamides (Yu *et al.*, 1997; Kozak *et al.*, 2002). This family of prostaglandin ethanolamides are known collectively as prostamides. Pharmacological investigation has revealed that prostamides are only weakly active at the CB₁ and CB₂ receptors and are much less active than their corresponding PG at the already established prostanoid receptors (Berglund *et al.*, 1999; Ross *et al.*, 2002; Woodward *et al.*, 2001). It is also speculated that the COX enzymes only metabolise AEA in conditions where FAAH is inhibited (Fowler, 2007).

In addition to COX enzymes metabolising AEA directly, there is also the possibility that COX enzymes can metabolise the arachidonic acid generated from the hydrolysis of AEA by FAAH; this in turn results in the generation of vasoactive prostanoids (Grainger *et al.*, 2001; Wahn *et al.*, 2005). Understanding the metabolic route of AEA and other endocannabinoids may be

useful experimentally and therapeutically to either increase endogenous cannabinoid activity or the production of beneficial metabolites.

4.1.3 Receptors involved in mediating cannabinoid responses in the vasculature

To date two types of cannabinoid receptor have been identified and cloned, the CB₁ and CB₂. AEA acts as a partial agonist at both these receptors, although it has slightly greater affinity for CB₁ (Devane *et al.*, 1992; Munro *et al.*, 1993; Pertwee *et al.*, 1999). There is substantial evidence, however, which suggests there are more than just two types of cannabinoid receptor. At least two novel receptors are thought to exist; the abnormal cannabidiol receptor (CB_x) which is located on the endothelium and is activated by abnormal cannabidiol (Begg *et al.*, 2005), and GPR55, an orphan G protein coupled receptor (Ryberg *et al.*, 2007; Baker *et al.*, 2006). It has not yet been established if GPR55 is present in the vasculature, although there is some evidence to suggest its presence in some vascular beds (Baker *et al.*, 2006). The ability of AEA to activate GPR55 is controversial and depends on the method used. In experiments using ERK phosphorylation as a marker for receptor activation, AEA was found to have no effect up to 10 μ M (Oka *et al.*, 2009), whereas in experiments using [³⁵S] GTP γ S binding assay both AEA and 2-AG were found to be potent GPR55 agonists (Ryberg *et al.*, 2007).

4.2 Aim

To date rat vessels have been the main subject of study to characterise the response to endocannabinoids, however there has been no such effort to characterise the response in the mouse. Little is known about the effects of AEA in the mouse vasculature. The previous chapter has highlighted both the presence of cannabinoid receptors in the murine vasculature and also that following injury the concentration of endogenous cannabinoids increases. The aim of this chapter was to investigate whether AEA could elicit a functional response in the murine vasculature and identify specific receptors or metabolic involvement.

4.3 Myography Method

Small vessel myography was used to investigate the vasoactive properties of the endogenous cannabinoid AEA. Selective cannabinoid receptor antagonists and enzyme inhibitors were used to investigate the pharmacological properties of the response produced by AEA.

Murine aortas and carotid arteries were freshly dissected and mounted onto a dual wire myograph (as detailed in chapter 2.2.2). Initial experiments involved one carotid segment and

one aortic segment being mounted in the bath to determine the optimum vessel under the same conditions. In subsequent experiments the main bath was divided into two (by a separator), with a carotid arterial segment in each allowing two pharmacological interventions to be performed at the same time.

4.3.1 Normalisation Procedure

Once the arteries were mounted onto the myograph (described in section 2.2) the vessels were then normalised. The purpose of the normalisation process was to determine the internal diameter that a vessel mounted on the myograph would have at a transmural pressure of 100mmHg (IC_{100}). Once this diameter was calculated the vessel was then set to 90% of this internal circumference denoted IC_1 (Danish Myo Technology, 2003).

The normalisation process was performed by stretching the vessel section in a stepwise manner (demonstrated in Figure 4.1), measuring both the micrometer and force readings until the pressure exceeded 100mmHg. These values were then converted by the software into values of internal circumference (μm) and wall tension (mN/mm) respectively.

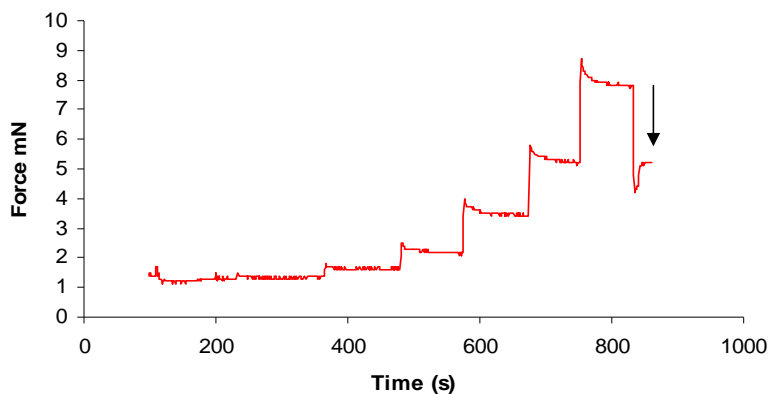


Figure 4.1 An example of a normalisation trace in the mouse carotid artery. The stepwise increments in force correspond to increasing the vessel diameter by $100\mu\text{m}$. The arrow indicates where the vessel was set to the optimum internal diameter (IC_1).

The software then plotted wall tension against the internal circumference values and fit an exponential curve (Figure 4.2). The IC_{100} was then calculated from the point on the curve which corresponds to 100mmHg, the IC_1 was then calculated as follows.

$$IC_1 = 0.9 \times IC_{100}.$$

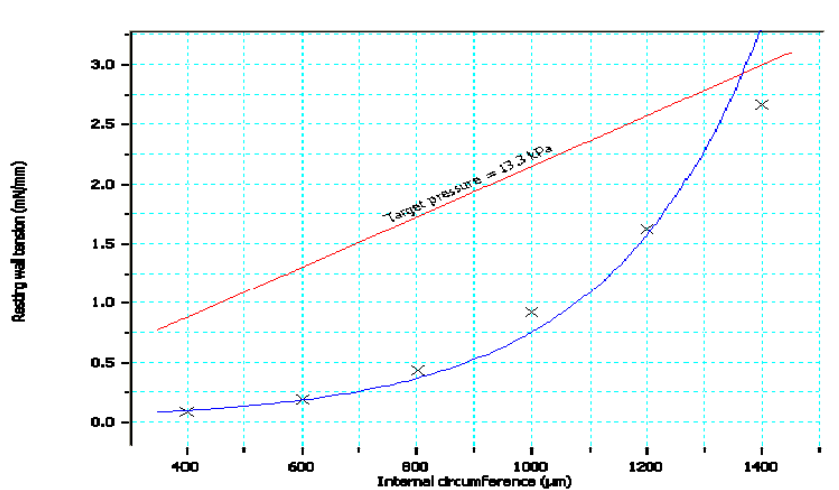


Figure 4.2 An example of a normalisation curve showing how the optimum internal diameter is determined.

Once the IC_1 value was calculated the vessel diameter was then manually adjusted to the micrometer reading calculated by the program corresponding to IC_1 , (DMT Auto Dual Wire Myograph System Model 510A User Manual version 2).

Following completion of the normalisation process the vessels were then left to equilibrate for 1 hour. To ensure vessel viability and to sensitise the tissue KCl was added to the bath to produce a concentration of 80mM; this was repeated a further 2 times with the tissue being washed with fresh Krebs solution in between each addition (example traces demonstrating this process are shown in Figure 4.5). Vessels that did not contract to 80mM KCl were deemed not viable, and so not included in experimentation. The vessels were then left for between 30 and 45 minutes before experimentation began and subsequently between each experiment to allow time for the vessels to recover. For concentration responses enough time was left between each drug addition to allow any effect to stabilise. Experimentation lasted for around 5 hours. Details of vessel characteristics are shown in table 4.1.

$$\text{Internal diameter} = IC_1 / \pi$$

Vessel	Mean Length (mm)	Internal Diameter (μm)
Aorta	1.475 \pm 0.08	348.58 \pm 37.38
Carotid	1.46 \pm 0.05	223.81 \pm 17.08

Table 4.1 Example measurements of the vessels used in this study. For the aorta a selection of 10 experiments were chosen at random and the vessel length noted and the internal diameter calculated as shown above. For the carotid artery 20 experiments were picked at random and the vessel length noted and internal diameter calculated. Values shown are mean \pm SEM.

4.4 Experimental Protocols

4.4.1 Determination of optimum contractile agent

In order to investigate the relaxant effect of AEA, the vessels had to be precontracted. To determine the optimum agent for this purpose the effects of three well established contractile agents KCl, 5HT and U46619 (a thromboxane A₂ (TXA₂) agonist) were investigated. Once the aortic tissue was successfully mounted and normalised the tissue segments were sensitised to KCl as described in the method section 3.3.1. The tissue was then left to stabilise under resting tension for 1 hour. Cumulative concentration responses to KCl ($3 \times 10^{-2}\text{M} - 1.6 \times 10^{-1}\text{M}$), 5-HT ($10^{-8}\text{M} - 3 \times 10^{-5}\text{M}$) and U46619 ($10^{-9}\text{M} - 3 \times 10^{-6}\text{M}$) were then obtained. Between each addition the contraction was left to reach a plateau to allow for accurate measurement. Results from these preliminary experiments determined that U46619 was the optimum contractile agent at a concentration of $5 \times 10^{-7}\text{M}$ and was subsequently employed throughout the study to precontract the tissue.

4.4.2 Production of relaxant responses

As relaxations in blood vessels are often induced by the endothelium, it was important to ensure endothelial viability in the vessel preparations. In order to confirm the functionality of the endothelium the effects of two endothelium dependent vasodilators, carbachol and calcimycin were investigated (Angus *et al.*, 1983; Singer *et al.*, 1982). Aortic segments were precontracted

with U46619 ($5 \times 10^{-7} \text{M}$) and allowed to stabilise. Cumulative concentrations of carbachol (10^{-5}M - $3 \times 10^{-2} \text{M}$) were then added to the bath, allowing adequate time between each addition for the relaxant effect to stabilise. The tissue was then washed 3-4 times with fresh Krebs solution and left to rest for 1 hour. This process was then repeated with calcimycin (10^{-9}M - $3 \times 10^{-5} \text{M}$). Drug solutions were made up daily from stock solutions and diluted in distilled water.

4.4.3 SNP relaxations

To confirm that the optimum resting tension determined by the normalisation process was not so high as to impede vessel relaxations in either the aorta or carotid artery, the NO donor, sodium nitroprusside (SNP), was added to the bath to relax the vessel. Following pre-contraction with U46619 ($5 \times 10^{-7} \text{M}$) cumulative concentration responses were obtained to SNP (10^{-9}M - $3 \times 10^{-5} \text{M}$). Solutions of SNP were made up daily from a stock solution and diluted with distilled water.

4.4.4 Vessel responses to anandamide

To investigate the effect of AEA on the murine carotid artery and aorta, an artery segment from each vessel was mounted in the bath, the vessels were precontracted with U46619 ($5 \times 10^{-7} \text{M}$) and left to reach a plateau. Once the contraction had reached its maximum, cumulative concentrations of AEA were added to the bath (10^{-9}M - $3 \times 10^{-5} \text{M}$). Further experiments using enzyme inhibitors or antagonists were performed in the carotid artery. Enzyme inhibitors and antagonists were added immediately following U46619 contraction and the tissues left to incubate for at least 15 minutes before the first concentration of AEA was added to the bath.

4.4.5 Vessel responses to the CB₁ receptor agonist ACEA

As the CB₁ receptor antagonist AM251 attenuated the relaxant response produced by AEA in the murine carotid artery, the effects of CB₁ activation by ACEA were investigated. To investigate the effect of CB₁ receptor activation, carotid artery segments were mounted onto the myograph normalised and sensitised (as described in section 3.3). The vessel was then precontracted using U46619 ($5 \times 10^{-7} \text{M}$). Once the contraction had reached its maximum and stabilised cumulative concentrations of ACEA were added to the bath (10^{-9}M - $3 \times 10^{-5} \text{M}$).

4.4.6 Vessel responses to the endogenous cannabinoid virodhamine

The endogenous cannabinoid virodhamine (Porter *et al.*, 2002) has been identified as a potent agonist of the novel cannabinoid receptor GPR55 (Ryberg *et al.*, 2007), and is also speculated to act at the novel abnormal canabidiol receptor (Ho *et al.*, 2004). In order to investigate whether activation of these receptors could induce a functional response in the carotid artery, vessel sections were precontracted with U46619 ($5 \times 10^{-7} \text{M}$) and then cumulative concentrations of virodhamine (10^{-9}M - $3 \times 10^{-5} \text{M}$) were added to the bath.

4.5 Drugs

The drugs used in this chapter were made daily from stock solutions which, unless otherwise stated, were kept aliquoted in 1.5ml tubes at -20°C ; concentrations, solvents and functions of agents are all detailed below. Prior to experimentation drug solutions were kept on ice but allowed to reach room temperature before addition to the myograph bath. In experiments using inhibitors or antagonists a control experiment of AEA+URB597 was always performed to ensure vessel viability.

- KCl (Sigma) salt was dissolved in distilled water to a stock solution of 2M this was then diluted daily to give the appropriate concentration.
- 5-HT (Sigma) was dissolved in distilled water to a stock solution concentration of $1 \times 10^{-2} \text{M}$ this was diluted with distilled water to provide the range of concentrations required for the concentration response studies.
- U46619 (Sigma) was made to a stock solution of $1 \times 10^{-3} \text{M}$ in ethanol, this was then diluted to $1 \times 10^{-4} \text{M}$ in distilled water then aliquoted into 1.5ml ependorffs then frozen. Concentration responses were obtained in the range of $1 \times 10^{-9} \text{M}$ – $3 \times 10^{-6} \text{M}$. A bath concentration of 5×10^{-7} was used as a contractile agent.
- Calcimycin (Sigma): An endothelium dependent vasodilator was dissolved in ethanol to a stock solution concentration of $1 \times 10^{-2} \text{M}$, this was subsequently diluted in distilled water. In concentration responses a bath concentration range of $1 \times 10^{-9} \text{M}$ – $3 \times 10^{-5} \text{M}$ was investigated.
- Carbachol (Sigma): An endothelium dependent vasodilator was dissolved in distilled water to a concentration of 1M stock solution. This was used at a concentration range of $1 \times 10^{-4} \text{M}$ - $3 \times 10^{-2} \text{M}$.
- SNP (Sigma): A NO donor which produced vasodilation was diluted in distilled water to a stock concentration of $1 \times 10^{-2} \text{M}$. The stock solution was diluted in distilled water a bath concentration range of $1 \times 10^{-9} \text{M}$ – $3 \times 10^{-5} \text{M}$ was investigated.

- AEA in Tocrisolve® (Tocris): 10mg of AEA was dissolved in 1ml of Tocrisolve® (a water soluble emulsion consisting of a 1:4 ratio of soya oil/water that is emulsified with the block copolymer Pluronic F68.). This was then diluted in distilled water to a stock solution of $1 \times 10^{-3} \text{M}$. The stock solution was aliquoted into 1ml samples and stored at 4°C . Before experiments the stock solution was diluted in distilled water to appropriate concentrations, bath concentrations of $1 \times 10^{-9} \text{M} - 3 \times 10^{-5} \text{M}$ were investigated.
- URB597 (Caymen Chemical): A FAAH inhibitor. This was diluted in ethanol to a stock solution of $2 \times 10^{-3} \text{M}$. This was diluted in distilled water before use to produce a bath concentration of $1 \times 10^{-7} \text{M}$.
- SC560 (Tocris): A COX-1 enzyme inhibitor. This was dissolved in ethanol to produce a stock solution of $2 \times 10^{-5} \text{M}$. This was diluted prior to experiments in distilled water to produce a bath concentration of $1 \times 10^{-7} \text{M}$.
- DUP697 (Tocris): A COX-2 inhibitor. This was dissolved in ethanol to a stock solution of $2 \times 10^{-5} \text{M}$, this was diluted prior to experiments in distilled water and used at a bath concentration of $1 \times 10^{-7} \text{M}$.
- AM251 (Tocris): A CB_1 receptor antagonist. 10mg was dissolved in ethanol to produce a stock solution $1 \times 10^{-4} \text{M}$. This was diluted prior to experiments in distilled water to give a bath concentration of $1 \times 10^{-6} \text{M}$.
- AM630 (Tocris): A CB_2 receptor antagonist. 10mg was dissolved in DMSO to produce a stock solution of $1 \times 10^{-2} \text{M}$ this was diluted prior to experiments in distilled water to allow a bath concentration of $1 \times 10^{-6} \text{M}$.
- ACEA (Tocris): A CB_1 receptor agonist. 5mg was dissolved in ethanol to produce a stock solution of $1 \times 10^{-2} \text{M}$, prior to experiments this was diluted in distilled water, bath concentration of $1 \times 10^{-9} - 3 \times 10^{-5} \text{M}$ were investigated.
- Virodhamine (Tocris): An endogenous cannabinoid. 5mg was diluted in ethanol to produce a stock solution of $1 \times 10^{-2} \text{M}$, this was then diluted in distilled water prior to experiments, concentrations of $1 \times 10^{-9} - 3 \times 10^{-5} \text{M}$ were investigated.

4.6 Data analysis and Statistics

The values recorded for each concentration point were based on an average reading of trace values over a 15 second period before the next addition to the bath. Experiments were disregarded if total relaxation was less than 5%, as this could purely be attributed to loss of tone over time. An example time control trace and the values recorded are shown in Figure 4.3 and Table 4.1. Experimental data was also disregarded if the values were out with the range of $\pm 2 \times \text{St Dev}$, or the vessel was non responsive to KCL, or if the contraction to U44619 was less than 1mN.

All results are shown as the mean values either + or - SEM (for clarity of graphs error bars are only shown in one direction); n= the number of mice used. Data shown regarding vessel contraction is shown as a mean of the response produced in mN, and data showing vessel relaxation is presented as % relaxation of the U46619 induced contraction. A two way repeated measures ANOVA with Bonferroni post test was used to analyse the data P<0.05 (*) was taken as significant, P<0.01 (**).

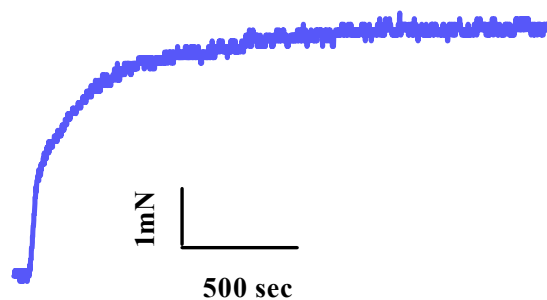


Figure 4.3 An example trace of a time control experiment. Vessels were pre-contracted with $5 \times 10^{-7} \text{M}$ of U46619 then left for a period of time that was equal to that required to add all the concentrations of AEA (approximately 30 minutes) in a concentration response. URB597 ($1 \times 10^{-6} \text{M}$) was present during the control time.

Time Control	% relaxation
1	5.67
2	-3.3
3	11.07
4	3.85
Mean	4.32 ± 2.56

Table 4.2 The % relaxation values produced by the time controls. Vessels were pre-contracted with $5 \times 10^{-7} \text{M}$ U46619. Values are shown as % relaxation. n=4

4.7 Results

4.7.1 Determination of optimum KCl sensitisation concentration

Increasing concentrations of KCL increased the magnitude of contraction produced by the aortic tissue (Figure 4.4 n=6). The contraction began to plateau at approximately 60mM before reaching a maximum contraction of 5.08 ± 0.958 mN at 160mM. A sub-maximal concentration of 80mM was chosen as the optimum concentration to sensitise the vessel and used in all subsequent experiments. Example traces demonstrating tissue sensitisation at 80mM in both the aorta and carotid artery can be visualised in Figure 4.5.

4.7.2 Determination of optimum contractile agent

Both 5-HT and U46619 produced concentration dependent contractile responses which produced a maximum response of 3.06 ± 0.39 nM and 13.16 ± 2.7 nM, respectively (Figures 4.6 and 4.7 n=4). As U46619 produced a contraction that was significantly greater in magnitude ($P < 0.05$ Student's t test) compared to 5-HT, it was deemed the optimum contractile agent (Figure 4.8). A sub maximal concentration of 5×10^{-7} M was employed throughout the study.

4.7.3 Determination of relaxant ability of blood vessel sections and endothelial integrity

Carbachol produced a biphasic concentration dependent relaxation (Fig 4.9 n=3) which peaked at 40% (1×10^{-2} M), above this concentration the relaxant response decreased with increasing drug concentration. Calcimycin produced a concentration dependent relaxation up to a concentration of 10^{-6} M, where relaxation reached a peak of 34% (Figure 4.10 n=3). Above this concentration the relaxation produced declined to 0% at concentrations greater than 10^{-5} M. The nitric oxide donor, SNP, produced a concentration dependent relaxation with a peak relaxation of 60% at a concentration of 3×10^{-5} M n=2 (Figure 4.11).

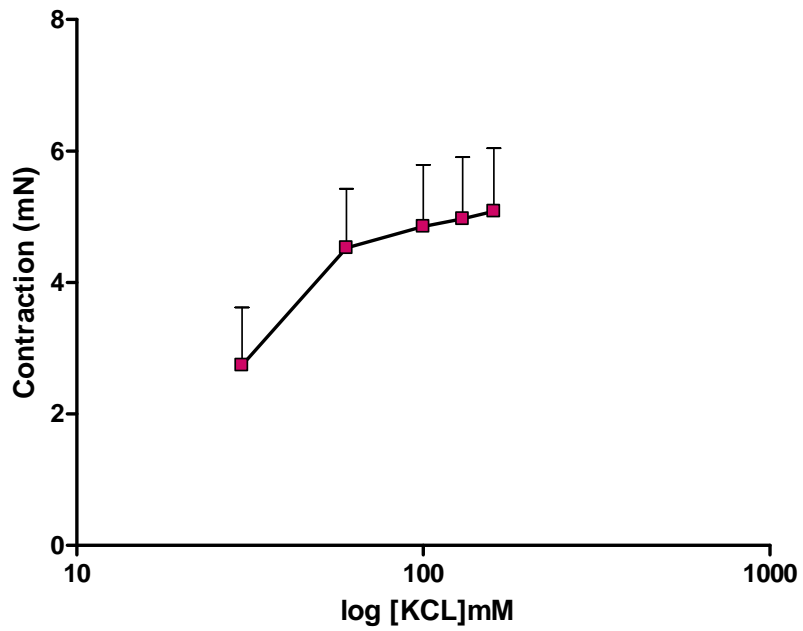
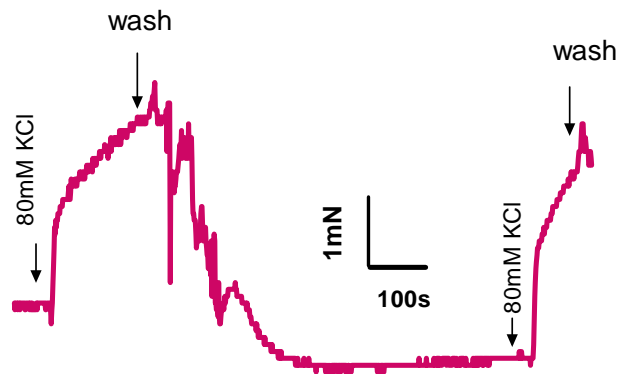


Figure 4.4 Concentration response curve to increasing concentrations of KCl. Contraction was measured as a mean increase in tension mN + SEM, n = 6.

(A)



(B)

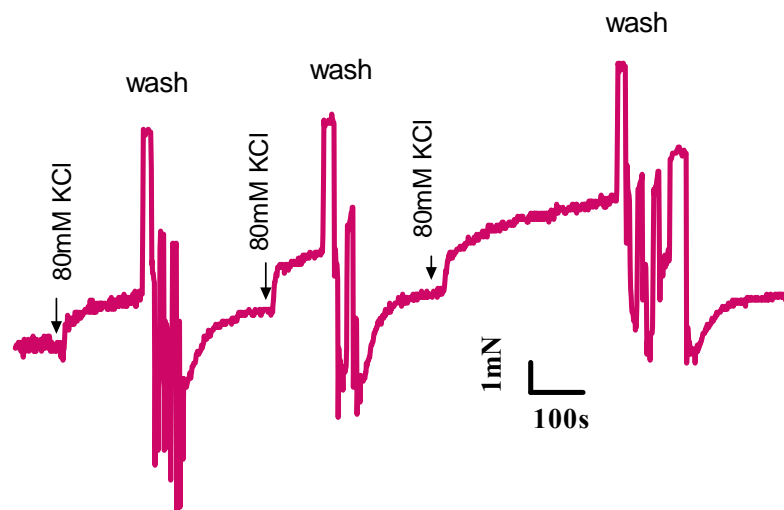


Figure 4.5 KCl sensitisation of vessels. Contractions induced by 80mM KCl in the aorta (A) and the carotid artery (B) performed prior to experiments to sensitise the tissue and ensure tissue viability.

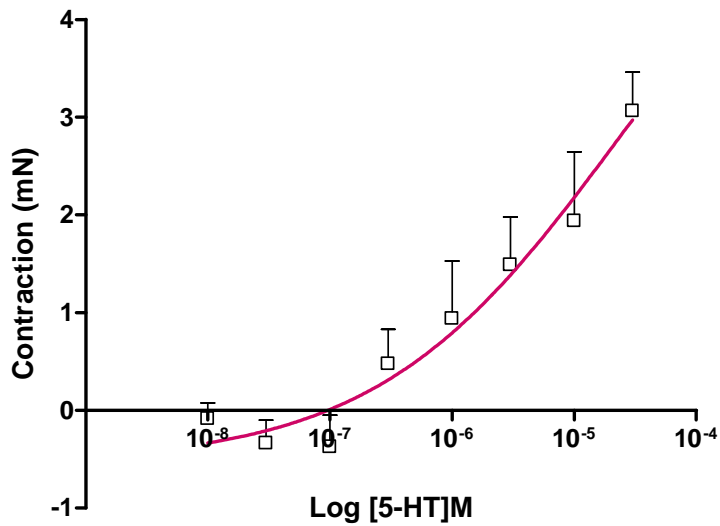


Figure 4.6 Concentration response curve to 5-HT in murine aorta. EC_{50} calculated from non linear curve fit using a variable Hill slope EC_{50} $2.2 \times 10^{-5}M$. Values shown are mean increase in tension +SEM, n=4.

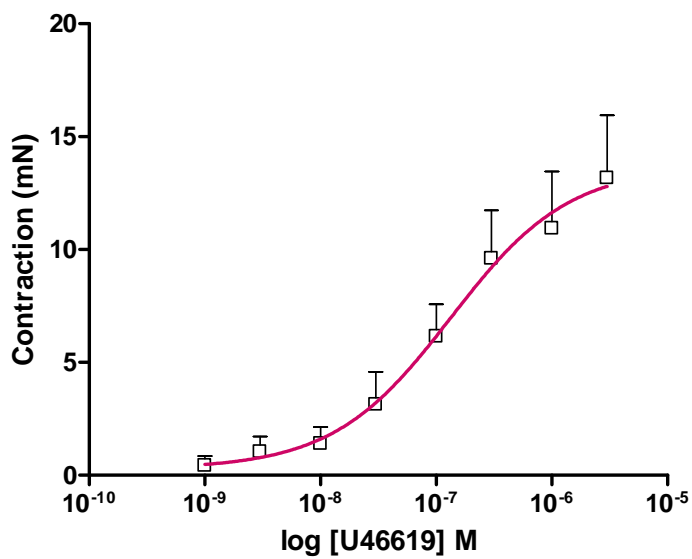


Figure 4.7 Concentration response curve to U46619 in murine aorta. EC_{50} calculated from non linear curve fit using a variable Hill slope EC_{50} $1.34 \times 10^{-7}M$. Values show mean increase in tension + SEM, n= 4.

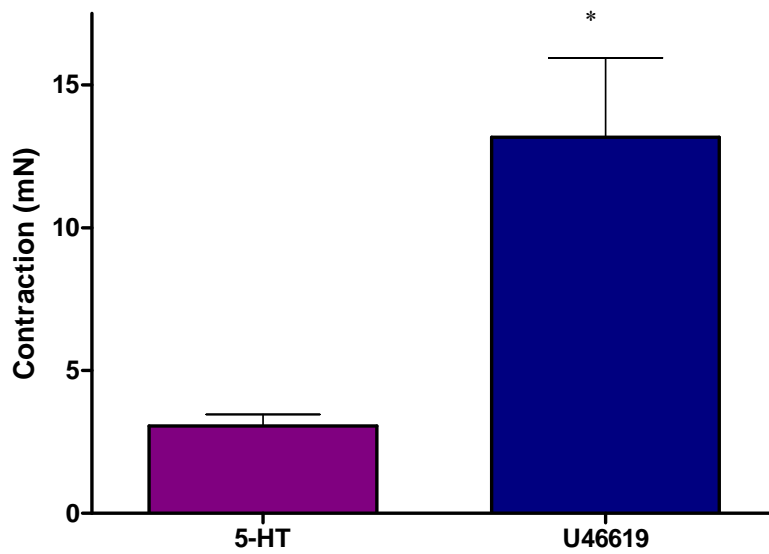


Figure 4.8 A comparison of the E_{max} values for 5-HT and U46619. Values obtained from concentration responses shown previously (Figure 4.6 and 4.8). Values represent mean increase in tension \pm SEM. $P < 0.05$ Students t test.

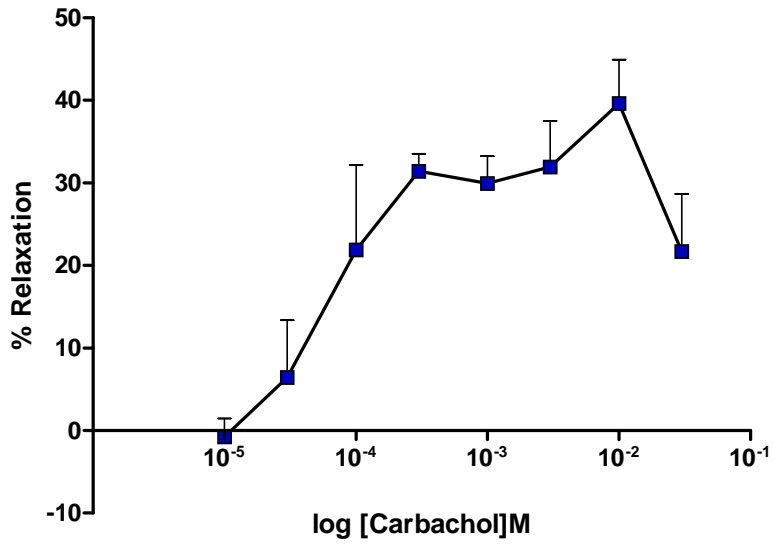


Figure 4.9 Concentration response curve to carbachol. Data shown as mean % relaxation of U46619 induced contraction + SEM, n =3.

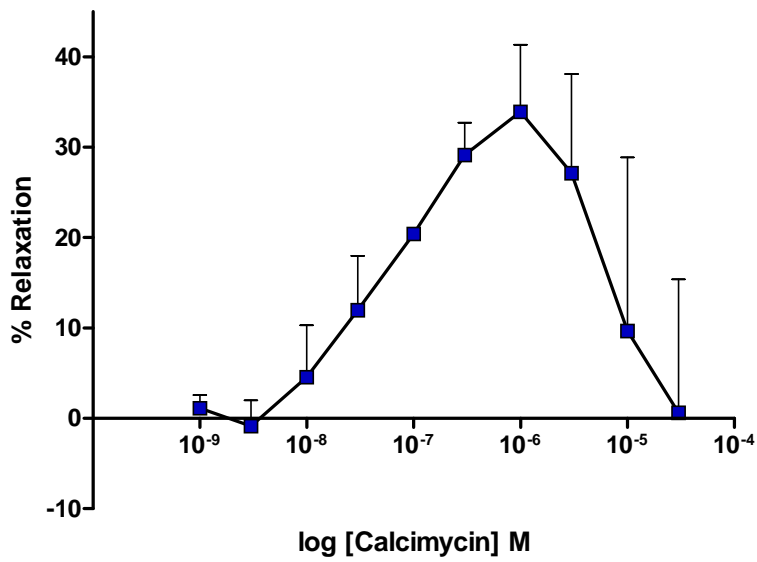


Figure 4.10 Concentration response curve to calcimycin. Data shown as mean % relaxation of U46619 induced tone + SEM N=3.

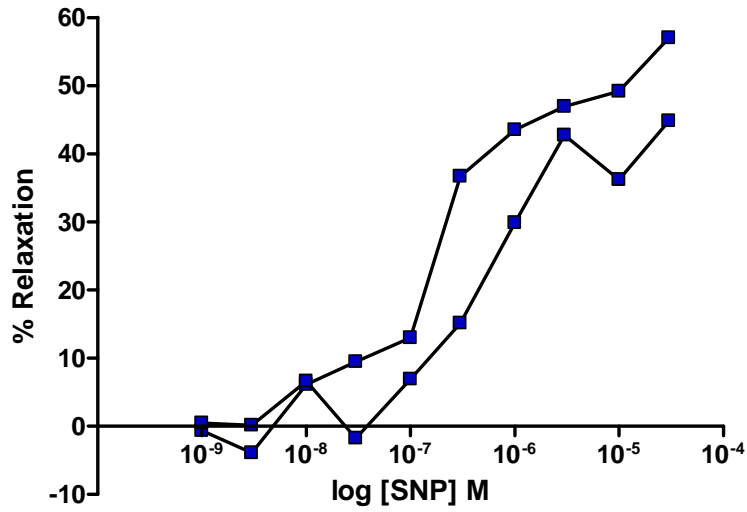
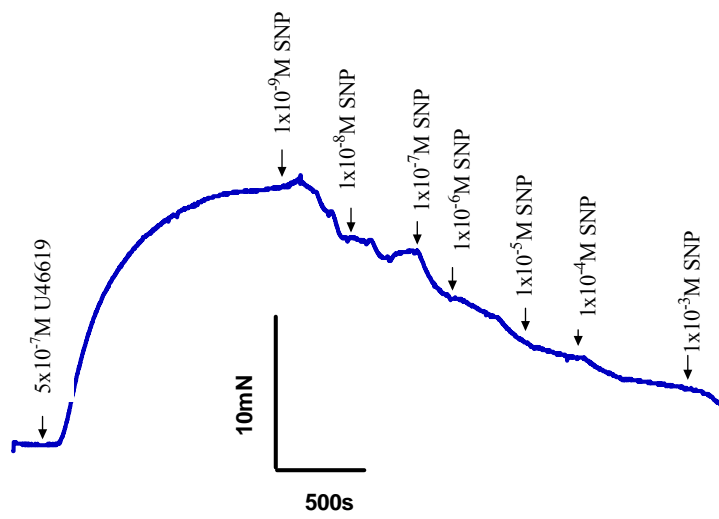


Figure 4.11 Concentration response curve of SNP. Relaxation produced by increasing concentrations of SNP in the aorta. n=2 each data set shown. Data shown as % relaxation of U46619 induced tone.

(A)



(B)

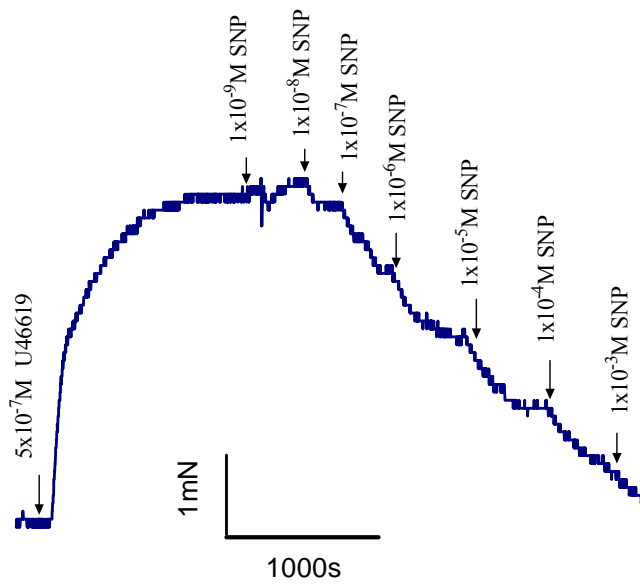


Figure 4.12 Example traces of SNP induced relaxations. A sample trace of the effects of SNP on the aorta (A) and mouse carotid artery (B).

4.7.4 Assessment of the relaxant response to anandamide and effect of FAAH inhibition in both the mouse aorta and carotid artery.

Increasing concentrations of anandamide produced a concentration dependent relaxation of both the thoracic aorta and carotid artery with E_{max} values of $29.09 \pm 7.09\%$ and $13.59 \pm 4.67\%$ respectively $n=5$ (Figure 4.13 and Figure 4.14). In the carotid artery the magnitude of the relaxation was increased in the presence of the FAAH inhibitor URB597 ($1 \times 10^{-7}M$), albeit not enough to generate statistical significance, however the E_{max} value increased to $34.32 \pm 14.1\%$ $n=5$. Although statistically (Two way ANOVA with Bonferroni post test) it appeared that FAAH had no impact on the relaxant response of anandamide in either vessel, it was decided that all subsequent experiments would include URB597 to eliminate any possible intervention from FAAH and ensure the highest available concentration of AEA.

To determine the optimum vessel to use, the relaxant responses of AEA in both the aorta and the carotid artery in the presence of URB597 were compared (Figure 4.15). The response produced in the carotid artery (E_{max} $34.32 \pm 14.1\%$ $n=5$) was marginally larger than that in the aorta (E_{max} $32.9 \pm 8.8\%$ $n=6$), and showed greater sensitivity at lower concentrations, for this reason the carotid artery was used in all subsequent experiments ($P > 0.05$, Two way ANOVA with Bonferroni post test). Sample traces illustrating the effect of AEA on both the carotid artery and the aorta can be seen in Figure 4.16

4.7.5 The effects of COX-1 and COX-2 inhibition on the relaxant response to anandamide

Anandamide in the presence of URB597 produced a relaxation that reached a maximum of 20.4%, this was not affected by the presence of a COX1 inhibitor (SC560 $1 \times 10^{-6}M$) $n=7$. In these experiments it can also be observed that the vehicle control (Tocrisolve at the same concentration range as AEA) showed no relaxant effect; statistical analysis could not be performed due to the small n number ($n=2$) of the vehicle control (Figure 4.17). AEA produced a relaxation with an E_{max} of $22.3 \pm 5.42\%$ (Figure 4.18); this was unaffected by the presence of a COX-2 inhibitor (DUP697 $1 \times 10^{-6}M$, E_{max} $22.42 \pm 8\%$) $n=6$. $P > 0.05$ (Two way ANOVA with Bonferroni post test).

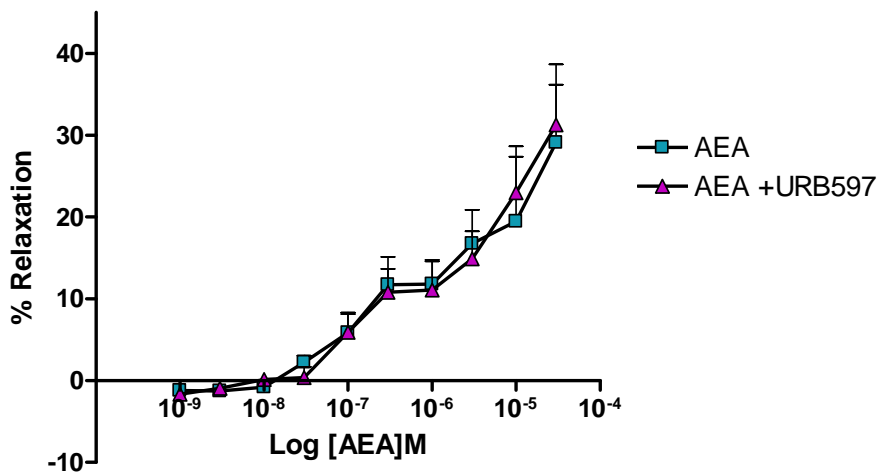


Figure 4.13 Concentration response curve to AEA alone and in the presence of URB597 in the mouse aorta. Results are shown as mean % relaxation of U46619 ($5 \times 10^{-7} \text{M}$) induced tone + SEM, $n=5$ for AEA alone $n=6$ for AEA +URB597.

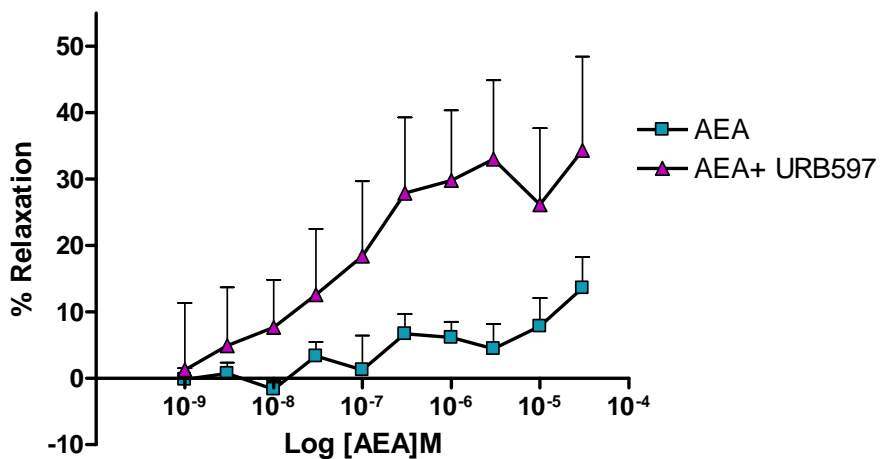


Figure 4.14 Concentration response curve to AEA alone or in the presence of URB597 in the mouse carotid artery. Results are shown as mean % relaxation of U46619 ($5 \times 10^{-7} \text{M}$) induced tone + SEM, $n=5$ $P > 0.05$ (Two way ANOVA with Bonferroni post test).

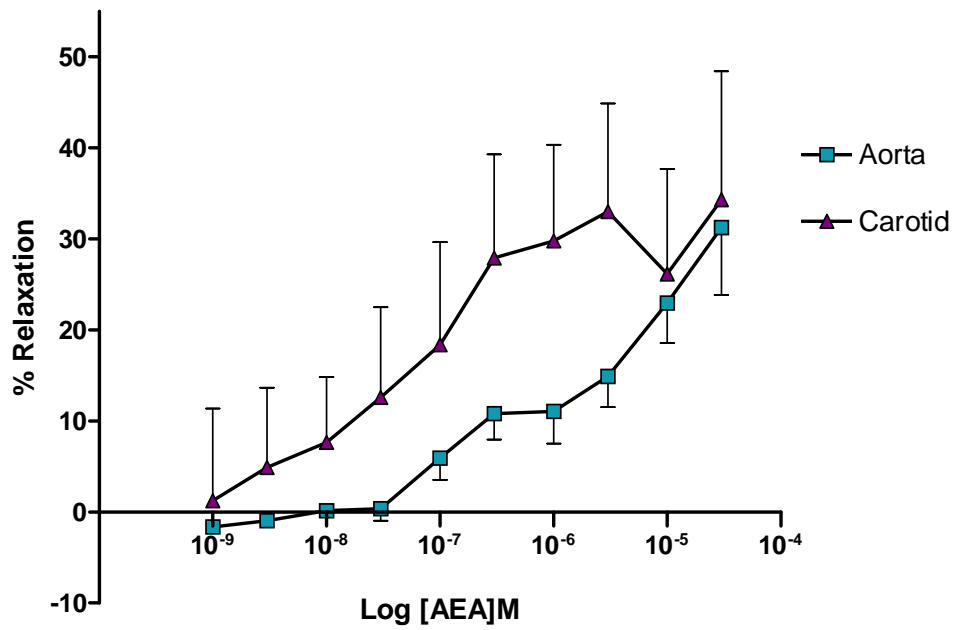
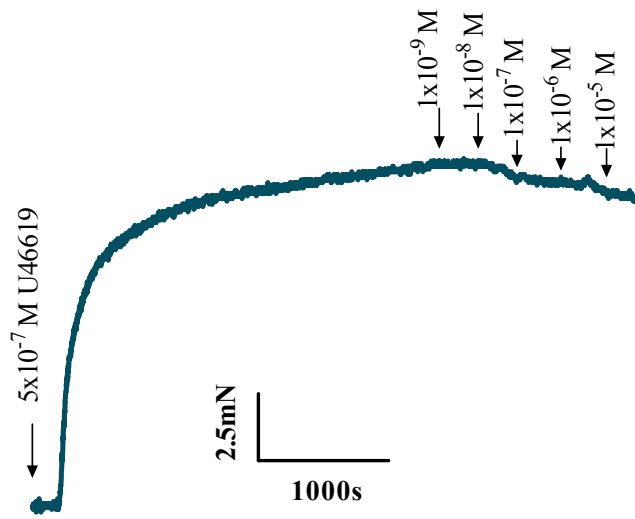


Figure 4.15 Comparison of AEA concentration response curves in the carotid artery and thoracic aorta in the presence of URB597. URB597 was included at a concentration of $1 \times 10^{-7} \text{M}$. Results are shown as mean % relaxation of U46619 ($5 \times 10^{-7} \text{M}$) induced tone \pm SEM. $n=6$ for aorta, $n=5$ for carotid $P>0.05$ (Two way ANOVA with Bonferroni post test).

(A)



(B)

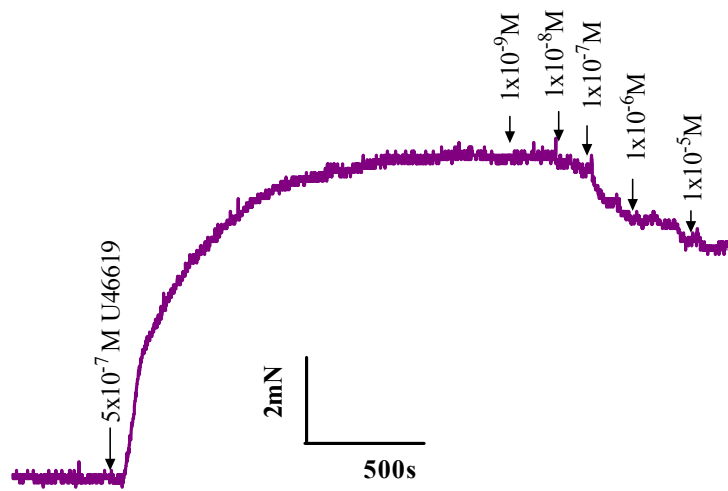


Figure 4.16 Responses produced in response to AEA in the aorta and carotid artery. Original traces of the response produced by AEA in the aorta (A) and carotid artery (B) vessels were pre-contracted with U46619 ($5 \times 10^{-7} \text{ M}$) and URB597 ($1 \times 10^{-7} \text{ M}$) was present in both responses.

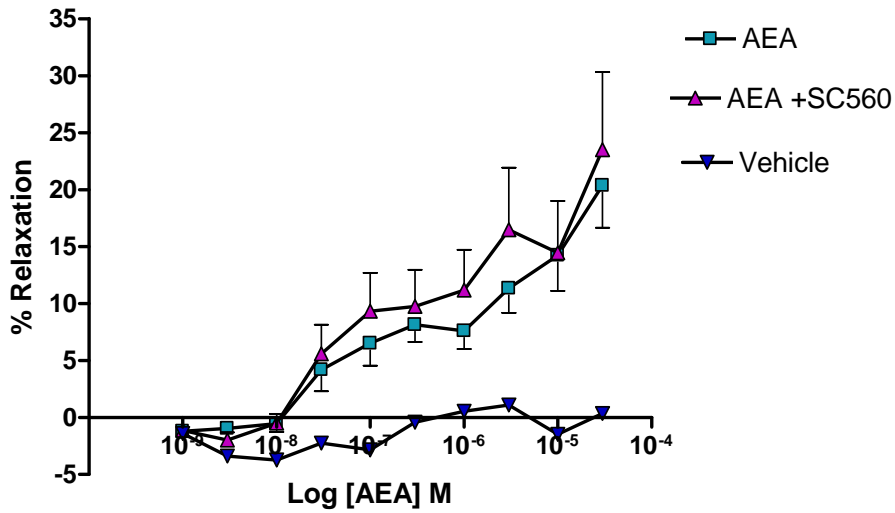


Figure 4.17 Concentration response curve to AEA alone and in the presence of a COX-1 inhibitor. SC560 ($1 \times 10^{-6} \text{M}$), and URB597 ($1 \times 10^{-7} \text{M}$) were included in the bath. Results are shown as mean % relaxation of U46619 ($5 \times 10^{-7} \text{M}$) induced tone \pm SEM $n = 7$ for AEA , $n = 7$ for SC560 and $n = 2$ for vehicle (Tocrisolve).

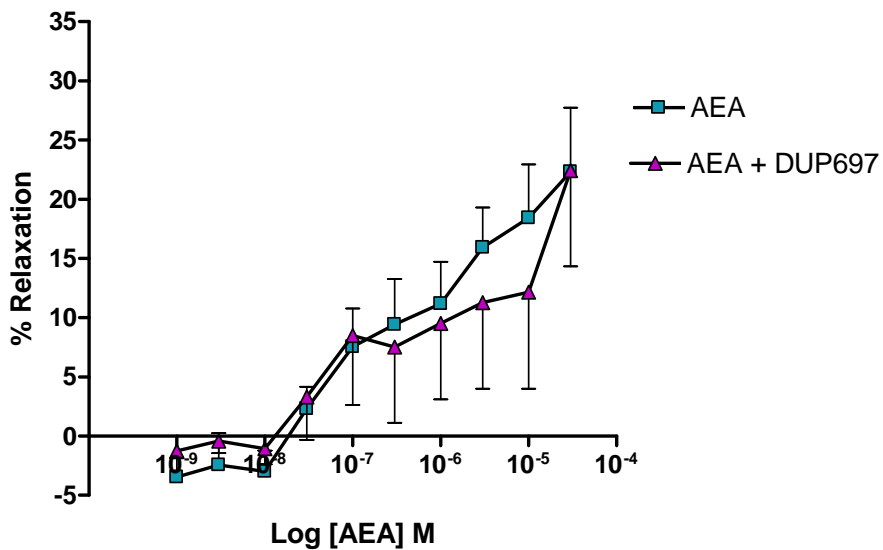


Figure 4.18 Concentration response curve to AEA alone and in the presence of the COX-2 inhibitor DUP697. DUP697 was used at a concentration of ($1 \times 10^{-7} \text{M}$) URB596 ($1 \times 10^{-6} \text{M}$) was included in all experiments. Results are shown as mean % relaxation of U46619 ($5 \times 10^{-7} \text{M}$) induced tone \pm SEM, $n = 6$ for all.

4.7.6 The effects of the CB₁ antagonist AM251 on the vasorelaxant response produced by AEA

AEA produced a maximum relaxation of $22.4 \pm 3.6\%$, this was significantly greater (at concentrations greater than $1 \times 10^{-6} \text{M}$) than the vehicle control which produced a maximum relaxation of $11.3 \pm 3.66\%$. It can be seen that the relaxation produced by AEA was significantly attenuated (at a concentration of $1 \times 10^{-5} \text{M}$) in the presence of the CB₁ receptor antagonist AM251 ($1 \times 10^{-6} \text{M}$), reducing the maximum relaxation to $12.10 \pm 3.87\%$ (Figure 4.19). There was no significant difference between the response produced by AEA in the presence of AM251 and the vehicle control (Two way ANOVA with Bonferroni post test $n=7$).

4.7.7 The effect of the CB₂ antagonist AM630 on the vasorelaxant response produced by AEA

AEA produced a maximum relaxation of $19.56 \pm 1.60\%$ (Figure 4.20); this was greater than the response produced by the vehicle (10.8 ± 3.4) but did not reach statistical significance due to the large standard errors. The presence of the CB₂ antagonist had no effect on the response produced by AEA ($18.8 \pm 4.6\%$) $n=5$.

4.7.8 The effect of the CB₁ agonist ACEA on the murine carotid artery

Increasing concentrations of the CB₁ agonist ACEA (Figure 4.21) produced a contractile response in carotid artery segments ($-19.87 \pm 1.69\%$) which was enhanced in the presence of the CB₁ antagonist AM251 ($-24.59 \pm 2.52\%$) $n=5$. The vehicle control (ethanol) also produced a contractile effect ($-21.92 \pm 2.84\%$) which was indistinguishable from that produced by ACEA $n=2$.

4.7.9 The effect of the endogenous cannabinoid virodhamine on the murine carotid artery

Cumulative concentrations of virodhamine produced a small relaxation of $9.9 \pm 3.4\%$ (Figure 4.22). However, the relaxation produced by virodhamine alone $n=8$, and in combination with the CB₁ antagonist AM251 ($11.70 \pm 2.65\%$) $n=6$, were indistinguishable from the ethanol vehicle control (9.3 ± 2.3) $n=4$.

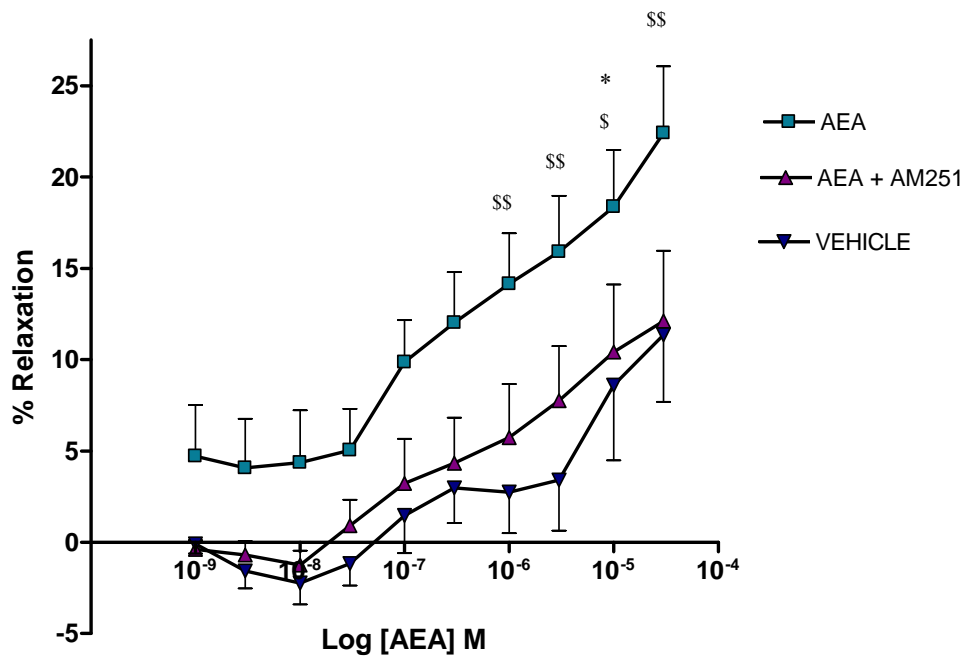


Figure 4.19 Concentration response for AEA alone and in combination with the CB₁ antagonist AM251. Results are shown as mean % relaxation of U46619 ($5 \times 10^{-7} \text{M}$) induced tone \pm SEM $n=7$ for all concentrations. * $P < 0.05$ compared to AEA+ AM251, \$\$ = $P < 0.01$, \$ = $P < 0.05$ AEA compared to vehicle.

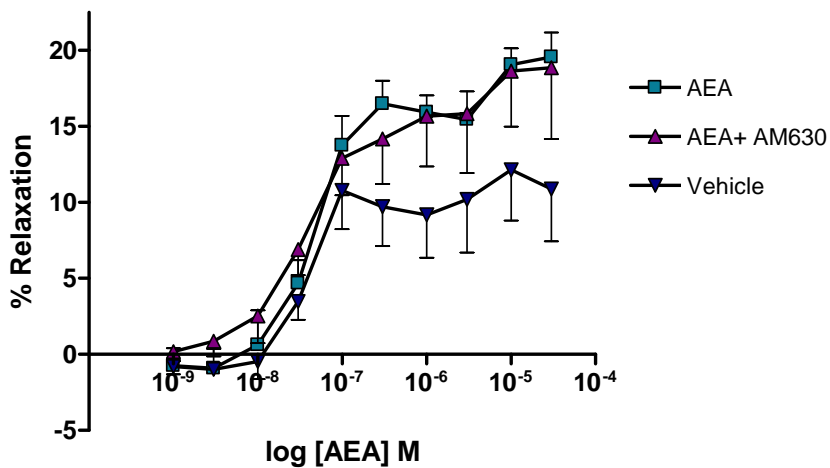


Figure 4.20 Concentration response curve to AEA alone and in combination with the CB₂ antagonist AM630. Results are shown as mean % relaxation of U46619 (5x10⁻⁷M) induced tone ± SEM. n= 5 for all. P > 0.05

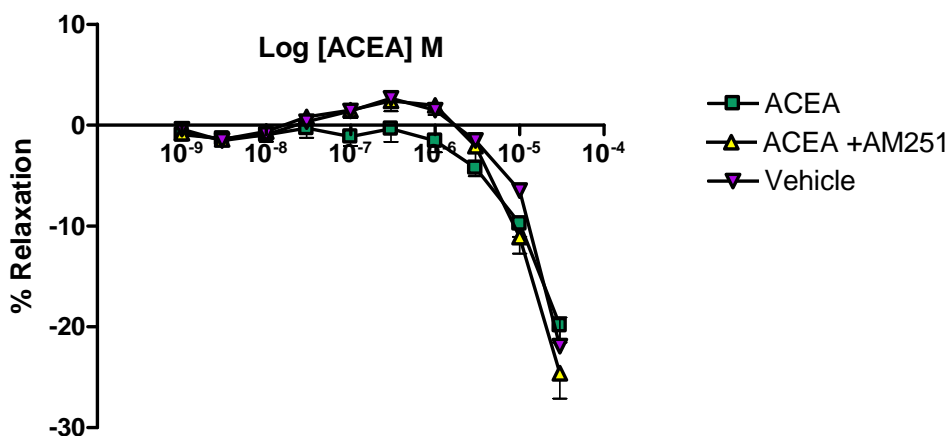


Figure 4.21 Concentration response curve for ACEA alone and in combination with the CB₁ antagonist AM251. Results are shown as mean % relaxation of U46619 (5x10⁻⁷M) induced tone ± SEM n=5, n=2 for vehicle.

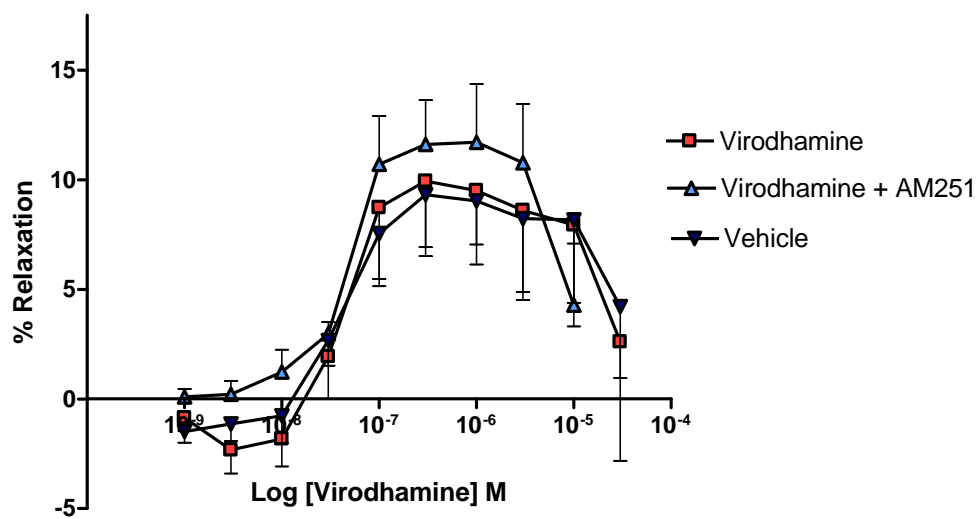


Figure 4.22 Concentration response for virodhamine alone and in the presence of AM251. Results are shown as mean % relaxation of U46619 ($5 \times 10^{-7} \text{M}$) induced tone \pm SEM n=8 for virodhamine, n= 6 for virodhamine +AM251 and n=4 for vehicle (ethanol).

4.8 Discussion

The aim of this study was to investigate whether AEA could elicit a functional response in the murine vasculature and to determine which receptors were involved. To maximise the concentration of AEA available to the tissue and ensure any effect observed was not due to the production of a vasoactive metabolite its metabolic breakdown was also investigated. AEA produced a small relaxation which increased in magnitude in the presence of a FAAH inhibitor. This, alongside the results of the experiments using COX inhibitors confirms that the response produced by AEA was not due to the production of an active metabolite. The relaxation produced by AEA was attenuated by a CB₁ receptor antagonist, while a CB₂ antagonist had no effect.

Optimum resting tension and determination of contractile agent

The thromboxaneA₂ (TXA₂) agonist U46619 produced a contraction that was of much greater magnitude than 5-HT and for this reason was chosen as the contractile agent to be used throughout this study. From studying the concentration response curve a concentration of 5×10^{-7} M was identified as optimum and used to precontract the vessels in all subsequent experiments. These initial optimising experiments were performed in only the mouse aorta, the carotid artery was used for the majority of experiments and therefore optimisation experiments should also have been performed in the carotid artery. Nonetheless U46619 (5×10^{-7} M) provided a large enough contraction to allow the effect of vasodilators to be investigated. From the literature it can be seen that U46619 is commonly used to precontract vessels, some examples include the rat mesenteric arterial bed (a concentration of between 10-100nM), the rat aorta and the sheep coronary artery (O'Sullivan *et al.*, 2005; Wheal *et al.*, 2007; Grainger *et al.*, 2001). An alternative contractile agent used to contract the rat thoracic aorta and rat mesenteric arterial bed is methoxamine (Wheal *et al.*, 2009; Ho *et al.*, 2004). In a study using murine mesenteric arteries phenylephrine was used as a contractile agent (Johns *et al.*, 2007).

Endothelium integrity

As many agents produce relaxation through direct action on the endothelium, it was important to ensure that following set up of the vessels on to the wire they retained an intact and functioning endothelium. Two endothelium dependent vasodilators were investigated to determine which one would be most suitable to determine endothelium viability. Carbachol, a muscarinic agonist, produces vasodilatation by endothelial release of NO. Experiments in this study demonstrated a maximum relaxation response of just over 40%. This is much lower than expected as administration of carbachol or ACh can induce complete reversal of the contraction (Zhou *et al.*, 2005; Van Hove *et al.*, 2009). At concentrations above 10mM carbachol reduced

relaxation may be due to a counter contractile effect. It has previously been reported that in the murine vasculature ACh can produce two opposing effects, the first being an endothelium dependent relaxation which is NO mediated, and the second being an endothelium dependent contraction which is reliant upon COX metabolism of arachidonic acid and activation of the TXA₂ receptor. The contractile effect produced by ACh was of greatest magnitude in the carotid artery followed by the aorta (Zhou *et al.*, 2005). It has also been found that ACh can induce vasoconstriction through activation of the muscarinic receptors present on smooth muscle cells (Zhou *et al.*, 2005).

Calcimycin is a calcium ionophore that produces vasodilatation by inducing pore formation in the endothelium allowing influx of Ca²⁺ resulting in the release of NO and subsequent relaxation. Previous studies have demonstrated that the effects of calcium ionophore are purely endothelium dependent and rely on nitric oxide (Furchgott *et al.*, 1983). Results of this study have shown that calcimycin produced a maximum relaxation of approximately 40%, at high concentrations the relaxation produced was reduced; a plausible explanation for this could be a counter acting contractile response produced by Ca²⁺ entry into the smooth muscle cells resulting in contraction.

Both calcimycin and carbachol produced a maximum relaxation of 40%, this is much lower than expected. In a study using the rat mesenteric artery, vessel sections were only included if the relaxation produced by 10µM carbachol was 90% or greater (Ho *et al.*, 2004) however, in a study using mouse aorta, vessels were deemed viable if a relaxation of more than 50% was produced (Sennoun *et al.*, 2009). Experiments using the NO donor, SNP, completely reversed vessel contraction confirming that the resting tension (predetermined through the normalisation process) was not too high as to inhibit the vessel sections from relaxing. It can therefore be suggested that either the aorta, being a large conduit vessel may have had a weak NO generating capacity, or that the endothelium had lost some of its integrity. As the carotid artery was used for the majority of experiments, concentration responses to both carbachol and calcimycin should have been performed in that vessel as well. Functioning endothelium tests were not done routinely as responses observed were minimal, if this was due to loss of endothelium integrity it could explain the large standard error observed in subsequent experiments. The injury to vessels induced during the mounting process could have been minimised by using smaller diameter wire.

Effects of AEA on vessel tone

As there is known to be both a wide species and vessel (within the same specie) variability in the responses produced by AEA the experiments were performed in both the murine carotid artery and thoracic aorta. This study has shown that a relaxation of approximately 20% occurs in both vessels. Although there is no evidence of previous studies for comparison these results are in contradiction to studies in the rat carotid artery where methanandamide (metabolically stable form of AEA) along with HU210 (potent CB₁ and CB₂ agonist) failed to have any relaxant effect (Holland *et al.*, 1999). In the rat aorta however, a similar response of 20-25% relaxation is produced in response to Δ^9 THC (O'Sullivan *et al.*, 2005). A relaxation of around 20% is much smaller than AEA responses observed in other animals which in resistance vessels can reach approximately 100% (Harris *et al.*, 2002; Zygmunt *et al.*, 1997).

It is known that AEA is readily metabolised by the enzyme FAAH. For this reason concentration responses were also obtained in the presence of the specific FAAH inhibitor, URB597. FAAH inhibition had no significant effect on the AEA response in either vessel. It has been suggested that the relaxation produced by AEA is a result of its metabolism into arachidonic acid, which then acts as a precursor for the synthesis of vasoactive prostanoids such as prostacyclin (Pratt *et al.*, 1998). The results obtained in this present study suggest that this is not the case for either vessel in the mouse. This is similar to previous studies in our laboratory in the porcine coronary artery (Skene *et al.*, 2006). Nevertheless, to eliminate any mouse to mouse variability in the levels of FAAH activity, all subsequent experiments were undertaken in the presence of URB597.

COX Metabolism

As detailed in chapter 1, due to its chemical composition AEA is susceptible to COX-2 metabolism. It has been shown that the products produced by enzymatic oxidation of AEA could bind and activate CB receptors (Berglund *et al.*, 1999). This study demonstrates that in the mouse carotid artery both COX-1 and COX-2 inhibition had no effect on the relaxant response produced by AEA, confirming that vasodilatation produced by AEA is not due to oxidative metabolism to an active metabolite. This is in contrast to previous studies in rats which have shown that COX-2 inhibition diminishes relaxations produced by AEA but only in female rats (Peroni *et al.*, 2007), this study did not separate animals according to gender but this may be an area for future work.

CB₁ and CB₂ receptor inhibition

The presence of a CB₁ receptor antagonist (AM251) resulted in an attenuation of the relaxant response produced by AEA, which reached significance at the highest concentration. This suggests that the response produced by AEA is due to activation of the CB₁ receptor. There was no statistically significant differences between the responses produced by AEA +AM251 and the vehicle, this could mean that the residual relaxation produced in the presence of AM251 was in fact just the effect of the vehicle and that AM251 had abolished all effects of AEA, however due to lack of significance this cannot be confirmed. The CB₂ receptor antagonist AM630 had no effect on the AEA response indicating a negligible role for the CB₂ receptor in the relaxation produced by AEA. Despite this study suggesting a role for the CB₁ receptor it may not be the only receptor involved, as a significant attenuation was only observed at the highest concentration. A number of other experimental studies have demonstrated a lack of involvement of CB₁ and CB₂ receptors in the vascular response to AEA, for example in the rat coronary artery and the rabbit aorta (Ford, *et al.*, 2002; Mukhopadhyay *et al.*, 2002). The CB₁ antagonist SR141716A has been shown to be effective in blocking the effects of AEA in the mouse mesenteric arterial system, however the concentration required to inhibit this effect was a lot higher than required to block CB₁ receptors suggesting that the antagonist was acting on another receptor type, possibly the putative “endothelial anandamide receptor” (White *et al.*, 1998; Offertaler *et al.*, 2003).

Studies have suggested that this novel receptor can be activated by abnormal cannabidiol, a synthetic analogue of the phytocannabinoid cannabidiol, which has been shown to produce relaxations in the mesentery of both wild type mice and CB receptor knockout mice (Jarai *et al.*, 1999; Wagner *et al.*, 1999). The antagonist O-1918 is a proposed antagonist of the endothelial AEA receptor (Offertaler *et al.*, 2003) and would thus be a useful tool to investigate the receptors mediating the AEA response in the mouse carotid.

The effect of the CB₁ agonist ACEA and the endocannabinoid virodhamine

As inhibition of the CB₁ receptor reduced the relaxant response produced by AEA it was important to investigate the physiological effect of stimulating the CB₁ receptor. Addition of ACEA (CB₁ agonist) produced a contractile response which could not be distinguished from the contractile response produced by the vehicle. Similar observations were made upon investigation of virodhamine, the effect of this endocannabinoid could not be separated from the relaxant effect of the vehicle, paradoxically the vehicle for both drugs was ethanol. Ethanol causes an increase in intracellular calcium in both the endothelial cells and smooth muscle cells

resulting in both vasodilatation and vasoconstriction, vasoconstriction was observed in porcine pulmonary artery vessels that had been denuded (Lawrence *et al.*, 1998). In another study it was found that following vasoconstriction ethanol produced a biphasic change in vascular tone, causing an initial vasodilatation followed by vasoconstriction (Lopez-Miranda *et al.*, 2004). To observe the true effects of these drugs an alternative solvent would have to be used for example DMSO.

Study Limitations

The active effect of Tocrisolve

As stated in the method section AEA was dissolved in a water-soluble emulsion called Tocrisolve, this was used as a vehicle control although unfortunately not routinely from the beginning. It can be seen that in some experiments the effect of the vehicle for AEA is easily dismissible, however in the experiments using the CB receptor antagonists a vehicle effect of nearly 10% can be observed. This vehicle effect is extremely problematic in a preparation where the maximum relaxation observed is only approximately 20%, as it makes investigating any possible mechanism involved highly challenging. The AEA response can only be statistically separated from the vehicle in the experiments involving the CB₁ receptor antagonist. The variability in vehicle effect could largely explain the large standard errors observed in all experiments in this chapter, and explain why no mechanism of action can be clearly identified. As mentioned in data analysis section 4.6 responses were excluded if the maximum relaxation produced to AEA was less than 5%. It was noted that 18% of functional vessel segments (as determined by KCL and U46619 responses) did not respond to AEA, this finding of AEA non responders was also observed in the rat coronary artery, where 30% of samples failed to respond to AEA. It was suggested that this may be due to differences in receptor expression (White *et al.*, 2001); this may also explain the variability in responses observed in this study.

It has been suggested that the conflicting evidence of mechanisms of AEA responses between vessels of the same species and between that of different species could be explained by the vehicle used to solubilise AEA. When AEA was dissolved in ethanol no relaxation was produced in either intact or denuded aortic rings, however when AEA was solubilised in DMSO relaxation was observed in intact vessels but not those that had been denuded (Lopez-Miranda *et al.*, 2004).

The effects of U46619 on the endocannabinoid system

As mentioned in chapter 1, endocannabinoids are synthesised on demand by an increase in intracellular Ca^{2+} and activation of signalling cascades. Vasoconstriction is accompanied by increases in Ca^{2+} this gives rise to the hypothesis that vasoconstrictor agents can lead to production of endocannabinoids. Rademacher (2005) have shown that tissue concentration of both AEA and 2-AG are increased following incubation with U46619 (the contractile agent used in this study), in the mouse cerebral artery. They hypothesise that activation of the TXA_2 receptor initiates production of endocannabinoids which activate the CB_1 receptor to “dampen its vasoconstriction effect”.

It was not possible in this study to investigate the size of response produced by U46619 in the presence of a CB_1 receptor antagonist as the antagonist was always added once the contraction had reached a maximum. However, if U46619 does interfere with the endocannabinoid system it may be a contributing factor to the large standard error observed in these experiments.

In conclusion, AEA produced a small relaxation which increased in magnitude in the presence of a FAAH inhibitor. This in combination with the findings from experiments using COX inhibitors confirmed that the response produced by AEA was not due to the production of an active metabolite. The relaxation produced by AEA was attenuated by a CB_1 receptor antagonist indicating that the relaxant response produced by AEA was CB_1 receptor mediated.

Chapter 5

The effects of cannabinoids on murine vascular smooth muscle cell proliferation

5.1 Introduction

5.1.1 Smooth muscle cells and neointimal formation

The process of neointimal formation is complex and involves a plethora of cell types including smooth muscle cells, endothelial cells, platelets and inflammatory cells. Of all these cell types the smooth muscle cell is arguably the most important. In physiological conditions smooth muscle cells exist in a quiescent state, however following injury induced by either balloon angioplasty or insertion of a stent, smooth muscle cells become activated and thus rapidly proliferate. The release of vasoactive mitogens such as bFGF, PDGF, FGF (Schwartz *et al.*, 1995) and inflammatory mediators such as IL-1 β and TNF α (Ikeda *et al.*, 1990; Selzman *et al.*, 1999) all stimulate smooth muscle cell proliferation and therefore enhance neointimal formation. Due to their reported cardiovascular (discussed extensively in Chapter 1), anti-inflammatory, and cardio protective effects (Montecucco *et al.*, 2009), drugs that target the cannabinoid system have been proposed as potential therapeutic agents for the prevention and treatment of a range of cardiovascular disorders.

5.1.2 Cannabinoids and cell proliferation

As discussed in Chapter 1, smooth muscle cell proliferation and the inflammatory response are key events in both restenosis and atherosclerosis. Therefore, an ideal agent for the treatment of these conditions would be one that could target both of these key processes. In 2005 Steffens *et al.* found that treatment of apolipoprotein E knockout mice with Δ^9 -THC significantly reduced atherosclerotic disease progression. A finding that was attributed to the anti-inflammatory effects produced by CB₂ receptor activation. This study did not however, consider the effects of cannabinoids on smooth muscle cells during atherosclerosis. In light of mounting evidence to suggest that cannabinoid receptor manipulation exerts anti-proliferative effects, it is feasible that cannabinoid drugs may present a novel treatment for cardiovascular diseases involving smooth muscle cell proliferation.

5.1.2.1 Cannabinoid receptors and intracellular growth signalling pathways

Both the CB₁ and CB₂ receptors are G protein coupled, belonging to the G_{i/o} family (Munro *et al.*, 1993). The downstream signalling of these receptors is complex involving inhibition of adenylate cyclase (Howlett *et al.*, 1985 a & b), modulation of ion channels (only CB₁), and most relevant to this chapter, activation of MAPK (Bouaboula *et al.*, 1995). The ability of cannabinoids to activate a variety of regulators of cellular growth (discussed in detail in Chapter

1), for example ERK, c-jun and p38 (Liu *et al.*, 2000; Rueda *et al.*, 2000) and the AKT/PKB pathway (discussed in Chapter 1), indicate that cannabinoids may play an important role in cellular proliferation and apoptosis (Guzman *et al.*, 2002). To date, most of our understanding of the antiproliferative nature of cannabinoids has come from experiments using cancer cells, with only a very few recent studies exploring the ability of cannabinoids to modify smooth muscle cell growth and proliferation.

5.1.2.2 Anti-tumour effects of cannabinoids

The antimitogenic effects of AEA were first investigated on human breast cancer cell lines, when AEA (at sub-micromolar concentrations) was found to significantly inhibit the cell cycle at the G1-S transition phase (De Petrocellis *et al.*, 1998). This effect was found to be CB₁ mediated and was a result of inhibition of adenylate cyclase, resulting in decreased cAMP levels and subsequent inhibition of MAPK. An antiproliferative effect has also been observed in prostate cancer cell lines following treatment with AEA. Micromolar concentrations of AEA inhibited EGF induced proliferation in a variety of cancer cell lines, again by G1 arrest (Mimeault *et al.*, 2003; Bifulco *et al.*, 2006). Incubation of these cells with AEA for 5-6 days caused severe apoptosis, mediated by CB_{1/2} induced ceramide accumulation. CB₁ receptor activation has been found to initiate the generation of ceramide by the hydrolysis of sphingomyelin (Kolesnick *et al.*, 1998). Ceramide is known to have an important influence on cellular metabolism, however CB receptor activation has been shown to induce sustained ceramide synthesis “de novo”, leading to induction of apoptosis through the canonical raf-MEK-ERK signalling pathway (Galve-Roperh *et al.*, 2000).

Although the majority of evidence points to an antiproliferative effect of cannabinoids, it is important to note that in some studies cannabinoids have been found to increase cellular proliferation. Δ^9 -THC (an agonist at both the CB receptors), AEA and HU210 (a potent CB₁ and CB₂ receptor agonist) all increased proliferation at nanomolar concentrations (Hart *et al.*, 2004). This suggests that the CB receptors, by signalling through MAPK and the AKT/PKB pathways can initiate cellular proliferation, cause growth arrest, or induce apoptosis, depending on the concentration (Bifulco *et al.*, 2006).

5.1.2.3 Cannabinoids and smooth muscle cells

Since smooth muscle cells replicate like other cells through entry into the cell cycle, there is reason to believe that cannabinoids may also influence cell growth by manipulation of the regulators of the cell cycle. Indeed two very recent studies have shown in human coronary

artery smooth muscle cells that the CB₁ antagonist, SR141716A, inhibits PDGF induced proliferation and migration by inhibition of Ras and ERK1/2 (Rajesh *et al.*, 2008 b). A study by the same group also demonstrated that treatment with a CB₂ agonist inhibits TNF α induced cellular proliferation and migration, a finding which was ascribed to the inhibition of Ras, p38 MAPK, ERK 1/2, SAPK/JNK and Akt cellular pathways (Rajesh *et al.*, 2008 a). Beyond this, however the influence of cannabinoids receptor agonists on smooth muscle cell growth is a relatively unexplored area.

5.2 Aim

In light of the findings in Chapter 3 that confirmed the presence of both the CB₁ and CB₂ receptors on murine vascular smooth muscle cells, alongside the observations that endocannabinoid concentration increases in tissue subjected to injury, suggests that cannabinoids may be able to influence smooth muscle cells. The aim of this study was to determine the effects of selective cannabinoid receptor agonists acting at the CB₁, CB₂ and the orphan GPR55 (proposed as a third CB receptor; Baker *et al.*, 2005; Ryberg *et al.*, 2007), as well as the endogenous cannabinoids AEA and 2-AG on vascular smooth muscle cell proliferation. ERK1/2 phosphorylation and BrdU incorporation were used as tools to detect smooth muscle cell proliferation. The effect of the agents on cell viability was also investigated using the MTT assay.

5.3 Method

5.3.1 Optimisation of PDGF concentration and incubation time for ERK1/2 ELISA

Primary smooth muscle cells were grown to 90% confluence, quiesced overnight then treated with 10, 30 or 100ng/ml PDGF for 20 minutes. The cells were then harvested and used in both the Phospho and Total ERK 1/2 ELISAs (as described in section 2.5). From these experiments (section 5.5.1), 30ng/ml was decided to be the optimum concentration and was therefore used in all subsequent ERK experiments. To determine the optimum incubation time to ensure maximal ERK phosphorylation, cells were incubated with 30ng/ml PDGF for either 10, 15 or 20 minutes. Again, based on the data reported in section 5.5.1, 15 minutes was identified as the optimum incubation time and was utilised in all further experiments.

5.3.2 Effects of cannabinoid treatment on PDGF induced ERK 1/2 phosphorylation

To determine the effects of cannabinoids on ERK1/2 phosphorylation the CB₁ agonist ACEA, the CB₂ agonist JWH015 and the GPR55 agonist 0-1602 were investigated at a concentration range of 1×10^{-8} to 1×10^{-5} M. The FAAH inhibitor URB597 was also investigated at a single concentration (1×10^{-7} M as used previously in myography studies) to determine the effects of raising endogenous cannabinoid levels. Quiesced cells were treated with the desired concentration of drug for 20 minutes before subsequent stimulation with 30ng/ml of PDGF for 15 minutes. Table 5.1 summarises the treatment protocols for each drug intervention.

Following completion of drug incubation and cell stimulation, cells were harvested by scraping then lysed by addition of lysis buffer as detailed in section 2.5.3. Cell lysates were then analysed for both phospho ERK1/2 and total ERK1/2 by ELISA (section 2.5.5-2.5.6.). To allow comparison of data a Bradford assay was performed on the cell lysates so that results could be standardised relative to the quantity of protein in each sample. Figure 5.2 shows an example of a standard curve used to calculate concentrations of the unknown samples.

Flask Number	Cell treatment
1	Cells without PDGF (un-stimulated control)
2	Cells + 30ng/ml PDGF (stimulated control)
3	Cells + 30ng/ml PDGF + vehicle
4	Cells + 30ng/ml PDGF + Drug (1×10^{-8})M
5	Cells + 30ng/ml PDGF + Drug (1×10^{-7})M
6	Cells + 30ng/ml PDGF + Drug (1×10^{-6})M
7	Cells + 30ng/ml PDGF + Drug (1×10^{-5})M

Table 5.1 Treatment protocols for drug interventions required for a single experiment.

Experiments were performed 3 times using cells from different mice and were measured in duplicate.

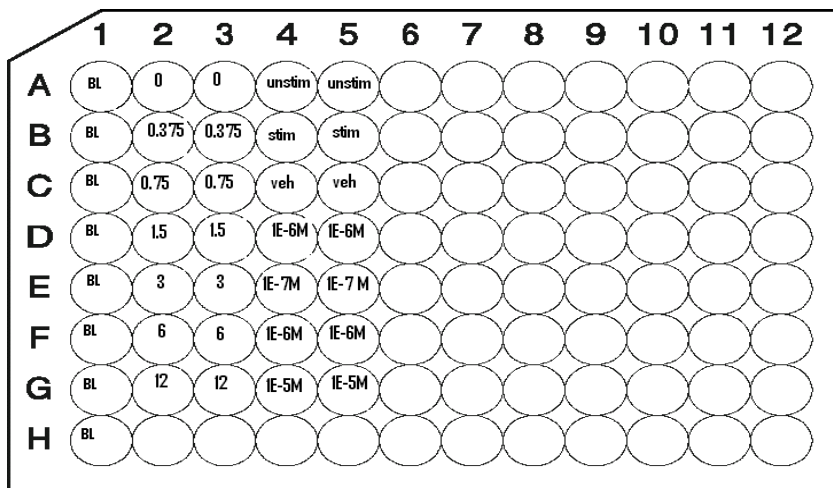


Figure 5.1 An example of the plate lay out used in the ELISAs and the typical arrangement of samples. Column 1 contained blanks (BL); Columns 2 & 3 contained standards (0-12ng/ml); Columns 4 & 5 contained drug treatments (unstim = cells untreated with PDGF; stim = cells treated with PDGF; veh = vehicle).

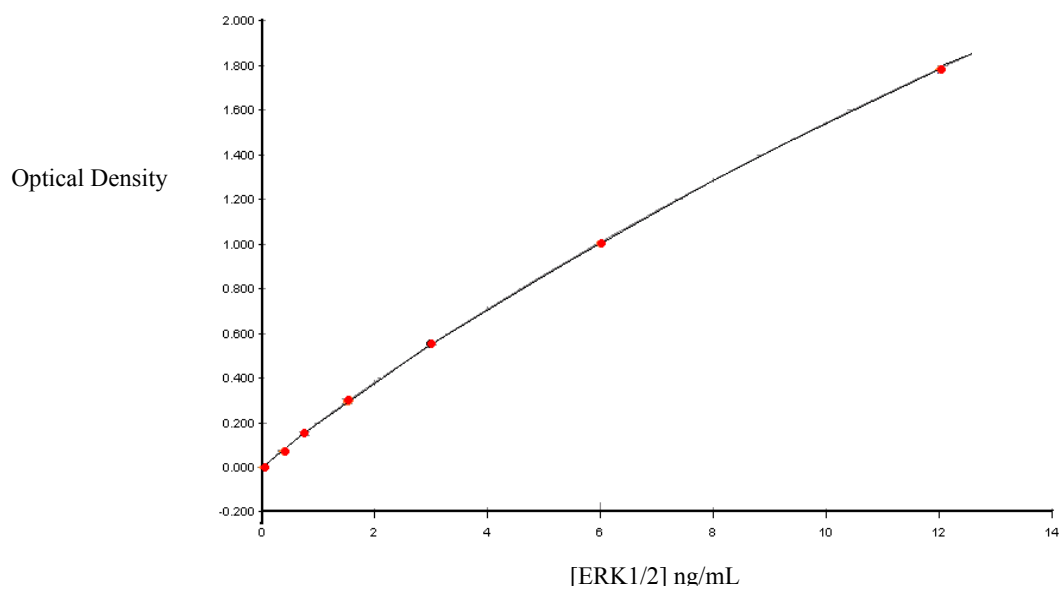


Figure 5.2 An example of a standard curve produced from phospho ERK standards. The absorbance of the standards was plotted against Phospho ERK concentration (ng/ml). From this curve the concentration of the unknown samples were calculated.

5.3.3 Data Expression of ERK1/2 phosphorylation

To allow accurate comparison of samples, results were normalised in accordance to their individual protein concentration (as established by Bradford Assay) to a uniform 2mg/ml as shown below, this was performed for both the phospho and total ERK samples.

$$[\text{Phospho ERK}] \text{ at } 2\text{mg/ml} = \frac{\text{2}}{[\text{Protein of sample}]} \times [\text{Phospho ERK}]$$

The normalised data was then expressed as % phosphorylation, this was calculated as follows.

$$\% \text{ Phosphorylation} = \frac{[\text{Phosphorylated ERK}]}{[\text{Total ERK}]} \times 100$$

Data was then expressed as fold change in % phosphorylation compared to un-stimulated control.

$$\text{Fold change} = \frac{\% \text{ phosphorylation of drug treatment}}{\% \text{ Phosphorylation of un-stimulated control}}$$

5.3.4 Optimisation of PDGF concentration, BrdU incorporation time and cell seeding density for BrdU assay.

Cells were seeded in a 96 well plate at a density of 2000 cells/well and 5000 cells/well, left to adhere for approximately 5 hours then quiesced overnight as detailed in section 2.5.7.1. To determine the concentration of PDGF-BB that would produce maximal stimulation of cells and the optimum BrdU incubation time, cells were stimulated with 10, 30 or 100ng/ml PDGF-BB for 24 hours then incubated for either 12 or 24 hours with BrdU reagent. The experiment was then completed as detailed in method section 2.5.7.2. From these experiments a concentration of 30ng/ml PDGF-BB was identified as the optimum stimulatory concentration, 5000 cells/ well was determined the optimum seeding density and a BrdU incubation time of 24 hours was chosen and utilised in all subsequent experiments (section 2.4.2).

5.3.5 Rationale for choice of cannabinoid ligands to study BrdU incorporation

CB₂ agonists: The data generated from the ERK experiments demonstrated that the CB₂ agonist JWH015 (1x10⁻⁵M) had the greatest effect on ERK phosphorylation. For this reason an equimolar concentration of the CB₂ agonist JWH015 (1x10⁻⁵M), was used as a starting point along with an additional CB₂ agonist JWH133 (1x10⁻⁵M), to confirm that any effects seen were

due to an action at CB₂ receptors. In addition, the CB₂ antagonist AM630 (1x10⁻⁶M), was studied alone and in the presence of each of the CB₂ agonists to further confirm the CB₂ receptor as the site of action. However, as the two CB₂ receptor agonists did not produce similar effects (Figure 5.1.1) a further series of experiments employing a wider concentration range of JWH133 was subsequently performed (1x10⁻⁸-1x10⁻⁵M).

CB₁ agonist: As the ERK phosphorylation data produced following cell treatment with CB₁ agonist ACEA was quite variable, the effect of ACEA was then confirmed using the BrdU assay at the same concentration range (1x10⁻⁸-1x10⁻⁵M) rather than using a single concentration.

Endocannabinoids: Since the FAAH inhibitor URB597 did not produce any effects in the ERK phosphorylation assay, the direct effects of the endocannabinoids AEA and 2-AG on BrdU incorporation were investigated at a concentration range of 1x10⁻¹² to 1x10⁻⁵M.

5.3.6 Cannabinoid treatment of cells

The 96 well plates containing quiesced cells were incubated with the desired concentration of drug for 15 minutes, after which time the media was then supplemented with 30ng/ml PDGF-BB. The cells were then left to incubate for 24 hours at 37° C and 5% CO₂. Following a 24 hour incubation BrdU reagent was prepared (as detailed in section 2.9.5), added to the cells, and left to incubate for a further 24 hours at 37° C and 5% CO₂. For all sample groups an un-stimulated control, a stimulated control and a vehicle control were included as detailed in Table 5.2.

Un-stimulated Control	Cells + 0.3% serum media
Stimulated control	Cells + PDGF
Vehicle Control	Cells+ PDGF + vehicle
Drug sample	Cells +PDGF+ drug

Table 5.2 Controls included for all drug treatment groups in the BrdU assay.

5.3.7 Data Expression

Data was expressed as a fold change in absorbance over the un-stimulated control.

$$\text{Fold change in absorbance} = \frac{\text{Absorbance of drug treated samples}}{\text{Absorbance of un-stimulated control}}$$

5.3.8 Drug treatments for MTT assay

To ensure that the reduction in BrdU incorporation (DNA synthesis) observed following drug treatment was a result of cellular actions as opposed to drug induced cytotoxicity, cell viability following exposure to a variety of drugs (detailed in Table 5.3) was investigated by MTT assay.

Cells were prepared for the assay as described in section 2.6 then incubated with drug for 24hours (as detailed in Table 5.3). Agents that had produced a significant effect on BrdU incorporation were tested following 48 hour incubation. PDGF-BB was included at a concentration of 30ng/ml in all treatments aside from the triton X control. Following drug incubation the assay was completed as detailed in section 2.6.

Cell treatments 24 hours	Cell treatment 48 hours	Concentration (M)
Triton X	Triton X	(see materials)
Media	Media	-
JWH015	JWH015	1x10 ⁻⁵
JWH133	-	1x10 ⁻⁵
Ethanol	-	1%
DMSO	-	1%
DMSO + Ethanol	DMSO + Ethanol	As above
AM630	AM630	1x10 ⁻⁶ M
AM630 + JWH133	AM630 + JWH133	As above
AM630 + JWH015	AM630 + JWH015	As above
AEA	AEA	1x10 ⁻⁵
2-AG	-	1x10 ⁻⁵

Table 5.3 Details of the concentrations of drugs investigated in the MTT assay.

5.3.9 Data Expression

Cell viability following drug treatment was calculated as % Cell viability as shown below.

$$\% \text{ Viability} = \frac{(\text{Sample absorbance} - \text{Triton X absorbance})}{(\text{Media absorbance} - \text{Triton X absorbance})} \times 100$$

5.4 Data Analysis

Statistical analysis was carried out using a one-way analysis of variance (ANOVA) with a Dunnetts post test (Graph pad Prism 4), unless otherwise stated, significance was accepted when P<0.05. Samples from the ERK ELISA were measured in duplicate and experiments were repeated 3 times with cells originating from 3 different mice. Samples for the BrdU assay and MTT assay were measured in triplicate and experiments were repeated 3 times with cells originating from three different mice.

5.5 Drugs

- ACEA (Tocris) A CB₁ receptor agonist, this was dissolved in ethanol to a stock solution of 1×10^{-2} M, this was diluted in ethanol and serum free media to required concentrations maximum ethanol concentration was 1%.
- JWH015 & JWH133 (Tocris) CB₂ receptor agonists, these were dissolved in ethanol to a stock solution of 1×10^{-2} M, this was diluted in ethanol and serum free media to required concentrations maximum ethanol concentration was 1%.
- 0-1602 (Tocris) A GPR55 agonist, this was dissolved in methyl acetate to a stock solution of 1×10^{-2} M, this was diluted in serum free media to the required concentrations
- Anandamide (Tocris) An endogenous cannabinoid, this was dissolved in ethanol to a stock solution of 1×10^{-2} M, this was diluted in ethanol and serum free media to required concentrations maximum ethanol concentration was 1%.
- 2-AG (Tocris) An endogenous cannabinoid, this was dissolved in ethanol to a stock solution of 1×10^{-2} M, this was diluted in ethanol and serum free media to required concentrations maximum ethanol concentration was 1%
- AM630 (Tocris) A CB₂ receptor antagonist, this was dissolved in ethanol to a stock solution of 1×10^{-2} M, this was diluted in DMSO and serum free media to required concentrations maximum DMSO concentration was 1%.

5.6 Results

5.6.1 Determination of optimum conditions

5.6.1.1. Determination of optimum conditions for measuring ERK1/2 phosphorylation

When cells were incubated with PDGF-AB for 20 minutes at concentrations of 10, 30 and 100ng/ml, over a 4 fold increase in % phosphorylation was observed at all concentrations (Figure 5.3) with no apparent concentration dependency. A maximum fold change was observed at 100ng/ml (5.6 ± 1.79) followed by 10ng/ml (5.2 ± 2.45) then 30ng/ml (4.41 ± 1.19) $n=3$ for all. As there was no statistical difference between any of the concentration responses, 30ng/ml was chosen as the optimum PDGF concentration, as it was shown to exhibit the least variability. To determine the optimum PDGF incubation time, cells were incubated with 30ng/ml PDGF for either 10, 15, or 20 minutes (Figure 5.4) $n=2$. A 15-minute incubation time produced the largest fold change in % phosphorylation and was therefore chosen as the optimum incubation time and was applied in all subsequent experiments.

5.6.1.2 Determination of optimum conditions for the BrdU assay

At concentrations of 10ng/ml to 100ng/ml, PDGF-BB produced an increase in absorbance of over 2 fold (compared to un-stimulated control) in cells that had been seeded at a density of both 2000 cells/well (Figure 5.5) and 5000 cells/well (Figure 5.6). Although the group size was too small (n=2) to perform any statistical analysis, the data indicates a trend of little difference in response to incubating the cells for 12 or 24hours with BrdU, at either seeding density. It can be seen that at both cell densities the highest fold increase in absorbance was produced at 100ng/ml PDGF at the 24 hour time point (2.86 fold increase at a density of 2000 cells/well and 3 fold increase at a density of 5000 cells/well). 30ng/ml PDGF induced an increase in absorbance of approximately 2.5 fold at 24 hours at both seeding densities. A seeding density of 5000 cells/well, 30ng/ml of PDGF and 24hour incubation with BrdU were thus chosen as the optimum conditions and were applied in all further BrdU incorporation experiments.

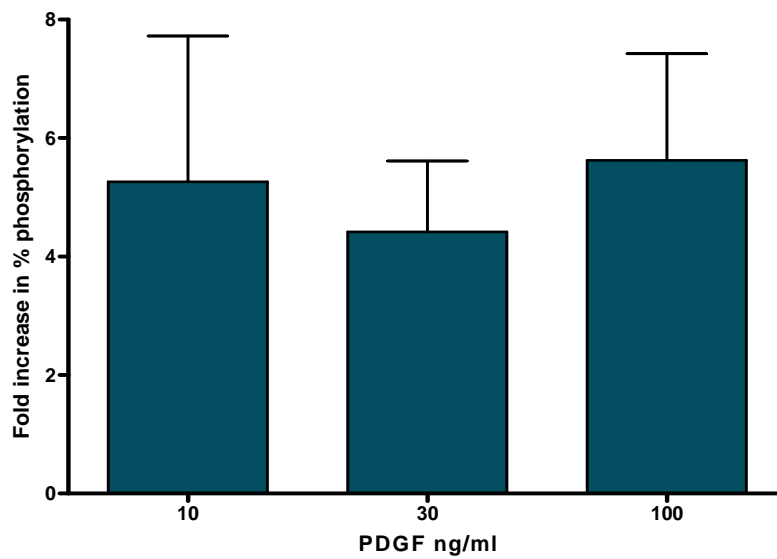


Figure 5.3. ERK1/2 phosphorylation in response to increasing PDGF concentrations in MVSMC. Cells were incubated with varying concentrations of PDGF-AB for 20 minutes. Results are expressed as a fold change in % phosphorylation compared to the % phosphorylation measured in cells that had not been treated with PDGF. Samples were measured in duplicate, n =3, mean + SEM.

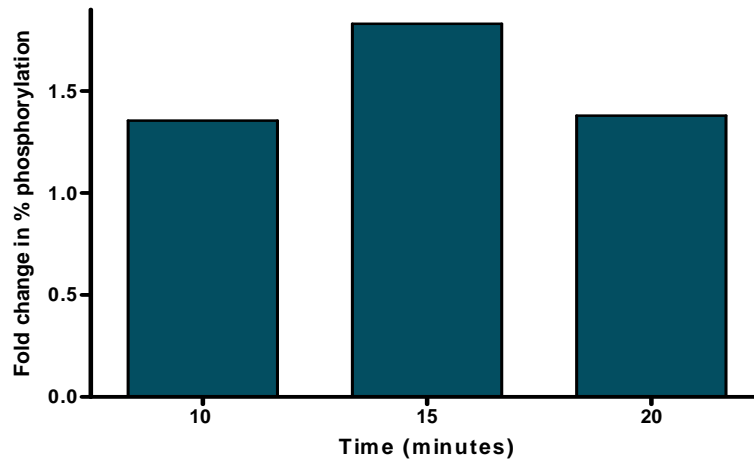


Figure 5.4 ERK1/2 phosphorylation in response to increasing PDGF incubation time in MVSMC. Cells were incubated with 30ng/ml PDGF-AB over varying incubation times. Results are expressed as a fold change in % phosphorylation compared to the % phosphorylation measured in cells that had not been treated with PDGF. Samples were measured in duplicate, n=2.

Incubation time (minutes)	Exp 1	Exp2
10	1.27	1.43
15	1.92	1.73
20	1.36	1.39

Table 5.4. The individual values of ERK1/2 phosphorylation in response to increasing PDGF incubation time. Results are expressed as a fold change in % phosphorylation compared to the % phosphorylation measured in cells that had not been treated with PDGF.

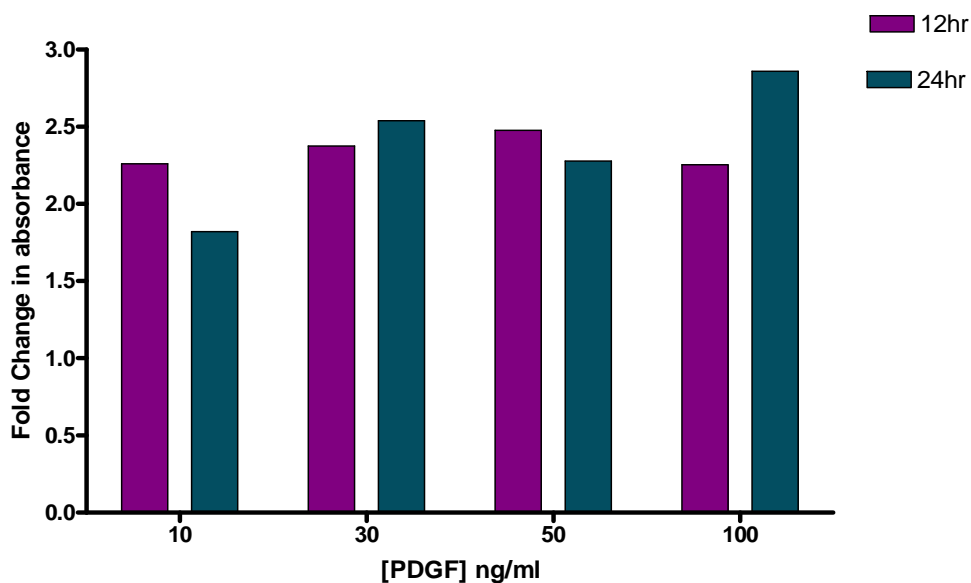


Figure 5.5. Increasing concentrations of PDGF on BrdU incorporation at both 12 and 24 hour time points at a cell seeding density of 2000 cells/ well. Results are expressed as a fold change in % phosphorylation compared to the % phosphorylation measured in cells that had not been treated with PDGF. Samples were measured in duplicate, n=2.

[PDGF] ng/ml	12 hours		24 hours	
	EXP 1	EXP 2	EXP 1	EXP 2
10	1.65	2.86	1.38	1.95
30	1.86	2.89	2.16	2.58
50	1.91	3.03	2.14	2.04
100	1.88	2.61	2.28	2.40

Table 5.5. Individual results of increasing PDGF concentration on BrdU incorporation at both 12 and 24 hour time points at a cell seeding density of 2000 cells/ well. Results are expressed as a fold change in % phosphorylation compared to the % phosphorylation measured in cells that had not been treated with PDGF.

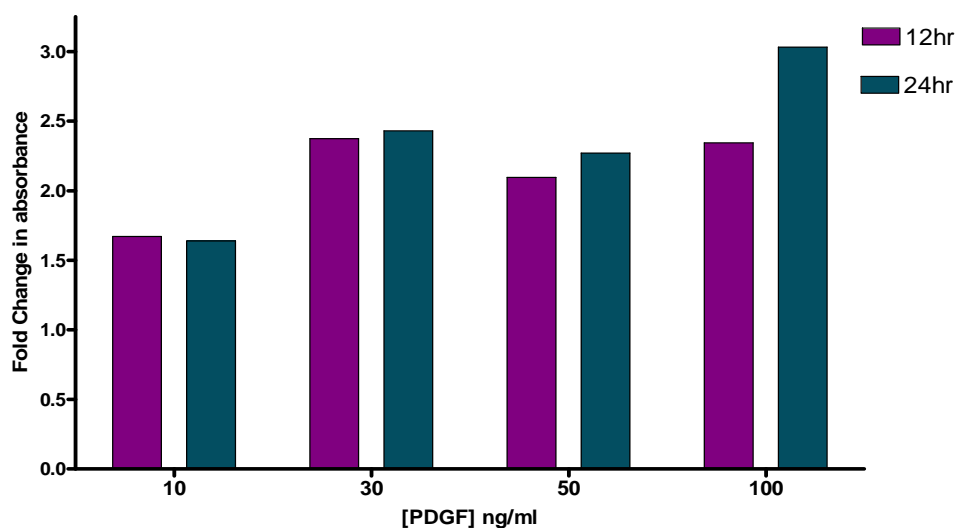


Figure 5.6. Increasing concentrations of PDGF on BrdU incorporation at both 12 and 24 hour time points at a cell seeding density of 5000 cells/ well. Results are expressed as a fold change in % phosphorylation compared to the % phosphorylation measured in cells that had not been treated with PDGF. Samples were measured in duplicate, n=2.

[PDGF] ng/ml	12 hours		24 hours	
	Exp 1	Exp 2	Exp 1	Exp 2
10	1.38	1.95	1.51	1.76
30	2.16	2.58	2.27	2.58
50	2.14	2.04	2.08	2.45
100	2.28	2.40	2.98	3.08

Table 5.6 Individual experimental values of increasing concentrations of PDGF on BrdU incorporation at both 12 and 24 hour time points at a cell seeding density of 5000 cells/ well. Results are expressed as a fold change in % phosphorylation compared to the % phosphorylation measured in cells that had not been treated with PDGF.

5.6.2 The effect of CB receptor ligands on ERK1/2 phosphorylation

5.6.2.1 CB₁ agonist ACEA

PDGF-AB stimulation of the cells (control) produced a 2.8 ± 1.08 fold increase in % ERK1/2 phosphorylation. The CB₁ agonist ACEA appeared to reduce ERK1/2 phosphorylation at higher concentrations (Figure 5.7), although there was no statistically significant effect across the concentration range (1×10^{-8} to 1×10^{-5} M); One way ANOVA with Dunnetts post-hoc test $n=3$ unless indicated). However, the vehicle (0.1% ethanol) alone induced a marked inhibitory effect (fold change in the presence of vehicle was 1.05 ± 0.41) which clearly masked any effect of ACEA itself. Statistical comparison of the highest concentration of ACEA with the vehicle (ethanol) did not reveal a significant difference. Statistical analysis could not be performed in comparison to the control as there was only an $n=2$.

5.6.2.2. CB₂ agonist JWH015

In these experiments PDGF-AB treatment induced a 2.0 ± 0.27 fold increase in ERK phosphorylation compared to an un-stimulated control (Figure 5.8), which was unaffected by the vehicle (0.1% ethanol). Low concentrations (10^{-8} M & 10^{-7} M) of JWH015 had no effect, but higher concentrations (10^{-6} & 10^{-5} M) showed a reduction in phosphorylation (from 2.0 ± 0.27 to 1.47 ± 0.44 and 0.49 ± 0.179 , respectively) although this did not reach statistical significance (One way ANOVA with Dunnett's post test $n=3$).

5.6.2.3 GPR55 agonist 0-1602

PDGF-AB stimulation of cells (control) produced a 3.6 ± 1.39 fold increase in ERK 1/2 phosphorylation (Figure 5.9). Treating cells with either the vehicle control, (0.1% methyl acetate), or increasing concentrations of 0-1602 (GPR55 agonist) had no effect on PDGF induced ERK1/2 phosphorylation (One way ANOVA with Dunnetts post test $n=3$).

5.6.2.4. Raising endogenous AEA concentration

Stimulating cells with PDGF-AB produced a 2.43 ± 1.25 fold increase in % phosphorylation (Figure 5.10). Treating cells with URB597 (1×10^{-7} M) and the vehicle control (0.1% DMSO) had a negligible effect on % phosphorylation (one way ANOVA with Dunnett's post test $n=3$).

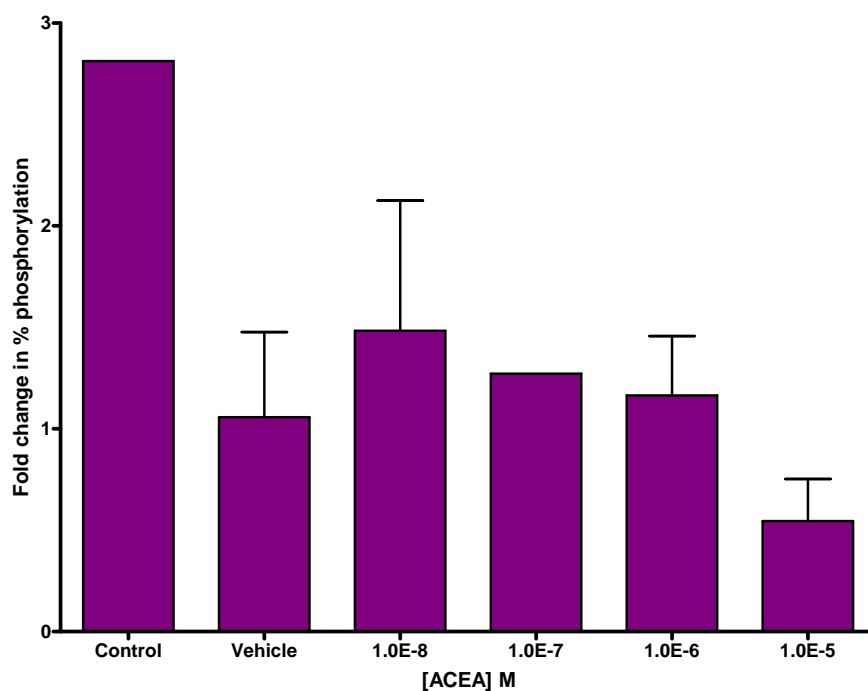


Figure 5.7 The effect of ACEA on PDGF stimulated ERK 1/2 phosphorylation. Cells were stimulated with 30ng/ml PDGF-AB for 15 minutes. Results are expressed as a fold change in % phosphorylation compared to the % phosphorylation measured in cells that had not been treated with PDGF. Samples were measured in duplicate, n=3, mean + SEM where error bars are not present samples are n=2.

Cell treatment	EXP 1	EXP2
Control	1.73	3.4
1x10 ⁻⁷ M ACEA	2.01	0.53

Table 5.7 Individual experimental values of the control cells and cells treated with 1x10⁻⁷M ACEA. Results are expressed as a fold change in % phosphorylation compared to the % phosphorylation measured in cells that had not been treated with PDGF.

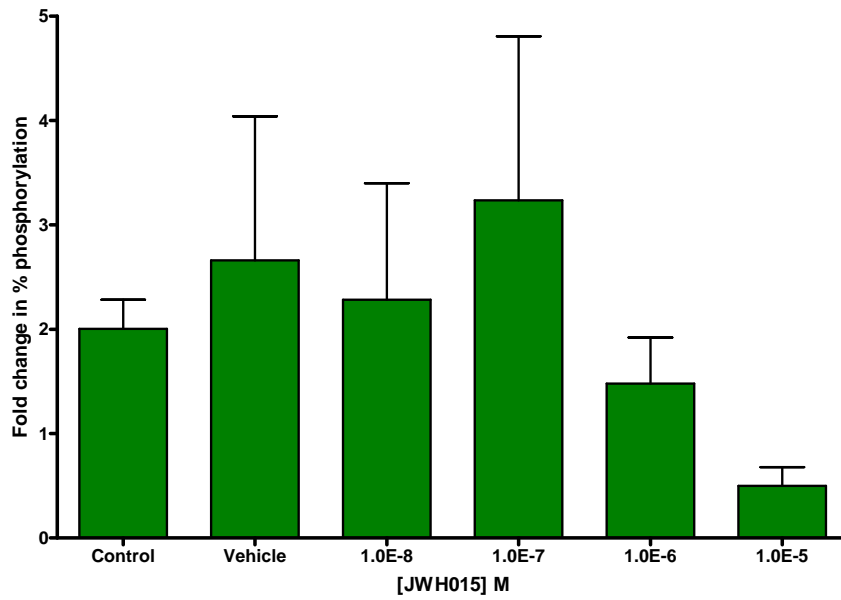


Figure 5.8. The effect of JWH015 on PDGF stimulated ERK 1/2 phosphorylation. Cells were stimulated with 30ng/ml PDGF-AB for 15 minutes. Results are expressed as a fold change in % phosphorylation compared to the % phosphorylation measured in cells that had not been treated with PDGF. Samples were measured in duplicate, n=3, mean + SEM.

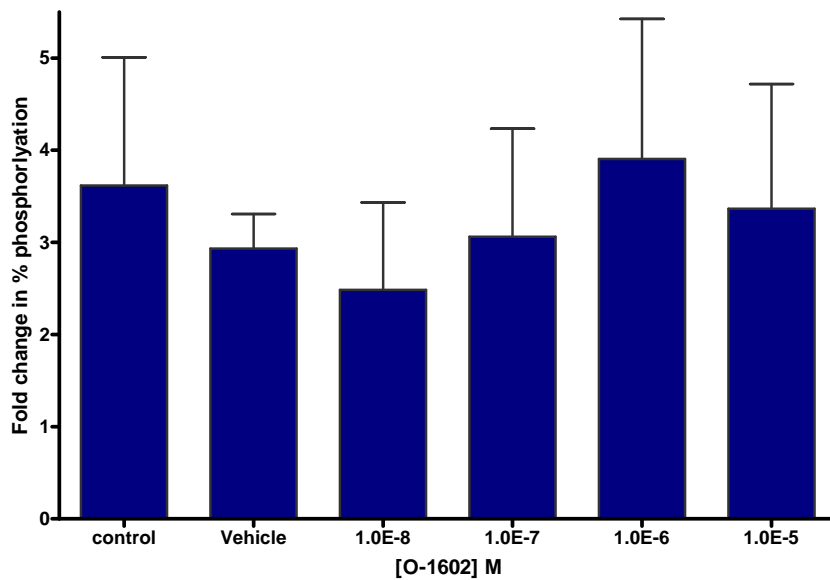


Figure 5.9. The effect of O-1602 on PDGF stimulated ERK 1/2 phosphorylation. Cells were stimulated with 30ng/ml PDGF-AB for 15 minutes. Results are expressed as a fold change in % phosphorylation compared to the % phosphorylation measured in cells that had not been treated with PDGF. Samples were measured in duplicate, n=3, mean + SEM.

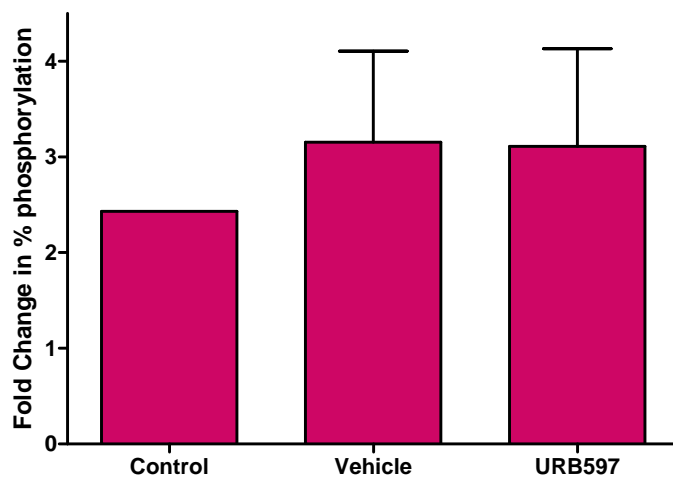


Figure 5.10. The effect of URB597 on PDGF induced ERK1/2 phosphorylation.

Cells were stimulated with 30ng/ml PDGF-AB for 15 minutes Results are expressed as a fold change in % phosphorylation compared to the % phosphorylation measured in cells that had not been treated with PDGF. Samples were measured in duplicate, n=3, mean + SEM, where no error bar is present n= 2.

Cell treatment	EXP1	EXP2
Control	1.2	3.7

Table 5.8 Individual experimental values of the control cells. Results are expressed as a fold change in % phosphorylation compared to the % phosphorylation in cells that had not been treated with PDGF.

5.6.3. The effect of CB receptor ligands on BrdU incorporation

5.6.3.1 The effect of CB₂ agonists and antagonist on BrdU incorporation

To investigate the effects of CB₂ agonists more thoroughly on cell proliferation their effect on BrdU incorporation was measured. BrdU incorporation is a marker of DNA synthesis and therefore a useful tool for investigating activation of the proliferation pathway. Stimulating cells with PDGF-BB produced a 1.8 ± 0.28 fold increase in BrdU incorporation (Figure 5.11). Treating cells with the CB₂ agonist JWH015 (1×10^{-5} M) culminated in a significant reduction in BrdU incorporation (0.78 ± 0.15) as did the CB₂ antagonist AM630 (1×10^{-6} M) alone (0.83 ± 0.156), and in combination with both CB₂ agonists (AM630 + JWH133 0.87 ± 0.17 ; AM630 + JWH015 0.82 ± 0.167). Cells treated with only JWH133 (1×10^{-5} M) exhibited a small attenuation in BrdU incorporation compared to the control; however this failed to reach statistical significance ($P < 0.05$ one way ANOVA with Dunnetts post test $n=3$). When a wider concentration of JWH133 (1×10^{-8} - 1×10^{-5} M) was studied (Figure 5.12) there was similarly a negligible effect on BrdU incorporation ($P > 0.05$ one way ANOVA with Dunnetts post test $n=3$).

5.6.3.2. CB₁ agonist ACEA

Stimulating cells with PDGF-BB produced a 2.3 ± 0.6 fold increase in BrdU incorporation (Figure 5.13) which was unaffected by the vehicle (1% ethanol). The CB₁ receptor agonist ACEA attenuated BrdU incorporation at 1×10^{-5} M, however this did not reach statistical significance; between 1×10^{-8} M - 1×10^{-6} M there was no effect on BrdU incorporation. $P > 0.05$ one way ANOVA with Dunnetts post test $n=4$.

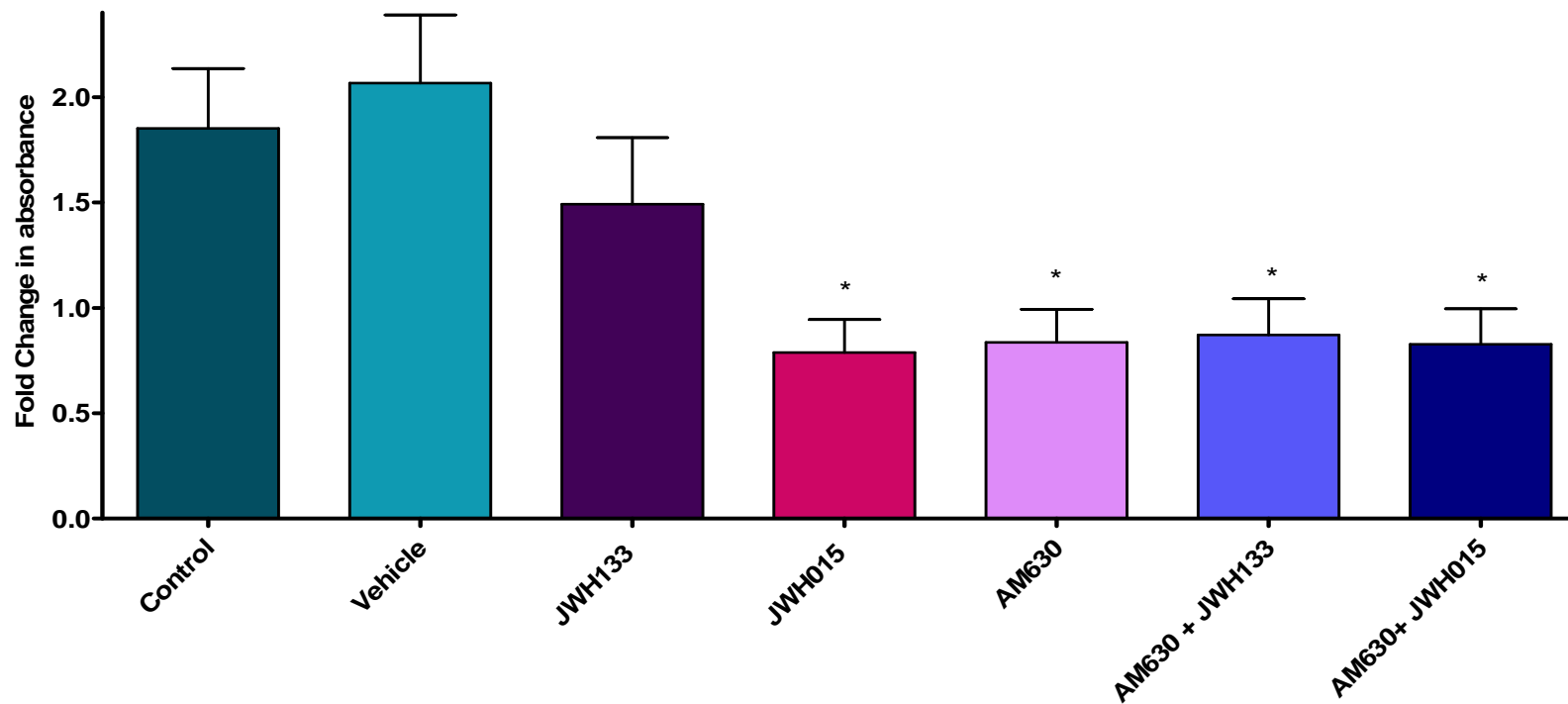


Figure 5.11. The effect of the CB₂ agonists JWH015 and JWH133, and CB₂ antagonist AM630 on PDGF stimulated BrdU incorporation. JWH133 and JWH015 were used at a concentration of $1 \times 10^{-5} \text{M}$, AM630 ($1 \times 10^{-6} \text{M}$) Results are expressed as a fold change in % absorbance compared to the absorbance measured in cells that had not been treated with PDGF. Samples were measured in triplicate, $n=3$, mean + SEM * Indicates $P < 0.05$ compare to stimulated control (one way ANOVA with a Dunnetts post test).

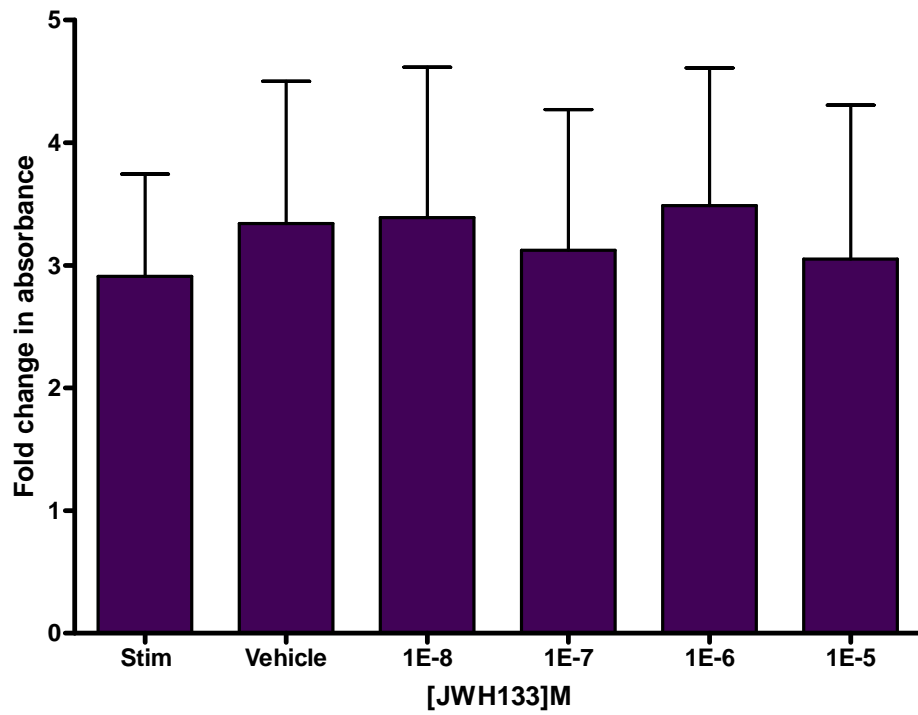


Figure 5.12 The effect of JWH133 on PDGF stimulated BrdU incorporation. Results are expressed as a fold change in % absorbance compared to the absorbance measured in cells that had not been treated with PDGF. Samples were measured in triplicate, n=3, mean + SEM.

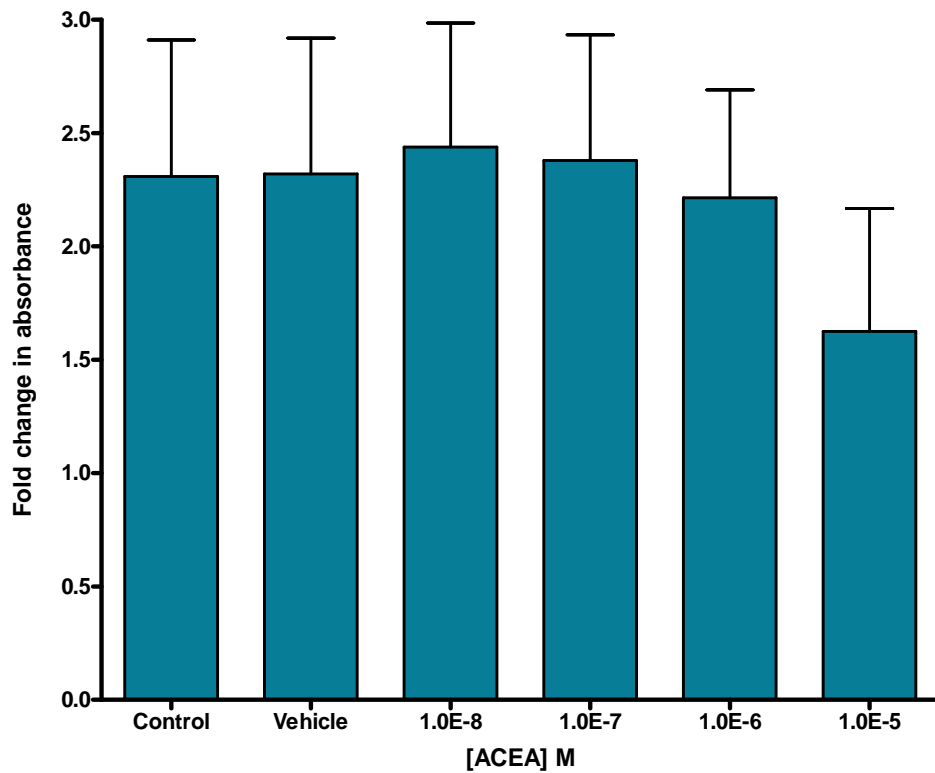


Figure 5.13. The effect of ACEA on PDGF stimulated BrdU incorporation. Results are expressed as a fold change in % absorbance compared to the absorbance measured in cells that had not been treated with PDGF. Samples were measured in triplicate, n=4, mean + SEM.

5.6.3.3 The effect of AEA on BrdU incorporation

PDGF-BB stimulation of control cells produced a 1.93 ± 0.36 fold increase in BrdU incorporation which was unaffected by the vehicle (1% ethanol). A concentration range of 10^{-12} M to 10^{-6} M AEA showed no effect (Figure 5.14) however, 1×10^{-5} M AEA induced a significant reduction in BrdU incorporation (Figure 5.15 $P < 0.05$ One-way ANOVA with a Dunnetts post test $n=3$).

5.6.3.4. The effect of 2-AG on BrdU incorporation

Stimulating cells with PDGF-BB (control cells) produced a 2.51 ± 0.82 fold increase in BrdU incorporation which was unaffected by the vehicle (1% ethanol). At a concentration range of 1×10^{-12} M to 1×10^{-7} M there was no effect (Figure 5.16) however 1×10^{-6} M 2-AG produced a small attenuation in BrdU incorporation, this did not reach significance ($n=3$). At a concentration of 1×10^{-5} M there was also no effect on BrdU incorporation (Figure 5.17).

5.6.3.5. The effect of AEA and 2-AG on BrdU incorporation

PDGF stimulation of control cells produced a 2.17 ± 0.27 fold increase in BrdU incorporation (Figure 5.18) which was unaffected by the vehicle (1%DMSO + 1% ethanol). A combination of AEA+2-AG (both 1×10^{-5} M) significantly reduced BrdU incorporation to 0.69 ± 0.19 fold ($P < 0.01$ Students t test $n=3$).

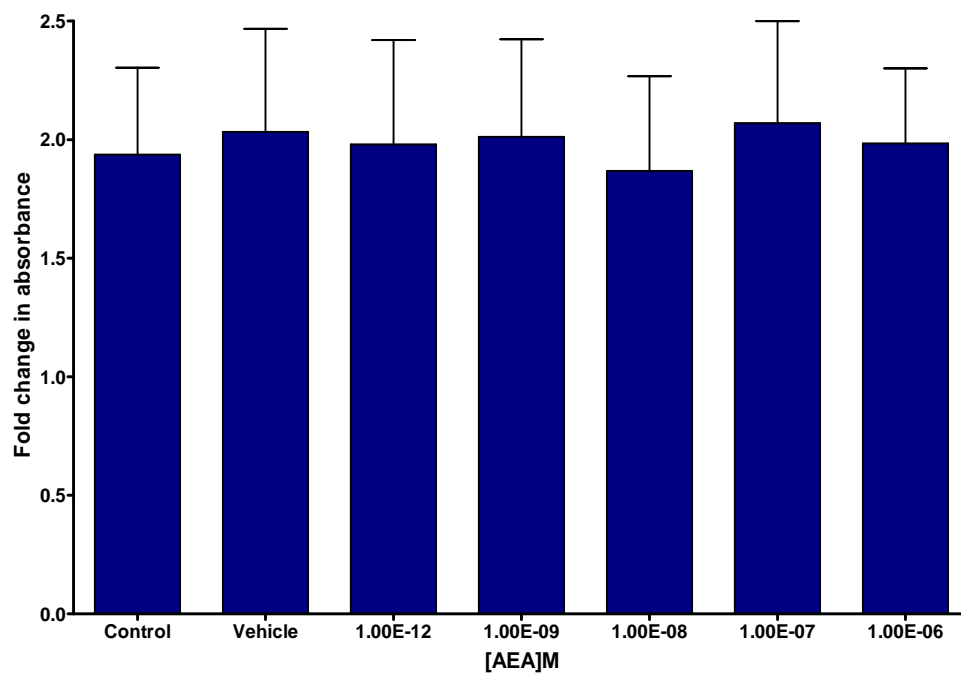


Figure 5.14 The effect of AEA on PDGF stimulated BrdU incorporation. Results are expressed as a fold change in % absorbance compared to the absorbance measured in cells that had not been treated with PDGF. Samples were measured in triplicate, n=3, mean + SEM

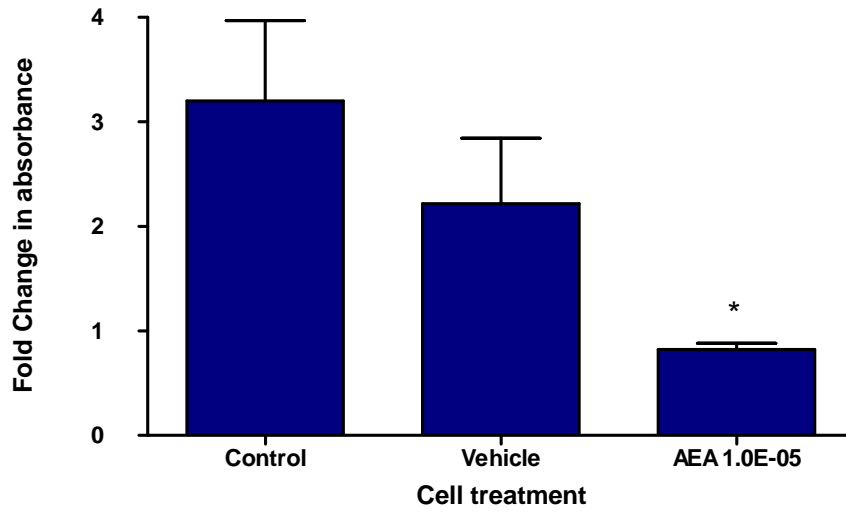


Figure 5.15 The effect of AEA ($1 \times 10^{-5} \text{M}$) on PDGF stimulated BrdU incorporation. Results are expressed as a fold change in % absorbance compared to the absorbance measured in cells that had not been treated with PDGF. Samples were measured in triplicate, $n=3$, mean + SEM. * Indicates $P < 0.05$ compared to stimulated control (one-way ANOVA with a Dunnetts post test). $P=0.06$ between AEA and vehicle control.

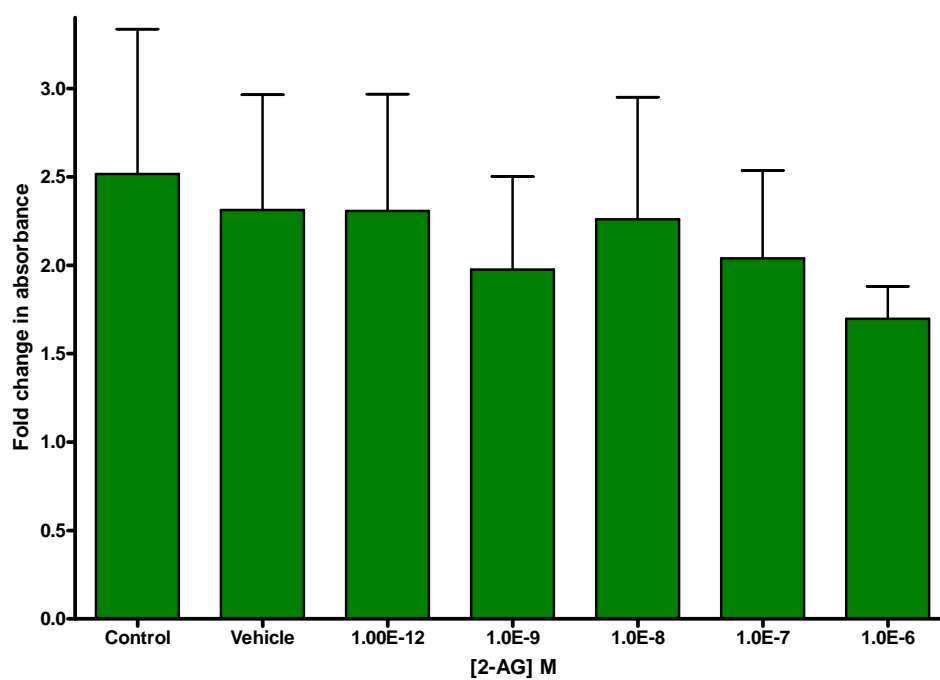


Figure 5.16 The effect of treating cells with 2-AG on PDGF stimulated BrdU incorporation. Results are expressed as a fold change in % absorbance compared to the absorbance measured in cells that had not been treated with PDGF. Samples were measured in triplicate, n=3, mean + SEM.

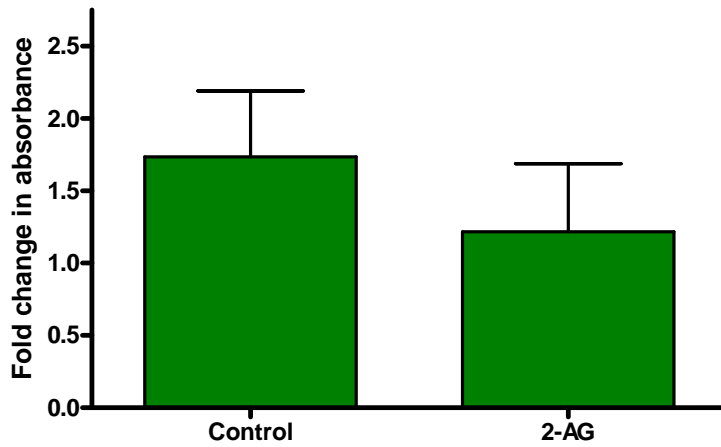


Figure 5.17 The effect of 2-AG ($1 \times 10^{-5} \text{M}$) on PDGF stimulated BrdU incorporation. Results are expressed as a fold change in % absorbance compared to the absorbance measured in cells that had not been treated with PDGF. Samples were measured in triplicate, $n=3$, mean + SEM.

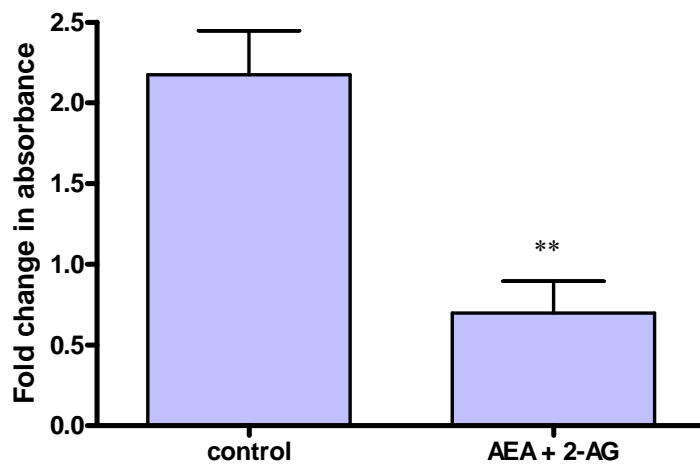


Figure 5.18 The effect of AEA and 2-AG combined on PDGF stimulated BrdU incorporation. Results are expressed as a fold change in % absorbance compared to the absorbance measured in cells that had not been treated with PDGF. Samples were measured in triplicate, $n=3$, mean + SEM ** Indicates $P < 0.01$ (Students t test).

5.6.4 The effect of the CB₂ agonists/antagonist and their corresponding vehicles on % cell viability

5.6.4.1 The effects of CB₂ agonists on % cell viability

Incubation with JWH015 (1×10^{-5} M) for either 24 or 48 hours elicited no detrimental effects on cell viability. Moreover cells that were treated with JWH133 (1×10^{-5} M) or the vehicle (1% ethanol) for 24 hours similarly did not have reduced % cell viability as measured by MTT assay, $n=3$ (Figure 5.19).

5.6.4.2 The effects of a CB₂ antagonist on cell viability.

Interestingly, cells that were treated with AM630 for both 24 and 48 hours exhibited a significant increase in % cell viability compared to the DMSO (1%) vehicle control (105.17 ± 3.0 and 82 ± 6.6 respectively), $P < 0.05$; Students *t* test $n=3$ (Figure 5.20).

5.6.4.3 The effects of a CB₂ antagonist in combination with a CB₂ agonist on cell viability.

Cells that were treated with the vehicle (1% DMSO + 1% ethanol) for 24 hours exhibited a cell viability of $72.87 \pm 9.9\%$ (Figure 5.21). In contrast when cells were incubated with AM630 in combination with JWH015, there was a significant increase in % cell viability compared to the vehicle ($P < 0.05$ one way ANOVA with Dunnetts post test $n=3$). Similarly, when cells were incubated with AM630 in combination with JWH133 cell viability was increased to over 100%, however this did not reach statistical significance ($P > 0.05$ one way ANOVA with Dunnetts post test $n=3$).

When the same combinations of drugs were incubated for 48 hours a dissimilar trend was observed (Figure 5.21). The vehicle control (DMSO + ethanol) similarly reduced cell viability to $88 \pm 13.85\%$, however the combination of AM630 and JWH133 had a negligible effect on cell viability compared with the control.

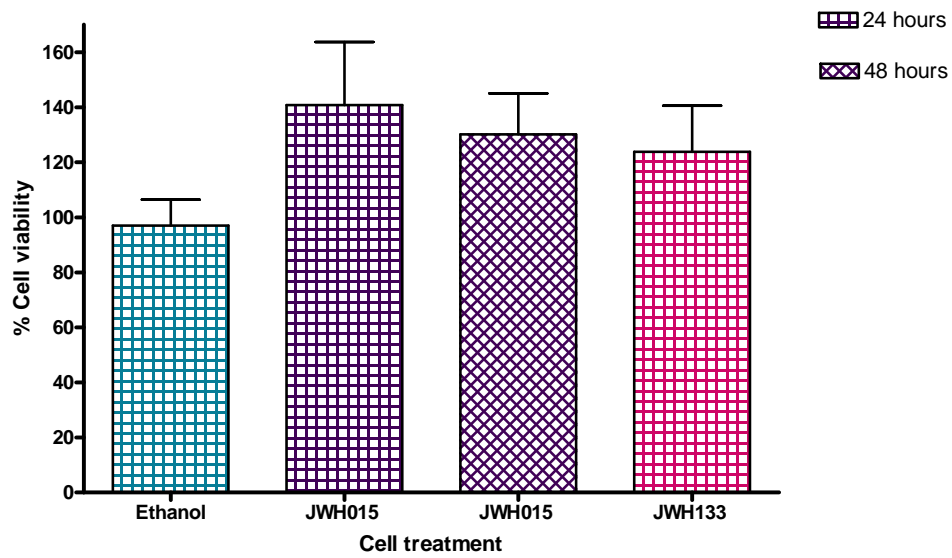


Figure 5.19 The effect on cell viability following treatment with vehicle, JWH015 and JWH133 ($1 \times 10^{-5} \text{M}$), measured by MTT assay. Data is shown as a % of cell viability, samples measured in triplicate, $n=3$, mean + SEM.

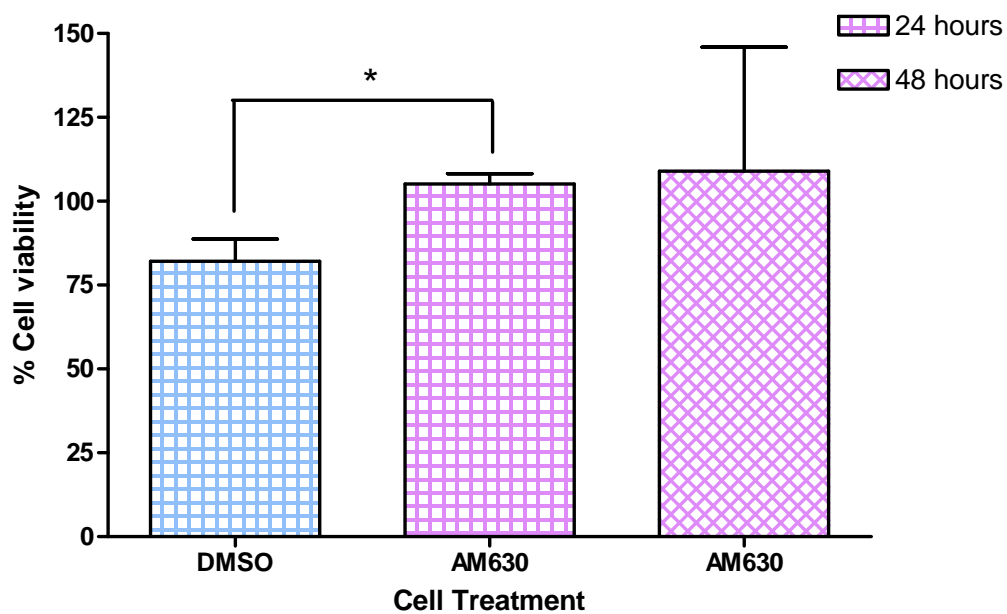


Figure 5.20 The effect on cell viability following 24 and 48 hour incubation with the CB₂ antagonist AM630 measured by MTT assay. AM630 1x10⁻⁶M, Data is shown as a % of cell viability, samples were measured in triplicate n =3, mean + SEM.

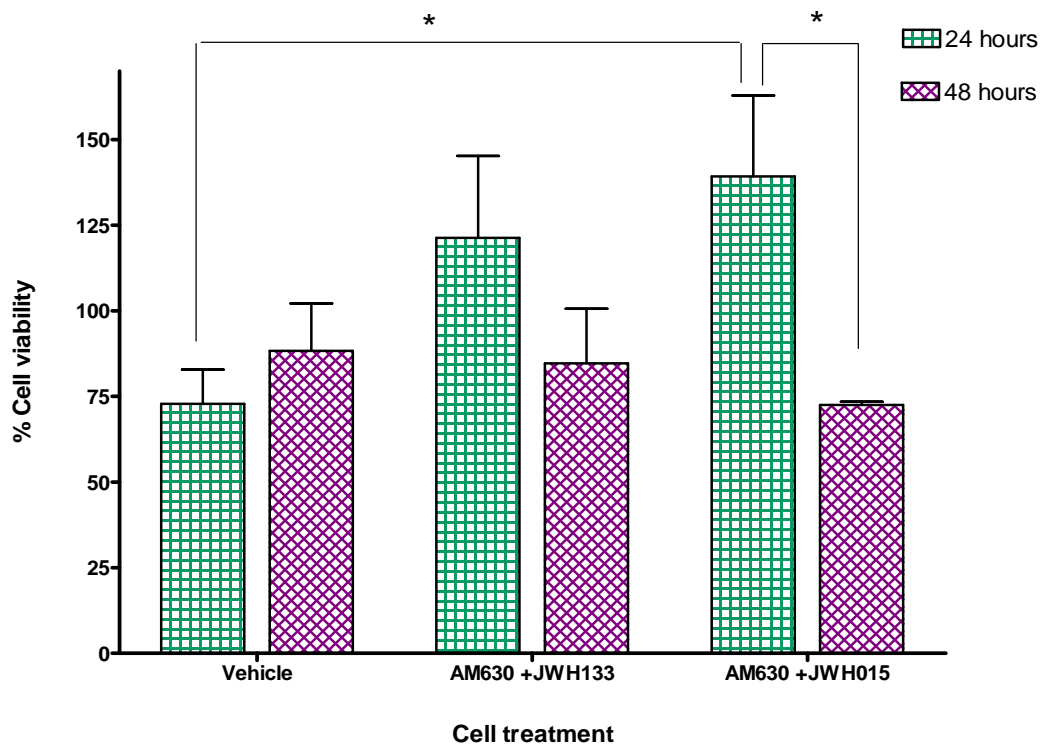


Figure 5.21 A comparison between the effect on cell viability following 24 hour or 48 hour incubation with the CB₂ antagonist AM630 in combination with CB₂ agonists, measured by the MTT assay. Vehicle = Ethanol + DMSO, AM630 was used at 1x10⁻⁶M, JWH133 and JWH015 were used at 1x10⁻⁵M. Data is shown as a % of cell viability. Samples were measured in triplicate, n=3, mean + SEM.

5.6.5 The effect of the endocannabinoids AEA and 2-AG on cell viability

Treating cells with AEA ($1 \times 10^{-5} \text{M}$) for 24 hours (Figure 5.22) resulted in a reduced % cell viability of $41\% \pm 19.6$ compared to the vehicle (1% ethanol) control ($96.97 \pm 16.38\%$), however this failed to reach statistical significance (Students t test $P > 0.05$ $n=3$). Paradoxically, when cells were treated with AEA ($1 \times 10^{-5} \text{M}$) for 48 hours % cell viability was normal (109.5 ± 15.9 ; $P=0.0556$; Students t test compared to 24 hour data $n=3$). Treating cells with 2-AG ($1 \times 10^{-5} \text{M}$) or the vehicle (1% ethanol) had no detrimental effects on % cell viability ($111.61 \pm 20.54\%$ and $96.9 \pm 9.46\%$ respectively; Figure 5.23).

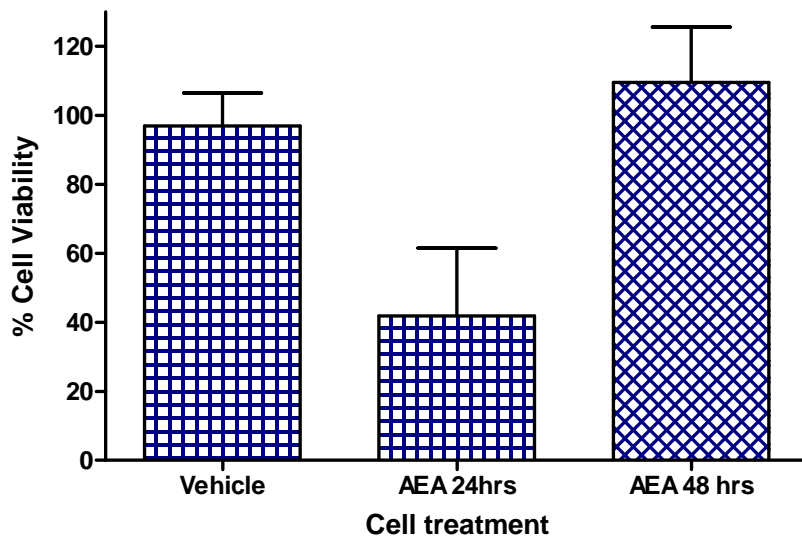


Figure 5.22 The effect of AEA ($1 \times 10^{-5} \text{M}$) at both 24 and 48hrs on cell viability, measured by MTT assay. Data is shown as % cell viability. $n=3$, mean + SEM $P = 0.0556$ Students t test.

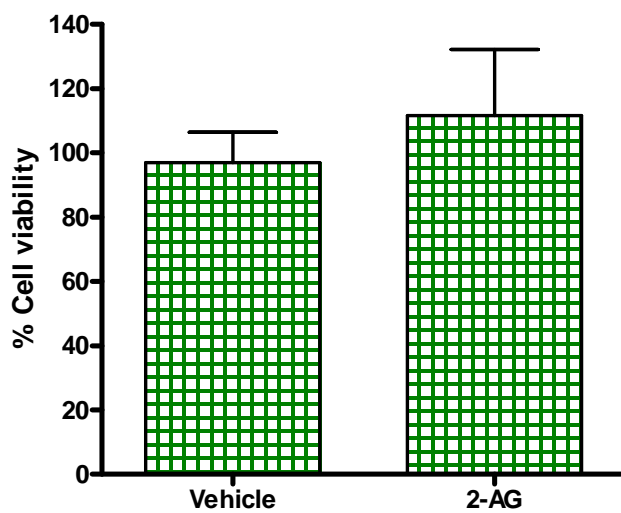


Figure 5.23 The effect of 2-AG ($1 \times 10^{-5} \text{M}$) on cell viability, measured by MTT assay. Data is shown as a % of cell viability. $n=3$, mean + SEM.

5.7 Discussion

The aim of this study was to investigate the effects of selective cannabinoid receptor agonists acting at the CB₁, CB₂ and the orphan GPR55 receptor, as well as the endogenous cannabinoids AEA and 2-AG, on vascular smooth muscle cell proliferation. ERK1/2 phosphorylation and BrdU incorporation were used as tools to detect smooth muscle cell proliferation. To ensure results were not due to cytotoxicity cell viability was investigated. The results of this study show that JWH015 and AM630 both induced a reduction in cell proliferation without any detrimental effects on cell viability, while high concentrations of AEA (10 μ M) reduced proliferation associated with an apparent transient cytotoxic effect.

Method optimisation

To avoid cells being stimulated to their maximum capability by PDGF, 30ng/ml was chosen as the optimum concentration. At this concentration the individual values for % phosphorylation were most reproducible, as evident by the small standard error. A PDGF incubation time of 15 minutes was determined to be optimal, as this time point yielded the highest % phosphorylation. Despite the sample size in this study being very small the values obtained for each time point were very reproducible. In comparison with information found in the literature an incubation time of 15 minutes is within the expected range. Bornfeldt *et al.*, 1994 reported that in human smooth muscle cells peak MAPK activation was observed 5 minutes following stimulation with PDGF. Similarly in rat embryonic thoracic aorta smooth muscle derived A7r5 cells, maximum PDGF (10ng/ml) stimulation of ERK phosphorylation occurred between 5 and 10 minutes (Sandirasegarane *et al.*, 2000). In this study the sampling time began at 10 minutes. Upon reflection shorter incubation times of 2 and 5 minutes should have been investigated to ensure the optimum phosphorylation time wasn't disregarded.

It was observed that the level of ERK phosphorylation produced by PDGF-AB was somewhat low and variable compared to previous findings in the literature. In rat embryonic thoracic aorta smooth muscle derived A7r5 cells, PDGF stimulation (10ng/ml) produced over a 7 fold increase in ERK 2 phosphorylation (Sandirasegarane *et al.*, 2000). Despite the levels of stimulated ERK1/2 phosphorylation being low, it was still possible to demonstrate any effect of drug. To confirm the findings of the ERK1/2 study, the BrdU assay was employed. As described in Chapter 1, there are different isoforms of PDGF, so to maximise stimulation PDGF-BB was used in the BrdU experiments.

Treatment with 30ng/ml PDGF-BB produced a measurable fold change in absorbance in cells that were seeded at both 2000 cells/well and 5000 cells/well, and that had been incubated with BrdU for both 12 and 24 hours. Despite the sample size for this experiment being too small to calculate standard errors, the values were most reproducible at a seeding density of 5000 cells/well and at a BrdU incubation time of 24 hours. For this reason these conditions were put into practise for all BrdU experiments. The optimum conditions determined here are very similar to those found in the literature. In a similar study using human smooth muscle cells, a PDGF-BB concentration of 25ng/ml and a seeding density of 5000 cells/well were applied, although the cells were incubated with BrdU for only 12 hours (Rajesh *et al.*, 2008). The fold change in BrdU incorporation produced in these present experiments is approximately 2-3 fold, which is low when compared to another study utilising primary murine smooth muscle cells, where 10ng/ml PDGF-BB induced a 10 fold increase in BrdU uptake (Willert *et al.*, 2010). Similarly, the stimulated response in human coronary artery smooth muscle cells, where a 7 fold increase in BrdU incorporation was observed (Rajesh *et al.*, 2008). Despite the stimulatory responses in this study being smaller than those previously reported, it was possible to determine a significant inhibitory effect of some of the drug interventions, demonstrating that the experimental system was sufficiently sensitive to be able to detect drug induced changes.

Studies with CB₂ agonists

The CB₂ agonist JWH015 ($K_i = 13.8\text{nM}$) appeared to inhibit ERK1/2 phosphorylation at high concentrations, although this reduction did not reach statistical significance due to the high level of variability of responses at the lower concentrations. Incidentally, if the highest concentration of JWH015 ($1 \times 10^{-5}\text{M}$) is compared to the control and analysed using a Students t test, then a significant reduction in ERK1/2 phosphorylation is observed ($P < 0.05$). Evidence from the BrdU incorporation studies supports this theory since JWH015 significantly inhibited DNA synthesis at high concentrations. This is in agreement with previous findings from Rajesh *et al.*, 2008a who demonstrated (by Western Blotting) that the CB₂ agonists JWH133 and HU308 ($4\mu\text{M}$) reduced ERK 1/2 phosphorylation in human coronary artery smooth muscle cells, an effect that was attenuated in the presence of a CB₂ antagonist (AM630). In an attempt to confirm that the response observed in this study was due to the activation of CB₂ receptors a second, more potent, CB₂ agonist (JWH133 $K_i = 3.4\text{nM}$) was investigated. Intriguingly, studies using this agonist over a wide concentration range did not confirm these findings, with only a small attenuation being observed at the highest concentration. This contradicts the findings from Rajesh *et al.*, 2008a who demonstrated that JWH133 and a second CB₂ agonist HU-308 reduced TNF α stimulated cell proliferation using the BrdU assay. The experimental conditions employed in that study were very similar to those used in this study, therefore the difference in results is most likely due to the species difference. The Rajesh study was performed in an

immortalised human smooth muscle cell line, whereas in this study primary murine smooth muscle cells were utilised. Moreover, rather than reversing the effects of JWH015, the CB₂ receptor antagonist (AM630) alone, and in combination with the two CB₂ agonists resulted in a reduction in cell proliferation. This was unexpected, if the reduction in cell proliferation produced by JWH015 was a result of CB₂ receptor activation, then the presence of an antagonist would have been expected to at least result in a partial reversal of the effect. These findings strongly suggest that JWH015 is acting through a non CB₂ mediated mechanism.

As mentioned above, AM630 both alone and in combination with JWH133 resulted in a significant reduction in cell proliferation. If the reduction in proliferation observed following treatment with AM630 was purely CB₂ mediated, then when given in conjunction with JWH133 there should be some reversal of the effect due to competition at the binding site. Although AM630 is primarily a competitive CB₂ receptor antagonist, it also has the capability to function as a CB₁ receptor agonist, antagonist or inverse agonist (Ross *et al.*, 1999). This study has shown a negligible effect of CB₁ receptor activation on cell proliferation making a CB₁ agonist role for AM630 unlikely. Therefore, due to its extremely complex pharmacology, further investigation would be required to establish the mechanism of action of AM630 in this experimental preparation.

To confirm that the results from the BrdU investigations were genuine effects on DNA synthesis, and not the result of drug induced cytotoxicity, the effects of the agonists and antagonist on cell viability were investigated. MTT investigation revealed that cell treatment with both the CB₂ agonists (JWH015 and JWH133) for 24 and 48 hours had no detrimental effects on cell viability. This is in contrast to findings in immune cells where JWH015 has been shown to induce apoptosis through activation of caspases, a finding that was attenuated in the presence of a CB₂ receptor antagonist (Lombard *et al.*, 2007). Cells incubated with AM630 for 24 and 48 hours did not exhibit reduced cell viability. In actuality AM630 significantly increased cell viability compared to the DMSO vehicle control (at 24 hours), suggesting that the DMSO was having a cytotoxic effect on the cells, and that the AM630 was acting as a cytoprotective agent. The MTT assay is reliant upon the enzymatic conversion of MTT to purple formazan. CB₁ activation is known to cause an immediate increase in ceramide concentration. This short term peak in ceramide has been linked to metabolic regulation of the cell, resulting in stimulation of glucose utilisation and the production of ketone bodies, processes that are regulated through the ERK cascade (Guzman *et al.*, 1999; Velasco *et al.*, 2005; Sanchez *et al.*, 1998). If ceramide can increase the metabolic capabilities of the cell, then

AM630 by acting as a CB₁ receptor agonist may increase the metabolism of MTT which could explain the significant increase in cell viability observed between cells treated with vehicle and AM630. It could be argued that this process is unlikely to be occurring in this experimental preparation due to the lack of effect of a CB₁ agonist on ERK1/2 phosphorylation. However, the experiments in this study were performed following stimulation by PDGF which would mask any stimulatory effects a CB₁ agonist had on ERK activity.

Cell incubation with AM630 in conjunction with both the CB₂ agonists (JWH133 and JWH015) had no detrimental effects on cell viability following 24 hour incubation. In fact, AM630 in combination with JWH015 induced a significant increase in cell viability compared to the vehicle control (AM630 +JWH133 also increased viability but this did not reach significance). This trend was not observed following 48 hour incubation. At 48 hours the antagonist-agonist combinations resulted in cell viability similar to the relative vehicle control, but significantly lower (JWH015+ AM630) compared to the corresponding 24 hour treated cells.

The 24 hour results suggest that either JWH015 or AM630 is protecting the cells against vehicle induced cytotoxicity. However, this effect is abolished following 48 hour incubation with the drug combination. It is possible that the initial cytoprotective effect (observed after 24 hours) was due to either JWH015 or AM630 activating the CB₁ receptor, which has been shown to actuate the cytoprotective PKB/Akt pathway (Gomez del Pulgar *et al.*, 2000), and it may be that this was simply not enough to protect from vehicle induced toxicity following 48 hour treatment.

These findings strongly suggest that the reduction in cell proliferation observed in this study, following incubation with the agonists and antagonist combined may be a result of vehicle induced cytotoxicity. However, this does not explain the differing effects of JWH015 and JWH133 as despite JWH015 being a selective CB₂ agonist it also has the potential to activate CB₁ receptors ($K_i = 383\text{nM}$). Since the concentration used in this study was very high (10 μM) perhaps CB₁ activity could explain the reduction in cell proliferation.

Studies with the CB₁ agonist ACEA

Treating cells with ACEA had no significant effect on either ERK 1/2 phosphorylation or similarly BrdU incorporation. This is in contradiction to the literature as there is evidence illustrating that CB₁ agonists can activate ERK 1/2 (Bosier *et al.*, 2008; Bouaboula *et al.*, 1995), however these studies were performed in N1E-115 neuroblastoma cells and CHO cells. The lack of activity produced by ACEA also rules out the possibility that JWH015 (discussed above)

reduced smooth muscle cell proliferation by acting on CB₁ receptors. It has recently been shown that the CB₁ antagonist SR141716A induced an inhibition of PDGF stimulated cell proliferation through inhibition of ERK in human smooth muscle cells (Rajesh *et al.*, 2008). Therefore, if anything, it might have been expected to see an increase in proliferation following cell treatment with ACEA. Perhaps if cells were treated with ACEA without stimulation by PDGF this may be observed, conformation of which would be an area for future work. ACEA is susceptible to metabolic breakdown in a similar fashion to AEA therefore for a more accurate picture these experiments should be confirmed with another metabolically stable selective CB₁ agonist.

Studies with GPR55 agonist O-1602

Treating cells with O-1602 had no effect on PDGF- induced ERK1/2 phosphorylation. As far as we are aware this is the first study of the effect of GPR55 activation on vascular smooth muscle cell proliferation as there is no literature available for direct comparison. However, it has been shown in both HEK293 and microglial cells that GPR55 activation can lead to rapid ERK phosphorylation (Oka *et al.*, 2007, Pietr *et al.*, 2009). It is important to note that due to the lack of specific antibodies for GPR55 we have not been able to provide evidence that GPR55 is present in the mouse vasculature and therefore a lack of any functional response may in fact be due to the lack of the receptor.

Studies using endocannabinoids

Increasing the concentration of AEA by inhibiting its metabolic breakdown using the selective FAAH inhibitor URB597, had a negligible effect on PDGF stimulated ERK1/2 phosphorylation. Similarly when cells were treated with anandamide there was only an effect on DNA synthesis at a concentration of 10 μ M. This is much higher than would be observed either physiologically or pathophysiologically. Indeed, results in this study (Chapter 3) show the tissue concentrations of endocannabinoids to be in the pico molar range. A similar growth inhibitory effect was observed in the gastric cancer cell line HGC-27 where 10 μ M AEA strongly inhibited cell proliferation (Miyato *et al.*, 2009). At 10 μ M, AEA reduced viability of cells treated for 24 hours (albeit not significantly); however cells treated with 10 μ M AEA for 48hours showed no loss of viability. This indicates that cell exposure to AEA (10 μ M) induces an immediate cytotoxic/cytostatic effect which over time the cells can recover from (as shown by the restoration of cell viability at 48 hours). When put into context, this confirms that the reduction in cell proliferation is due to cytotoxicity/ growth arrest. Although the cells were incubated

with drug for 48 hours they would not be able to recover from the initial toxic/static effect, as once they had taken up the BrdU they could no longer proliferate.

In contrast to the findings with AEA, treating cells with 2-AG had no effect on cell proliferation. Moreover, when cells were treated with both AEA and 2-AG there was a reduction in proliferation similar to that observed when cells were treated with AEA, suggesting the two cannabinoids do not work in tandem to control cell growth. Furthermore, the lack of a concentration dependent effect of AEA on proliferation strongly implies a cytotoxic effect.

It has been suggested that endocannabinoids can control cell fate by either inducing cell proliferation or inducing apoptosis, depending on the environmental cue. As already stated in section 5.1.3.2 ceramide is produced following CB₁ and CB₂ receptor activation (Sanchez *et al.*, 2001) by two mechanisms. The first mechanism occurs within minutes and involves activation of sphingomyelinase which induces production of ceramide; the second requires the “de novo” synthesis of ceramide through activation of a serine palmitoyltransferase (Gomez del Pulgar *et al.*, 2002 a & b) a process which takes days (Galve-Roperh *et al.*, 2000). AEA has been shown to induce apoptosis in immune cells (Reviewed in Rieder *et al.*, 2009) and HGC-27 cells (Miyato *et al.*, 2009). It may be possible therefore that AEA is activating the ceramide pathway and is a notion that requires further investigation.

Limitations of the study

Despite paying careful attention to experimental technique the major limitation plaguing this study was the high level of variability present in both the ERK1/2 and BrdU incorporation studies, which resulted in some data failing to reach statistical significance. For the ERK1/2 studies a possible source of the variation could have been the method employed, as this involved many stages all of which could introduce error. Each experimental sample was taken from a 75cm² flask, primary murine smooth muscle cells are extremely slow growing and give a low yield of cells per flask, making the ERK 1/2 studies extremely time consuming. On reflection an alternative method would be to use a cell based ELISA. This would be advantageous in terms of involving fewer steps in the protocol thus reducing the opportunities to introduce variability and would have been less time consuming, as both phospho ERK and total ERK could have been measured in the same experiment. Western Blotting would also have been an alternative method to the cell lysate ELISA as this is frequently used in the literature.

Another explanation for the variability may be that both types of ELISA used in this study were not sensitive enough to detect any subtle changes, especially at lower levels of BrdU incorporation. The primary cell line may also be a contributor to the large variation between experiments. Due to the slow growing nature of the cells they were utilised for experimentation between passage 5-7, perhaps passage number affected the cells ability to respond to both the stimulus and to drug intervention

Perhaps another limitation to this study is that the effects of the drugs were not investigated in cells untreated with PDGF. The majority of the evidence from the literature suggests a stimulatory effect of CB₁ agonists on ERK (Wartmann *et al.*, 1995; Bouaboula *et al.* 1995; Bouaboula *et al.* 1996, although ERK activation does not necessarily lead to proliferation Grewal *et al.*, 1999) and either an inhibitory or pro-proliferative effect of AEA (Mimeault *et al.*, 2003; Bifulco *et al.*, 2006 Hart *et al.*, 2004). It is therefore possible that the drugs used in this study have a pro-proliferative effect that was masked by activation of PDGF and the resulting overlapping signalling pathways.

A final consideration arising from this study is apparent lack of selectivity of the cannabinoid ligands used. JWH133 and JWH015 are both reported to be selective CB₂ agonists yet in this study they did not act in the same manner, with the overall evidence suggesting that in the present studies JWH015 was acting through a non CB₂ mediated mechanism.

Conclusions

In conclusion the results of these studies show that the CB₂ agonist JWH015 and the CB₂ antagonist AM630 both inhibited PDGF stimulated cell proliferation, although their effects appear to be through mechanisms independent of the CB₂ receptor. Studies investigating CB₁ receptor activation and also drug induced cytotoxicity provided evidence to eliminate these factors from possible mechanisms. Further investigation would be required to determine the precise mechanism of action of these drugs. The endogenous cannabinoid AEA also produced an inhibition of PDGF stimulated smooth muscle cell proliferation, albeit this is most likely due to a cytotoxic effect of the cannabinoid.

Chapter 6

The effect of cannabinoids on vascular smooth muscle cell migration

6.1 Introduction

6.1.1 Smooth muscle cells and neointimal formation

As described in Chapter 1 restenosis is a disease in which luminal area is reduced following vascular injury. The key events which induce this pathology are smooth muscle cell proliferation and migration. Smooth muscle cells normally exist in a quiescent non motile state, however immediately following vascular injury the smooth muscle cells undergo phenotypic modulation from the contractile to the synthetic phenotype and begin to rapidly divide and migrate (Raines *et al.*, 1993). Once the injured cells are replaced, the majority of cells return to the original contractile quiescent state. However an important sub population of cells resist growth inhibition and migrate towards the lumen (Casscells *et al.*, 1992). Once these migrating cells reach the lumen they continue to divide and produce extracellular matrix resulting in the formation of a neointima (Majesky *et al.*, 1994).

In order for smooth muscle cells to migrate towards the lumen, they rely upon a chemoattractant gradient produced by cells within the vessel wall, the degradation of surrounding matrix proteins, and the synthesis of new matrix proteins. The mechanisms by which smooth muscle cells generate force and move in response to a chemoattractant are described in detail in Chapter 1. There are multiple signalling pathways involved in cell migration, some of which overlap with the pathways involved in cell proliferation (reviewed in Bornfeldt 1996). Cell migration in response to a chemoattractant begins following stimulation of either a G protein coupled receptor (GPCR) or receptor tyrosine kinase (RTK). These receptors then activate a multitude of signalling molecules (including the G proteinases Rho, Rac and Cdc42), which activate membrane phospholipids that subsequently activate lipid kinases. These induce an increase in Ca^{2+} that ultimately activates Ca^{2+} dependant kinases. These signalling molecules function to activate proteins which lead to actin polymerisation, the activation of myosin motors and therefore induce cell migration (Reviewed in Huang *et al.*, 2004; Gerthoffer *et al.*, 2009; Newby *et al.*, 2000; Gerthoffer *et al.*, 2007).

6.1.2 Cannabinoids and cell migration

The effects of cannabinoids on cell migration has been studied primarily in immune cells. An anti-inflammatory role for cannabinoids has been suggested since 1974, when it was discovered that Δ^9 -THC elicited an inhibitory effect on the migration of leukocytes (Schwartzfarb *et al.*, 1974). Low concentrations of Δ^9 -THC have also been shown to inhibit the migration of

macrophages in response to monocyte chemoattractant protein-1 (Steffens *et al.*, 2005). In contrast, studies investigating the endogenous cannabinoid 2-AG have shown it to induce the migration of human monocytic cells (Kishimoto *et al.*, 2003) and microglia cells. Interestingly, the effect was abolished by an inhibitor of ERK phosphorylation and an antagonist of the novel abnormal cannabidiol receptor (Walter *et al.*, 2003). 2-AG has also been shown to induce directional migration of B lymphocytes in a CB₂ dependant manner (Jorda *et al.*, 2002) and to regulate CB₂ mediated migration of myeloid leukaemia cells (Jorda *et al.*, 2002). Intriguingly, AEA does not share the same pro-migratory profile as 2-AG. AEA only weakly stimulates migration of microglia cells and showed only 20% of the migratory response produced by 2-AG in a leukaemia cell line (Walter *et al.*, 2003; Jorda *et al.*, 2002). The poor ability of AEA to stimulate immune cell migration has been attributed to the finding that AEA only weakly activates the CB₂ receptor (Hillard *et al.*, 1999). Interestingly, 2-AG was found to have no effect on human neutrophil migration, whereas both AEA and virodhamine (another endogenous cannabinoid) have both been shown to inhibit migration (McHugh *et al.*, 2008).

Studies have also looked at the effects of cannabinoids on cell migration out with the immune system. Synthetic cannabinoids as well as AEA have been found to stimulate migration in CB₁ transfected human embryonic kidney cells (Song and Zhong 2000). In a study using vascular endothelial cells, abnormal cannabidiol stimulated migration through a PI3K/Akt dependant pathway (Mo *et al.*, 2004), whereas the CB₂ agonist JWH133 has been shown to reduce migration of human umbilical vein endothelial cells (Blazquez *et al.*, 2003). As endothelial cells are pivotal to the formation of new blood vessels in cancer progression, cannabinoids are also being investigated as potential anti cancer agents.

6.1.3 Cannabinoids and smooth muscle cells

Recent studies have shown that, in human coronary artery smooth muscle cells, the CB₁ antagonist SR141716A inhibits PDGF induced migration by inhibition of Ras and ERK1/2 (Rajesh *et al.*, 2008 b). Moreover, the same group also found that CB₂ agonists inhibits TNF- α induced cellular migration, a finding which was ascribed to the inhibition of Ras, p38 MAPK, ERK 1/2, SAPK/JNK and Akt cellular pathways (Rajesh *et al.*, 2008 b). Beyond this however, the influence of cannabinoid receptor agonists and endocannabinoids on smooth muscle cell migration is a relatively un explored area.

6.2 Aim

In light of the findings in Chapter 3 that confirmed the presence of both the CB₁ and CB₂ receptors on murine vascular smooth muscle cells, alongside the observations that

endocannabinoid concentration increases in tissue subjected to injury suggests that cannabinoids may be able to influence smooth muscle cells. The previous chapter has shown the ability of cannabinoids to influence cell proliferation. The pathways involved in proliferation overlap with those involved in cell migration, therefore the aim of this study was to determine the effects of selective cannabinoid receptor agonists acting at the CB₁ and CB₂ receptors as well as the endogenous cannabinoids AEA and 2-AG on vascular smooth muscle cell migration.

6.3 Method

6.3.1 Method optimisation

The most common approach to investigating cell migration *in vitro* is to use a modified Boyden chamber, the principle of which measures the migration of cells through a porous membrane in response to a chemoattractant. Cultured cells are placed on top of a porous membrane/filter (8µm), they then migrate through the polycarbonate membrane towards a chemoattractant agent located in the lower chamber (PDGF-BB). The migrated cells are then stained and quantified. The benefit of using this technique over some other methods of measuring cell migration (for example wounding assays) is that multiple cell treatments may be investigated in one experiment. The chamber used in this study was a 48 well chemotaxis chamber.

Due to the nature of the assay a variety of conditions had to be optimised before drug investigation could commence. These involved the identification of: (i) the incubation time to allow optimum cell migration. (ii) a staining technique which would enable clear visualisation of the nuclei for cell counting, (iii) the optimum number of cells seeded in each well and (iv) the optimum concentration of PDGF-BB to stimulate migration.

6.3.2 Determination of optimum incubation time and cell number

As a starting point the conditions utilised in a recent migratory study using human coronary artery smooth muscle cells were used (Rajesh *et al.*, 2008a). Primary murine smooth muscle cells were grown to 95% confluence in 75cm² flasks, the cells were harvested from the flask and counted as detailed in method section 2.4.4. In all experiments bar the initial ones, cells were quiesced over night in medium containing 0.3% serum prior to experimentation. Cells were suspended at the appropriate dilution in medium containing 0.3% serum until ready to be added to the chamber. A starting cell number of 30,000 cells/ well was employed.

In parallel to cell harvesting the polycarbonate filter was coated in a solution of 0.2% gelatine (as detailed in section 2.7.2) and the PDGF solutions were prepared (as detailed in section 2.7.2) and added to the lower wells. The chemotaxis chamber was assembled, the cell suspension was gently vortexed, and 50µl of cell suspension was added to the upper wells. The chemotaxis chamber was placed in a humidifying chamber and incubated at 37°C and 5% CO₂ for 8 hours. The chamber was removed from the incubator, inverted and the filter removed. The unmigrated cells were removed from the filter using a wiper blade (as described in section 2.7.3) and the remaining migrated cells were then fixed in 100% methanol for 7 minutes before subsequent staining with Coomassie brilliant blue (as detailed in section 6.3.3.1.). Once dry the filter was mounted using Shandon xylene substitute mountant.

To determine the optimum conditions, this process was then repeated reducing the incubation time to 6 hours and then subsequently to 2 hours (this proved to be too short and was subsequently increased to 3). The cell number was also reduced to 5000 cells/well and 10,000 cells/well. An incubation time of 3 hours and a cell number of 10,000 cells/well were identified as the optimum experimental conditions and were utilised throughout this study.

6.3.3 Determination of optimum staining technique

As smooth muscle cells are large with lamellipodial processes, in order to be able to quantify the number of cells accurately their nuclei had to be clearly visible. Five staining techniques were investigated Coomassie brilliant blue, Giemsa, haematoxylin, H&E and a modified H&E technique.

6.3.3.1 Coomassie brilliant blue stain

The migration experiment was carried out as detailed above and in section 2.7. Once the migrated cells had been fixed the filter was allowed to dry before complete immersion in a petri dish containing Coomassie brilliant blue stain for 15 minutes. The filter was transferred and immersed in another petri dish containing de-stain and was gently agitated until the excess stain had been removed (usually a few minutes). The filter was left to air dry then mounted on a glass slide.

6.3.3.2 Giemsa stain

Once the migration experiment had been completed and the cells fixed and left to dry, the filter was immersed in a petri dish containing 0.5% Giemsa solution for 15 minutes. The filter was briefly dipped in a petri dish containing distilled water to remove the excess stain then left to air dry. The filter was then mounted on a glass slide.

6.3.3.3 Haematoxylin

Once the migration experiment had been completed and the cells fixed and left to dry, the filter was immersed in a petri dish containing haematoxylin for 10 minutes. The filter was briefly dipped in a petri dish containing distilled water to remove the excess stain and allowed to air dry. The filter was then mounted on a glass slide.

6.3.3.4 Haematoxylin and Eosin

Once the migration experiment had been completed and the cells fixed and left to air dry the filter was stained using the following technique:

1. Distilled Water	1 min
2. Haematoxylin	1 min
3. Distilled Water	2 min
4.0.5% Acid Alcohol	1 min
5. Distilled Water	2 min
6. STWS	2 min
7. Distilled Water	2 min
8. Eosin	30 secs
9. Distilled Water	2 mins

The filter was then allowed to air dry and mounted on a glass slide. Due to poor nuclear staining using this technique, the protocol was altered by increasing the incubation time with haematoxylin and adding another haematoxylin step at the end of the staining procedure as detailed below.

1. Distilled Water	1 min
2. Haematoxylin	5 min
3. Distilled Water	2 min
4.0.5% Acid Alcohol	1 min

5. Distilled Water	2 min
6. STWS	2 min
7. Distilled Water	2 min
8. Eosin	30 secs
9. Distilled Water	2 min
10. Haematoxylin	5 min
11. Distilled water	2 min

This staining protocol produced the clearest visualisation of the cell nuclei and was therefore used throughout this study.

6.3.4 Determination of the optimum PDGF concentration

Cells were grown to 95% confluence, quiesced overnight then harvested and diluted appropriately to give cell suspensions which would yield 10,000 cells/ well and 5000 cells/well. PDGF solutions of increasing concentration (0, 10, 20, 30 or 50ng/ml), were added to the lower wells (26.5µl) as illustrated in Figure 6.1. The chamber was assembled and the cell solutions added to the upper wells; it was then placed in a humidifying chamber and incubated for 3 hours at 37°C and 5% CO₂. The chamber was removed from the incubator, inverted and the filter removed. Unmigrated cells were removed by wiping the underside of the filter against a wiper blade (as detailed in section 2.7.3) carefully dipping the underside in PBS between each wipe. The filter was fixed in 100% methanol for 7 minutes and allowed to dry. It was then stained using the modified H&E method described above, allowed to dry then mounted on a glass slide. The cells were then counted as detailed in section 6.4. A concentration of 30ng/ml PDGF-BB and 10,000 cells/well were identified as optimum and used throughout this study.

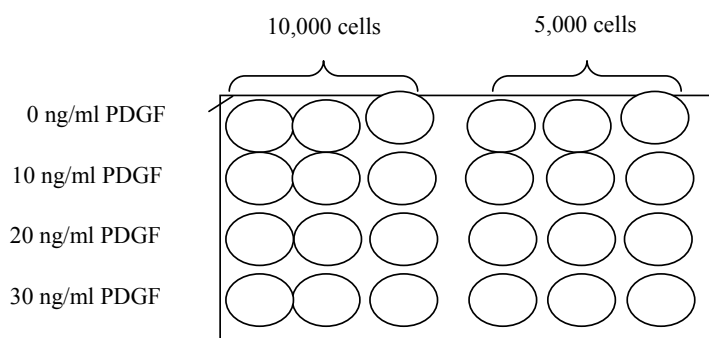


Figure 6.1 An example of the layout of the chamber. With the notch at the top left hand corner (to indicate filter orientation), the unstimulated control at the top with increasing concentrations of PDGF downwards. Samples were measured in triplicate.

6.3.5 Cannabinoid treatment of cells prior to migration assay

To investigate the effects of cannabinoids on smooth muscle cell migration, cells were incubated with a variety of cannabinoid agents (detailed in Table 6.1) prior to their addition to the chemotaxis chamber. Smooth muscle cells were quiesced, harvested (as detailed in section 2.4.4), diluted appropriately (at a density to yield 10,000 cells/well) and suspended in a 1.5ml tube containing 1ml of serum free media supplemented with cannabinoid drug (for drugs used and concentrations see Table 6.1). The 1.5ml tubes were placed in a rack and incubated for 30 minutes at 37°C and 5% CO₂. During this time the lower wells were filled with either serum free media or a solution containing 30ng/ml PDGF-BB, the chamber was assembled and 50µl of the cell solutions were added to the upper wells. The effect of each drug was investigated on both unstimulated cells and stimulated cells as illustrated in Figure 6.2. The chamber was then placed in the humidifying chamber and incubated for 3 hours at 37°C and 5% CO₂. Once removed from the incubator the chamber was inverted and the filter isolated, the unmigrated cells were removed from the underside of the filter using a wiper blade (as detailed in method section 2.7.3). The migrated cells were fixed in 100% methanol for 7 minutes and left to air dry, the filter was then stained using the modified H & E method (as described above) and mounted on a glass slide.

6.4 Data Expression and Analysis

Migrated cells were quantified by counting the cells in 5 non overlapping fields of vision at x400 magnification (as illustrated in Figure 6.3). To ensure impartiality counting was both blinded (labels were covered up) and randomised (filters were mixed up). Data from unstimulated cells was expressed as fold change in cell number compared to the control, as shown below. Samples were measured in triplicate and repeated in cells originating from at least three different mice.

$$\text{Fold change in cell number} = \frac{\text{Number of unstimulated drug treated cells}}{\text{Number of unstimulated control cells}}$$

Data from stimulated cells was expressed as fold change in cell number compared to unstimulated cells treated with the same drug.

$$\text{Fold change in cell number} = \frac{\text{Number of drug treated stimulated cells}}{\text{Number of drug treated un- stimulated cells}}$$

Statistical analysis was carried out using a one-way analysis of variance (ANOVA) with a Dunnetts post test (Graph pad Prism 4) unless otherwise stated, significance was accepted when $P < 0.05$.

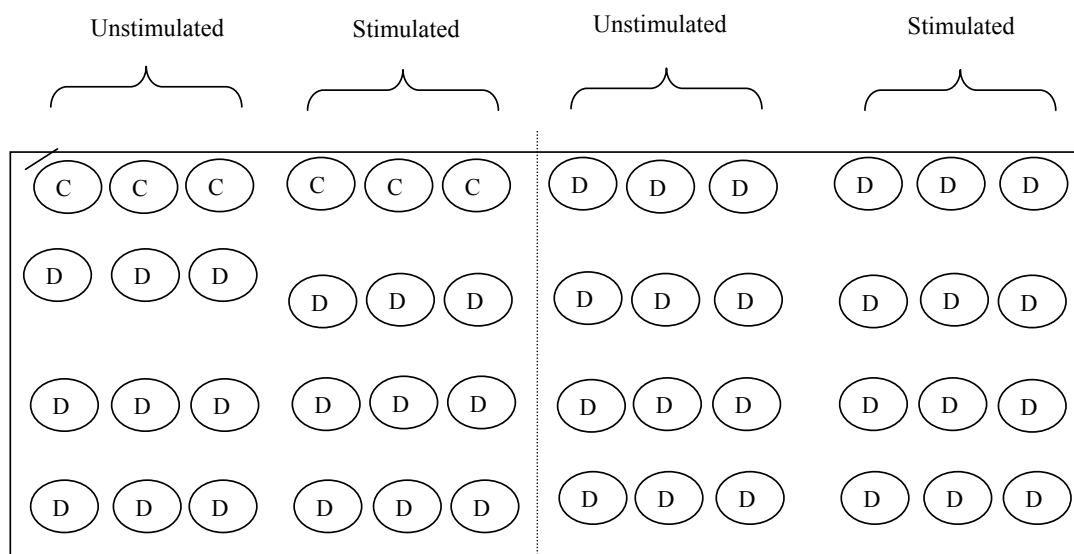


Figure 6.2 An illustration of the layout of the chemotaxis chamber for the cannabinoid drug study. Each drug was investigated in wells that were not exposed to PDGF (unstimulated) and wells that were exposed to 30ng/ml PDGF (Stimulated). C stands for control (where no cannabinoid was present), D stands for drug.

Drug Treatment	Well concentration M
Ethanol	0.1%
JWH133	1×10^{-6}
JWH133	1×10^{-5}
ACEA	1×10^{-6}
ACEA	1×10^{-5}
DMSO	0.1%
AM630	1×10^{-6}
AEA	1×10^{-9}
AEA	1×10^{-7}
2-AG	1×10^{-9}
2-AG	1×10^{-7}

Table 6.1 Drugs used in this study and the well concentrations at which they were used.

Drugs and concentrations were chosen on the basis of the data generated in the cell proliferation studies described in Chapter 5.

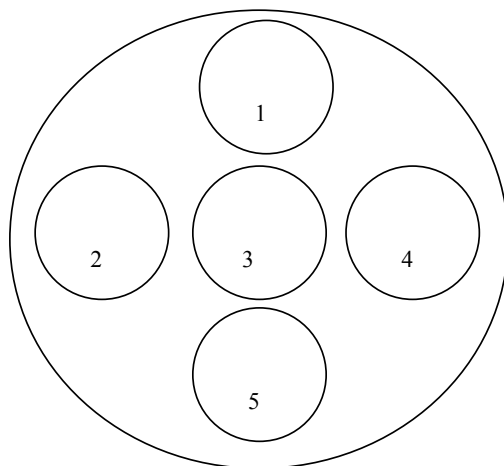


Figure 6.3. Illustration of the five non overlapping fields of vision used to count the migrated cells.

6.5 Drugs

- ACEA (Tocris) A CB_1 receptor agonist, this was dissolved in ethanol to a stock solution of $1 \times 10^{-2}M$, this was diluted in ethanol and serum free media to required concentrations maximum ethanol concentration was 0.1%.
- JWH133 (Tocris) CB_2 receptor agonist, this was dissolved in ethanol to a stock solution of $1 \times 10^{-2}M$, this was diluted in ethanol and serum free media to required concentrations maximum ethanol concentration was 0.1%.
- Anandamide (Tocris) An endogenous cannabinoid, this was dissolved in ethanol to a stock solution of $1 \times 10^{-2}M$, this was diluted in ethanol and serum free media to required concentrations maximum ethanol concentration was 0.1%.
- 2-AG (Tocris) An endogenous cannabinoid, this was dissolved in ethanol to a stock solution of $1 \times 10^{-2}M$, this was diluted in ethanol and serum free media to required concentrations maximum ethanol concentration was 0.1%
- AM630 (Tocris) A CB_2 receptor antagonist, this was dissolved in ethanol to a stock solution of $1 \times 10^{-2}M$, this was diluted in DMSO and serum free media to required concentrations maximum DMSO concentration was 0.1%.

6.6 Results

6.6.1. Determination of optimum experimental conditions

6.6.1.1 Determination of optimum incubation time for measuring cell migration

Incubation of 30,000 cells/ well for 8 hours produced substantial cell migration (Figure 6.4). When compared to the unstimulated control (Figure 6.4 A) a PDGF-BB concentration dependent increase in the number of migrated cells was observed up to a concentration of 30ng/ml. Above this concentration the number of migrated cells appears to be reduced. However it is visually apparent that the number of migrated cells was too numerous for quantification and that both the incubation time and cell number needed to be reduced. Cell counting was performed at x400 magnification. It was impossible to distinguish a single cell or individual cell nuclei under these conditions (Figure 6.5).

Following reduction of the incubation period to 6 hours and the cell number to 10,000 cells/well, substantial cell migration remained (Figure 6.6). Paradoxically, at this reduced incubation time, it can be observed that there are a considerable number of unstimulated cells migrating, so much so that there was a negligible difference between the unstimulated cells and those treated with PDGF. Due to the dense clustering of the cells and poor nuclear staining it was again impossible to distinguish individual cells and therefore quantify the response.

Reducing the incubation time to 2 hours still permitted cell migration (Figure 6.7). It can be seen that there is a marked difference in the number of un-stimulated cells migrating through the membrane compared to cells exposed to PDGF. Increasing concentrations of PDGF-BB produced a concentration dependent increase in cell migration, with a maximum at 30ng/ml as evident by the dense clustering of cells (Figure 6.7D). However, due to poor nuclear staining only a few cell nuclei could be visualised.

6.6.1.2 Determination of optimum staining technique

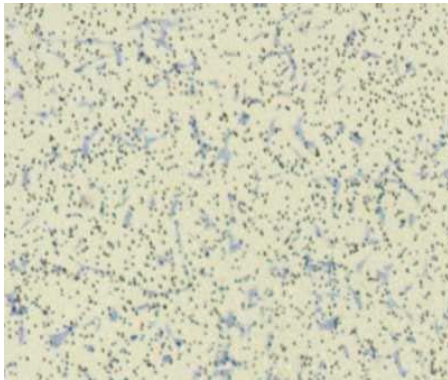
Staining smooth muscle cells with haematoxylin did permit some visualisation of the nuclei but not very clearly (Figure 6.8 A); this was also the case when smooth muscle cells were stained with 0.5 % Giemsa. At high magnification (x400) the nuclei were distinguishable however the staining proved to be inconsistent (Figure 6.8 B). H&E staining using a protocol routinely used for staining tissue was not successful, no definition between the cytoplasm and the nucleus could be observed (Figure 6.5C). Due to the lack of distinguishable nuclear staining the incubation time with haematoxylin was increased, this method proved to be very successful

with clear definition between the red cytoplasm and the purple nucleus (Figure 6.9B). For this reason this staining protocol was used throughout this study.

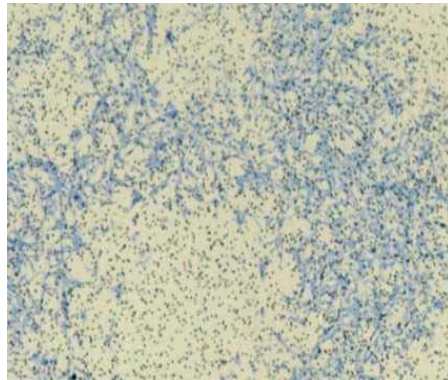
6.6.1.3 Determination of optimum PDGF concentration

An increase in the concentration of PDGF-BB produced a concentration dependent increase in cell migration (Figures 6.10 and 6.11). Fold change in migration increased from 2.89 ± 1.0 (10ng/ml PDGF) to 6.49 ± 1.7 following exposure to 30ng/ml PDGF-BB (n=3). As 30ng/ml PDGF produced the maximum fold change in migration it was identified as the optimum stimulatory concentration and used throughout the study.

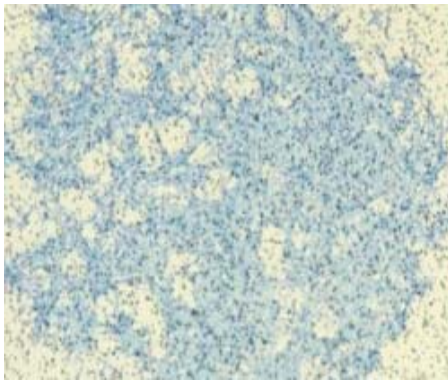
(A)



(B)



(C)



(D)

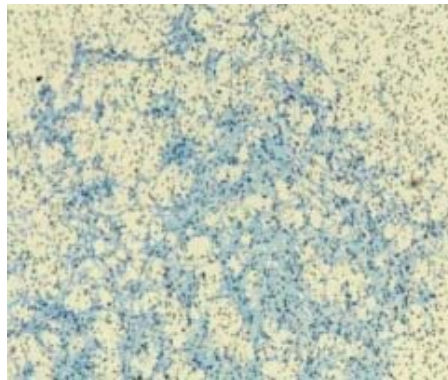
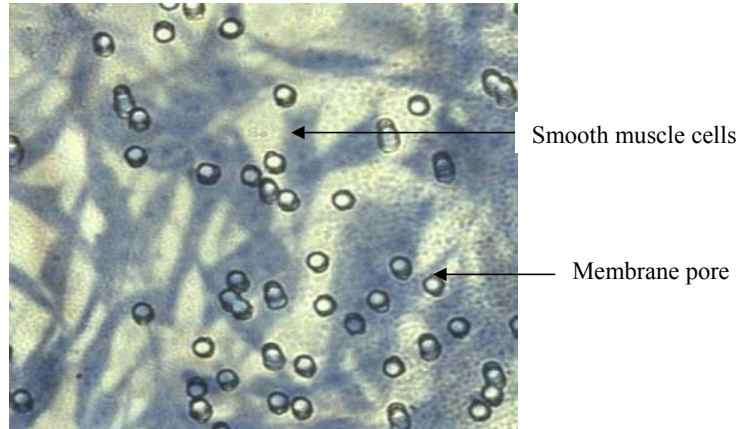


Figure 6.4 The effect of increasing concentrations of PDGF on smooth muscle cell migration. Light micrographs (x25) of primary aortic smooth muscle cells (30,000 cells/ well) stained with Coomassie brilliant blue following 8 hour incubation. (A) The unstimulated control cells were not exposed to PDGF. (B) Cells were exposed to 10ng/ml PDGF. (C) Cells were exposed to 30ng/ml PDGF. (D) Cells were exposed to 50ng/ml PDGF.

(A)



(B)

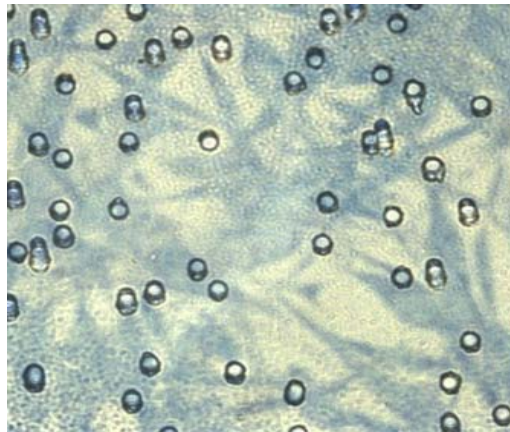
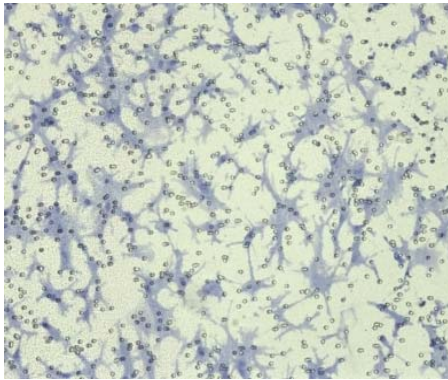
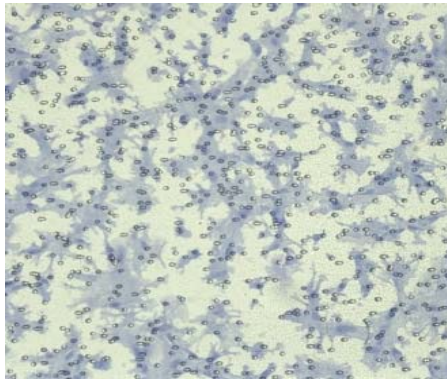


Figure 6.5 Smooth muscle cells stained with Coomassie brilliant blue. Light micrographs (x400) of primary aortic smooth muscle cells (30,000 cells/ well) stained with Coomassie brilliant blue following 8 hour incubation. (A) Cells exposed to 10ng/ml PDGF. (B) Cells exposed to 30ng/ml PDGF.

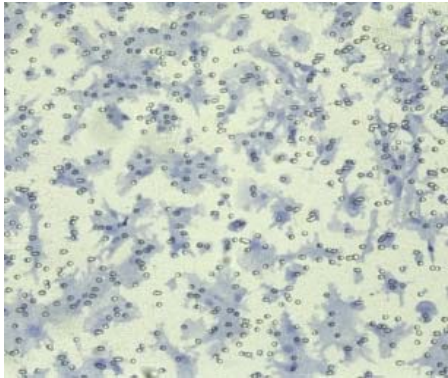
(A)



(B)



(C)



(D)

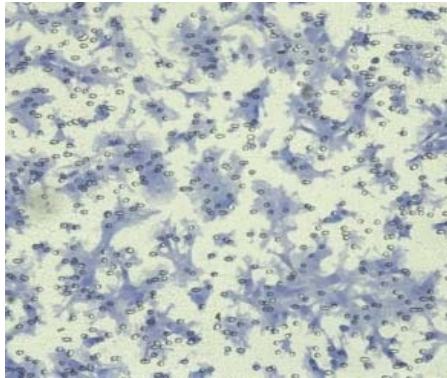
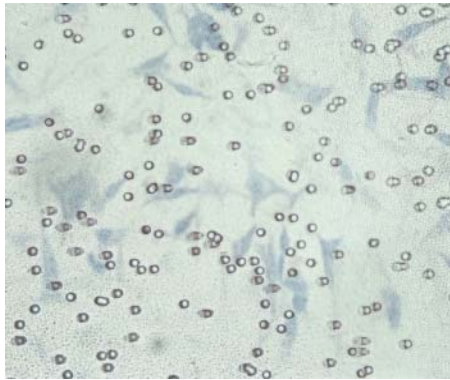
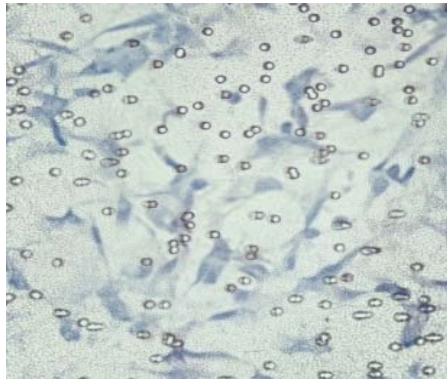


Figure 6.6 The effect of increasing concentrations of PDGF on smooth muscle cell migration. Light micrographs (x250) of primary aortic smooth muscle cells (10,000 cells/ well) stained with Coomassie brilliant blue following 6 hour incubation. (A) The unstimulated control, cells were not exposed to PDGF. (B) Cells were exposed to 10ng/ml PDGF. (C) Cells were exposed to 30ng/ml PDGF. (D) Cells were exposed to 50ng/ml PDGF.

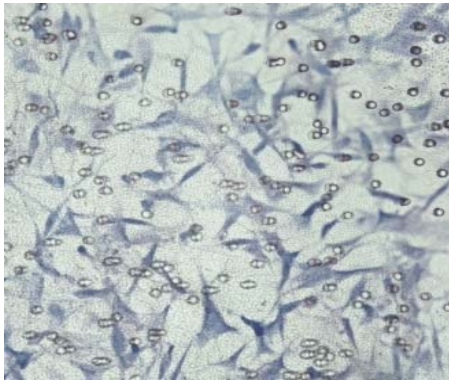
(A)



(B)



(C)



(D)

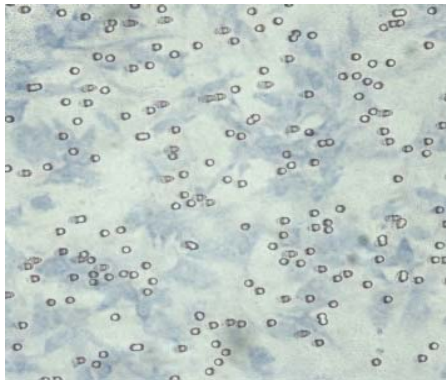
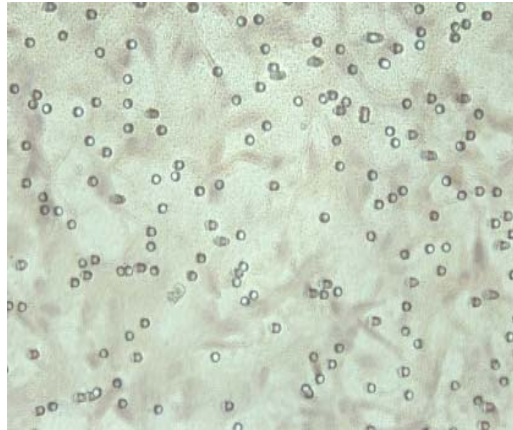
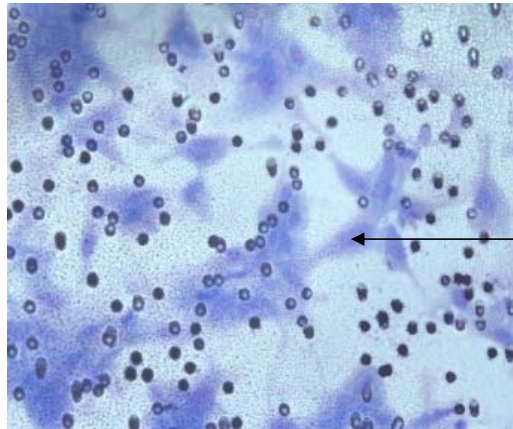


Figure 6.7 The effect of increasing concentrations of PDGF on smooth muscle cell migration. Light micrographs (x250) of primary aortic smooth muscle cells (10,000 cells/ well) stained with Coomassie brilliant blue following 2 hour incubation. (A) The unstimulated control, cells were not exposed to PDGF. (B) Cells were exposed to 10ng/ml PDGF. (C) Cells were exposed to 20ng/ml PDGF. (D) Cells were exposed to 30ng/ml PDGF.

(A)



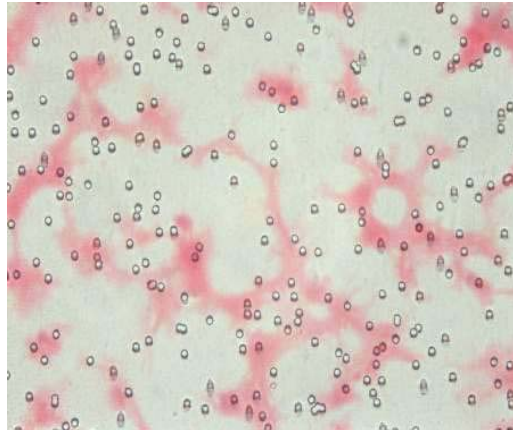
(B)



Cell nucleus

Figure 6.8 Smooth muscle cells stained using a variety of techniques. Light micrographs (x250) showing smooth muscle cells stained using different staining methods. (A) Smooth muscle cells stained with haematoxylin only. (B) Smooth muscle cells stained with giemsa.

(A)



(B)

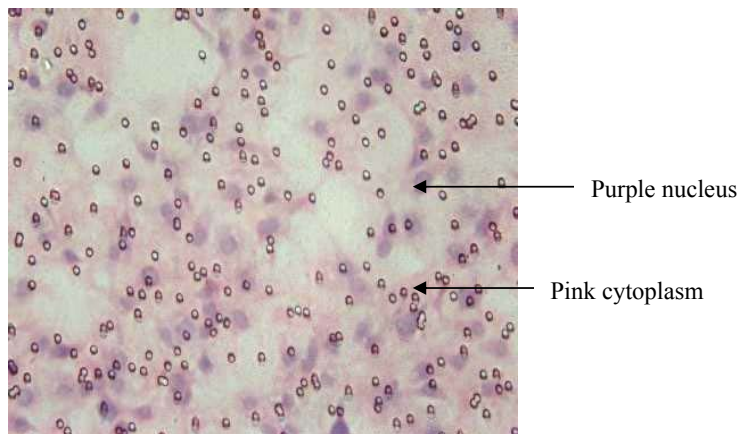


Figure 6.9 Smooth muscle cells stained using a variety of techniques. Light micrographs (x250) showing smooth muscle cells stained using different staining methods. (A) Smooth muscle cells stained with haematoxylin and eosin. (B) Smooth muscle cells stained using a modified H&E technique.

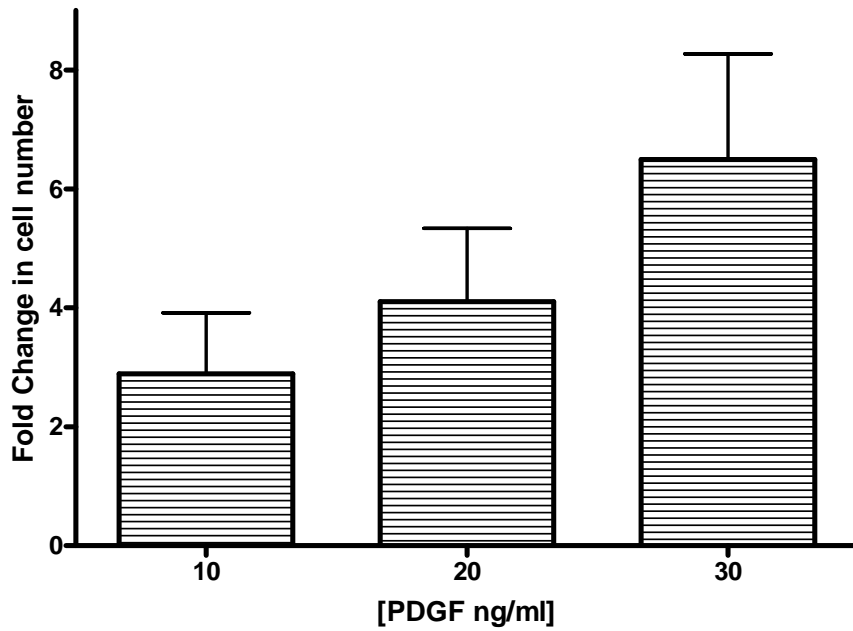
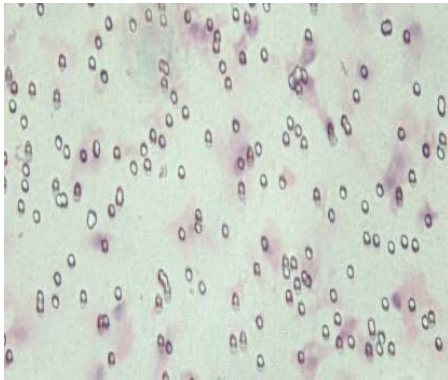
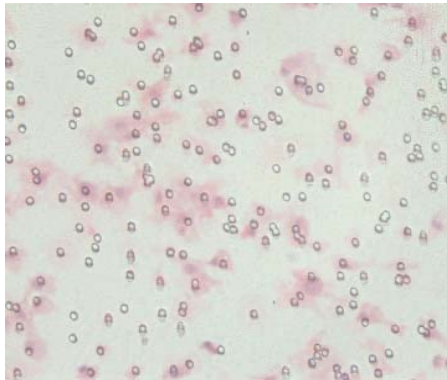


Figure 6.10. The effect of increasing concentrations of PDGF on fold change in cell number. Smooth muscle cells (10,000 cells/ well) were exposed to increasing concentrations of PDGF for 2 hours; results are expressed as fold change in cell number compared to cells not exposed to PDGF. Samples were measured in triplicate, n=3, mean + SEM.

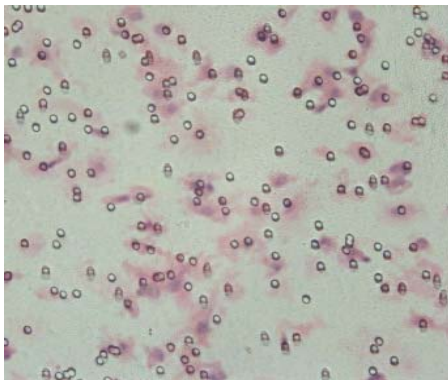
(A)



(B)



(C)



(D)

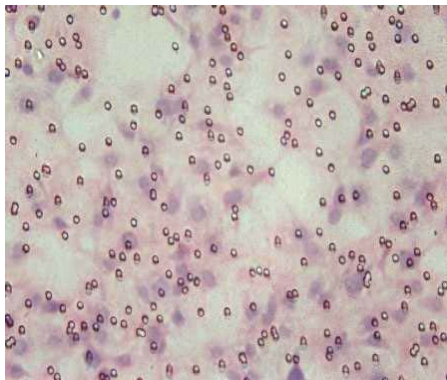


Figure 6.11 The effect of increasing concentrations of PDGF on smooth muscle cell migration. Light micrographs (x250) of primary aortic smooth muscle cells (10,000 cells/ well) stained with H&E following 2 hour incubation. (A) The unstimulated control, cells were not exposed to PDGF. (B) Cells were exposed to 10ng/ml PDGF. (C) Cells were exposed to 20ng/ml PDGF. (D) Cells were exposed to 30ng/ml PDGF.

6.6.2 The effect of cannabinoid agonists on cell migration

6.6.2.1 The effect of a CB₁ agonist on both un-stimulated and stimulated cell migration

Pre-treating cells with 0.1% ethanol (the vehicle for ACEA) induced a 2.4 ± 0.72 fold increase in unstimulated cell migration (Figure 6.12). Treating cells with ACEA (1×10^{-6} M) increased cell migration to 4.7 ± 1.6 fold; however 1×10^{-5} M ACEA reduced cell migration back to the level of the vehicle. Due to the large standard errors there was no significant difference $P > 0.05$ (One way ANOVA with Dunnetts post test $n=3$).

Stimulating cells with 30ng/ml PDGF produced an increase of 3.6 ± 2.2 fold in cell migration (Figure 6.13), this was reduced to 1.9 ± 0.7 when cells were pre-treated with ethanol. Pre-treating cells with both 1×10^{-6} M and 1×10^{-5} M ACEA induced a reduction in cell migration (0.8 ± 0.2 and 0.9 ± 0.1 respectively) compared to the stimulated control (Figure 6.13). This did not reach significance $P > 0.05$ (One way ANOVA with Dunnetts post test $n=3$).

6.6.2.2 The effect of a CB₂ agonist on both un-stimulated and stimulated cell migration

Treating cells with 0.1% ethanol (the vehicle for JWH133) induced a 2.4 ± 0.7 fold increase in un-stimulated cell migration compared to control cells (Figure 6.14). Treating cells with either 1×10^{-6} or 1×10^{-5} M JWH133 had a negligible effect on unstimulated cell migration (1.2 ± 0.6 , 0.8 ± 0.5 fold change respectively $n=3$).

Stimulating cells with 30ng/ml PDGF produced a 3.5 ± 2.2 fold increase in cell migration compared to the unstimulated control (Figure 6.15). Pre-treating cells with ethanol prior to PDGF exposure induced a reduction in cell migration (1.9 ± 0.7), which was reduced further following pre treatment with 1×10^{-6} and 1×10^{-5} M JWH133 (1.3 ± 0.2 , 1.9 ± 1.1 respectively) albeit there was no significant difference between any of the treatments $P > 0.05$. One way ANOVA with Dunnetts post test $n=3$.

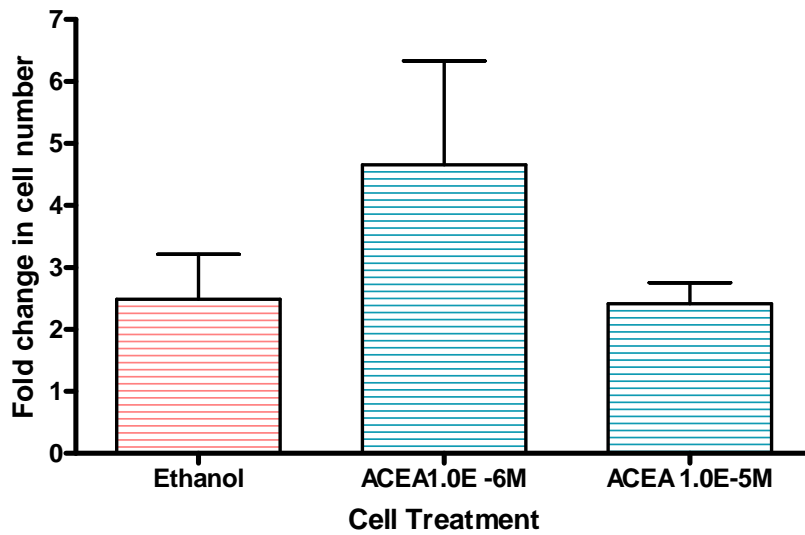


Figure 6.12. The effect of ACEA on un-stimulated cell migration. Cells were incubated with ACEA without stimulation of PDGF. Results are shown as fold change in cell number compared to cells alone. Samples were measured in triplicate n=3 + SEM.

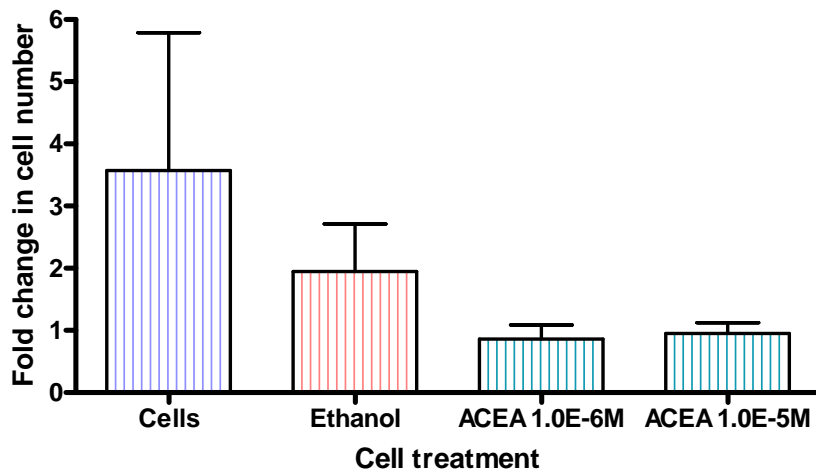


Figure 6.13. The effect of ACEA on PDGF stimulated cell migration. Results are shown as fold change in cell number compared to un-stimulated cells treated with the same intervention. Samples were measured in triplicate n=3 + SEM.

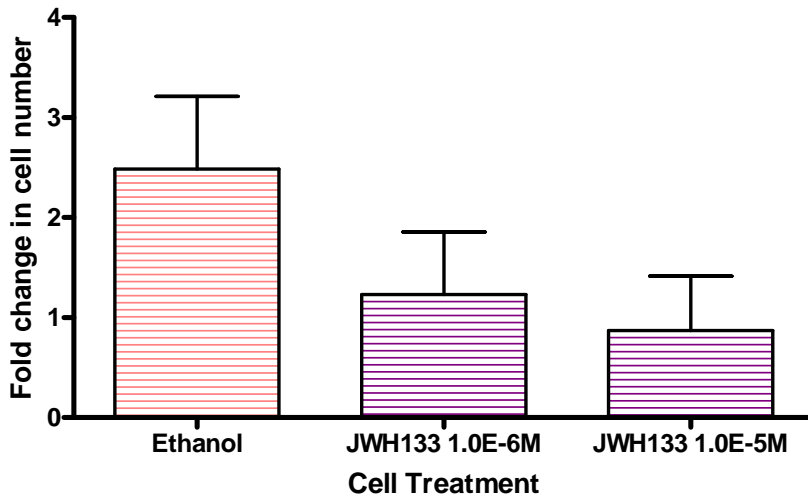


Figure 6.14 The effect of JWH133 on un-stimulated cell migration. Cells were incubated with JWH133 without stimulation of PDGF. Results are shown as fold change in cell number compared to cells alone. Samples were measured in triplicate n=3 mean + SEM.

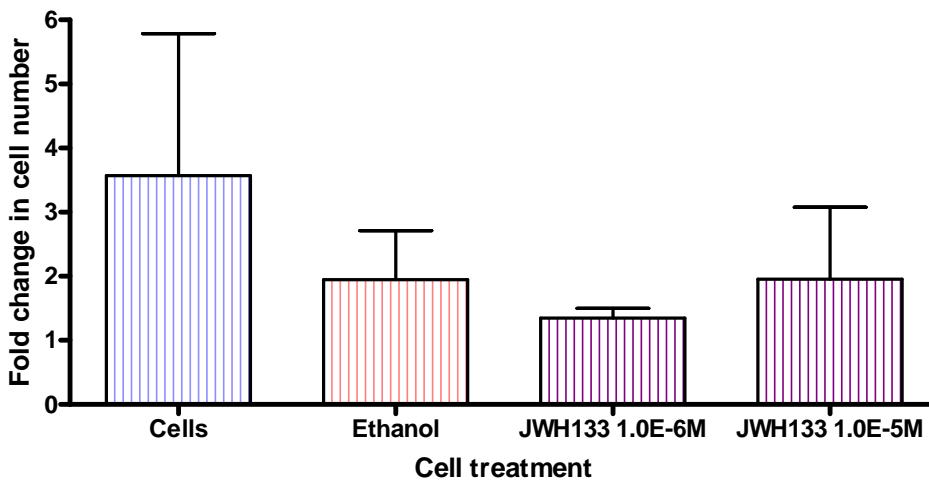


Figure 6.15 The effect of JWH133 on PDGF stimulated cell migration. Results are shown as fold change in cell number compared to un-stimulated cells treated with the same intervention. Samples were measured in triplicate n=3 mean+SEM.

6.6.2.3 The effect of a CB₂ antagonist on both un-stimulated and stimulated cell migration

Pre-treating cells with 0.1% DMSO induced a 3.46±1.52 fold increase in unstimulated cell migration (Figure 6.16). Cells treated with AM630 were found to have a 2.28±0.43 fold increase in un-stimulated migration n=3.

Exposing cells to 30ng/ml PDGF induced a 3.573±2.21 fold increase in cell migration compared to the unstimulated control (Figure 6.17). Cells treated with DMSO and AM630 (1x10⁻⁶M) exhibited a reduction in cell migration to 1.13±0.32 and 0.81±0.29 fold respectively. P>0.05, (One way ANOVA with Dunnetts post test n=3).

6.6.2.4 The effect of the endogenous cannabinoid AEA on both un-stimulated and stimulated cell migration.

Cells treated with either 0.1% ethanol or AEA (1x10⁻⁹ and 1x10⁻⁷M) demonstrated no increase in unstimulated cell migration (1.5±0.63: 1.14±0.5 and 2.08±0.15 respectively, Figure 6.18 n=4).

Exposing cells to 30ng/ml PDGF induced a 1.37±0.50 fold increase in cell migration, pre-treatment with ethanol reduced migration to 0.89±0.15 (Figure 6.19). Cell pre-treatment with AEA (1x10⁻⁹M) had no effect (0.88±0.26) on cell migration compared to the vehicle control however; pre-treatment with 1x10⁻⁷M AEA reduced the fold change in migration to 0.57±0.15 P>0.05, (One way ANOVA with Dunnetts post test n=4).

6.6.2.5 The effect of the endogenous cannabinoid 2-AG on both un-stimulated and stimulated cell migration

Cells treated with 0.1% ethanol showed no increase in un-stimulated cell migration (1.5±0.6, Figure 6.20), pre-treatment with 2-AG (both 1x10⁻⁹ and 1x10⁻⁷M) induced an increase in un-stimulated cell migration to 4.1±3.4 and 3.9±2.6 respectively, albeit there was no significant difference (P>0.05 One way ANOVA with Dunnetts post test n=3).

Cells exposed to 30ng/ml PDGF produced a 1.3±0.5 fold increase in migration (Figure 6.21). Pre-treating cells with either ethanol or 2-AG (1x10⁻⁹ and 1x10⁻⁷M) had no effect on fold change in cell migration (0.9±0.2, 0.9±0.3, 1.4±0.5, respectively n=3).

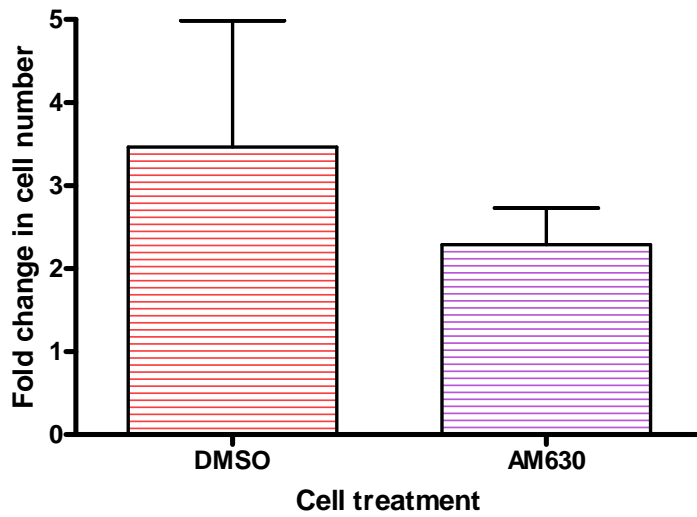


Figure 6.16. The effect of AM630 on un-stimulated cell migration. Cells were incubated with AM630 ($1 \times 10^{-6} \text{M}$) without stimulation of PDGF. Results are shown as fold change in cell number compared to cells alone. Samples were measured in triplicate $n=3$ mean \pm SEM.

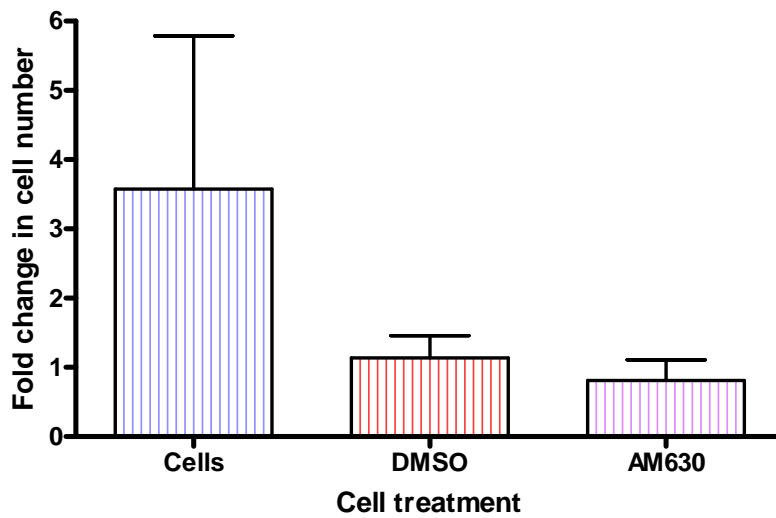


Figure 6.17 The effect of AM630 on PDGF stimulated cell migration. Results are shown as fold change in cell number compared to un-stimulated cells treated with the same AM630 ($1 \times 10^{-6} \text{M}$). Samples were measured in triplicate $n=3$ mean \pm SEM.

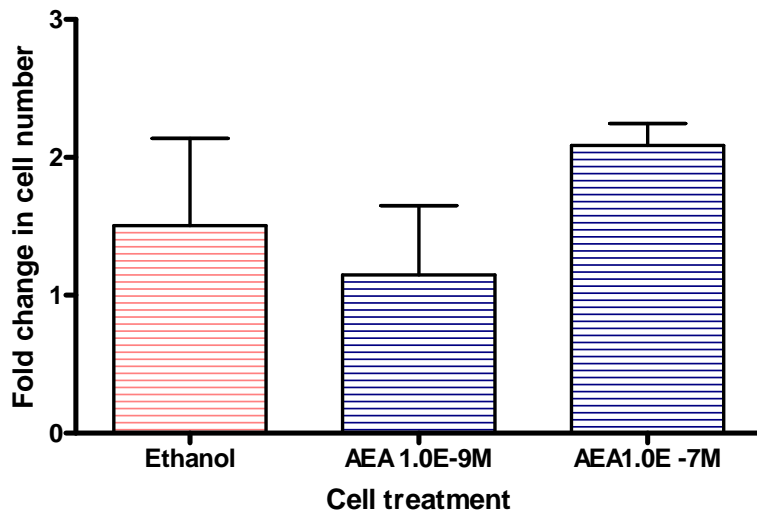


Figure 6.18. The effect of AEA on un-stimulated cell migration. Cells were incubated with AEA without stimulation of PDGF. Results are shown as fold change in cell number compared to cells alone. Samples were measured in triplicate n=4 mean +SEM.

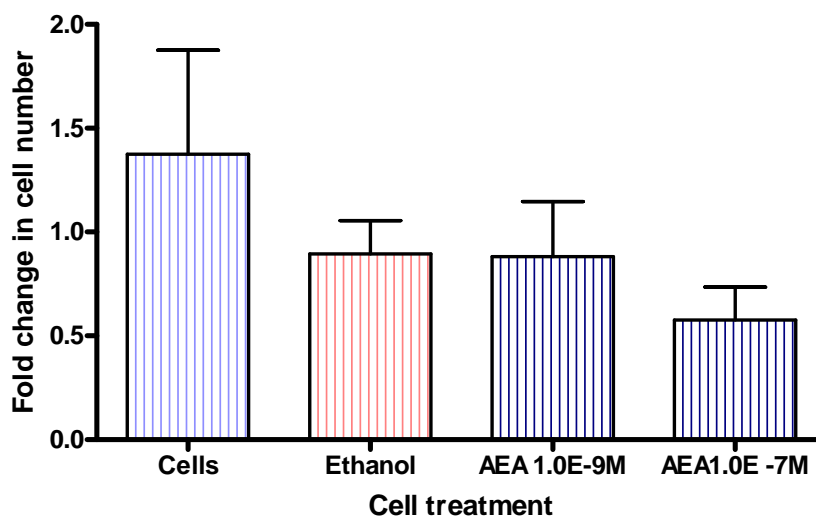


Figure 6.19. The effect of AEA on PDGF stimulated cell migration. Results are shown as fold change in cell number compared to un-stimulated cells treated with the same intervention. Samples were measured in triplicate n=4 mean +SEM.

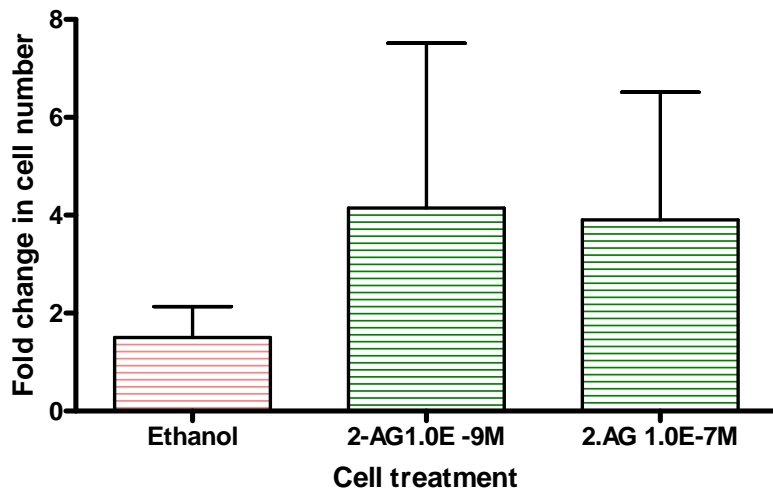


Figure 6.20. The effect of 2-AG on un-stimulated cell migration. Cells were incubated with 2-AG without stimulation of PDGF. Results are shown as fold change in cell number compared to cells alone. Samples were measured in triplicate n=3 mean +SEM.

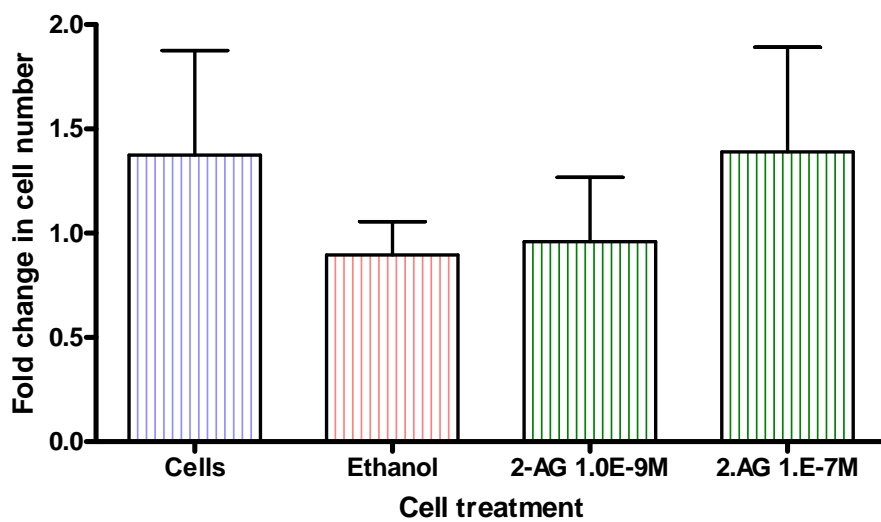


Figure 6.21 The effect of 2-AG on PDGF stimulated cell migration. Results are shown as fold change in cell number compared to un-stimulated cells treated with the same intervention. Samples were measured in triplicate n=3 mean +SEM.

6.7 Discussion

The aim of this study was to investigate the effects of both synthetic and endogenous cannabinoids on vascular smooth muscle cell migration using a chemotaxis chamber. Although this is a preliminary study the results suggest that both ACEA and 2-AG induce cell migration in cells not exposed to PDGF. Moreover JWH133 and ACEA demonstrate a trend for reducing migration of cells exposed to PDGF.

Method Optimisation

Since assessment of smooth muscle cell migration was a completely new technique to the laboratory all conditions had to be optimised. A starting incubation time of 8 hours was implemented as this was used in a similar study using human smooth muscle cells (Rajesh *et al.*, 2008). However, this incubation time resulted in too many cells migrating through the porous membrane. Subsequent experiments where the incubation time was reduced proved highly problematic as too large a number of unstimulated cells migrated through the membrane, making comparison to those exposed to PDGF impossible. To try and overcome this (i) the cell number was reduced, (ii) the type of gelatine the filter was coated with was changed (iii) the cells were quiesced (prior to addition to the chamber) (iv) cells were used at a lower passage number and (v) the layout of the chamber was altered to avoid any possible overspill of PDGF solution into the un-stimulated wells, however all these interventions proved ineffectual. Since there is evidence in the literature of incubation times ranging from 1 hour to 8 hours (Rajesh *et al.*, 2008; Fayon *et al.*, 2006) a shorter period of two hours was investigated, to determine if this would reduce the number of unstimulated cells migrating through the membrane. This approach resulted in a visible difference in migration between cells that were not exposed to PDGF and those that were stimulated. For that reason 2 hour incubation was used in subsequent experiments to determine the optimum PDGF-BB concentration. From these studies it was evident that many cells that had not fully migrated through the pore following the 2 hour incubation, for this reason the drug intervention experiments employed a 3 hour incubation period.

Due to the shape and nature of smooth muscle cells, it was impossible to count migrated cells unless the nucleus was clearly visible. To begin with cells were stained with Coomassie brilliant blue. This did not provide enough clarity to enable accurate counting, as there was no definition between the nucleus and the cytoplasm. Information from the literature suggested Giemsa stain and haematoxylin, however neither of these were successful. Eventually a modified method of H&E staining was developed which provided clear nuclear visualisation, this method was used

throughout the remainder of the study. Despite this method providing adequate clarification between the cytoplasm and nucleus, in some cases the filter had to be left in the haematoxylin for longer than the extra 10 minutes to ensure clear staining. An alternate stain that is often used to stain smooth muscle cells following migration is Diff Quick, on reflection this may have been a more suitable alternative.

To stimulate cell migration so that any inhibitory effect of a drug could be measured, cells were stimulated with PDGF-BB. 30ng/ml PDGF-BB was identified as the optimum concentration as it produced approximately a 6 fold increase in migration compared to an unstimulated control. This is similar to reports in the literature, where human smooth muscle cells stimulated with 20ng/ml PDGF produced an approximate 7 fold increase in migration, compared to an unstimulated control (Rajesh *et al.*, 2008a). Also, in a study utilising primary rat aortic smooth muscle cells 10ng/ml PDGF-BB induced a 4 fold increase in cell migration (Freyhaus *et al.*, 2006).

The effects of synthetic cannabinoids on smooth muscle cell migration

The CB₁ agonist ACEA produced over a 4 fold increase in migration of unstimulated cells at 1μM. At the higher concentration (10μM) there was no difference between the drug treated cells and the vehicle (ethanol) treated cells. When cells were stimulated with PDGF, ACEA reduced cell migration at both concentrations, albeit not significantly due to the vehicle effect. There is no report of the effects of ACEA on smooth muscle cells in the literature, however in human smooth muscle cells it was found that a CB₁ antagonist inhibited PDGF stimulated smooth muscle cell migration, through inhibition of Ras and ERK1/2 (Rajesh *et al.*, 2008b). If a CB₁ antagonist reduced stimulated cell migration, then a CB₁ agonist might be expected to stimulate migration, therefore supporting the results of this study. In Human embryonic kidney 293 cells transfected with human CB₁ gene, it was found that HU-210, WIN55212-2, and AEA all induced cell migration through activation of the CB₁ receptor (Song *et al.*, 2000), again supporting the promigratory role of the CB₁ receptor suggested from this study. The inability of ACEA to enhance migration in cells stimulated with PDGF may be explained by the overlapping of cell signalling pathways. PDGF stimulation results in the activation of a plethora of signalling pathways including the Ras, PI3K, PLC and Src pathways (all discussed in Chapter 1, reviewed in Hughes *et al.*, 1996). Cannabinoid receptor activation is complex involving coupling to G₁/G₀ proteins, activation of MAPK and the PI3K/Akt pathways (Howlett *et al.*, 2002, Bouaboula *et al.*, 1995; Molina-Holgado *et al.*, 2002). MAPK and Ras have been shown to be involved in cannabinoid induced migration (Song *et al.*, 2000; Rajesh *et al.*, 2008 a & b), the overlap of these pathways may explain the lack of a clear effect produced by ACEA in stimulated cells.

Compared to the vehicle, the CB₂ agonist JWH133 did not induce migratory activity on cells that were not exposed to PDGF-BB. In cells that were stimulated with PDGF JWH133 appeared to have an inhibitory effect compared to control cells; however a similar reduction in migration was observed with the vehicle control (ethanol). These findings are similar to the results of a study in human smooth muscle cells, where it was found that the CB₂ agonists JWH133 and HU-308 (4μM) had no effect on unstimulated cell migration and that they inhibited migration of TNF-α stimulated cells. This was reduced in the presence of a CB₂ antagonist. The inhibitory effect on migration was shown to be due to inhibition of the signalling molecules Ras, P38, ERK1/2, SAPK/JNK and Akt (Rajesh *et al.*, 2008). Similarly JWH133 was found to inhibit cell migration in human umbilical vein endothelial cells (Blazquez *et al.*, 2003).

The CB₂ antagonist AM630 produced a small increase in unstimulated cell migration, but since the vehicle DMSO induced over a 3 fold increase in migration, it is likely that any effect of AM630 was due to the vehicle. Moreover, while AM630 reduced cell migration in cells stimulated with PDGF this effect was mirrored by the vehicle, again pointing to a vehicle effect. In the human smooth muscle cells study mentioned above treatment with AM630 had no effect on basal cell migration (Rajesh *et al.*, 2008).

The effects of endogenous cannabinoids on smooth muscle cell migration

AEA had no effect on unstimulated cell migration; there was a slight increase compared to the vehicle control at 100nM but due to the large standard errors this did not reach significance. In cells exposed to PDGF, AEA (1nM and 100nM) reduced migration however a similar effect was observed following treatment with the vehicle (ethanol). What also must be noted is that in these experiments the number of control cells migrating in response to PDGF was very low (not even 2 fold). In the literature there is contradicting evidence as to the role of AEA on cell migration depending on the cell type. In human CB₁ transfected HEK cells AEA induced cell migration (Song *et al.*, 2000), whereas in both breast and colon cancer cells AEA inhibited cell migration in culture (Joseph *et al.*, 2004; Grimaldi *et al.*, 2006).

2-AG induced an increase in the migration of unstimulated cells to approximately 4 fold, although the data did not achieve statistical significance due to an effect of the vehicle (ethanol). In cells that were exposed to PDGF there was no difference between control cells or cells that were treated with 2-AG or vehicle. Again it must be noted that the fold change in migrated cells for the stimulated experiments was very low, again not reaching a 2 fold increase. Comparing the results it can be seen that the unstimulated cells treated with 2-AG produced a larger increase in cell migration than those treated with PDGF.

The finding that 2-AG stimulates cell migration is in agreement with the literature. In immune cells 2-AG has been shown to be a powerful mitogen in a human monocyte cell line, a murine microglia cell line, a leukaemia cell line, human eosinophils and natural killer cells (Kishimoto *et al.*, 2003; Walter *et al.*, 2003; Jorda *et al.*, 2002; Oka *et al.*, 2004; Kishimoto *et al.*, 2005). An effect that has been attributed to 2-AG activating the CB₂ receptor. Interestingly, the effect produced by 2-AG in microglia cells was also abolished by an antagonist of the abnormal canabidiol receptor (0-1918) (Walter *et al.*, 2003). Aside from immune cells 2-AG has also been shown to induce the migration of hematopoietic cells, an apposite effect to AEA which in the same cell line inhibited cell migration (Patinkin *et al.*, 2008). The finding in this study that 2-AG induces more migration than AEA has also been observed in leukaemia cells where AEA induced only 20% of the migratory response observed by 2-AG (Jorda *et al.*, 2002).

Limitations of the study

It can be seen from this study that the ethanol vehicle had a stimulatory response on cell migration. Cells treated with ethanol regardless of whether they were exposed to PDGF-BB or not, exhibited approximately a 2 fold increase in migration. The concentration of ethanol used in these experiments was only 0.1% but for future work this should be reduced if possible. Similarly, unstimulated cells that were treated with DMSO also demonstrated an increase in migration of over 3 fold, again the concentration of DMSO was low but for future work this should be reduced if possible. Finally, another limitation to this study was that due to time restrictions the effects of the cannabinoids as chemoattractants or on chemokinesis could not be investigated. In this study the effect of cannabinoids were measured by incubating cells with drug then measuring their unstimulated migration or their migratory response to stimulation by PDGF. As discussed in Chapter 1, stimulated cell migration can either be directional i.e. dependant on a concentration gradient (chemotaxis), or be random, with increases in motility independent of a concentration gradient (chemokinesis) (Gerthoffer *et al.*, 2007). Further experiments could be undertaken to determine whether any of the agents used in this study induced (a) directional migration by having the drug in the lower wells or (b) random increases in migration by having the drug in the lower chamber, the upper chamber or both.

Due to the length of time taken to minimise unstimulated cell migration, there was little time left to perform a thorough analysis of the effects of cannabinoids on cell migration. An example of this is that only two concentrations of each drug could be investigated as opposed to a whole range. This could mean that an effect of one of the drugs was missed. Another major limitation to this study was the large standard errors present due to the variability in results. A possible explanation for this could be that the incubation time was too short. Ideally the staining

technique should have been optimised before identifying the optimum incubation time. This would have been more accurate and may also have saved time. To begin with the conditions employed in the assay seemed adequate to measure cell migration as evident by the large stimulatory response produced in the PDGF-BB experiments; however, as experiments progressed the stimulatory response produced by PDGF-BB decreased and was highly variable.

Conclusions

The preliminary data shown in this study suggest that ACEA and possibly JWH133 reduce stimulated cell migration and that 2-AG can increase migration of unstimulated smooth muscle cells. However to increase reliability of results a more thorough investigation into incubation time staining cells with either the modified H&E technique or using the Diff Quick stain should be performed.

Chapter 7

General Discussion

7.1 Main findings

Δ^9 -THC has been shown to reduce the progression of atherosclerosis by means of its immunoregulatory effects (Steffen *et al.*, 2005), in a separate more recent study a synthetic CB₂ agonist inhibited stimulated human smooth muscle cell proliferation *in vitro* (Rajesh *et al.*, 2008). Despite this the effects of cannabinoids, especially the endogenous cannabinoids AEA and 2-AG, have not been investigated in terms of restenosis. This study was designed to investigate whether the endocannabinoid system is present and functional in a murine model of neointimal formation, and to identify whether or not endogenous cannabinoids play a negative or positive role in disease progression by investigating their effects on SMC proliferation and migration. This study has demonstrated that AEA elicits a dilatory effect on the murine carotid artery, through a mechanism independent of active metabolites but mediated through the CB₁ receptor, demonstrating the functional presence of this receptor in murine blood vessels. Moreover, the presence of both cannabinoid receptors on murine smooth muscle cells was confirmed. In an organ culture model of neointimal formation it was found that endocannabinoid concentration was increased, suggesting a further functional role for these compounds in vascular injury. Further study revealed that the CB₂ receptor agonist JWH015 reduced cell proliferation through a non-CB₂ receptor mediated mechanism, a finding that was mimicked with a CB₂ antagonist. AEA also reduced stimulated cell proliferation, however this was most likely due to cytotoxicity. Finally it was found that both CB₁ and CB₂ agonists tended to reduce stimulated SMC migration whereas the endogenous cannabinoid 2-AG stimulated cell migration.

Presence of a functional endocannabinoid system

As described in section 3.5.6 and 3.5.7 the concentrations of endogenous cannabinoids were significantly (2-AG) increased in an *in vitro* model of vessel injury, compared to healthy vessels. Despite this being the first report linking increased endocannabinoid concentration with neointimal formation, these findings are in agreement with a vast quantity of studies which demonstrate an increase in endogenous cannabinoid concentration in pathological conditions (reviewed in Di Marzo *et al.*, 2008). This study did not investigate the location of endocannabinoid synthesis; however evidence from the literature can provide a basis for speculation. Endothelial progenitor cells have been shown to release both AEA and 2-AG in a basal manner, which is increased following stimulation with TNF α (Opitz *et al.*, 2007). Similarly endothelial cells synthesise and release 2-AG in response to stimulation by thrombin (Sugiura *et al.*, 1998), the endothelium of bovine coronary arteries has also been shown to secrete 2-AG (Gauthier *et al.*, 2005). Evidence also suggests that endocannabinoids can be released from sensory neurones, as this has been shown to be the case in the CNS (Di Marzo *et*

al., 1994). Evidence of non-endothelium derived endocannabinoids in the vasculature has come from a study by Rademacher *et al.*, 2005, who showed that endocannabinoid concentration increased in the rat cerebral artery preparations without an endothelium. As the injured arteries in this study were devoid of an endothelium (as a result of the injury process), it is most likely that the source of endocannabinoid production is the smooth muscle cells, however experimental investigation would be required to confirm or contradict this.

This study did however confirm the presence of both CB₁ and CB₂ receptors on murine smooth muscle cells (discussed in section 3.5.5). The finding that endocannabinoid concentration increases during the vessel response to injury strongly suggests that endocannabinoids play a role in either disease progression or limitation.

Direct vascular effect of AEA

Anandamide produced a concentration dependant relaxation of the murine carotid artery that reached a maximum of approximately 20%. This is dissimilar to previous findings in the rat carotid artery which demonstrated no functional response to methanandamide (Holland *et al.*, 1999). As discussed in both chapter 1 and chapter 4, a wide species variation exists regarding the response to cannabinoids in the vasculature. A 20% relaxation is similar however to the response produced by Δ^9 -THC in the rat aorta (O'Sullivan *et al.*, 2005). Inhibition of FAAH tended to increase the relaxant response of AEA (although not significantly), thus confirming that the vasodilatation produced by AEA was not attributable to the FAAH mediated production of arachidonic acid and its vasoactive metabolites, as observed in some species (Pratt *et al.*, 1998). Similarly, COX produced metabolites were not involved in the vasodilatation produced by AEA. A CB₁ receptor antagonist significantly attenuated the AEA response suggesting that AEA elicits its functional effect through activation of the CB₁ receptor. Inhibition of the CB₂ receptor had no effect on the response produced by AEA. In addition to these findings it was also discovered that the vehicle in which AEA was dissolved in (Tocrisolve®) was vasoactive. When put in context with the previous findings, it can be speculated that in diseased conditions an artery produces AEA to induce a vasodilatory effect through means of the CB₁ receptor.

Effect of cannabinoids on vascular smooth muscle cell proliferation

The CB₂ agonist JWH015 reduced ERK1/2 phosphorylation at high concentrations (albeit this did not reach statistical significance). As discussed in detail in Chapter 1, ERK activation does not necessarily lead to cell proliferation; to provide a further indication of cell proliferation DNA synthesis was measured by BrdU incorporation. In a similar fashion JWH015 significantly inhibited DNA synthesis at high concentrations, agreeing with previous findings which demonstrated that CB₂ agonists can reduce stimulated cell proliferation (Rajesh *et al.*, 2008). In

contradiction to this however, when these experiments were repeated with an alternative CB₂ agonist a dissimilar effect was observed. JWH133, a more potent CB₂ agonist, had no effect on DNA synthesis over a wide concentration range producing only a small attenuation at the highest concentration. Further controversy arose when a CB₂ antagonist alone and in the presence of CB₂ agonists significantly reduced DNA synthesis. If the CB₂ antagonist was having a genuine CB₂ antagonistic effect, then canonical pharmacology would mean that in the presence of an agonist there would be some reversal of the inhibition of DNA synthesis, due to competition at the binding site. As this was not observed it can be concluded that both JWH015 and the CB₂ receptor antagonist were acting independently of CB₂.

Further investigation revealed that the reduction in DNA synthesis observed when the agonist and antagonist were combined could be explained by drug induced cytotoxicity. Toxicity testing revealed no adverse effects on cell viability for either agonist, or the antagonist on its own. This study also revealed no functional effect of CB₁ or GPR55 activation on stimulated cell proliferation.

AEA significantly reduced DNA synthesis at a concentration of 10µM; this is much higher than would be found either physiologically or pathophysiologically, information from cell viability studies indicates that this reduction in DNA synthesis was most likely due to cytotoxicity or growth arrest. 2-AG had no effect on stimulated cell DNA synthesis. To put these findings back into context of increased endocannabinoid concentration following injury, no certain conclusions can be made from this study as to the role endocannabinoids play on stimulated cell proliferation. Information from the literature showing an inhibitory effect of CB₂ agonists on stimulated cell proliferation (Rajesh *et al.*, 2008) might indicate that endogenous cannabinoids are released to combat excess cell proliferation through their actions on CB₂ receptors. This study has also highlighted the need for caution when using CB₂ agonists, as they may not be entirely selective.

Effect of cannabinoids on vascular smooth muscle cell migration

The CB₁ agonist ACEA had a tendency to increase the migration of unstimulated cells; however this did not reach significance due to a vehicle effect. When cells were stimulated with PDGF, ACEA appeared to reduce cell migration, again this failed to achieve significance due to a vehicle effect. There are no reports of the effects of ACEA on smooth muscle cells in the literature to compare these findings. However, in human smooth muscle cells it was found that a

CB₁ antagonist inhibited PDGF stimulated smooth muscle cell migration (Rajesh *et al.*, 2008b). If a CB₁ antagonist reduced stimulated cell migration then a CB₁ agonist might be expected to stimulate migration, therefore supporting the results of this study. A similar finding was observed in human embryonic kidney 293 cells transfected with human CB₁ gene, where it was found that HU-210, WIN55212-2, and anandamide all induced cell migration through activation of the CB₁ receptor.

JWH133 had no effect on unstimulated cell migration, but demonstrated a tendency to reduce migration in cells that were stimulated; however a similar reduction in migration was observed with the vehicle control. These findings are similar to the results of a study in human smooth muscle cells, where it was found that the CB₂ agonists JWH133 and HU-308 (4µM) had no effect on unstimulated cell migration and that they inhibited migration in TNFα stimulated cells, which was reduced in the presence of a CB₂ antagonist (Rajesh *et al.*, 2008). Similarly JWH133 was found to inhibit cell migration in human umbilical vein endothelial cells (Blazquez *et al.*, 2003).

AEA had a negligible effect on unstimulated and stimulated cell migration, however 2-AG exhibited a trend for inducing migration in unstimulated cells (this did not reach significance due to some activity of the vehicle). The finding that 2-AG stimulates cell migration is in agreement with the literature, as 2-AG has shown powerful mitogenic effects in a variety of immune cells (Kishimoto *et al.*, 2003; Walter *et al.*, 2003; Jorda *et al.*, 2002; Oka *et al.*, 2004; Kishimoto *et al.*, 2005). Due to the lack of any statistically significant effects on cell migration, no decisive answer can be provided to the question of whether or not the increase in endocannabinoid concentrations seen in injured arteries has any effects on cell migration and the subsequent formation of a neointimal, although this is an attractive concept.

Investigation of cannabinoid agents in an organ culture model of neointimal formation

One of the key aims of this study was to develop an organ culture model of neointimal formation that would permit the investigation of cannabinoid agents on the injury response. The ultimate goal was to identify a target that would reduce the development of a neointima. The agent that was identified to be used in this study was the CB₂ agonist JWH133. Despite complex results obtained in the DNA synthesis experiments, a CB₂ agonist did reduce DNA synthesis and demonstrated a trend of reducing stimulated cell migration.

The organ culture model developed in chapter 3 provided an injury response that had many characteristics of a neointimal formation, including medial thickening, adventitial thickening, cell infiltration into the lumen and production of extracellular matrix. A pilot study using this model was employed for a drug study (detailed in Appendix 1), although the outcome was disappointing. Firstly neither the control cultured nor injured artery segments developed a substantial injury response. Second, due to shrinkage of the vessel sections and problems with the embedding process a number of tissue samples were lost. Due to constraints of time it was decided not to continue with these experiments. However, the data that was collected is shown in Appendix 1. In theory, the use of a murine organ culture model of neointimal formation has immense potential, it would allow the screening of a variety of agents at the same time, and therefore reduce the number of animals used for experimentation. Also the availability of transgenic mice would make for extremely valuable experimental tools. Despite this, the organ culture model developed in this chapter proved difficult to reproduce, and therefore may be unsuitable as a screening model. As mentioned previously the C57BL/6 strain of mice can be resistant to neointimal hyperplasia following endothelial denudation *in vivo* (Hui *et al.*, 2008), therefore perhaps a different strain of mouse may be more successful.

7.2 Clinical relevance

Drug eluting stents have proved to be very effective in reducing restenosis rates when compared to bare metal stents. Despite the effectiveness of the two most established DES (which elute rapamycin and paclitaxel), safety concerns over the possible link with thrombus formation in response to incomplete revascularisation, surrounding endothelial dysfunction, and complications with diabetic patients mean that further research is required to identify novel agents that may eliminate these problems (Babapulle *et al.*, 2004; Inoue *et al.*, 2009; Costa *et al.*, 2005). This study has shown that the endocannabinoid system becomes activated in a mouse model of vessel injury, a CB₂ agonist inhibited smooth muscle cell proliferation, and AEA induced a small vasodilatation. When these findings are put into context with previous findings in the literature, for example that a CB₂ agonist reduces human smooth muscle cell proliferation (Rajesh *et al.*, 2008), and that cannabinoids reduce atherosclerosis progression through both their immunomodulatory effects (Steffens *et al.*, 2005) and through the decreased expression of adhesion molecules (Zhao *et al.*, 2010), it can be seen that modulation of the cannabinoid system has great potential to prevent/treat both atherosclerosis and restenosis.

A previous clinical trial (STRADIVARIUS) investigated the effectiveness of rimonabant (a CB₁ antagonist) on progression of coronary disease in patients with abdominal obesity and metabolic syndrome. The findings of this trial showed some favourable properties of

rimonabant but the overall outcome was a non significant effect on percent atheroma volume (Nissen *et al.*, 2008), however there has been no investigation into the effects of a CB₂ agonist. One fundamental issue that needs to be overcome to permit the use of cannabinoid agents as a treatment for vascular disease would be the eradication of psychological effects. This negative side effect of cannabinoids was recently observed in the removal of rimonabant from the commercial market due to increased suicidality (Christensen *et al.*, 2007).

7.3 Future work

Completion of smooth muscle cell proliferation and migration studies.

As discussed in Chapter 5 the results of the DNA synthesis experiments regarding the CB₂ agonist were conflicting. If these experiments were repeated then a more thorough understanding of the effects of the CB₂ agonist and its mechanisms of action may be obtained. Similarly as mentioned in Chapter 6, the preliminary studies on cell migration require further investigation to obtain a more thorough understanding of the functional role of cannabinoids (both endogenous and synthetic) on cell migration. Another problem experienced throughout this study was the interference from the vehicle, a vehicle effect was observed with both ethanol and DMSO (both at 1% for proliferation studies, 0.1% for migration studies) therefore experiments should be repeated with a lower concentration of solvent.

Cannabinoids and endothelial cells

One of the major limitations to the currently available drug eluting stents is the antiproliferative effect the eluting drugs have on endothelial cell proliferation. Previous studies have shown that endothelial cells express the CB₁ receptor and that it is functionally coupled to MAP kinase (Liu *et al.*, 2000), leading to the speculation that perhaps cannabinoids could stimulate endothelial cell proliferation. A more recent study has also shown meth-AEA to induce NO production in rabbit aortic endothelial cells through the novel AEA receptor (McCollum *et al.*, 2007). If cannabinoids could increase endothelial cell proliferation and increase NO production these would be extremely desirable qualities to have in an antirestenotic drug. Therefore an area for further work would be to characterise the effects of cannabinoid agents on endothelial cell proliferation.

Effects of virodhamine

Virodhamine is an endogenous cannabinoid that has been found to demonstrate antagonistic effects at the CB₁ receptor but be a full agonist at CB₂ receptors (Porter *et al.*, 2002). Results from both this study and the literature, have shown an inhibitory effect of CB₂ agonists in smooth muscle cell proliferation. Similarly Rajesh *et al.*, 2008 demonstrated that a CB₁ antagonist reduced cell proliferation. These functional effects of a CB₂ agonist and a CB₁ antagonist bear striking similarity to the agonist/antagonist properties of virodhamine. Due to these similarities it could be speculated that virodhamine would inhibit SMC proliferation. Virodhamine is also thought to function through the abnormal canabidiol/anandamide receptor (Ho *et al.*, 2004), which, as mentioned above, is thought to induce NO release from endothelial cells. Therefore in theory this endocannabinoid might reduce SMC proliferation through CB₁ inhibition/CB₂ activation and may induce the release of NO through the endothelial abnormal canabidiol/anandamide receptor, and is a future avenue for investigation.

***In vivo* model of neointimal formation**

There are many established *in vivo* models of neointimal formation; the next step in this study would be to investigate the effects of cannabinoid agents (primarily CB₂ agonists) on neointimal formation in an *in vivo* environment. This would provide a more reproducible and physiologically relevant setting compared to the use of an organ culture model, as both the circulatory and inflammatory response would be present. The benefit of utilising a murine model means that the effects of cannabinoid agonists on neointimal formation could be investigated in wild type, ApoE^{-/-}, and CBR^{-/-} transgenic mice (Karshovska *et al.*, 2007; Zerneck *et al.*, 2008). If these studies showed positive results, then a possible avenue for further investigation would be to develop a stent designed to elute the appropriate agent, which could then be tested in a larger animal model, such as the porcine coronary artery.

7.4 Conclusion

In conclusion this study has shown for the first time that endocannabinoid concentrations increase in a mouse model of vessel injury, thus suggesting they play a role in the arterial response to injury. This study has also confirmed the presence of both CB₁ and CB₂ receptors on murine smooth muscle cells. The endogenous cannabinoid AEA produced a small but measurable relaxation in the mouse carotid artery, a response that was independent of both FAAH, and COX mediated metabolites, but requiring activation of the CB₁ receptor. Despite

conflicting data, this study suggests that CB₂ receptor agonists reduce stimulated cell proliferation and possibly migration, and that the endogenous cannabinoid 2-AG may stimulate cell proliferation. Unfortunately due to the un-reproducibility of the organ culture model the effects of cannabinoid agents on the development of neointima could not be investigated. Despite the inability to form a clear cut conclusion over the question do endogenous cannabinoids enhance or inhibit neointimal formation, the evidence does lean towards an inhibitory effect on disease progression. Therefore, this study along with findings in the literature highlights that although further research is required, the endocannabinoid system may have the potential to be manipulated for therapeutic gains in terms of restenosis.

Appendix

Drug incubation study

8.1 Aim

The aim of this study was to investigate the effects of cannabinoid agents in an organ culture model of neointimal formation.

8.2 Method

8.2.1 Tissue preparation and drug incubation method

C57/B16J mice of either sex were euthanized by cervical dislocation, sprayed with ethanol and the aortas dissected and cleared of adherent tissue using sterile technique. The vessels were placed in a 6-well plate containing 3ml of sterile medium (composed of 42% Waymouths, 42% Hams F-12, 1% penicillin streptomycin, 15% foetal bovine serum (FBS), 0.05% fungizone) and transferred to the laminar flow hood, the vessels were then cut in half. One half was used to investigate drug effects on cultured tissue, the other half was used to investigate the effects of cannabinoid agents on injured tissue (vessels were injured as described in section 3.3.2.3).

The segments (injured or non-injured) were then transferred to a sterile 6-well plate containing 3ml medium, supplemented with cannabinoid agent (see Table 8.1), and placed in an incubator at 5%CO₂ at 37°C. The vessel segments were maintained in culture for 14 days with the medium being aspirated and replaced every alternate day, fresh drug solutions were added at each media change. The aortic sections were removed from culture and fixed in 10% neutral buffered formalin for subsequent histological analysis as previously described in section 2.3.1. (method summarised in Figure 8.1.) Tissue measurements were performed in the same as as described in section 3.3.3

Drug	Media concentration
JWH133	1x10 ⁻⁵ M
AM630	1x10 ⁻⁶ M
JWH133 +AM630	As above

Table 8.1 Drugs and their media concentrations used in the drug incubation study.

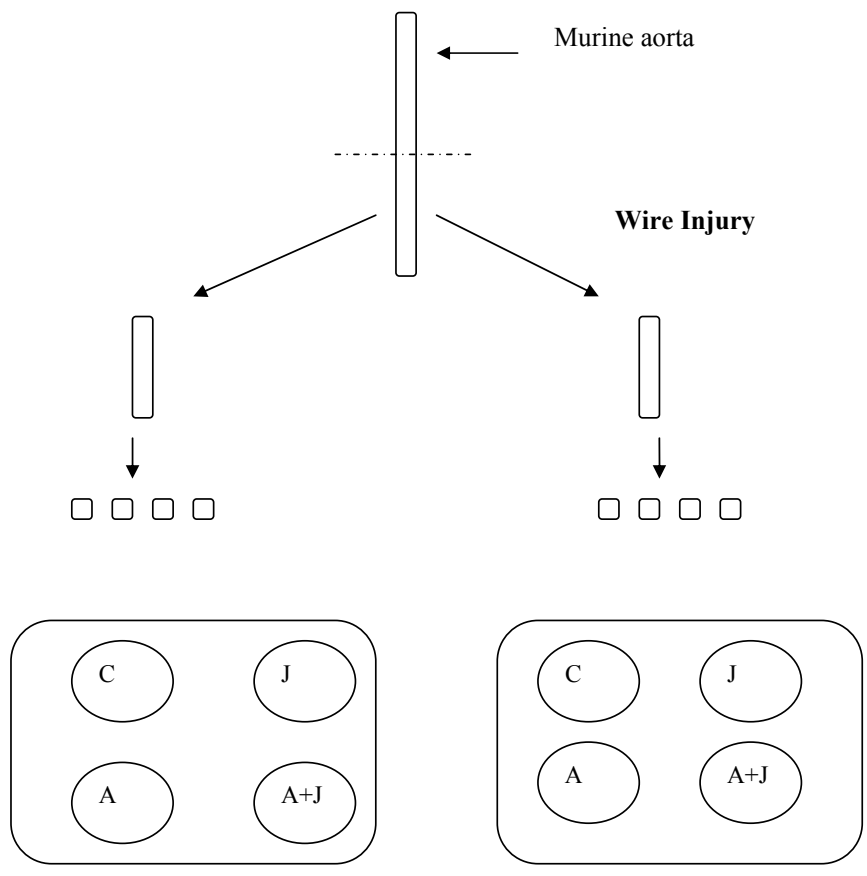


Figure 8.1 Illustrates the method by which tissue samples either injured or non injured were incubated with cannabinoid drugs. C =control (no drug), J=JWH133, A =AM630, A+J =AM630 + JWH133.

8.3 Results

Despite earlier work demonstrating that this organ culture model produced a measurable injury response, only one wire injured tissue segment displayed any sign of neointimal cell growth. As can be seen from the raw data shown in Tables 8.2-8.8, many samples do demonstrate increased medial or adventitial area/thickness in response to culture and injury. However, some samples demonstrate no difference between the uncultured control and the wire injured samples. Unfortunately, due to the shrinkage of vessels and issues with wax embedding, a number of samples were lost in the process. Since most of these samples were in the groups where the segments were incubated with the cannabinoid agents, it was impossible to determine from these pilot studies whether or not they had any effect.

Medial Area mm ²					
Sample	Un cultured	Cultured			
		Control	JWH133	JWH133 +AM630	AM630
1					
2	0.092	0.32			0.084
3	0.106				
4		0.073	0.104		
5		0.051			
6					0.099
7	0.071	0.304			
8	0.053	0.054		0.073	
9	0.07				
10		0.049		0.078	
11				0.098	
12		0.047		0.227	

Tables 8.2 The individual medial areas of samples that had been cultured in combination with cannabinoid agents.

Medial Area mm ²					
Sample	Un cultured	Injured			
		Control	JWH133	JWH133 +AM630	AM630
1			0.055		
2	0.092				
3	0.106				
4					
5		0.08			
6		0.051			0.064
7	0.071	0.075		0.089	
8	0.053	0.079			0.125
9	0.07				
10		0.139			
11		0.058			
12		0.082			

Table 8.3 The individual areas of tissue samples that had been injured then cultured in the presence of cannabinoid agents.

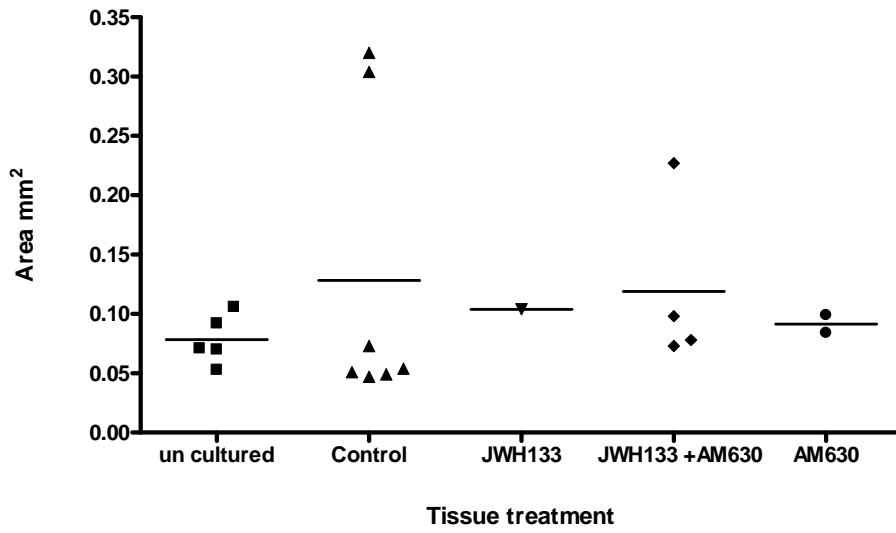


Figure 8.2 The individual areas of samples that had been cultured in the presence of cannabinoid agents.

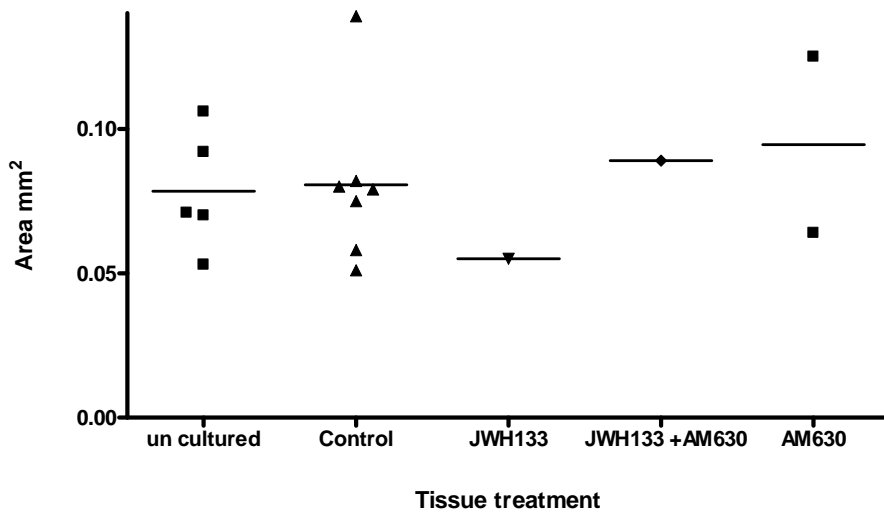


Figure 8.3 The individual areas of samples that had been injured prior to culture in the presence of cannabinoid agents

Adventitial Area mm ²					
Sample	Un cultured	Cultured			
		Control	JWH133	JWH133 +AM630	AM630
1					
2	0.051	0.144			0.02
3	0.004				
4		0.016	0.052		
5		0.029			
6					0.042
7	0.018	0.115			
8	0.02	0.026		0.05	
9	0.01				
10		0.015		0.061	
11				0.026	
12		0.001		0.163	

Table 8.4 The individual adventitial areas of samples that were cultured in the presence of cannabinoid agents.

Adventitial Area mm ²					
Sample	Un cultured	Injured			
		Control	JWH133	JWH133 +AM630	AM630
1			0.012		
2	0.051				
3	0.004				
4					
5		0.086			
6		0.01			0.018
7	0.018	0.05		0.147	
8	0.02	0.033			0.071
9	0.01				
10		0.059			
11		0.002			
12		0.048			

Table 8.5 The individual adventitial areas of tissue samples that had been injured then cultured in the presence of cannabinoid agents.

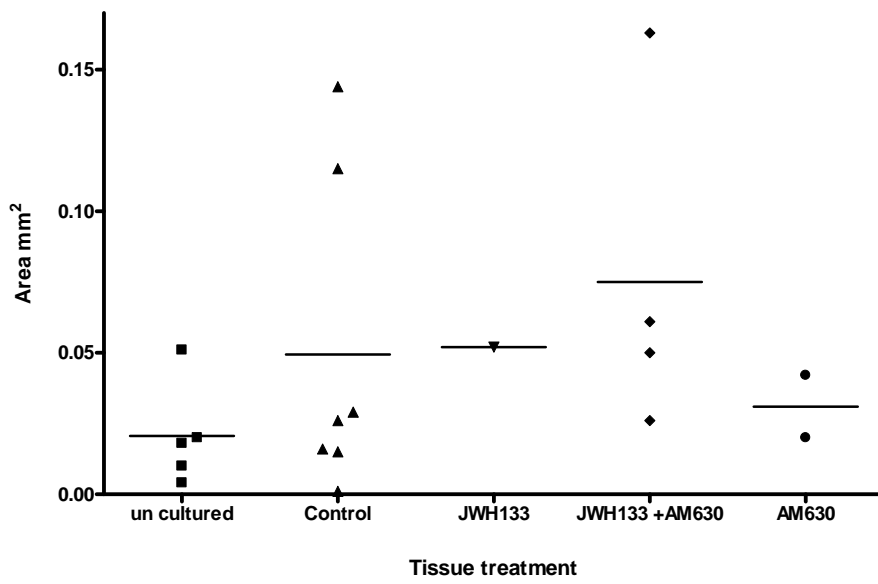


Figure 8.4 The individual adventitial areas of samples that were cultured in the presence of cannabinoid agents.

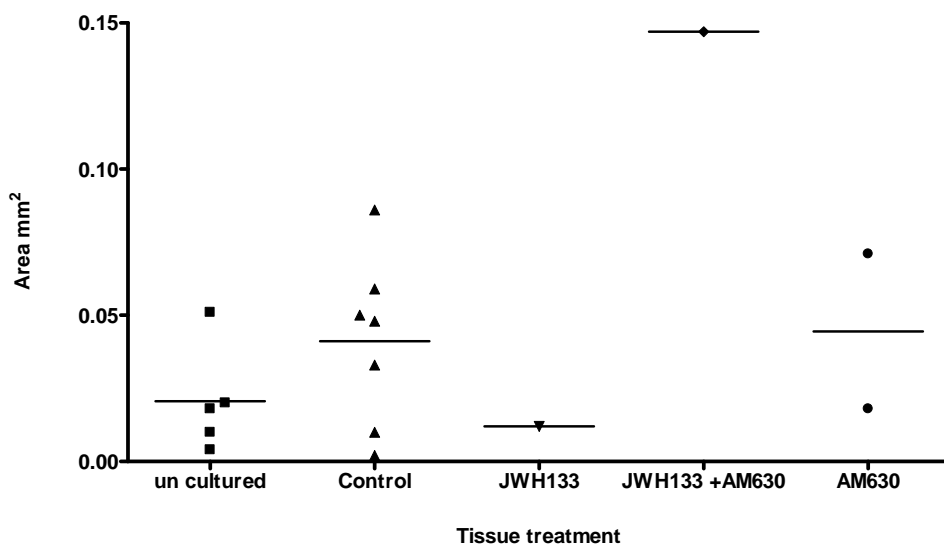


Figure 8.5 The individual adventitial areas of samples that were injured prior to culture in the presence of cannabinoid agents.

Medial Thickness mm ²					
Sample	Un cultured	Cultured			
		Control	JWH133	JWH133 +AM630	AM630
1					
2	0.061	0.07925			0.04875
3	0.04975	0.1115			
4		0.036	0.0675		
5		0.04225			
6					0.07425
7	0.042	0.1165			
8	0.036	0.04725		0.11475	
9	0.03025				
10		0.03125		0.05225	
11				0.075	
12		0.034		0.13925	

Table 8.6 The mean medial thickness value for each sample that had been cultured along with cannabinoid agents.

Medial Thickness mm ²					
Sample	Un cultured	Injured			
		Control	JWH133	JWH133 +AM630	AM630
1			0.03475		
2	0.061				
3	0.04975				
4					
5		0.0535			
6		0.036			0.0355
7	0.042	0.043		0.0655	
8	0.036	0.0515			0.055
9	0.03025				
10		0.05175			
11		0.032			
12		0.058			

Table 8.7 The mean medial thickness values for each sample that had been injured prior to culture, along with cannabinoid agents.

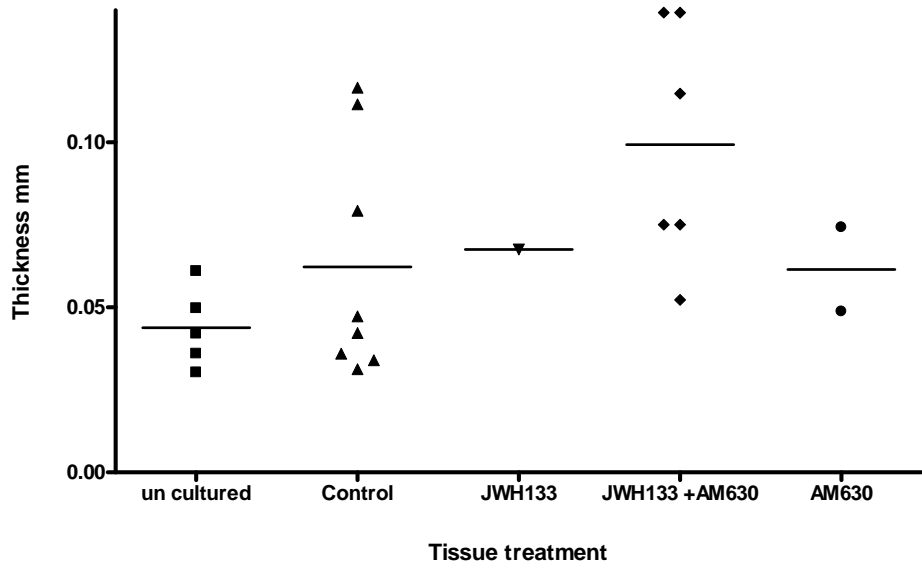


Figure 8.6 The mean medial thickness value for each sample that had been cultured along with cannabinoid agents.

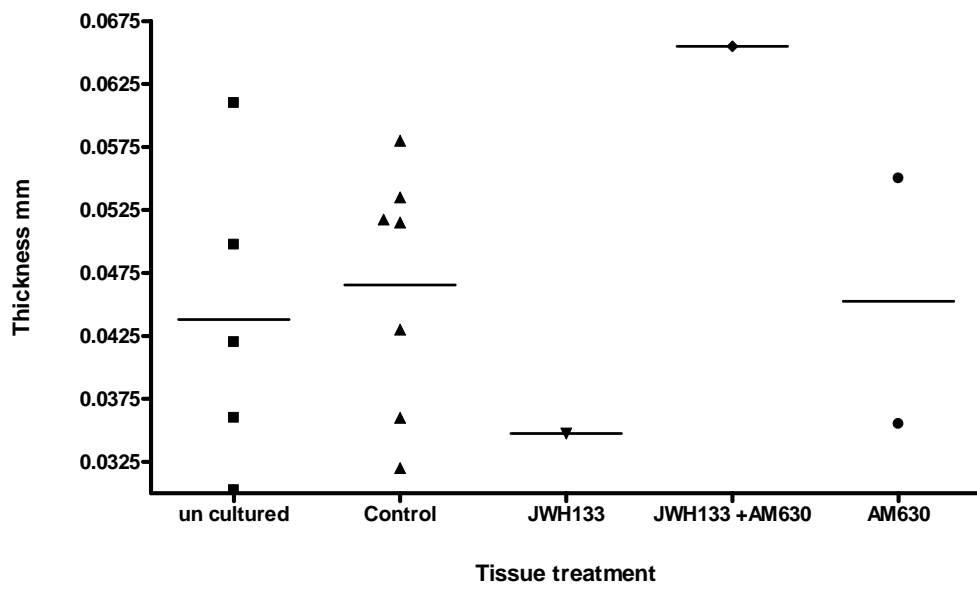


Figure 8.7 The mean medial thickness value for each sample that had been injured prior to culture along with cannabinoid agents.

Adventitial Thickness mm ²					
Sample	Un cultured	Cultured			
		Control	JWH133	JWH133 +AM630	AM630
1					
2	0.03	0.0585			0.02625
3	0.01275	0.048			
4		0.01875	0.059667		
5		0.02			
6					0.0395
7	0.017	0.05875			
8	0.01575	0.0185		0.02	
9	0.01975				
10		0.01125		0.04175	
11				0.02275	
12		0.002		0.062	

Table 8.8 The mean adventitial thickness values for each sample that had been cultured along with cannabinoid agents.

Adventitial Thickness mm ²					
Sample	Un cultured	Injured			
		Control	JWH133	JWH133 +AM630	AM630
1			0.008		
2	0.03				
3	0.01275				
4					
5		0.05275			
6		0.00925			0.01875
7	0.017	0.03725		0.0275	
8	0.01575	0.018			0.063
9	0.01975				
10		0.0235			
11		0.032			
12		0.0455			

Table 8.9. The mean adventitial thickness values for each sample that had been injured prior to culture, along with cannabinoid agents.

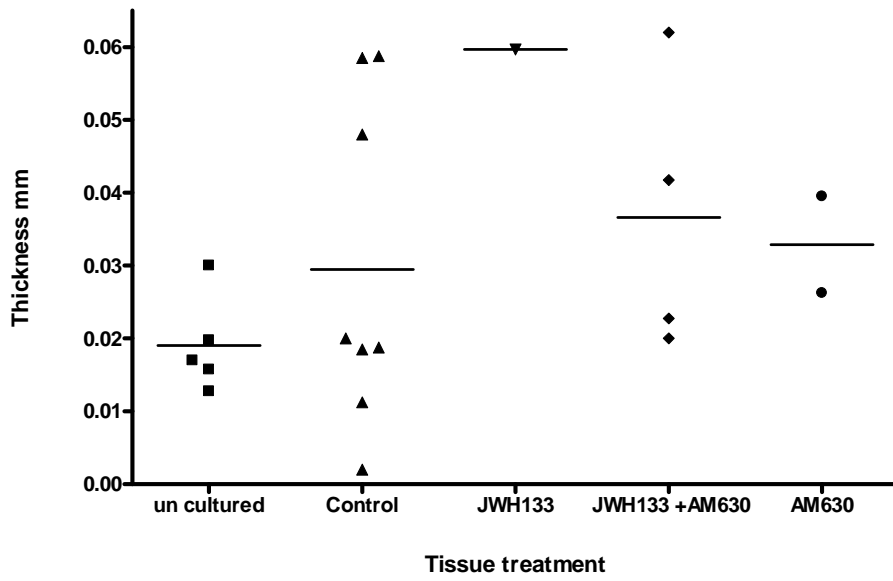


Figure 8.8 The mean adventitial thickness values for each sample that had been cultured along with cannabinoid agents.

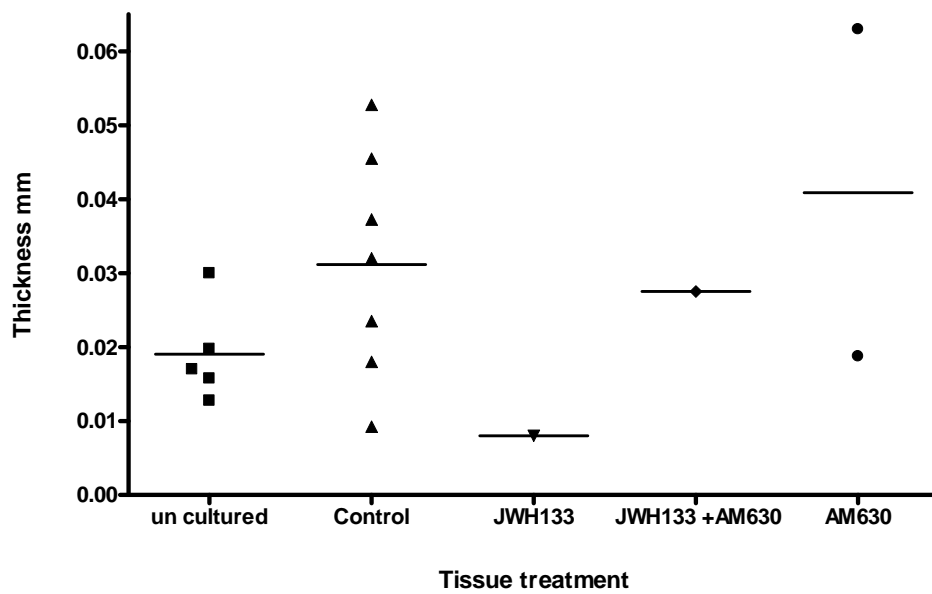


Figure 8.9. The mean adventitial thickness values for each sample that had been injured prior to culture along with cannabinoid agents.

Chapter 8

References

- AHANCHI, S., TSIHLIS, N. and KIBBE, M., 2007. The role of nitric oxide in the pathophysiology of intimal hyperplasia. *Journal of Vascular Surgery*, 45, pp. A64-A73
- AHN, S. et al., 2004. Tumor necrosis factor-alpha induces fractalkine expression preferentially in arterial endothelial cells and mithramycin A suppresses TNF-alpha-induced fractalkine expression. *American Journal of Pathology*, 64(5), pp. 1663-1672
- ALPINI, G. and DEMORROW, S., 2009. Changes in the Endocannabinoid System May give Insight into new and effective Treatments for Cancer. *Vitamins and Hormones*, 81, pp. 469-485
- ARTURO, G. and SCHWARTZ, R., 2006. Preclinical Restenosis Models: Challenges and Successes. *Toxicologic Pathology*, 34, pp. 11-18
- ASAHARA, T. et al., 1995. Local delivery of vascular endothelial growth factor accelerates reendothelialization and attenuates intimal hyperplasia in balloon-injured rat carotid artery. *Circulation*, 91(11), pp. 2793-2801
- BABAPULLE, M. et al., 2004. A hierarchical Bayesian meta-analysis of randomised clinical trials of drug-eluting stents. *Lancet*, 364, pp. 583-591
- BAKER, D. et al., 2006. In silico patent searching reveals a new cannabinoid receptor. *TRENDS in pharmacological sciences*, 27, pp. 1-4
- BANAI, S. et al., 1991. Rabbit ear model of injury-induced arterial smooth muscle cell proliferation. Kinetics, reproducibility, and implications. *Circulation Research*, 69, pp. 748-756
- BARILLARI, G. et al., 2003. Inflammatory cytokines stimulate vascular smooth muscle cells locomotion and growth by enhancing $\alpha 5\beta 1$ integrin expression and function *Atherosclerosis*, 154, pp. 377-385
- BARISH, G., NARKAR, V. and EVANS, R., 2006. PPAR delta: a dagger in the heart of the metabolic syndrome. *Journal of Clinical Investigation*, 116, pp. 590-597
- BÁTKAI, S. et al., 2004. Endocannabinoids acting at cannabinoid-1 receptors regulate cardiovascular function in hypertension. *Circulation*, 110(14), pp. 1996-2002

- BÁTKAI, S. et al., 2007. Decreased age-related cardiac dysfunction, myocardial nitrate stress, inflammatory gene expression, and apoptosis in mice lacking fatty acid amide hydrolase. *American Journal of Heart and Circulatory Physiology*, 293, pp. H909-H918
- BÁTKAI, S. et al., 2001. Endocannabinoids acting at vascular CB1 receptors mediate the vasodilated state in advanced liver cirrhosis. *Nature Medicine*, 7, pp. 827-832
- BEGG, M. et al., 2005. Evidence for novel cannabinoid receptors. *Pharmacology and Therapeutics*, 106, pp. 133-145
- BELTRAMO, M. et al., 1997. Functional role of high-affinity anandamide transport, as revealed by selective inhibition. *Science*, 277(5329), pp. 1094-1097
- BENDECK, M. et al., 1994. Smooth muscle cell migration and matrix metalloproteinase expression after arterial injury in the rat. *Circulation Research*, 75, pp. 539-545
- BENHAM, C., DAVIS, J. and RANDALL, A., 2002. Vanilloid and TRP channels: a family of lipid-gated cation channels. *Neuropharmacology*, 42(7),
- BENTZON, J. et al., 2006. Smooth muscle cells in atherosclerosis originate from the local vessel wall and not circulating progenitor cells in ApoE knockout mice. *Arteriosclerosis, Thrombosis and Vascular Biology*, 26(12), pp. 2696-2702
- BERDYSHEV, E., 2000. Cannabinoid receptors and the regulation of immune response. *Chemistry and Physics of Lipids*, 108, pp. 169-190
- BERGLUND, B., BORING, D. and HOWLETT, A., 1999. Investigation of structural analogs of prostaglandin amides for binding to and activation of CB1 and CB2 cannabinoid receptors in rat brain and human tonsils. *Advances in Experimental Medicine and Biology*, 469, pp. 527-533
- BERGSTEN, E. et al., 2001. PDGF-D is a specific, protease-activated ligand for the PDGF beta-receptor. *Nature cell biology*, 3(5), pp. 512-516

- BEST, P. et al., 1999. Apoptosis: Basic Concepts and Implications in Coronary Artery Disease. *Arteriosclerosis, Thrombosis and Vascular Biology*, 19, pp. 14-22
- BHARGAVA, B. et al., 2003. New approaches to preventing restenosis. *British Medical Journal*, 327, pp. 274-279
- BIDAUT-RUSSELL, M., DEVANE, W. and HOWLETT, A., 1990. Cannabinoid receptors and modulation of cyclic AMP accumulation in the rat brain. *Journal of Neurochemistry*, 55(1), pp. 21-26
- BIFULCO, M. et al., 2006. Cannabinoids and cancer: pros and cons of an antitumour strategy. *British journal of Pharmacology*, 148, pp. 123-135
- BIFULCO, M. et al., 2001. Control by the endogenous cannabinoid system of ras oncogene-dependent growth. *FASEB*, 15(14), pp. 2745-2747
- BISOGNO, T. et al., 1999. Brain Regional Distribution of Endocannabinoids: Implications for Their Biosynthesis and Biological Function. *Biochemical and biophysical Research Communications*, 256, pp. 377
- BISOGNO, T., LIGRESTI, A. and DI MARZO, V., 2005. The endocannabinoid signaling system: biochemical aspects. *Pharmacology, Biochemistry and behavior*, 81, pp. 224-238
- BLANKMAN, J., SIMON, G. and CRAVATT, B., 2007. A comprehensive profile of brain enzymes that hydrolyze the endocannabinoid 2-arachidonoylglycerol. *Chemical Biology*, 14(12), pp. 1347-1356
- BLAZQUEZ, C. et al., 2003. Inhibition of tumor angiogenesis by cannabinoids. *FASEB*, 17, pp. 529-531
- BOBIK, A., 2006. Transforming Growth Factor-B and Vascular Disorders. *Arteriosclerosis, Thrombosis and Vascular Biology*, 26, pp. 1712-1720
- BORNFELDT, K. et al., 1994. Insulin-like growth factor-I and platelet-derived growth factor-BB induce directed migration of human arterial smooth muscle cells via signaling

pathways that are distinct from those of proliferation. *Journal of Clinical Investigation*, 93(3), pp. 1266-1274

BORNFELDT, K., 1996. Intracellular signaling in arterial smooth muscle migration versus proliferation. *Trends in cardiovascular medicine*, 6, pp. 143-151

BORNHEIM, L. et al., 1995. Microsomal cytochrome P450-mediated liver and brain anandamide metabolism. *Biochemical Pharmacology*, 50(5), pp. 677-686

BOSIER, B., LAMBERT, D. and HERMANS, E., 2008. Reciprocal influences of CB₁ cannabinoid receptor agonists on ERK and JNK signaling in N1E-115 cells. *FEBS letters*, 582, pp. 3861-3867

BOUABOULA, M. et al., 1996. Signaling pathway associated with stimulation of CB₂ peripheral cannabinoid receptor. Involvement of both mitogen-activated protein kinase and induction of Krox-24 expression. *European Journal of Biochemistry*, 237, pp. 704-711

BOUABOULA, M. et al., 1995. Activation of mitogen activated protein kinases by stimulation of the central cannabinoid receptor CB₁. *Biochemical Journal*, 312, pp. 637-641

BOUANOULA, M. et al., 2005. Anandamide induced PPAR gamma transcription activation and 3T3-L1 pre-adipocyte differentiation. *European Journal of Pharmacology*, 517, pp. 174-181

BRAUN, M. et al., 1999. Cellular adhesion molecules on vascular smooth muscle cells. *Cardiovascular Research*, 41(2), pp. 395-401

BROWN, A., 2007. Novel cannabinoid receptors. *British journal of Pharmacology*, 152, pp. 567-575

BROWN, D. and LONDON, E., 2000. Structure and Function of Sphingolipid- and Cholesterol-rich Membrane Rafts. *The journal of biological chemistry*, 275(23), pp. 17221-17224

- BUI, Q., PREMPEH, M. and WILENSKY, R., 2009. Atherosclerotic plaque development. *The international Journal of Biochemistry and Cell Biology*, 41, pp. 2109-2113
- CAI, Q., LANTING, L. and NATARAJAN, R., 2004. Interaction of monocytes with vascular smooth muscle cells regulates monocyte survival and differentiation through distinct pathways. *Arteriosclerosis, Thrombosis and Vascular Biology*, 24, pp. 2263-2270
- CASSCELLS, W., 1992. Migration of smooth muscle and endothelial cells. Critical events in restenosis. *Circulation Research*, 86(3), pp. 723-729
- CASSCELLS, W., ENGLER, D. and WILLERSON, J.T., 1994. Mechanisms of Restenosis. *Texas Heart Institute Journal*, 21, pp. 68-77
- CHANG, Y., LEE, S. and LIN, W., 2001. Effects of cannabinoids on LPS-stimulated inflammatory mediator release from macrophages: involvement of eicosanoids. *Journal of Cellular Biochemistry*, 81(4), pp. 715-723
- CHRISTEN, T. et al., 2001. Mechanisms of neointima formation and remodeling in the porcine coronary artery. *Circulation*, 106(6), pp. 882-888
- CHRISTENSEN, R. et al., 2007. Efficacy and safety of the weight-loss drug rimonabant: a meta-analysis of randomised trials. *Lancet*, 370(9600), pp. 1706-1713
- CLOWES, A.'R., MA. and CLOWES, M., 1983. Mechanisms of stenosis after arterial injury. *Laboratory Investigation*, 49, pp. 208-215
- CLOWES, A. et al., 1990. Smooth muscle cells express urokinase during mitogenesis and tissue-type plasminogen activator during migration in injured rat carotid artery. *Circulation Research*, 67(1), pp. 61-67
- COSTA, B. et al., 2005. Effect of the cannabinoid CB1 receptor antagonist, SR141716, on nociceptive response and nerve demyelination in rodents with chronic constriction injury of the sciatic nerve. *Pain*, 116, pp. 62-61

COSTA, M. and SIMON, D., 2005. Molecular Basis of Restenosis and Drug Eluting Stents. *Circulation*, 111, pp. 2257-2273

CRAIB, S. et al., 2001. A possible role of lipoxygenase in the activation of vanilloid receptors by anandamide in the guinea-pig bronchus. *British journal of Pharmacology*, 134, pp. 30-37

CRAVATT, B. et al., 1996. Molecular characterization of an enzyme that degrades neuromodulatory fatty-acid amides. *Nature*, 384(6604), pp. 83-87

CRAVATT, B. et al., 2001. Supersensitivity to anandamide and enhanced endogenous cannabinoid signaling in mice lacking fatty acid amide hydrolase. *PNAS*, 98, pp. 9371-9376

CROXFORD, J., 2005. Cannabinoids and the immune system: potential for the treatment of inflammatory diseases? *Journal of Neuroimmunology*, 166, pp. 3-18

Danish Myograph Technology (2003) Dual Wire Myography System Model 510 A. User manual Version 2. Aarhus, Denmark.

DARTSCH, P., ISCHINGER, T. and BETZ, E., 1990. Differential effect of PhotofrinII on growth of human smooth muscle cells from nonatherosclerotic arteries and atheromatous plaques in vitro. *Arteriosclerosis, Thrombosis and Vascular Biology*, 10, pp. 616-624

DAUGHERTY, A. et al., 2005. Cytokine regulation of macrophage functions in atherogenesis. *Journal of Lipid Research*, 46, pp. 1812-1822

DAVIGNON, J. and GRANZ, P., 2004. Role of Endothelial Dysfunction in Atherosclerosis. *Circulation*, 109, pp. III-27-III-32

DAY, T. et al., 2001. Role of fatty acid amide hydrolase in the transport of the endogenous cannabinoid anandamide. *Molecular Pharmacology*, 59, pp. 1369-1375

DE MARTIN, R. et al., 2000. The transcription factor NF-kappa B and the regulation of vascular cell function. *Arteriosclerosis, Thrombosis and Vascular Biology*, 20(11), pp. 83-8

- DE PETROCELLIS, L., DAVIS, J. and DI MARZO, V., 2001. Palmitoylethanolamide enhances anandamide stimulation of human vanilloid VR1 receptors. *FEBS letters*, 506(3), pp. 253-256
- DE PETROCELLIS, L. et al., 1998. The endogenous cannabinoid anandamide inhibits human breast cancer cell proliferation. *PNAS*, 95(14), pp. 8375-8380
- DECHERT, M., HOLDER, J. and GERTHOFFER, W., 2001. p21-activated kinase 1 participates in tracheal smooth muscle migration by signaling to p38 MAPK. *American Journal of Cell Physiology*, 281, pp. 123-132
- DEMUTH, D. and MOLLEMAN, A., 2006. Cannabinoid Signalling. *Life Sciences*, 78, pp. 549-563
- DEROCQ, J. et al., 1998. The endogenous cannabinoid anandamide is a lipid messenger activating cell growth via a cannabinoid receptor-independent pathway in hematopoietic cell lines. *FEBS letters*, 425, pp. 419-425
- DEUTSCH, D. et al., 2001. The cellular uptake of anandamide is coupled to its breakdown by fatty-acid amide hydrolase. *Journal of Biological Chemistry*, 276(10), pp. 6967-6973
- DEVANE, W. et al., 1992. Isolation and structure of a brain constituent that binds to the cannabinoid receptor. *Science*, 258(5090), pp. 1946-1949
- DI MARZO, V., 2008. Targeting the endocannabinoid system: to enhance or reduce?. *Nature Reviews Drug Discovery*, 7(5), pp. 438-455
- DI MARZO, V., BISOGNO, T. and DE PETROCELLIS, L., 2001. Anandamide: some like it hot. *Trends in Pharmacological Sciences*, 22, pp. 346-349
- DI MARZO, V., BLUMBERG, P. and SZALLASI, A., 2002. Endovanilloid signaling in pain. *Current opinion in neurobiology*, 12(4), pp. 372-379
- DI MARZO, V. et al., 1994. Formation and inactivation of endogenous cannabinoid anandamide in central neurons. *Nature*, 372(6507), pp. 686-691

- DI MARZO, V., 1999. Biosynthesis and inactivation of endocannabinoids: Relevance to their proposed role as neuromodulators. *Life Sciences*, 65, pp. 645-655
- DINH, T., FREUND, T. and PIOMELLI, D., 2002. A role for monoglyceride lipase in 2-arachidonoylglycerol inactivation. *Chemistry and Physics of Lipids*, 121, pp. 149-158
- DOL-GLEIZES, F. et al., 2009. Rimonabant, a selective cannabinoid CB1 receptor antagonist, inhibits atherosclerosis in LDL receptor-deficient mice. *Arteriosclerosis, Thrombosis and Vascular Biology*, 29, pp. 12-18
- DROZDOFF, V. and PLEDGER, W., 1991. Cellular response to platelet-derived growth factor (PDGF)-AB after down regulation of PDGF α receptors/. *The journal of biological chemistry*, 266, pp. 17165-17172
- DUBEY, R., JACKSON, E. and LUSCHER, T., 1995. Nitric Oxide Inhibits Angiotensin II-induced Migration of Rat Aortic Smooth Muscle Cell. *Journal of Clinical Investigation*, 96, pp. 141-149
- DUBOIS, R. et al., 1998. Cyclooxygenase in biology and disease. *FASEB*, 12(12), pp. 1063-1073
- EBISUYA, M., KONDOH, K. and NISHIDA, E., 2005. The duration, magnitude and compartmentalization of ERK MAP kinase activity: mechanisms for providing signaling specificity. *Journal of Cell Science*, 118, pp. 2997-3002
- ELLIS, E., MOORE, S. and WILLOUGHBY, K., 1995. Anandamide and delta 9-THC dilation of cerebral arterioles is blocked by indomethacin. *American Journal of Physiology*, 269, pp. H1859-H1864
- EPSTEIN, H. et al., 2008. Predicting in vivo efficacy of potential restenosis therapies by cell culture studies: species-dependent susceptibility of vascular smooth muscle cells. *The open Cardiovascular Medicine Journal*, 2, pp. 60-69
- FAXON, D. et al., 1982. Acute effects of transluminal angioplasty in three experimental models of atherosclerosis. *Arteriosclerosis, Thrombosis and Vascular Biology*, 2, pp. 125-133

- FAYON, M. et al., 2006. Increased secretion of leukemia inhibitory factor by immature airway smooth muscle cells enhances intracellular signaling and airway contractility. *American Journal of Physiology, Lung Cellular and Molecular Physiology*, 291(2), pp. L244-L251
- FEGLEY, D. et al., 2004. Anandamide transport is independent of fatty-acid amide hydrolase activity and is blocked by the hydrolysis-resistant inhibitor AM1172. *PNAS*, 101(23), pp. 8756-8761
- FELDMAN, L. et al., 2000. Interleukin-10 inhibits intimal hyperplasia after angioplasty or stent implantation in hypercholesterolemic rabbits. *Circulation*, 101(8), pp. 908-916
- FERNS, G. et al., 1991. Inhibition of neointimal smooth muscle accumulation after angioplasty by an antibody to PDGF.. *Science*, 253, pp. 1129-1132
- FERNS, G.A. and AVADES, T.Y., 2000. The mechanisms of coronary restenosis: insights from experimental models. *International Journal of Experimental Pathology*, 81, pp. 63-88
- FIÉVET, C., FRUCHART, J. and STAELS, B., 2006. PPAR alpha and PPAR gamma dual agonists for the treatment of type 2 diabetes and the metabolic syndrome. *Current opinion in Pharmacology*, 6(6), pp. 606-614
- FIMIANI, C. et al., 1999. Morphine and anandamide stimulate intracellular calcium transients in human arterial endothelial cells: coupling to nitric oxide release. *Cell signaling*, 11(3), pp. 189-193
- FINGERLE, J. et al., 1989. Role of platelets in smooth muscle cell proliferation and migration after vascular injury in rat carotid artery. *PNAS*, 86(21), pp. 8412-8416
- FLEENOR, B. and BOWLES, D., 2009. Negligible contribution of coronary adventitial fibroblasts to neointimal formation following balloon angioplasty in swine. *American Journal of Heart and Circulatory Physiology*, 296(5), pp. 1532-1539
- FORCE, T. and BONVENTRE, J., 1998. Growth Factors and Mitogen-Activated Protein Kinase. *Hypertension*, 31, pp. 152-161

- FORD, W.R. et al., 2002. Evidence of a novel site mediating anandamide-induced negative inotropic and coronary vasodilator responses in rat isolated hearts. *British journal of Pharmacology*, 135, pp. 1191-1198
- FOWLER, C.J., 2007. The contribution of cyclooxygenase-2 to endocannabinoid metabolism and action. *British journal of Pharmacology*, , pp. 1-8
- FREYHAUS, H. et al., 2006. Novel Nox inhibitor VAS2870 attenuates PDGF-dependent smooth muscle cell chemotaxis, but not proliferation. *Cardiovascular Research*, 71(2), pp. 331-341
- FURCHGOTT, R., 1983. Role of endothelium in responses of vascular smooth muscle. *Circulation Research*, 53(5), pp. 557-573
- FURUKAWA, Y. et al., 1999. Anti-monocyte chemoattractant protein-1/monocyte chemotactic and activating factor antibody inhibits neointimal hyperplasia in injured rat carotid arteries. *Circulation Research*, 84(3), pp. 306-314
- GALVE-ROPERH, I. et al., 2002. Mechanism of extracellular signal-regulated kinase activation by the CB(1) cannabinoid receptor. *Molecular Pharmacology*, 62(6), pp. 1385-1392
- GALVE-ROPERH, I. et al., 2000. Anti-tumoral action of cannabinoids: Involvement of sustained ceramide accumulation and extracellular signal-regulated kinase activation. *Nature Medicine*, 6, pp. 313-319
- GARDINER, S. et al., 2002. Complex regional haemodynamic effects of anandamide in conscious rats. *British journal of Pharmacology*, 135(8), pp. 1889-1896
- GAUTHIER, K. et al., 2005. Endothelium-derived 2-arachidonylglycerol: an intermediate in vasodilatory eicosanoid release in bovine coronary arteries. *American Journal of Heart and Circulatory Physiology*, 288(3), pp. H1344-H1351
- GERTHOFFER, W., 2007. Mechanisms of vascular smooth muscle cell migration. *circulation Research*, 100, pp. 607-621

- GERTHOFFER, W., 2008. Migration of airway smooth muscle cells. *Proceedings of the American Thoracic Society*, 5, pp. 97-105
- GIANG, D. and CRAVATT, B., 1997. Molecular characterization of human and mouse fatty acid amide hydrolases. *PNAS*, 94(6), pp. 2238-2242
- GLASER, S. et al., 2003. Evidence against the presence of an anandamide transporter. *PNAS*, 100, pp. 4269-4274
- GLASS, M. and FELDER, C., 1997. Concurrent stimulation of cannabinoid CB1 and dopamine D2 receptors augments cAMP accumulation in striatal neurons: evidence for a Gs linkage to the CB1 receptor. *Journal of Neuroscience*, 17(14), pp. 5327-5333
- GOETZE, S. et al., 1999. TNF-alpha-induced migration of vascular smooth muscle cells is MAPK dependent. *Hypertension*, 33, pp. 183-189
- GÓMEZ DEL PULGAR, T., VELASCO, G. and GUZMÁN, M., 2000. The CB1 cannabinoid receptor is coupled to the activation of protein kinase B/Akt. *Biochemical Journal*, 347, pp. 369-373
- GÓMEZ DEL PULGAR, T. et al., 2002. De novo-synthesized ceramide is involved in cannabinoid-induced apoptosis. *The Biochemical Journal*, 363(1), pp. 183-188
- GONSIOREK, W. et al., 2000. Endocannabinoid 2-arachidonoyl glycerol is a full agonist through human type 2 cannabinoid receptor: antagonism by anandamide. *Molecular Pharmacology*, 57(5), pp. 1045-1050
- GRAINGER, J. and BOACHIE-ANSAH, G., 2001. Anandamide-induced relaxation of sheep coronary arteries: the role of the vascular endothelium, arachidonic acid metabolites and potassium channels. *British journal of Pharmacology*, 134(5), pp. 1003-1012
- GRANT, M. et al., 1994. Localisation of insulin-like growth factor I and inhibition of coronary smooth muscle cell growth by somatostatin analogues in human coronary smooth muscle cells. A potential treatment for restenosis? *Circulation*, 89, pp. 1511-1517

- GREENHOUGH, A. et al., 2007. The cannabinoid delta(9)-tetrahydrocannabinol inhibits RAS-MAPK and PI3K-AKT survival signaling and induces BAD-mediated apoptosis in colorectal cancer cells. *International Journal of Cancer*, 121(10), pp. 2172-2180
- GRIENGLING, K. et al., 2000. Modulation of Protein Kinase Activity and Gene Expression by Reactive Oxygen Species and Their Role in Vascular Physiology and Pathophysiology . *Arteriosclerosis, Thrombosis and Vascular Biology*, 20, pp. 2175-2183
- GRIMALDI, C. et al., 2006. Anandamide inhibits adhesion and migration of breast cancer cells. *Experimental Cell Research*, 312(4), pp. 363-373
- GUYTON, J. et al., 1980. Inhibition of rat arterial smooth muscle cell proliferation by heparin. In vivo studies with anticoagulant and nonanticoagulant heparin. *Circulation Research*, 46, pp. 625-634
- GUZMÁN, M. and SÁNCHEZ, C., 1999. Effects of cannabinoids on energy metabolism. *Life Sciences*, 65, pp. 657-664
- GUZMAN, M., SANCHEZ, C. and GALVE-ROPERH, I., 2002. Cannabinoids and cell fate. *Pharmacology and Therapeutics*, 95, pp. 175-184
- HADOKE, P. et al., 1995. Characterization of the morphological and functional alterations in rabbit subclavian artery subjected to balloon angioplasty. *Coronary artery Disease*, 6(5), pp. 403-415
- HAGA, J., LI, Y. and CHIEN, S., 2007. Molecular basis of the effects of mechanical stretch on vascular smooth muscle cells. *Journal of Biomechanics*, 40, pp. 947-960
- HAMADA, N. et al., 2009. Tacrolimus-eluting stent inhibits neointimal hyperplasia via calcineurin/NFAT signaling in porcine coronary artery model. *Atherosclerosis*, 1016, pp. In Press
- HANSSON, G. and LIBBY, P., 2006. The immune response in atherosclerosis: A double-edged sword. *Nature Reviews Immunology*, 6, pp. 508-519

- HANUS, L. et al., 2001. 2-Arachidonyl glyceryl ether, an endogenous agonist of the cannabinoid CB1 receptor. *PNAS*, 98(7), pp. 3662-3665
- HAO, H. and GABBIANI, G., 2003. Arterial Smooth Muscle Heterogeneity: Implications for Atherosclerosis and Restenosis Development. *Arteriosclerosis, Thrombosis and Vascular Biology*, 23, pp. 1510-1520
- HARRIS, D. et al., 2002. Characterization of vasorelaxant responses to anandamide in the rat mesenteric arterial bed. *The Journal of Physiology*, 539.3, pp. 893-902
- HART, C. et al., 1988. Two classes of PDGF receptor recognize different isoforms of PDGF. *Science*, 240, pp. 1529-1531
- HART, S., FISCHER, O. and ULLRICH, A., 2004. Cannabinoids Induce Cancer cell proliferation via tumor necrosis factor alpha converting enzyme (TACE/ADAM17)-Mediated Transactivation of the Epidermal Growth Factor Receptor. *Cancer Research*, 64, pp. 1943-1950
- HATANO, N. et al., 2003. Essential role for ERK2 mitogen-activated protein kinase in placental development.. *Genes to Cells*, 8, pp. 847-856
- HAUCK, C., HSIA, D. and SCHLAEPFER, D., 2000. Focal adhesion kinase facilitates platelet derived growth factor-BB stimulated ERK2 activation required for chemotaxis migration of vascular smooth muscle cells. *The Journal of biological chemistry*, 275, pp. 41092-41099
- HEDIN, U. et al., 1988. Diverse Effects of Fibronectin and Laminin on Phenotypic Properties of Cultured Arterial Smooth Muscle Cells. *Journal of Cell Biology*, 107, pp. 307-319
- HELDIN, C. and WESTERMARK, B., 1999. Mechanism of Action and In Vivo Role of Platelet-Derived Growth Factor. *Physiological Reviews*, 79(4), pp. 1283-1316
- HENSTRIDGE, C. et al., 2009. The GPR55 ligand L-alpha-lysophosphatidylinositol promotes RhoA-dependent Ca²⁺ signaling and NFAT activation. *FASEB*, 23, pp. 183-193

- HERRERA, B. et al., 2006. The CB2 cannabinoid receptor signals apoptosis via ceramide-dependent activation of the mitochondrial intrinsic pathway. *Experimental cell research*, 312, pp. 2121-2131
- HICKEY, M. et al., 1997. Inducible nitric oxide synthase-deficient mice have enhanced leukocyte- endothelium interactions in endotoxemia. *FASEB*, 11, pp. 955-964
- HIGASHI, Y. et al., 2009. Endothelial Function and Oxidative Stress in Cardiovascular Diseases. *Circulation Journal*, 73, pp. 411-418
- HILLARD, C. et al., 1999. Synthesis and characterization of potent and selective agonists of the neuronal cannabinoid receptor (CB1). *Journal of Pharmacology and Experimental Therapeutics*, 289(3), pp. 1427-1433
- HILLARD, C., 2000. Endocannabinoids and Vascular Function. *Journal of Pharmacology and Experimental Therapeutics*, 294, pp. 27-32
- HILLARD, C. and JARRAHIAN, A., 2000. The movement of N-arachidonylethanolamine (anandamide) across cellular membranes. *Chemistry and Physics of Lipids*, 108, pp. 123-134
- HILLARD, C. and JARRAHIAN, A., 2003. Cellular accumulation of anandamide: consensus and controversy. *British Journal of Pharmacology*, 140, pp. 802-808
- HO, W. and HILEY, R., 2004. Vasorelaxant activities of the putative endocannabinoid virodhamine in rat isolated small mesenteric artery. *Journal of Pharmacy and Pharmacology*, 56, pp. 869-875
- HOFMA, S. et al., 2006. Indication of long-term endothelial dysfunction after sirolimus-eluting stent implantation. *European Heart Journal*, 27(2), pp. 166-170
- HOGESTATT, E. and ZYGMUNT, P., 2002. Cardiovascular Pharmacology of Anandamide. *Prostaglandins, Leukotrienes and Essential Fatty Acids*, 66, pp. 343-351
- HOLLAND, M. et al., 1999. Cannabinoid CB1 receptors fail to cause relaxation, but couple via Gi/Go to the inhibition of adenylate cyclase in carotid artery smooth muscle. *British journal of Pharmacology*, 128, pp. 597-604

- HOLT, C. et al., 1994. Release of platelet derived growth factor in serum-free organ culture of human coronary artery. *Cardiovascular Research*, 28, pp. 1170-1175
- HOLT, C. et al., 1992. Intimal proliferation in an organ culture of human internal mammary artery. *Cardiovascular Research*, 26, pp. 1189-1194
- HORVATH, C. et al., 2002. Targeting CCR2 or CD18 inhibits experimental in-stent restenosis in primates: inhibitory potential depends on type of injury and leukocytes targeted. *Circulation Research*, 90(4), pp. 488-494
- HOWLETT, A. et al., 2002. International Union of Pharmacology. XXVII Classification of cannabinoid Receptors. *Pharmacological reviews*, (54), pp. 161-202
- HOWLETT, A. and FLEMING, R., 1984. Cannabinoid Inhibition of Adenylate Cyclase. *Molecular Pharmacology*, 26, pp. 532-538
- HOWLETT, A., 1985a. Cannabinoid Inhibition of Adenylate Cyclase Biochemistry of the response in neuroblastoma Cell Membranes. *Molecular Pharmacology*, 27, pp. 429-436
- HOWLETT, A., QUALY, J. and KHACHATRIAN, L., 1985b. Involvement of Gi in the inhibition of Adenylate Cyclase by cannabimimetic drugs. *Molecular pharmacology*, 29, pp. 307-313
- HUANG, C., JACOBSON, K. and SCHALLER, M., 2004. MAP kinases and cell migration. *Journal of cell science*, 117, pp. 4619-4628
- HUGHES, A. et al., 1996. Platelet derived growth factor (PDGF): Actions and mechanisms in vascular smooth muscle. *Gen. Pharmac*, 27, pp. 1079-1089
- HUI, D., 2008. Intimal Hyperplasia in Murine Models. *Current Drug Targets*, 9, pp. 251-260
- HUO, Y., HAFEZI-MOGHADAM, A. and LEY, K., 2000. Role of vascular cell adhesion molecule-1 and fibronectin connecting segment-1 in monocyte rolling and adhesion on early atherosclerotic lesions. *Circulation Research*, 87, pp. 153-159

- HWANG, S. et al., 2000. Direct activation of capsaicin receptors by products of lipoxygenases: endogenous capsaicin-like substances. *PNAS*, 97(11), pp. 6155-6160
- I, M. et al., 2006. Changes in endocannabinoid and palmitoylethanolamide levels in eye tissue of patients with diabetic retinopathy and age-related macular degeneration. *Prostaglandins, Leukotrienes and Essential Fatty Acids*, 75, pp. 413-418
- IKARI, Y. et al., 1999. Neonatal Intima Formation in the Human Coronary Artery. *Arteriosclerosis, Thrombosis, and Vascular Biology*, 19, pp. 2036-2040
- IKEDA, U. et al., 1990. Mitogenic action of interleukin-1B on vascular smooth muscle cells mediated by PDGF. *Atherosclerosis*, 84, pp. 183-188
- INOUE, T. and NODE, K., 2009. Molecular Basis of Restenosis and Novel Issues of Drug-Eluting Stents. *Circulation Journal*, 73, pp. 615-621
- INOUE, T. et al., 2003. Stent-Induced Expression and Activation of the Leukocyte Integrin Mac-1 Is Associated With Neointimal Thickening and Restenosis. *Circulation*, 107, pp. 1757
- ISHIDA, A. et al., 1997. Induction of the Cyclin-dependent Kinase Inhibitor p21 by Nitric oxide-generating Vasodilator in Vascular Smooth Muscle Cells. *The journal of Biological Chemistry*, 272, pp. 10050-10057
- JÁRAI, Z. et al., 1999. Cannabinoid-induced mesenteric vasodilation through an endothelial site distinct from CB1 or CB2 receptors. *PNAS*, 96(24), pp. 14136-14141
- JARRAHIAN, A. et al., 2000. Structure—Activity Relationships Among N-Arachidonylethanolamine (Anandamide) Head Group Analogues for the Anandamide Transporter. *Journal of Neurochemistry*, 74(6), pp. 2597-2606
- JAWIEN, A. et al., 1992. Platelet-derived growth factor promotes smooth muscle migration and intimal thickening in a rat model of balloon angioplasty. *Journal of Clinical Investigation*, 89(2), pp. 507-511

JHAVERI, M., RICHARDSON, D. and CHAPMAN, V., 2007. Endocannabinoid metabolism and uptake: novel targets for neuropathic and inflammatory pain. *British journal of Pharmacology*, 152(5), pp. 624-632

JOHNS, D.G. et al., 2007. The novel endocannabinoid receptor GPR55 is not activated by atypical cannabinoids but does not mediate their vasodilator effects. *British journal of Pharmacology*, 152, pp. 825-831

JONER, M. et al., 2006. Pathology of drug-eluting stents in humans: delayed healing and late thrombotic risk. *Journal of the American College of Cardiology*, 48(1), pp. 193-202

JORDÀ, M. et al., 2002. Hematopoietic cells expressing the peripheral cannabinoid receptor migrate in response to the endocannabinoid 2-arachidonoylglycerol. *Blood*, 99(8), pp. 2786-2793

JOSEPH, J. et al., 2004. Anandamide is an endogenous inhibitor for the migration of tumor cells and T lymphocytes. *Cancer, Immunology and Immunotherapy*, 53(8), pp. 723-728

KAARTINEN, M., PENTTILÄ, A. and KOVANEN, P., 1996. Mast cells accompany microvessels in human coronary atheromas: implications for intimal neovascularization and hemorrhage. *Atherosclerosis*, 123, pp. 123-131

KAGOTA, S. et al., 2001. 2-Arachidonoylglycerol, a candidate of endothelium-derived hyperpolarizing factor. *European Journal of Pharmacology*, 415, pp. 233-238

KANTOR, B. et al., 1999. The experimental animal models for assessing treatment of restenosis. *Cardiovascular Radiation Medicine*, 1, pp. 48-54

KARSHOVSKA, E. et al., 2007. Expression of HIF-1alpha in injured arteries controls SDF-1alpha mediated neointima formation in apolipoprotein E deficient mice. *Arteriosclerosis, Thrombosis and Vascular Biology*, 27(12), pp. 2540-4547

KENNEDY, S. et al., 2000. Correlation of leukocyte adhesiveness, adhesion molecule expression and leukocyte- induced contraction following balloon angioplasty. *British Journal of Pharmacology*, 130, pp. 95-103

KHAN, B. et al., 1995. Modified low density lipoprotein and its constituents augment cytokine-activated vascular cell adhesion molecule-1 gene expression in human vascular endothelial cells. *Journal of Clinical Investigation*, 95, pp. 1262-1270

KIBBE, M., BILLIAR, T. and TZENG, E., 1999. Inducible nitric oxide synthase and vascular injury. *Cardiovascular Research*, 43(3), pp. 650-657

KIPSHIDZE, N. et al., 2004. Role of the Endothelium in Modulating Neointimal Formation. *Journal of the American College of Cardiology*, 44, pp. 733

KIRKILES-SMITH, N. et al., 2004. IL-11 protects human microvascular endothelium from balloon injury in vivo by induction of survivin expression. *Journal of Immunology*, 172(3), pp. 1391-1396

KISHIMOTO, S. et al., 2005. Endogenous cannabinoid receptor ligand induces the migration of human natural killer cells. *Journal of Biochemistry*, 137(2), pp. 217-223

KISHIMOTO, S. et al., 2003. 2-Arachidonoylglycerol Induces the Migration of HL-60 Cells Differentiated into Macrophage-like Cells and Human Peripheral Blood Monocytes through the Cannabinoid CB2 Receptor-dependent Mechanism *Journal of Biological Chemistry*, 278, pp. 24469-24475

KLEIN, T. et al., 2000. The cannabinoid system and cytokine network. *Proc Soc Exp Biol Med*, 255(1), pp. 1-8

KLEIN, T., NEWTON, C. and FRIEDMAN, H., 1998. Cannabinoid receptors and immunity. *Immunology Today*, 19(8), pp. 373-381

KLEIN, T. et al., 2003. The cannabinoid system and immune modulation. *Journal of Leukocyte Biology*, 74, pp. 486-496

- KOBAYASHI, Y. et al., 2001. Activation by 2-arachidonoylglycerol, an endogenous cannabinoid receptor ligand, of p42/44 mitogen-activated protein kinase in HL-60 cells. *Journal of biochemistry*, 129, pp. 665-669
- KOLCH, W., 2005. Coordinating ERK/MAPK signaling through scaffolds and inhibitors. *Nature Reviews*, 6, pp. 827-837
- KOLESNICK, R. and KRÖNKE, M., 1998. Regulation of ceramide production and apoptosis. *Annual Review of Physiology*, 60, pp. 643-665
- KOLODIE, F. et al., 2003. Intraplaque hemorrhage and progression of coronary atheroma. *New England Journal of Medicine*, 349, pp. 2316-2325
- KOZAK, K.R. et al., 2003. Amino acid determinants in cyclooxygenase-2 oxygenation of the endocannabinoid anandamide. *Biochemistry*, 42, pp. 9041-9049
- KOZAK, K. et al., 2002. 15-Lipoxygenase metabolism of 2-arachidonoylglycerol. Generation of a peroxisome proliferator-activated receptor alpha agonist. *The journal of biological chemistry*, 277(26), pp. 23278-23286
- KOZAK, K. et al., 2001. Amino acid determinants in cyclooxygenase-2 oxygenation of the endocannabinoid 2-arachidonoylglycerol. *Journal of Biological Chemistry*, 276(32), pp. 30072-30077
- KOZAK, K., ROWLINSON, S. and MARNETT, L., 2000. Oxygenation of the endocannabinoid, 2-arachidonoylglycerol, to glyceryl prostaglandins by cyclooxygenase-2. *Journal of Biological Chemistry*, 275(43), pp. 33744-33749
- KOZAK, K. and MARNETT, L., 2002. Oxidative metabolism of endocannabinoids. *Prostaglandins, Leukotrienes and Essential Fatty Acids*, 66(2&3), pp. 211-220
- KRAFT, B. and KRESS, H., 2005. Indirect CB₂ receptor and mediator-dependent stimulation of human whole-blood neutrophils by exogenous and endogenous cannabinoids. *Journal of Pharmacology and Experimental Therapeutics*, 315(2), pp. 641-647

- KRAFT, B., WINTERSBERGER, W. and KRESS, H., 2004. Cannabinoid receptor-independent suppression of the superoxide generation of human neutrophils (PMN) by CP55 940, but not by anandamide. *Life Sciences*, 75(8), pp. 969-977
- KROHN, R. et al., 2007. γ -box binding protein-1 controls CC chemokine ligand-5 (CCL5) expression in smooth muscle cells and contributes to neointima formation in atherosclerosis-prone mice. *Circulation*, 116(16), pp. 1812-1820
- KWOLEK, G. et al., 2005. Central and peripheral components of the pressor effect of anandamide in urethane-anaesthetized rats. *British journal of Pharmacology*, 145(5), pp. 567-575
- LAKE, K. et al., 1997. Cannabinoid-induced hypotension and bradycardia in rats mediated by CB1-like cannabinoid receptors. *Journal of Pharmacology and Experimental Therapeutics*, 281(3), pp. 1030-1037
- LAUCKNER, J. et al., 2008. GPR55 is a cannabinoid receptor that increases intracellular calcium and inhibits M current. *PNAS*, 105(7), pp. 2699-2704
- LAWRENCE, R., DUNN, W. and WILSON, V., 1998. Endothelium-dependent relaxation in response to ethanol in the porcine isolated pulmonary artery. *The Journal of Pharmacy and Pharmacology*, 50(8), pp. 885-890
- LEDENT, C. et al., 1999. Unresponsiveness to cannabinoids and reduced addictive effects of opiates in CB1 receptor knockout mice. *Science*, 283(5400), pp. 401-404
- LEE, P., GIBBONS, G. and DZAU, V., 1993. Cellular and molecular mechanisms of coronary artery restenosis. *Coronary Artery Disease*, 4(3), pp. 254-259
- LEMOS, P. et al., 2003. Coronary restenosis after sirolimus-eluting stent implantation: morphological description and mechanistic analysis from a consecutive series of cases. *Circulation*, 108(3), pp. 257-260
- LÉPICIER, P. et al., 2003. Endocannabinoids protect the rat isolated heart against ischaemia. *British journal of Pharmacology*, 139(4), pp. 805-815

- LEUNG, D. et al., 2006. Inactivation of N-acyl phosphatidylethanolamine phospholipase D reveals multiple mechanisms for the biosynthesis of endocannabinoids. *Biochemistry*, 45(15), pp. 4720-4726
- LEWIS, S., 2009. Prevention and Treatment of Atherosclerosis: A Practitioner's Guide for 2008. *The American Journal of Medicine*, 122, pp. S38-S50
- LI, S. et al., 2003. Signal transduction in matrix contraction and the migration of vascular smooth muscle cells in three-dimensional matrix.. *Journal of Vascular Research*, 40, pp. 378-388
- LI, G. et al., 2000. Direct in vivo evidence demonstrating neointimal migration of adventitial fibroblasts after balloon injury of rat carotid arteries. *Circulation*, 101(12), pp. 1362-1365
- LI, Q. et al., Overexpression of Insulin-like Growth Factor-1 in Mice Protects from Myocyte Death after Infarction, Attenuating Ventricular Dilation, Wall Stress, and Cardiac Hypertrophy. *Journal of Clinical Investigation*, 100, pp. 1991-1999
- LI, X. et al., 2000. PDGF-C is a new protease-activated ligand for the PDGF alpha-receptor. *Nature cell biology*, 2, pp. 302-309
- LIBBY, P. et al., 1988. Production of platelet-derived growth factor-like mitogen by smooth-muscle cells from human atheroma. *New England Journal of Medicine*, 318(23), pp. 1493-1498
- LIGRESTI, A. et al., 2004. Further evidence for the existence of a specific process for the membrane transport of anandamide. *Biochemical Journal*, 380, pp. 265-272
- LINDNER, V., MAJACK, R. and REIDY, M., 1990. Basic fibroblast growth factor stimulates endothelial regrowth and proliferation in denuded arteries. *Journal of Clinical Investigation*, 85(6), pp. 2004-2008
- LINDNER, V. and REIDY, M., 1991. Proliferation of smooth muscle cells after vascular injury is inhibited by an antibody against basic fibroblast growth factor. *PNAS*, 88(9), pp. 3739-3743

- LIU, J. et al., 2008. Multiple pathways involved in the biosynthesis of anandamide. *Neuropharmacology*, 54(1), pp. 1-7
- LIU, J. et al., 2000. Functional CB1 cannabinoid receptors in human vascular endothelial cells. *Biochemical Journal*, 346, pp. 835-840
- LIU, J. et al., 2006. A biosynthetic pathway for anandamide. *PNAS*, 103(36), pp. 13345-13350
- LO VERME, J. et al., 2005. The nuclear receptor peroxisome proliferator-activated receptor- α mediates the anti-inflammatory actions of palmitoylethanolamide. *Molecular Pharmacology*, 67, pp. 15-19
- LOMBARD, C., NAGARKATTI, M. and NAGARKATTI, P., 2007. CB2 cannabinoid receptor agonist, JWH-015, triggers apoptosis in immune cells: potential role for CB2-selective ligands as immunosuppressive agents. *Clinical Immunology*, 122(3), pp. 259-270
- LÓPEZ-MIRANDA, V. et al., 2004. Anandamide vehicles: a comparative study. *European Journal of Pharmacology*, 505(1-3), pp. 151-161
- LOVERME, J. et al., 2006. Rapid Broad-Spectrum Analgesia through Activation of Peroxisome Proliferator-Activated Receptor. *Journal of Pharmacology and Experimental Therapeutics*, 319, pp. 1051-1061
- LUNDBERG, M. et al., 1998. Regulation of vascular smooth muscle migration by mitogen activated protein kinase and calcium/calmodulin dependent protein kinase II signaling pathways. *Journal of molecular and cellular cardiology*, 30, pp. 2377-2389
- MACCARRONE, M. et al., 2000. Anandamide uptake by human endothelial cells and its regulation by nitric oxide. *The journal of biological chemistry*, 275(18), pp. 13484-13492
- MACCARRONE, M. et al., 2001. Human platelets bind and degrade 2-arachidonoylglycerol, which activates these cells through a cannabinoid receptor. *European Journal of Pharmacology*, 268, pp. 819-825

- MACCARRONE, M. et al., 2000. Human mast cells take up and hydrolyze anandamide under the control of 5-lipoxygenase and do not express cannabinoid receptors. *FEBS letters*, 468(2-3), pp. 176-180
- MAJESKY, M. et al., 1990. PDGF ligand and Receptor Gene Expression during Repair of Arterial Injury. *The Journal of Cell Biology*, 111, pp. 2149-2158
- MAJESKY, M.W., 1994. Neointima Formation after Acute Vascular Injury. *Texas Heart Institute Journal*, 21, pp. 78-85
- MALINOWSKA, B. et al., 2008. Role of endocannabinoids in cardiovascular shock. *Journal of Physiology and Pharmacology*, 59(8), pp. 91-107
- MALLAT, Z. and TEDGUI, A., 2000. Apoptosis in the vasculature: mechanisms and functional importance. 130, pp. 947-962
- MARSHALL, C., 1995. Specificity of receptor tyrosine kinase signaling: transient versus sustained extracellular signal-regulated kinase activation. *Cell*, 80, pp. 179-185
- MARTIN, R. et al., 2000. The Transcription Factor NF-kB and the Regulation of Vascular Cell Function. *Arteriosclerosis, Thrombosis and Vascular Biology*, 20, pp. 83-88
- MARX, S. et al., 1995. Rapamycin-FKBP inhibits cell cycle regulators of proliferation in vascular smooth muscle cells. *Circulation Research*, 76(3), pp. 412-417
- MATALLANAS, D. et al., 2006. Distinct utilization of effectors and biological outcomes resulting from site-specific Ras activation: Ras functions in lipid rafts and Golgi complex are dispensable for proliferation and transformation.. *Molecular and Cellular Biology*, 26(1), pp. 100-116
- MATIAS, I. et al., 2004. Prostaglandin ethanolamides (prostamides): in vitro pharmacology and metabolism. *Journal of Pharmacology and Experimental Therapeutics*, 309(2), pp. 745-757
- MATIAS, I. and DI MARZO, V., 2007. Endocannabinoids and the control of energy balance. *Trends in Endocrinology and Metabolism*, 18(1), pp. 27-37

- MATSUDA, L. et al., 1990. Structure of a cannabinoid receptor and functional expression of the cloned cDNA. *Nature*, 346(6284), pp. 561-564
- MAZIGHI, M. et al., 2004. IL-10 inhibits vascular smooth muscle cell activation in vitro and in vivo. *American Journal of Heart and Circulatory Physiology*, 287(2), pp. 866-871
- MCCOLLUM, L., HOWLETT, A. and MUKHOPADHYAY, S., 2007. Anandamide-mediated CB1/CB2 cannabinoid receptor--independent nitric oxide production in rabbit aortic endothelial cells. *Journal of Pharmacology and Experimental Therapeutics*, 321(3), pp. 930-937
- MCFARLAND, M. and BARKER, E., 2005. Lipid rafts: a nexus for endocannabinoid signaling? *Life Science*, 77(14), pp. 1640-1650
- MCFARLAND, M. and BARKER, E., 2004. Anandamide Transport. *Pharmacology and Therapeutics*, 104, pp. 117-135
- MCHUGH, D. et al., 2008. Inhibition of human neutrophil chemotaxis by endogenous cannabinoids and phytocannabinoids: evidence for a site distinct from CB1 and CB2. *Molecular Pharmacology*, 73(2), pp. 441-450
- MECHOULAM, R. et al., 1995. Identification of an endogenous 2-monoglyceride, present in canine gut, that binds to cannabinoid receptors. *Biochemical Pharmacology*, 50(1), pp. 83-90
- MECHOULAM, R., FRIDE, E. and DI MARZO, V., 1998. Endocannabinoids. *European Journal of Pharmacology*, 359(1), pp. 1-18
- MELCK, D. et al., 1999. Involvement of the cAMP/protein kinase A pathway and of mitogen-activated protein kinase in the anti-proliferative effects of anandamide in human breast cancer cells. *FEBS letters*, 463, pp. 235-240
- MESTAS, J. and LEY, K., 2008. Monocyte-endothelial cell interactions in the development of atherosclerosis. *Trends in cardiovascular medicine*, 18, pp. 228-232

- MILLER, A. et al., 2001. Inhibition by leukocyte depletion of neointima formation after balloon angioplasty in a rabbit model of restenosis. *Cardiovascular Research*, 49, pp. 838-850
- MIMEAULT, M. et al., 2003. Anti-proliferative and apoptotic effects of anandamide in human prostatic cancer cell lines: implication of epidermal growth factor receptor down-regulation and ceramide production. *The prostate*, 56, pp. 1-12
- MITRA, A. and AGRAWAL, D., 2006. In stent restenosis: bane of the stent era. *Journal of Clinical Pathology*, 59, pp. 232-239
- MIYATO, H. et al., 2009. Pharmacological synergism between cannabinoids and paclitaxel in gastric cancer cell lines. *Journal of surgical research*, 155, pp. 40-47
- MO, F., OFFERTÁLER, L. and KUNOS, G., 2004. Atypical cannabinoid stimulates endothelial cell migration via a G_i/G_o- coupled receptor distinct from CB₁, CB₂ or EDG-1. *European Journal of Pharmacology*, 489, pp. 21-27
- MOLINA-HOLGADO, E. et al., 2002. Cannabinoids promote oligodendrocyte progenitor survival: involvement of cannabinoid receptors and phosphatidylinositol-3 kinase/Akt signaling. *The Journal of Neuroscience*, 22(22), pp. 9742-9753
- MONTECUCCO, F. et al., 2009. Regulation and possible role of endocannabinoids and related mediators in hypercholesterolemic mice with atherosclerosis. *Atherosclerosis*, 205(2), pp. 433-441
- MONTECUCCO, F. et al., 2009. CB₂ cannabinoid receptor activation is cardioprotective in a mouse model of ischemia/reperfusion. *Journal of molecular and cellular cardiology*, 46, pp. 612-620
- MORENO, S., FARIOLI-VECCHIOLI, S. and CERÙ, M., 2004. Immunolocalization of peroxisome proliferator-activated receptors and retinoid X receptors in the adult rat CNS. *Neuroscience*, 123(1), pp. 131-145
- MORRIS, S. and BILLIAR, T., 1994. New insights into the regulation of inducible nitric oxide synthesis. *American Journal of Physiology*, 266, pp. E829-E839

- MOSES, J. et al., 2003. Sirolimus-eluting stents versus standard stents in patients with stenosis in a native coronary artery. *New England Journal of Medicine*, 349(14), pp. 1315-1323
- MOURA, R. et al., 2007. Thrombospondin-1 activates medial smooth muscle cells and triggers neointima formation upon mouse carotid artery ligation. *Arteriosclerosis, Thrombosis and Vascular Biology*, 27(10), pp. 2163-2169
- MUKHOPADHYAY, S., CHAPNICK, B. and HOWLETT, A., 2002. Anandamide-induced vasorelaxation in rabbit aortic rings has two components: G protein dependant and independent. *Am J Physiol Heart Circ Physiol*, 282, pp. H2046-H2054
- MUNRO, S., THOMAS, K. and ABU-SHAAR, M., 1993. Molecular characterisation of a peripheral receptor for cannabinoids. *Nature*, 365, pp. 61-65
- MUTHIAN, S. et al., 2000. Synthesis and characterization of a fluorescent substrate for the *N*-arachidonylethanolamine (anandamide) transmembrane carrier. *Journal of Pharmacology and Experimental Therapeutics*, 293(1), pp. 289-295
- MUTO, A. et al., 2007. Smooth Muscle Cell Signal Transduction: Implications of vascular biology for vascular surgeons. *Journal of Vascular Surgery*, 45, pp. 15-24
- NATHAN, C. and XIE, Q., 1994. Nitric oxide synthases: roles, tolls, and controls. *Cell*, 78(6), pp. 915-918
- NEUMANN, B. et al., 1996. Crucial role of 55-kilodalton TNF receptor in TNF-induced adhesion molecule expression and leukocyte organ infiltration. *Journal of Immunology*, 156, pp. 1587-1593
- NEWBY, A., 2007. Metalloproteinases and Vulnerable Atherosclerotic Plaques. *Trends in Cardiovascular Medicine*, 17, pp. 253-258
- NEWBY, A. and ZALTSMAN, A., 2000. Molecular mechanisms in intimal hyperplasia. *Journal of Pathology*, 190, pp. 300-309
- NGUYEN, T. et al., 1992. Co-regulation of the mitogen-activated protein kinase, extracellular signal-regulated kinase 1, and the 90-kDa ribosomal S6 kinase in PC12

cells. Distinct effects of the neurotrophic factor, nerve growth factor, and the mitogenic factor, epidermal growth factor. *The journal of biological chemistry*, 268(13), pp. 9803-9810

NISSEN, S. et al., 2008. Effect of rimonabant on progression of atherosclerosis in patients with abdominal obesity and coronary artery disease: the STRADIVARIUS randomized controlled trial. *JAMA*, 299(13), pp. 1547-1560

O' SULLIVAN, S., 2007. Cannabinoids go nuclear: evidence for activation of peroxisome proliferator-activated receptors. *British journal of Pharmacology*, , pp. 1-7

O' SULLIVAN, S., KENDALL, D. and RANDALL, A., 2005. Vascular effects of tetrahydrocannabinol (THC), anandamide and N-arachidonoyldopamine (NADA) in the rat isolated aorta. *European Journal of Pharmacology*, 507, pp. 211-221

OFFERTÁLER, L. et al., 2003. Selective ligands and cellular effectors of a G protein-coupled endothelial cannabinoid receptor. *Molecular Pharmacology*, 63, pp. 469-470

OHAYON, J. et al., 2008. Necrotic core thickness and positive arterial remodeling index: emergent biomechanical factors for evaluating the risk of plaque rupture.. *American Journal of Heart and Circulatory Physiology*, 295, pp. H717-H727

OKA, S. et al., 2004. 2-arachidonoylglycerol, an endogenous cannabinoid receptor ligand, induces the migration of EoL-1 human eosinophilic leukemia cells and human peripheral blood eosinophils. *Journal of Leukocyte Biology*, 76(5), pp. 1002-1009

OKA, S. et al., 2007. Identification of GPR55 as a lysophosphatidylinositol receptor. *Biochemical and biophysical Research Communications*, 362(4), pp. 928-934

OKA, S. et al., 2009. 2-Arachidonoyl-sn-glycero-3-phosphoinositol: a possible natural ligand for GPR55. *Journal of Biochemistry*, 145(1), pp. 13-20

OKA, S. et al., 2006. Analgesic effects of fatty acid amide hydrolase inhibition in a rat model of neuropathic pain. *Journal of Neuroscience*, 26(51), pp. 13318-13327

- OKA, S. et al., 2006. Involvement of the cannabinoid CB2 receptor and its endogenous ligand 2-arachidonoylglycerol in oxazolone-induced contact dermatitis in mice. *Journal of Immunology*, 177(12), pp. 8796-8805
- OKAMOTO, Y. et al., 2004. Molecular characterization of a phospholipase D generating anandamide and its congeners. *Journal of Biological Chemistry*, 279(7), pp. 5298-5305
- OKAMOTO, Y. et al., 2005. Mammalian cells stably overexpressing N-acylphosphatidylethanolamine-hydrolysing phospholipase D exhibit significantly decreased levels of N-acylphosphatidylethanolamines. *Biochemical Journal*, 389, pp. 241-247
- OPITZ, C. et al., 2007. Production of the endocannabinoids anandamide and 2-arachidonoylglycerol by endothelial progenitor cells. *FEBS*, 581, pp. 4927-4931
- O'SULLIVAN, S., KENDALL, D. and RANDALL, M., 2004. Heterogeneity in the mechanisms of vasorelaxation to anandamide in resistance and conduit rat mesenteric arteries. *British journal of Pharmacology*, 142, pp. 435-442
- O'SULLIVAN, S., KENDALL, D. and RANDALL, M., 2005. Vascular effects of tetrahydrocannabinol (THC), anandamide and N-arachidonoyldopamine (NADA) in the rat isolated aorta. *European Journal of Pharmacology*, 507, pp. 211-221
- OWENS, G., KUMAR, M. and WAMHOFF, B., 2004. Molecular regulation of vascular smooth muscle cell differentiation in development and disease. *Physiological reviews*, 84(3), pp. 767-801
- OWENS, L. et al., 2001. Overexpression of the focal adhesion kinase (p125FAK) in the vascular smooth muscle cells of intimal hyperplasia. *Journal of Vascular Surgery*, 34, pp. 344-349
- OWENS, G.K., KUMAR, M. and WAMHOFF, B., 2004. Molecular regulation of vascular smooth muscle cell differentiation in development and disease. *Physiological Reviews*, 84, pp. 767-801

PACHER, P., BATKAI, S. and KUNOS, G., 2005. Blood pressure regulation by endocannabinoids and their receptors. *Neuropharmacology*, 48, pp. 1130-1138

PAGÈS, G. et al., 1999. Defective thymocyte maturation in p44 MAP kinase (ERK 1) knockout mice. *Science*, 286, pp. 1374-1377

PAROLARO, D. et al., 2002. Endocannabinoids in the immune system and cancer. *Prostaglandins, Leukotrienes and Essential Fatty Acids*, 66, pp. 319-332

PATINKIN, D. et al., 2008. Endocannabinoids as positive or negative factors in hematopoietic cell migration and differentiation. *European Journal of Pharmacology*, 595(1-3), pp. 1-6

PATRICELLI, M. et al., 1998. An endogenous sleep-inducing compound is a novel competitive inhibitor of fatty acid amide hydrolase. *Bioorganic & Medicinal Chemistry Letters*, 8, pp. 613-618

PAULHE, F. et al., 2001. Vascular smooth muscle cell spreading onto fibrinogen is regulated by calpains and phospholipase C. *Biochemical and Biophysical Research Communications*, 288, pp. 875-881

PEKKNY, M. et al., 1994. Differences in binding to the solid substratum and extracellular matrix may explain isoform-specific paracrine effects of platelet derived growth factor. *Growth Factors*, 10, pp. 77-87

PENG, D. et al., 1996. Anti-Epidermal Growth Factor Receptor Monoclonal Antibody 225 Up-regulates p27^{kip1} and induces G1 arrest in Prostatic Cancer Cell Line DU145. *Cancer Research*, 56, pp. 3666-3669

PERLMAN, H. et al., 1997. Evidence for the rapid onset of apoptosis in medial smooth muscle cells after balloon injury. *Circulation*, 95(4), pp. 981-987

PERONI, R.N. et al., 2007. Participation of CGRP and prostanoids in the sex-linked differences of vascular anandamide effects in mesenteric beds of Sprague-Dawley rats. *European Journal of Pharmacology*, 557, pp. 49-57

- PERTWEE, R., 1999. Pharmacology of cannabinoid receptor ligands. *Current Medicinal Chemistry*, 6, pp. 635-664
- PERTWEE, R., 2006. Cannabinoid Pharmacology: the first 66 years. *British Journal of Pharmacology*, 147, pp. S163-S171
- PERTWEE, R. and ROSS, R., 2002. Cannabinoid receptors and their ligands. *Prostaglandins, Leukotrienes and Essential Fatty Acids*, 66, pp. 101-121
- PICHON, S., BRYCKAERT, M. and BERROU, E., 2004. Control of actin dynamics by p38 MAP kinase-Hsp27 distribution in the lamellipodium of smooth muscle cells. *Journal of cell science*, 117, pp. 2569-2577
- PIETR, M. et al., 2009. Differential changes in GPR55 during microglial cell activation. *FEBS letters*, 583(12), pp. 2071-2076
- PIKE, L. et al., 2002. Lipid rafts are enriched in arachidonic acid and plasmenylethanolamine and their composition is independent of caveolin-1 expression: a quantitative electrospray ionization/mass spectrometric analysis. *Biochemistry*, 41(6), pp. 2075-2088
- PIOMELLI, D. et al., 1999. Structural determinants for recognition and translocation by the anandamide transporter. *PNAS*, 96(10), pp. 5802-5807
- PISANTI, S. et al., 2009. Use of cannabinoid receptor agonists in cancer therapy as palliative and curative agents. *Best practice and research clinical endocrinology and metabolism*, 23, pp. 117-131
- POLLMAN, M., HALL, J. and GIBBONS, G., 1999. Determinants of vascular smooth muscle cell apoptosis after balloon angioplasty injury. Influence of redox state and cell phenotype.. *Circulation Research*, 84(1), pp. 113-121
- POON, M. et al., 1996. Rapamycin inhibits vascular smooth muscle cell migration. *Journal of Clinical Investigation*, 98(10), pp. 2277-2283

- PORTER, A. et al., Characterisation of a Novel Endocannabinoid, Virodhamine, with Antagonist Activity at the CB₁ Receptor. *The Journal of pharmacology and Experimental Therapeutics*, 301, pp. 1020-1024
- PRASS, M. et al., 2006. Direct measurement of the lamellipodial protrusive force in a migrating cell. *Journal of Cell Biology*, 174, pp. 767-772
- PRATT, P.F. et al., 1998. N-arachidonylethanolamide relaxation of bovine coronary artery is not mediated by CB₁ cannabinoid receptor. *American Journal of Physiology*, 274, pp. H375-H381
- PRESCOTT, S. and MAJERUS, P., 1983. Characterization of 1,2-diacylglycerol hydrolysis in human platelets. Demonstration of an arachidonoyl-monoacylglycerol intermediate. *Journal of Biological Chemistry*, 258(2), pp. 764-769
- PULLIKUTH, A. and CATLING, A., 2007. Scaffold mediated regulation of MAPK signaling and cytoskeletal dynamics: A perspective. *Cell Signal*, 19(8), pp. 1621-1632
- RADEMACHER, D. et al., 2005. U-46619 but not serotonin increases endocannabinoid content in middle cerebral artery: evidence for functional relevance. *American Journal of Heart and Circulatory Physiology*, 288, pp. H2694-H2701
- RAINES, E. and ROSS, R., 1993. Smooth muscle cells and the pathogenesis of the lesions of atherosclerosis. *British Heart Journal*, 69(1), pp. S30-S37
- RAINES, E., 2004. PDGF and Cardiovascular disease. *Cytokine and Growth Factor Reviews*, 15, pp. 237-254
- RAINES, E. and FERRI, N., 2005. Cytokines affecting endothelial and smooth muscle cells in vascular disease. *Journal of Lipid Research*, 46, pp. 1081-1092
- RAJESH, M. et al., 2008a. CB₂ cannabinoid receptor agonists attenuate TNF- α -induced human vascular smooth muscle cell proliferation and migration. *British journal of Pharmacology*, 153, pp. 347-357

- RAJESH, M. et al., 2008b. Cannabinoid CB₁ receptor inhibition decreases vascular smooth muscle migration and proliferation. *Biochemical and biophysical Research Communications*, 377, pp. 1248-1252
- RAKSHAN, F. et al., 2000. Carrier-mediated uptake of the endogenous cannabinoid anandamide in RBL-2H3 cells. *Journal of Pharmacology and Experimental Therapeutics*, 292(3), pp. 960-967
- RANDALL, M. and KENDALL, D., 1997. Involvement of a cannabinoid in endothelium-derived hyperpolarizing factor-mediated coronary vasorelaxation. *European Journal of Pharmacology*, 335, pp. 205-209
- RANDALL, M. et al., 2002. Cardiovascular effects of cannabinoids. *Pharmacology and Therapeutics*, 95, pp. 191-202
- RANDALL, M., KENDALL, D. and O'SULLIVAN, S., 2004. The complexities of the cardiovascular actions of cannabinoids. *British Journal of Pharmacology*, 142, pp. 20-26
- RIEDER, S. et al., 2009. Cannabinoid-induced apoptosis in immune cells as a pathway to immunosuppression. *Immunobiology*, doi:10.1016/J.imbio.2009.04.001
- ROBERTS, L., CHRISTIE, M. and CONNOR, M., 2002. Anandamide is a partial agonist at native vanilloid receptors in acutely isolated mouse trigeminal sensory neurons. *British journal of Pharmacology*, 137, pp. 421-428
- ROCKWELL, C. and KAMIINSKI, N., 2004. A cyclooxygenase metabolite of AEA causes inhibition of IL-2 secretion in murine splenocytes. *Journal of Pharmacology and Experimental Therapeutics*, 311, pp. 683-690
- RODRIGUEZ-MENOCAL, L. et al., 2009. The origin of post-injury neointimal cells in the rat balloon injury model. *Cardiovascular Research*, 81(1), pp. 46-53
- RODRIGUEZ-MENOCAL, L. et al., 2009. A novel mouse model of in-stent restenosis. *Atherosclerosis*, In Press

- ROGERS, C., EDELMAN, E. and SIMON, D., 1998. A mAb to the beta2-leukocyte integrin Mac-1 (CD11b/CD18) reduces intimal thickening after angioplasty or stent implantation in rabbits. *PNAS*, 95(17), pp. 10134-10139
- ROSS, R., 1981. George Lyman Duff Memorial Lecture. Atherosclerosis: a problem of the biology of arterial wall cells and their interactions with blood components. *Arteriosclerosis*, 1(5), pp. 293-311
- ROSS, R., 1999. Atherosclerosis--an inflammatory disease. *New England Journal of Medicine*, 340(2), pp. 115-126
- ROSS, R., BROCKIE, H. and PERTWEE, R., 2000. Inhibition of nitric oxide production in RAW264.7 macrophages by cannabinoids and palmitoylethanolamide. *European Journal of Pharmacology*, 401(2), pp. 121-130
- ROSS, R. et al., 1999. Agonist-inverse agonist characterization at CB1 and CB2 cannabinoid receptors of L759633, L759656, and AM630. *British journal of Pharmacology*, 126(3), pp. 665-672
- ROSS, R., 2003. Anandamide and Vanilloid TRPV1 Receptors. *British Journal of Pharmacology*, 140, pp. 790-801
- ROSS, R. et al., 2002. Pharmacological Characterisation of the Anandamide Cyclooxygenase Metabolite: Prostaglandin E2 Ethanolamide. *The Journal of pharmacology and Experimental Therapeutics*, 301, pp. 900-907
- ROSS, R., 2009. The enigmatic pharmacology of GPR55. *Trends in Pharmacological Sciences*, 30(3), pp. 156-163
- RUAN, X. et al., 2006. Mechanisms of dysregulation of low-density lipoprotein receptor expression in vascular smooth muscle cells by inflammatory cytokines. *Arteriosclerosis, Thrombosis and Vascular Biology*, 26(5), pp. 1150-1155
- RUEDA, D. et al., 2000. The CB(1) cannabinoid receptor is coupled to the activation of c-Jun N-terminal kinase. *Molecular Pharmacology*, 58, pp. 814-820

- RYAN, D. et al., 2009. Cannabidiol targets mitochondria to regulate intracellular Ca²⁺ levels. *The Journal of Neuroscience*, 29, pp. 2053-2063
- RYBERG, E. et al., 2007. The orphan receptor GPR55 is a novel cannabinoid receptor. *British journal of Pharmacology*, 152, pp. 1092-1101
- SABERS, C. et al., 1995. Isolation of a protein target of the FKBP12-rapamycin complex in mammalian cells. *Journal of Biological Chemistry*, 270(2), pp. 815-822
- SÁNCHEZ, C. et al., 1998. Involvement of sphingomyelin hydrolysis and the mitogen-activated protein kinase cascade in the Delta9-tetrahydrocannabinol-induced stimulation of glucose metabolism in primary astrocytes. 54(5), pp. 834-843
- SANCHEZ, C. et al., 2001. Inhibition of glioma growth *in vivo* by selective activation of the CB₂ Cannabinoid Receptor. *Cancer Research*, 61, pp. 5784-5789
- SANDIRASEGARANE, L. et al., 2000. NO regulates PDGF-induced activation of PKB but not ERK in A7r5 cells: implications for vascular growth arrest. *American Journal of Cell Physiology*, 279(1), pp. C225-C235
- SARKAR, R. et al., 1997. Cell cycle effects of nitric oxide on vascular smooth muscle cells. *American Journal of Physiology*, 272, pp. 1810-1818
- SATA, M. et al., 2002. Hematopoietic stem cells differentiate into vascular cells that participate in the pathogenesis of atherosclerosis. *Nature Medicine*, 8(4), pp. 403-409
- SCHACHTER, M., 1997. The pathogenesis of atherosclerosis. *International Journal of Cardiology*, 62, pp. S3-S7
- SCHELLER, B. et al., 2008. Short- and long-term effects of a novel paclitaxel coated stent in the porcine coronary model. *Clinical Research in Cardiology*, 97, pp. 118-123
- SCHILINGER, M. and MINAR, E., 2005. Restenosis after percutaneous angioplasty: the role of vascular inflammation. *Vascular Health and Risk Management*, 1, pp. 73-78
- SCHOBBER, A., 2008. Chemokines in vascular dysfunction and remodeling. *Arteriosclerosis, Thrombosis and Vascular Biology*, 28(11), pp. 1950-1959

- SCHOBBER, A. et al., 2004. Crucial role of the CCL2/CCR2 axis in neointimal hyperplasia after arterial injury in hyperlipidemic mice involves early monocyte recruitment and CCL2 presentation on platelets. *Circulation Research*, 95(11), pp. 1125-1133
- SCHRIJVERS, D. et al., 2007. Phagocytosis in atherosclerosis: Molecular mechanisms and implications for plaque progression and stability. *Cardiovascular Research*, 73, pp. 470-480
- SCHWARTZ, R. et al., 1990. Restenosis after balloon angioplasty. A practical proliferative model in porcine coronary arteries. *Circulation*, 82, pp. 2190-2200
- SCHWARTZ, S., CAMPBELL, G. and CAMPBELL, J., 1986. Replication of smooth muscle cells in vascular disease. *Circulation Research*, 58, pp. 427-444
- SCHWARTZ, S., DEBLOIS, D. and O'BRIEN, E., 1995. The Intima Soil for Atherosclerosis and Restenosis. *Circulation Research*, 77, pp. 445-465
- SCHWARTZ, S., MAJESKY, M. and MURRY, C., 1995. The intima: development and monoclonal responses to injury. *Atherosclerosis*, 118, pp. 125-142
- SCHWARTZFARB, L., NEEDLE, M. and CHAVEZ-CHASE, M., 1994. Dose-related inhibition of leukocyte migration by marijuana and delta-9-tetrahydrocannabinol (THC) in vitro. *Journal of Clinical Pharmacology*, 14(1), pp. 35-41
- SCOTT, N. et al., 1996. Identification of a potential role for the adventitia in vascular lesion formation after balloon overstretch injury of porcine coronary arteries. *Circulation*, 93, pp. 2178-2187
- SELZMAN, C.H., SHAMES, B.D. and REZNIKOV, L.L., 1999. Liposomal delivery of purified inhibitory-kBa inhibits tumor necrosis factor- α -induced human vascular smooth muscle cell proliferation. *Circulation Research*, 84, pp. 867-875
- SEN, P. et al., 2003. Involvement of the Akt/PKB signaling pathway with disease processes. *Molecular and Cellular Biochemistry*, 253, pp. 241-246

- SENNOUN, N. et al., 2009. Recombinant human activated protein C improves endotoxemia-induced endothelial dysfunction: a blood-free model in isolated mouse arteries. *American Journal of Heart and Circulatory Physiology*, 297(1), pp. H277-H282
- SHAUL, Y. and SEGER, R., 2007. The MEK/ERK cascade: from signaling specificity to diverse functions. *Biochimica et biophysica Acta*, 1773, pp. 1213-1226
- SHI, Y. et al., 1997. Origin of extracellular matrix synthesis during coronary repair. *Circulation*, 95(4), pp. 997-1006
- SHI, Y. et al., 1996. Adventitial myofibroblasts contribute to neointimal formation in injured porcine coronary arteries. *Circulation*, 94(7), pp. 1655-1664
- SIMON, D. et al., 2000. Decreased neointimal formation in Mac-1(-/-) mice reveals a role for inflammation in vascular repair after angioplasty. *Journal of clinical investigation*, 105(3), pp. 293-300
- SIMON, G. and CRAVATT, B., 2006. Endocannabinoid biosynthesis proceeding through glycerophospho-N-acyl ethanolamine and a role for alpha/beta-hydrolase 4 in this pathway. *Journal of Biochemical Chemistry*, 821(36), pp. 26465-26472
- SIMPER, D. et al., 2002. Smooth muscle cells in human blood. *Circulation*, 106, pp. 1199-1204
- SIOW, R. and CHURCHMAN, A., 2007. Adventitial growth factor signaling and vascular remodeling: potential of perivascular gene transfer from the outside-in. *Cardiovascular Research*, 75(4), pp. 659-668
- SKENE, K. et al., 2006. Studies on the receptors mediating relaxant responses to the endocannabinoid anandamide in the porcine coronary artery. *ICRS abstract book*, pp. 173
- SMART, D. et al., 2002. 'Entourage' effects of N-acyl ethanolamines at human vanilloid receptors. Comparison of effects upon anandamide-induced vanilloid receptor activation

and upon anandamide metabolism. *British journal of Pharmacology*, 136(3), pp. 452-458

SOLLOTT, S. et al., 1995. Taxol inhibits neointimal smooth muscle cell accumulation after angioplasty in the rat.. *Journal of Clinical Investigation*, 95, pp. 1869-1876

SONG, Z. and AND ZHONG, M., 2000. CB1 Cannabinoid Receptor-Mediated Cell Migration. *The Journal of pharmacology and Experimental Therapeutics*, 294, pp. 204-209

SPRAGUE, A. and KHALIL, R., 2009. Inflammatory cytokines in vascular dysfunction and vascular disease. *Biochemical Pharmacology*, 78, pp. 539-552

SRIRAM, V. and PATTERSON, C., 2001. Cell cycle in Vasculoproliferative Diseases Potential Interventions and Routes of Delivery. *Circulation*, 103, pp. 2414-2419

STANFORD, S. et al., 2001. Cytokine-activated human vascular smooth muscle delays apoptosis of neutrophils: relevance of interactions between cyclo-oxygenase-2 and colony-stimulating factors. *FASEB*, 15, pp. 1813-1815

STAROWICZ, K., NIGAM, S. and DI MARZO, V., 2007. Biochemistry and pharmacology of endovanilloids. *Pharmacology and Therapeutics*, 114(1), pp. 13-33

STARY, H. et al., 1992. A definition of the intima of human arteries and of its atherosclerosis-prone regions. A report from the Committee on Vascular Lesions of the Council on Arteriosclerosis, American Heart Association. *Arteriosclerosis, Thrombosis and Vascular Biology*, 12(1), pp. 120-134

STARY, H. et al., 1994. A definition of initial, fatty streak, and intermediate lesions of atherosclerosis. A report from the Committee on Vascular Lesions of the Council on Arteriosclerosis, American Heart Association. *Arteriosclerosis, Thrombosis and Vascular Biology*, 14(5), pp. 840-856

STARY, H., 2000. Natural history and histological classification of atherosclerotic lesions: an update. *Arteriosclerosis, Thrombosis and Vascular Biology*, 20(6), pp. 1177-1178

- STEFFENS, S. et al., 2005. Low dose oral Cannabinoid therapy reduces progression of atherosclerosis in mice. *Nature*, 434, pp. 782-786
- STEIN, E. et al., 1996. Physiological and behavioural effects of the endogenous cannabinoid, arachidonylethanolamide (anandamide), in the rat. *British journal of Pharmacology*, 119(1), pp. 107-114
- STELLA, N., SCHWEITZER, P. and PIOMELLI, D., 1997. A second endogenous cannabinoid that modulates long-term potentiation. *Nature*, 388(6644), pp. 773-778
- STIENSTRA, R. et al., 2007. PPARs, Obesity, and Inflammation. *PPAR research*, 2007, pp. 95974
- STOCKER, R. and KEANEY, J., 2004. Role of Oxidative Modifications in Atherosclerosis. *Physiological reviews*, 84, pp. 1381-1478
- STONE, G. et al., 2009. Paclitaxel-eluting stents versus bare-metal stents in acute myocardial infarction. *New England Journal of Medicine*, 360(19), pp. 1946-1959
- STONE, G. et al., 2007. Safety and Efficacy of Sirolimus-and Paclitaxel-Eluting Coronary Stents. *The New England Journal of Medicine*, 356, pp. 998-1008
- STORR, M. and SHARKEY, K., 2007. The endocannabinoid system and gut-brain signalling. *Current Opinion in Pharmacology*, 7(6), pp. 575-582
- STREMMEL, W. et al., 2001. A new concept of cellular uptake and intracellular trafficking of long-chain fatty acids. *Lipids*, 36(9), pp. 981-989
- SUGAMURA, K. et al., 2009. Activated endocannabinoid system in coronary artery disease and anti-inflammatory effects of cannabinoid 1 receptor blockade on macrophages. *Circulation*, 119, pp. 28-36
- SUGIURA, T. et al., 1998. Detection of an endogenous cannabimimetic molecule, 2-arachidonoylglycerol, and cannabinoid CB1 receptor mRNA in human vascular cells: is 2-arachidonoylglycerol a possible vasomodulator. *Biochemical and biophysical Research Communications*, 243(3), pp. 838-843

- SUGIURA, T. et al., 1995. 2-Arachidonoylglycerol: a possible endogenous cannabinoid receptor ligand in brain. *Biochemical and biophysical Research Communications*, 215(1), pp. 89-97
- SUGIURA, T., KOBAYASHI, Y. and WAKU, K., 2002. Biosynthesis and degradation of anandamide and 2-AG and their possible physiological significance. *Prostaglandins, Leukotrienes and Essential Fatty Acids*, 66(2&3), pp. 173-192
- SUN, J. et al., 2007. Mast cells promote atherosclerosis by releasing proinflammatory cytokines. *Nature Medicine*, 13(6), pp. 719-724
- SUN, Y. et al., 2004. Biosynthesis of anandamide and N-palmitoylethanolamine by sequential actions of phospholipase A2 and lysophospholipase D. *Biochemical Journal*, 380, pp. 749-756
- SUN, Y. et al., 2006. Cannabinoids and PPAR alpha signaling. *Biochemical Society Transactions*, 34, pp. 1095-1094
- SZALLASI, A., Vanilloid (capsaicin) receptors in health and disease. *American Journal of Clinical Pharmacology*, 118(1), pp. 110-121
- TAKAHASHI, S. et al., 2007. Late angiographic stent thrombosis after sirolimus-eluting stent implantation. *Circulation Journal*, 71(2), pp. 226-228
- TANAKA, H. et al., 1993. Sustained activation of vascular cells and leukocytes in the rabbit aorta after balloon injury. *Circulation*, 88, pp. 1788-1803
- TEDGUI, A. and MALLAT, Z., 2006. Cytokines in atherosclerosis: pathogenic and regulatory pathways. *Physiological Reviews*, 86(2), pp. 515-581
- TORSNEY, E., HU, Y. and XU, Q., 2005. Adventitial progenitor cells contribute to arteriosclerosis. *Trends in cardiovascular medicine*, 15(2), pp. 64-68
- TOUTOUZAS, K., COLOMBO, A. and STEFANADIS, C., 2004. Inflammation and restenosis after percutaneous coronary interventions. *European Heart Journal*, 25, pp. 1679-1687

- TRAVERSE, S. et al., 1994. EGF triggers neuronal differentiation of PC12 cells that overexpress the EGF receptor. *Current Biology*, 4(8), pp. 694-701
- UEDA, N. et al., 1995. Lipoxygenase-catalyzed oxygenation of arachidonylethanolamide, a cannabinoid receptor agonist. *Biochimica et biophysica Acta*, 1254(2), pp. 127-134
- UNDERDOWN, N., HILEY, C. and FORD, W., 2005. Anandamide reduces infarct size in rat isolated hearts subjected to ischaemia-reperfusion by a novel cannabinoid mechanism. *British journal of Pharmacology*, 146, pp. 809-816
- VAN HOVE, C. et al., 2009. Vasodilator efficacy of nitric oxide depends on mechanisms of intracellular calcium mobilization in mouse aortic smooth muscle cells. *British journal of Pharmacology*, 158(3), pp. 920-930
- VAN SICKLE, M. et al., 2005. Identification and functional characterization of brainstem cannabinoid CB2 receptors. *Science*, 310, pp. 329-332
- VARGA, K. et al., 1995. Novel antagonist implicates the CB1 cannabinoid receptor in the hypotensive action of anandamide. *European Journal of Pharmacology*, 278(3), pp. 279-283
- VARGA, K. et al., 1996. Mechanism of the hypotensive action of anandamide in anesthetized rats. *Hypertension*, 28(4), pp. 682-686
- VARGA, K. et al., 1998. Platelet- and macrophage-derived endogenous cannabinoids are involved in endotoxin-induced hypotension. *FASEB*, 12(11), pp. 1035-1044
- VELASCO, G. et al., 2005. Cannabinoids and ceramide: Two lipids acting hand by hand. *Life Sciences*, 77, pp. 1723-1731
- VIRMANI, R. et al., 2006. Pathology of the Vulnerable Plaque. *Journal of American College of Cardiology*, 47, pp. 13-18
- VOISARD, R. et al., 1999. A human arterial organ culture model of postangioplasty restenosis: results up to 56 days after ballooning. *Atherosclerosis*, 144, pp. 123-134

- WAGNER, J. et al., 2001. Endogenous cannabinoids mediate hypotension after experimental myocardial infarction. *Journal of the American College of Cardiology*, 38(7), pp. 2048-2054
- WAGNER, J. et al., 2003. CB(1) cannabinoid receptor antagonism promotes remodeling and cannabinoid treatment prevents endothelial dysfunction and hypotension in rats with myocardial infarction. *British journal of Pharmacology*, 138(7), pp. 1251-1258
- WAGNER, J. et al., 1997. Activation of peripheral CB1 cannabinoid receptors in haemorrhagic shock. *Nature*, 390(6659), pp. 518-521
- WAGNER, J. et al., 1999. Mesenteric Vasodilation Mediated by Endothelial Anandamide Receptors. *Hypertension*, 33(II), pp. 429-434
- WAHN, H. et al., 2005. The endocannabinoid arachidonyl ethanolamide (anandamide) increases pulmonary arterial pressure via cyclooxygenase-2 products in isolated rabbit lungs. *The American journal of Physiology- Heart and Circulatory Physiology*, 289, pp. H2491-H2496
- WAINWRIGHT, C.L., MILLER, A.M. and WADSWORTH, R.M., 2001. Inflammation as a key event in the development of neointima following vascular balloon injury. *Clinical and Experimental Pharmacology and Physiology*, 28, pp. 891-895
- WALTER, L. et al., 2003. Nonpsychotropic Cannabinoid Receptors Regulate Microglial Cell Migration. *Journal of neuroscience*, 23, pp. 1398-1405
- WANG, Y. et al., 2001. Simultaneous measurement of anandamide and 2-arachidonoylglycerol by polymyxin B-selective adsorption and subsequent high-performance liquid chromatography analysis: increase in endogenous cannabinoids in the sera of patients with endotoxic shock. *Analytical Biochemistry*, 294(1), pp. 73-82
- WANG, Y. et al., 2007. Andrographolide inhibits NF-kappa Beta activation and attenuates neointimal hyperplasia in arterial restenosis. *Cell Research*, 17(11), pp. 933-941

WARD, M. et al., 2001. Low blood flow after angioplasty augments mechanisms of restenosis: inward vessel remodeling, cell migration, and activity of genes regulating migration. *Arteriosclerosis, Thrombosis and Vascular Biology*, 21, pp. 208-213

WARTMANN, M. et al., 1995. The MAP kinase signal transduction pathway is activated by the endogenous cannabinoid anandamide. *FEBS letters*, 359, pp. 133-136

WELT, F.G. and ROGERS, C., 2002. Inflammation and Restenosis in the Stent Era. *Arteriosclerosis Thrombosis and Vascular Biology*, 22, pp. 1769-1776

WHEAL, A. and RANDALL, M., 2009. Effects of hypertension on vasorelaxation to endocannabinoids in vitro. *European Journal of Pharmacology*, 603, pp. 79-85

WHEAL, A. et al., 2007. Effects of chronic nitric oxide synthase inhibition on the cardiovascular responses to cannabinoids in vivo and in vitro. *British journal of Pharmacology*, 150, pp. 662-671

WHITE, R. and HILEY, C., 1998. The actions of some cannabinoid receptor ligands in the rat isolated mesenteric artery. *British journal of Pharmacology*, 125(3), pp. 533-541

WHITE, R. et al., 2001. Mechanisms of anandamide-induced vasorelaxation in rat isolated coronary arteries. *British journal of Pharmacology*, 134(4), pp. 921-929

WILLERT, M. et al., 2010. Transcriptional regulation of Pim-1 kinase in vascular smooth muscle cells and its role for proliferation. *Basic Research in Cardiology*, 105(2), pp. 267-277

WINSLOW, R., SHARMA, S. and KIM, M., 2005. Restenosis and drug eluting stents. *The Mount Sinai Journal of Medicine*, 72, pp. 81-89

WOODWARD, D. et al., 2001. The pharmacology of bimatoprost. *Survey of Ophthalmology*, 45(Supp 4), pp. S337-S345

WOODWARD, D. et al., 2007. Identification of an antagonist that selectively blocks the activity of prostamides (prostaglandin-ethanolamides) in the feline iris. *British journal of Pharmacology*, 150, pp. 342-352

- YAN, Z. et al., 2007. Exercise reduces adipose tissue via cannabinoid receptor 1 which is regulated by peroxisome proliferator-activated receptor-delta. *Biochemical and Biophysical Research Communications*, 354, pp. 427-433
- YANG, W. et al., 2005. Enzymatic formation of prostamide F2alpha from anandamide involves a newly identified intermediate metabolite, prostamide H2. *Journal of Lipid Research*, 46(12), pp. 2745-2751
- YAO, Y. et al., 2003. Extracellular signal-regulated kinase 2 is necessary for mesoderm differentiation. *PNAS*, 100, pp. 12759-12764
- YAU, L. et al., 2008. Meta-iodobenzylguanidine, an inhibitor of arginine-dependent mono(ADP-ribosyl)ation, prevents neointimal hyperplasia. *Journal of Pharmacology and Experimental Therapeutics*, 326(3), pp. 717-724
- YU, M., IVES, D. and RAMESHA, C., 1997. Synthesis of prostaglandin E2 ethanolamide from anandamide by cyclooxygenase-2. *Journal of Biological Chemistry*, 272(34), pp. 21181-21186
- ZALEWSKI, A. and SHI, Y., 1997. Vascular myofibroblasts. Lessons from coronary repair and remodeling. *Arteriosclerosis, Thrombosis and Vascular Biology*, 17(3), pp. 417-422
- ZAND, T. et al., 1999. Lipid deposition in rat aortas with intraluminal hemispherical plug stenosis. A morphological and biophysical study. *American Journal of Pathology*, 155, pp. 85-92
- ZARGHAM, R., 2008. Preventing restenosis after angioplasty: a multi stage approach. *Clinical Science*, 114, pp. 257-264
- ZEIFFER, U. et al., 2004. Neointimal smooth muscle cells display a proinflammatory phenotype resulting in increased leukocyte recruitment mediated by P-selectin and chemokines. *Circulation Research*, 94(6), pp. 776-784

ZERNECKE, A. et al., 2008. Protective role of CXC receptor 4/CXC ligand 12 unveils the importance of neutrophils in atherosclerosis. *Circulation Research*, 102(2), pp. 209-217

ZHAO, Y. et al., 2010. Activation of Cannabinoid CB2 Receptor Ameliorates Atherosclerosis Associated with Suppression of Adhesion Molecules. *Journal of Cardiovascular Pharmacology*, In Press

ZHOU, Y. et al., 2005. Acetylcholine causes endothelium-dependent contraction of mouse arteries. *American Journal of Heart and Circulatory Physiology*, 289(3), pp. H1027-H1032

ZICHE, M. et al., 1994. Nitric Oxide Mediates Angiogenesis in Vivo and Endothelial Cell Growth and Migration In Vitro Promoted by Substance P. *Journal of Clinical Investigation*, 94, pp. 2036-2044

ZYGMUNT, P. et al., 1997. Studies on the effects of anandamide in rat hepatic artery. *British journal of Pharmacology*, 122(8), pp. 1679-1686

ZYGMUNT, P. et al., 1999. Vanilloid receptors on sensory nerves mediate the vasodilator action of anandamide. *Nature*, 400(6743), pp. 452-457